# Draft

Prepared for:

## Rijkswaterstaat

# SCOUR manual

Desk study

August 1991

**Draft**

SCOUR manual

M. van der Wal, G. van Driel en H.J. Verheij

**delft hydraulics**

# CONTENTS

CONTENTS(continued)

**CONTENTS**(continued)

# CONTENTS (continued)

**APPENDICES**

# FIGURES

**FIGURES** (continued)

## SYMBOLS

| | | |
|---|---|---|
| A | area of a cross section | $m^2$ |
| a | constant | – |
| B | width of a river or canal | m |
| $B_p$ | pier projected width | m |
| $B_t$ | total width of a river | m |
| $B_s$ | width of a scour hole | m |
| b | width of a structure, constant | m, – |
| C | Chezy coefficient | $m^{\frac{1}{2}}s^{-1}$ |
| c | coefficient | var. |
| c | concentration (usually by volume) | – |
| $c_k$ | coefficient $(B_t - 1)/B_t$ | – |
| D | hydraulic mean depth | m |
| D | diffusion coefficient | $m^2/s$ |
| D | grain size (main grain size) | m |
| $d_*$ | dimensionless grainsize $d_* = D \{\Delta \cdot g/\nu^2\}^{0.33}$ | – |
| $D_x$ | grain diameter, a sieve-width of which x% of the grains of the material passes | m |
| Fr | Froude number | – |
| f | Darcy-Weissbach friction factor | – |
| f | Lacey silt factor | – |
| $f_s$ | shape factor | – |
| g | acceleration due to gravity | $m/s^2$ |
| H | total energy head loss | m |
| h | water level | m |
| $h_d$ | dune height | m |
| $h_e$ | scour depth (equilibrium) | m |
| $h_{s,t}$ | scour depth as a function of time | m |
| I | contents of a scour hole | $m^3$ |
| L | width of the sill | m |
| K | factor | – |
| $k_s$ | roughness height according to Nikuradse | m |
| $L_p$ | length bed protection | m |
| l | length | |
| n | porosity, Manning coefficient | –,– |
| n | scale factor | |

| | | |
|---|---|---|
| $p$ | pressure, constant | $N/m^2$, - |
| $Q$ | discharge (water) | $m^3/s$ |
| $Q_s$ | discharge (sediment) (volume of grains) | $m^3/s$ |
| $q$ | discharge/m width (water) | $m^2/s$ |
| $q_s$ | discharge/m width (sediment) | $m^2/s$ |
| $q_{s,b}$ | bed load sediment discharge/m width | $m^2/s$ |
| $q_{s,s}$ | suspended load sediment discharge/m width | $m^2/s$ |
| $q_{s,t}$ | total load sediment discharge/m width | $m^2/s$ |
| $q_o$ | discharge/m width, upstream of structure | $m^2/s$ |
| $q_c$ | discharge/m width, in the constraction | $m^2/s$ |
| $R$ | hydraulic mean radius | m |
| $Re$ | Reynolds number ($u . y_o/v$) | - |
| $Re_*$ | Reynolds number ($u_* . D/v$) | - |
| $r$ | radius, relative turbulence intensity | m, - |
| $S$ | hydraulic gradiënt, sediment transport | -, $m^3/ms$ |
| $t$ | time | s, days |
| $t_1$ | reference time, as $y_{s,max} = y_o$ | s, days |
| $T$ | period of unsteady flow | s |
| $te$ | time after which the equilibruim scour depth is reached | s |
| $U$ | velocity (depth averaged flow) | m/s |
| $U_{cr}$ | critical flow velocity at the initiation of movement | m/s |
| $U_o$ | undisturbed flow velocity | m/s |
| $U_1$ | local flow velocity at the edge of the bed protection | m/s |
| $u$ | local flow velocity | m/s |
| $u_*$ | shear stress velocity | m/s |
| $u_{*,cr}$ | critical shear stress at the initiation of motion | m/s |
| $u'$ | root mean square value of the turbulent velocity fluctuations | m/s |
| $v$ | velocity (average velocity), constants | m/s, - |
| $v_*$ | shear stress velocity | m/s |
| $w$ | fall velocity of sediment | m/s |
| $y_D$ | sill height | m |
| $y_o$ | depth (uniform flow depth) | m |
| $y_r$ | depth (regime depth) | m |
| $y_{s,max}$ | maximum scour depth | m |
| $z$ | bed level | m |

## SYMBOLS (continued)

| | | |
|---|---|---|
| $\alpha$ | angle, factor in Breusers formula | °,− |
| $\alpha_e$ | local value of the factor in Breusers formula | − |
| $\beta$ | angle | ° |
| $\gamma$ | exponent in Breusers formula | − |
| $\Delta$ | relative density | − |
| $\varepsilon$ | turbulent diffusion coefficient for sediment | $m^2/s$ |
| $\kappa$ | von Karman constant | − |
| $\mu$ | dynamic viscosity | $Ns/m^2$ |
| $\nu$ | kinematic viscosity | $m^2/s$ |
| $\rho$ | density of water | $kg/m^3$ |
| $\rho_s$ | density of sediment | $kg/m^3$ |
| $\sigma_g$ | geometric standard deviation of the grain size | − |
| $\tau$ | shear stress | $N/m^2$ |
| $\tau_{cr}$ | critical shear stress | $N/m^2$ |
| $\theta$ | flow parameter, dimensionless shear stress | − |

# 1. **Introduction**

## 1.1 *General*

During the last decades many research projects, directed to the phenomena of local scour, have been realised in the Netherlands. Now The Dutch Public Works Department wishes to summarise the main results of all these research projects in a local scour manual, which should contain guidelines to solve problems related to local scour in engineering practise. Finally all these results will implemented in a software information system SCOUR.

DELFT HYDRAULICS is commissioned by Dutch Public Works Department, Locks and Weirs Department in letter BSW/WB 89-4136, dated August 17th, 1989. Specially for the incorporation of local scour near bridge piers in this report DELFT HYDRAULICS is commissioned by the Locks and Weirs Department in letter BSW 90-4656, dated July 17th, 1990.

This project has been realised in the period October 1989 to September 1990.

The author of this draft manual is M. van der Wal, project engineer of Delft Hydraulics, in cooperation with Mr R. Jorissen of the Road and Hydraulic Department of the Dutch Public Works Department.

## 1.2 **Scope of this manual**

The treatment of the local scour phenomena in this manual is classified by different types of structures. Each structure type is necessarily schematized to a simple, basic lay-out, which is applied frequently in The Netherlands. Some characteristic lay-outs of each structure type are considered in this manual. The choice of the structures is based on a representative selection of the hydraulic structures in The Netherlands. The following types of structures have been included in this report: sills or bars (chapter 2), spurdikes and abutments (chapter 3), bridge piers (chapter 4), outlets (chapter 5), jets (chapter 6), scour by waves (chapter 7) and scour of cohesive soils (chapter 8).

A brief description is given of the main parameters of a structure and of the main parts of the flow pattern near a structure. Detailed and theoretical descriptions of the flow phenomena are not included, because at this stage the consequences of these descriptions for engineering practice are minimal.

The available theory of scour phenomena is not complete to match each scour problem, therefore some approximations are proposed. The mainly one-dimensional theory, which is presented in this manual, can be applied directly in engineering practice. The semi-empirical theory for the developing phase of a scour hole can be considered as a continuation and an expansion of the approach of Breusers, lit.[1.2]. With this approach a lot of experience has been gained mainly in the Netherlands, but also abroad, during last decades.

For the maximum scour depth in the equilibrium phase some preliminary formulas are given.

Complex two-dimensional computer models are developed now to calculate a scour hole depth, but these models will not be available for engineering practice in the near future.

The scope of this scour manual is to provide the civil engineer with practical calculation methods for the dimensions of scour holes and an introduction to the most relevant literature. The main aspects are the determination of the maximum scour depth and the initial slopes of a scour hole. If such calculation methods are not available for a certain situation, probably a possible future research topic can be identified.

A complete review of all the available references on local scour is out of the scope of this manual. For a more general introduction to local scour we refer for example to the monograph no A8 ´Scouring´ by Breusers and Raudkivi, lit.[1.1].

In this draft version of the manual insufficient attention is paid to the validity ranges and limitations of the formulas, and the information about the accuracy of the calculated parameters (mainly scour depth and initial slope of the scour hole) is complete. The methods to prevent local scour are only mentioned in the chapter about bridge piers.

In a specific, complex situation we recommend a physical scale model investigation for the most detailed information about the development of a scour hole.

## 1.3 Summary and conclusions

Sills

A sill with a broad or a sharp crest and a sill with and without a bed protection are distinguished in this manual. Normally the flow above a sill is subcritical, but depending on the downstream waterlevel the flow can become also supercritical.

For a broad crested sill with a bed protection the maximum scour depth can be calculated with the formulas of Breusers and Dietz. The differences between these formulas have been described. For the coefficient $\alpha$ as a function of the height of the sill and the length of the bed protection a new expression has been derived and compared with the measurements of systematic test series. As an alternative for these expressions a promising formula for $\alpha$ as a function of the relative turbulence intensity has been given by de Graauw and Jorissen.

The supply of sediment from upstream reduces the maximum scour depth, which is measured in clear water tests. An approximate calculation method is described. A method to adjust the calculation method for unsteady flow, especially tidal flow, is given. These methods have been applied successfully during the design of the Eastern Scheldt Storm Surge barrier.

The formulas to determine the equilibrium scour depths according to Dietz and Zanke have been confirmed by some tests of Delft Hydraulics. The complete formula of Zanke is considered to be too complicated for prediction purposes. A further examination of these formulas is recommended.

The time dependent development of a scour hole behind a broad crested sill without a bed protection can be calculated with the formulas of Bormann. He studied a sill with supercritical flow downstream of the sill. The structure of these formulas show a good similarity with the Breusers formula. Also for this case a further examination and development of Bormann´s formulas is recommended.

The time dependent development of the maximum scour depth downstream of an hydraulic jump has been studied by Fahroudi, Smith and Popova. The formulas of Fahroudi and Smith show some similarity with the Breusers method.

For the initial slope of a two-dimensional scour hole some values are recommended.

If the scour hole has a three dimensional shape, the initial slope needs a more extensive description.

Spurdikes and abutments

After a description of the geometry of a spurdike, the flow pattern around a spurdike and some remarks about the failure mechanism of a spurdike, the calculation of the maximum scour depth is treated more in detail.

In the developing phase of a scour hole the maximum scour depth can be calculated with the Breusers method also. The coefficient $\alpha$ can be determined as a function of the constriction of the flow by the spurdike, the length of the bed protection and the slope of the head of the spur dike. The coefficient $\gamma$ as a function of the maximum scour depth has been confirmed roughly by the results published by da Cunha.
For the situation of a spurdike combined with a sill and a constant constriction of 10% a special formula for the calculation of the value of $\alpha$ is given as a function of sill height and the length of the bed protection.

In the equilibrium phase of a scour hole the maximum scour depth can be estimated by a number of semi-empirical formulas. These formulas are compared globally and a general applicable expression is proposed.

It is recommended to extend the Breusers method in such a way that the development of the maximum scour depth can be predicted during a design flood or an extreme flood in a river.

The analysis of the semi-empirical formulas for the maximum scour depth in the equilibrium phase can be completed with more data and more formulas from the literature.
As further extensions are proposed to include the initial slope of a scour hole and rules for spurdike spacing and for the height of the crest.

The total depth of a scour hole near an abutment follows from the superposition of general river bed degradation, constriction scour and local scour. In principle the dimensions of a local scour hole can be estimated with the formulas for spurdikes. General river bed degradation

and constriction scour can be calculated with the results of a mathematical flood routing model. As an alternative for such a mathematical model the manual can be extended with some formulas to approximate the constriction scour depth. The soil mechanical aspects of the stability of wing walls near a scour hole need more attention.

Bridge piers

The geometry of a bridge pier can differ considerably, but most studies on local scour around bridge piers have been focussed on a prismatic bridge pier, which has a circular cross section and which has been placed into a non-cohesive bed. The description of the flow pattern around a bridge pier is restricted to a global description of the main parts of that flow pattern.

The methods to prevent bridge pier scour have been reviewed and some design rules for the length of a riprap protection have been mentioned.

In the developing phase of a scour hole around a bridge pier the Breusers method can be used also. In this three dimensional scour hole the exponent y depends also on the maximum scour depth and for a first approach a formula has been given to determine the value of the coefficient y. In this formula the two states of clear water scour and live bed scour are distinguished.

The ratio bridge pier width and water depth determines if the maximum scour depth depends on the bridge pier width or on the water depth.

A start has been made to adjust the formula for the reference time $t_1$ in the two-dimensional scour holes, to the bridge pier scour holes. It is recommended to complete this analysis of an adjusted formula for $t_1$.

Some rather high values of the coefficient $\alpha$ (up to 7.8) have been determined from the measurements in a scale model of a bridge pier without a bed protection.

In the equilibrium phase of a scour hole around a bridge pier a general formula has been proposed as a combination of three existing formulas.

In this formula the influence of the shape of the pier, the direction of the flow, the gradation of the bed material and a goup of piers have been presented in K-factors.

In this manual only local scour near a bridge pier is treated. In general, bridge pier scour is the result of the superposition of constriction scour, general bed degradation and local scour. It is recommended to include constriction scour also in this manual.

Further recommendations for a completion of this chapter concern the aspects of slopes of the scour hole, the influence of ice, waves and the combination of wave and currents.

## Outlets

The scour hole downstream of an outlet with a rectangular cross section, a horizontal or gentle sloped bed protection and diverging wing walls is considered in this manual.
In the developing phase of a scour hole the Breusers method can be used also for scour holes downstream of an outlet. For a first estimation of the coefficient $\alpha$ as a function of the length of the bed protection a special formula has been derived, based on the results of several scale model tests.

## Jets

Flow over, under and through hydraulic structures can result in submerged or free jets. Both types of jets can be a circular (three dimensional) or plane (two dimensional) jet, while also a distinction can be made into horizontal or vertical jets.
For design purpose it suffices to calculate with the equilibrium scour depth, because the developing phase of the scour hole requires only a few hours. Generally applicable calculation methods are hardly available. These methods are based on the efflux velocity and the efflux opening, however, most of the methods are derived from small-scale experiments. Because of the lack of calculation methods it is recommended to carry out detailed studies for each particular design.

## Waves

The orbital velocities as a result of the wave conditions near a hydraulic structure can result in scour holes. Important parameters that influence the scour depth are the geometry of the structure, local water depth and wave reflection by the structure. Up to now hardly any quantitative

prediction formulas are available. Nevertheless, some simple equations are presented in order to enable for design purpose to determine approximately the maximum scour depth for pipelines, piles, seawalls, breakwaters and submerged structures.

Cohesive soils

Quantitative information about scour in cohesive sediments is scarce, because the erosion characteristics of cohesive sediments are not fully understand at the moment. This is due to the physico-chemical and mechanical properties of these sediments, of which probably the cohesion and the size of the particle diameter appear to be the most significant features. In addition, salinity, cation exchange capacity, pH-level, sodium adsorption ratio and the sand concentration also play a role.

Two approaches are presented which can be applied for design purpose although they result in indicative scour depth values only. Detailed designs require the determination of the scour resistance by laboratory or full-scale tests.

One calculation method is based on permissible nonscouring velocities which can be substituted in the scour formulas for noncohesive sediments. The other method enables to calculate the critical velocity using an equivalent particle diameter.

## 1.4 References

1.1 H.N.C. BREUSERS, AND A.J. RAUDKIVI
    Scouring, Hydr. Structures design manual no. 8,
    Published by the International Association for Hydraulic Research
    A.A. Balkema, Rotterdam, 1991

1.2 H.N.C. BREUSERS
    The time scale of two dimensional local scour
    Proc. 12th IAHR Congress, Fort Collins, United States, 3 pp. 275 -
    28, 1967

## 2. **Sills**

### 2.1  **Introduction**

In an estuary or a river a sill is often a part of a closure dam, which has to  be founded on a bed of alluvial material. Sometimes a sill is also used to reduce mixing of different types of water in an estuary. In an estuary a sill  has  to  be  designed  for flow in two directions: flood flow and ebb flow. In a river the flow over a sill  is  mostly  unidirectional.  And  in rivers  for  example  a  sill can be used to maintain a minimum water level upstream of the sill, or to protect a pipe line crossing, or to protect the foundation of a bridge.

The geometry of a sill can be schematized to some basic  types  of  layout: broad  and  sharp-crested sills, with and without a bed protection (section 2.2).  In a general description of the different flow  patterns  subcritical and  supercritical  flow have been distinguished (section 2.3). The failure mechanism induced by local scour near a sill is treated in section 2.4. The one-dimensional  calculation  formulas  of  the  maximum  scour  depths are summarised in section 2.5, which section  has  different  subsections.  The initial  slope  of  a  scour  hole  is  treated  also  in that section. The dimensions of the scour hole  depend  on  the  soil  type  (in  calculation methods  mostly  the  soil is supposed to be non-cohesive), the density $\rho_s$, the characteristic diameter $D_{50}$ and the  gradation  of  the  bed  material, mostly  sand.  Other  parameters  are  the contents of a scour hole and the downstream slope and the side slopes of a scour hole.
The  sedimentation  area downstream of a scour hole has not been dealt with in this manual.

The review and the analysis of the available formulas for the maximum scour depth and the initial slope have demonstrated some basic situations,  which are not covered by these formulas. Such situations are identified as future research topics, section 2.6. In the final section a list of references  is given, section 2.7.

## 2.2 Characteristic geometric parameters

A structure of a sill or a bar on a more or less horizontal bed in a canal, river or tidal channel can be characterised by the following geometric parameters (see figures 2.1 and 2.2):

- The height of the sill, $y_D$, is the vertical distance between the (horizontal) crest and the bed level.
- The width of the sill, L, measured at the base of the sill, at the elevation of the adjacent bed level.
- The slope $\beta_s$ of the downstream side slope of the sill; sometimes the downstream face is divided in sections with different slopes.
- The surface roughness of the sill is represented by the equivalent Nikuradse sand-roughness, $k_s$.

In principle, the height $y_D$ can vary along the axis of the sill. This variation is not treated in this manual.

The downstream, horizontal bed-protection is characterised by
- the length $L_p$, and
- the Nikuradse roughness $k_s$ of the surface of the bed protection.
- the edge of the bed protection:

    a constant or increased permeability at an edge, the edge perpendicular to the main flow direction or a more complex edge, and the flexibility of the edge of the bed protection. The edge of the bed protection can be equipped with reinforcements in estuaries to prevent the mattress of the bed protection to flap.

In general, an upstream bed protection does not have any influence on the local scour downstream of the sill, except if in a tidal region the direction of the flow changes regularly.

The following types of sills are distinguished, see figures 2.1 and 2.2:
- short-crested or broad-crested sills, and
- sills with or without a downstream bed protection.

In this manual schematized constructions will be considered with the axis of the sill perpendicular to the main flow direction, and the sill or bar is supposed to be impermeable. For the sake of simplicity only sills with a constant height along the sill axis will be considered, so the flow pattern

is basically two dimensional. The downstream bed protection is supposed to be schematized to a horizontal layer, if not specified. In a scale model this bed protection is often a rigid plate and in the prototype a flexible layer.


## 2.3  Characteristic flow pattern

The two-dimensional flow above a sill or a bar is characterised by an acceleration from upstream to a cross-section somewhere above the sill. First, the case is considered that the flow is still subcritical after this acceleration. Downstream this cross-section the flow will decelerate. Normally, the downstream side slope of a sill or dam is so steep that the flow separates and a bottom eddy will be generated. At the reattachment point the flow near the bottom is dominated by high turbulence intensities. From the reattachment point the flow approaches the normal uniform flow gradually.

If the sill is rather high relative to the upstream water-depth the flow can become supercritical just downstream of the sill. The supercritical flow will decelerate with an hydraulic jump. In an hydraulic jump very high relative turbulence intensities can be observed. However, downstream of a hydraulic jump the relative turbulence intensity near the bottom can be lower than in steady and uniform flow, (less than 5 % compared with 5 to 10 % in uniform and steady flow) according to Resh and Leutheusser lit.[2.28]. The hydraulic jump can be drowned just downstream of the sill. In that case normally a stilling basin is applied.

In general, a subcritical main flow induces in a two-dimensional scour hole a flow field, which is generally similar to that of a highly turbulent mixing zone. A weak return current is formed in an eddy near the bed in the most upstream part of the scour hole, this return current ends at a reattachment point, in general this point is also the point of maximum scour depth. In this region the flow is very turbulent, and large vortices erode and transport bed material intermittently.
Downstream of the deepest point of the scour hole the flow accelerates, the vertical velocity profiles return slowly to normal and the turbulence decreases (Breusers [2.4], Raudkivi [2.27], Pilarczyk [2.24]).

## 2.4 Failure mechanism

If the upstream slope of the scour hole exceeds a critical value, and if the depth of the scour hole and the volume of the scour hole have developed well, the risk for a soil mechanical failure becomes high. The following types of soil mechanical phenomena can be distinguished in the situation of a sill with an adjacent bed protection and a scour hole downstream of this bed protection:
- sliding
- flow slide

By sliding or flow slide a part of the bed protection will be lost, in an worse case even the stability of the sill will be endangered, (serviceability limit state) and a complete collapse of the structure can result: the ultimate limit state of the structure has been reached. In a sliding a coherent volume of the soil moves downward into the scour hole, along a sliding plane. In a flow slide a big volume of the non-cohesive soil ´verweekt´ and flows like a density current into the scour hole.

The susceptibility to a soil mechanical instability depends on the type of soil and on the groundwater flow, and an important parameter for these phenomena is the slope of the sliding plane [2.20]. Some examples of types of soils are:
- homogeneous fine sand,
- layers of fine, consolidated sand covered by a layer of coarse, unconsolidated sand.

From a detailed analysis of around 200 soil mechanical instabilities by sliding or flow slide in the fore shores in The Netherlands the criteria in table 2.1 have been deduced by Silvis [2.20]. From these 200 instabilities the locations with a rather homogeneous sand have been selected for the analysis.

| bulk density of fine sand | critical initial slope of scour hole | phenomena |
|---|---|---|
| very loose | 1 : 2.25 | flow slide |
| loose | 1 : 2.00 | flow slide |
| dense | 1 : 1.75 | sliding |
| very dense | 1 : 1.50 | sliding |

*Table 2.1 Critical initial slopes of a scour hole for soil mechanical instabilities.*

The criteria in table 2.1 are probably on the safe side. For the maintenance of the coastal protection system of dikes and dunes in The Netherlands the rule to strenghten the protection of the scour hole, if the initial slope becomes steeper than 1 : 3 has been applied successfully to prevent flow slide or sliding. The average width of the mentioned 200 soil mechanical instabilities is about 100 m.

In engineering practise the risk of a soil mechanical instability near the edge of a bed protection is taken into account in the design of a hydraulic structure, if the maximum scour depth is expected to become more than 5 m.

Measures to prevent a sliding or flow slide:
- densification of the subsoil to prevent flow slides, but this measure is very expensive,
- to increase the lenght of the bed protection by protecting the adjacent part of the scour hole,
- to end the bed protection with a falling apron of an imperfect filter construction,
- filling the scour holes with rubble to prevent soil sliding,

The load by the weight of the sill can create unfavourable sliding planes if the lenght of the bed protection is less than the height of the sill, lit.[2.20]. In general, the length of the bed protection is much more than the height of the sill, and therefore these sliding planes are in general not decisive for the design of a hydraulic structure.

The length of expected damage of the bed protection by a slide can be determined with a standard calculation method, as developed for example by Bishop, Fellenius or Spencer, lit.[2.20].
The length of the expected damage of the bed protection by a flow slide can be estimated by the following formula, see for more details Silvis [2.20]:

- Two dimensional schematization in which the length of the scour hole and forms no limitation in storage capacity for a flow slide, see figure 2.3:

$$L_s = 0.5 \ y_{s,max} \cdot \{ \ 16.3 \ - \cot g \ \beta \ \} - 4.35 \qquad (2.1)$$

in which:

$L_s$ = length of expected damage from the edge of the bed protection (m)

$\beta$ = initial slope of scour hole, see section 2.5.7 (degrees)

$Y_{s,max}$ = maximum scour depth (m)

This simple formula has been obtained by substituting default values for the parameters in the complete formula.

Formula (2.1) underestimates $L_s$ if flow slide has a more three dimensional character, e.g. flows sideways into the scour hole.

-Three dimensional schematization in which the length of the scour hole forms no limitation in storage capacity for a flow slide, figure 2.4. Silvis gives a formula for the calculation of $L_s$, but in that formula not all parameters are well defined. He has used the approach of Wilderom and this approach should be elaborated in more detail.

If the shape of the scour hole limits the storage capacity of the flow slide then the following formula has been developed by Silvis and also by de Graauw:

$$L_s = \frac{- e_s + [ e_s^2 + (16.3 - \cot g\ \beta - 2.e_s).0.5.\{ 1.09 + e_s\} ]^{0.5}}{16.3 - \cot g\ \beta - 2.\ e_s} \cdot y_{s,max}.$$

$$. 2.(16.3 - \cot g\ \beta) - 5.45\ y_{s,max} \qquad (2.2)$$

in which

$$e_s = 4.42\ .\ \sin(\beta - 3.5)\ .\ \sin(\beta + 3)\ .\ [\ \sin \beta^{-2}] \qquad (2.3)$$

Formulas (2.2) and (2.3) are obtained by substituting default values into the general formula. A same type of formula has been derived by de Graauw based on a less accurate schematization [ 2.10]. If the same default values are used, he found a very simple formula:

$$L_s = 16\ y_{s,max}$$

In engineering practise this criterion is only applied if the soil consists of fine, unconsolidated sand, and the storage capacity of the scour hole is unlimited. If this capacity is limited then $L_s = 10\ y_{s,max}$ for very deep scour holes and $L_s = 8\ y_{s,max}$ for rather shallow scour holes ($y_{s,max} < 40$ m).

If the soil is inhomogeneous no general rules or formulas are available for estimating the length of damage at the bed protection.


## 2.5  Calculation methods

### 2.5.1  Introduction

The development of a scour hole is a time dependent process, which results in an equilibrium scour hole after some time. This time dependent development of a scour hole is characterised by an increasing scour depth as a function of time (section 2.5.2). Some types of sills and flow patterns are sketched in figures 2.1 and 2.2.

A broad-crested sill with a horizontal bed protection:
The following conditions for the development of the maximum scour depth can be distinguished:
- clear-water scour of a non-cohesive sediment in a steady, subcritical flow, without supply of sediment (section 2.5.2),
- extension with upstream supply of sediment, $u_* > 2\ u_{*,cr}$, (section 2.5.3),
- extension with a non-steady flow, for example tidal flow (section 2.5.4),
- equilibrium maximum scour depth, (section 2.5.5).

A broad-crested sill without a bed protection and supercritical flow:
- equilibrium maximum scour depth (Bormann), (section 2.5.6) with clear water scour of a non-cohesive sediment in a steady, supercritical flow, a submerged jet and without upstream supply of sediment.

A short-crested spillway with a bed protection and supercritical flow:
- clear-water scour of a non-cohesive sediment in a steady flow downstream of a hydraulic jump, (Fahroudi and Smith, and Popova), (section 2.5.7).

Most attention has been paid to scour holes in non-cohesive sediments. In general, these scour holes have a bigger size than scour holes in consolidated cohesive sediments.

The initial upstream slope of the scour hole is treated in section 2.5.7. In this section a sill with a horizontal bed protection and subcritical flow is considered.

## 2.5.2    A broad-crested sill with bed protection, maximum scour depth

### 2.5.2.1    Breusers approach

The time development of a scour hole can be divided into the following phases:

1    initiation of the scour hole,
2    development of the scour hole,
3    stabilization of the scour hole, and
4    equilibrium shape of the scour hole.

The maximum scour depth in these 4 phases has been sketched in figure 2.5 (see Pilarzcyk 1984, lit.[2.24]).
In this section the formulas for the time dependent maximum scour depth are restricted to the development phase. Formulas for an approximation of the maximum scour depth in the equilibrium phase are treated in section 2.5.5.

In case of clear water scour observations in model investigations on two dimensional scour holes in various bed materials, due to different flow velocities, and different geometries of the sill and the bed protection, showed that for a given geometry, similarity of scour hole shape was satisfied by the functional relation according to Breusers [2.5]:

$$\frac{y_s(x,t)}{y_o} = f\left[\frac{t}{t_1}\right] \tag{2.4}$$

in which

$y_s(x,t)$    = maximum scour depth of a scour hole, measured from the
               original bed level                                      (m)
$y_o$         = water depth just upstream from the scour hole      (m)
$t$           = time                                              (hours)
$t_1$         = time at which $y_{s,max} = y_o$                    (hours)

In these model investigations sand, bakelite and polystyrene have been used as bed material. The density $\rho_s$ of these materials had the following values, see table 2.2:

| bed material | density $\rho_s$ |
|---|---|
| sand | 2650 kg/m³ |
| brown coal or lignite | 1370 kg/m³ |
| bakelite | 1350 kg/m³ |
| polystyrene | 1050 kg/m³ |

*Table 2.2 Density of bed materials*

In other model studies many other non-cohesive materials were used, as brown coal, see for example lit.[2.16]. Up to now no proved formulas to predict the maximum scour depths in cohesive materials are available. One of the reasons is the insufficient understanding of the complex erosion process of cohesive soils.

The maximum scour depth as a function of time was:

$$\frac{y_{s,max}}{y_o} = \{t_o/t_1\}^y \qquad (2.5)$$

in which $y$ = constant $\qquad\qquad$ (-)

Formula (2.5) has been fitted to the results of about 250 tests, see figure 2.6: $y = 0.38$. Dietz, lit.[2.16], analysed also the results of a systematic scale model study and he found $0.34 < y < 0.38$ with an average value of 0.36. The difference between these values is so small that Dietz's results can be considered as a confirmation of the Breusers's results. It is recommended to use $y = 0.38$, and for engineering practice the value of $y$ is often rounded off to 0.4.

In all two-dimensional tests with clear water scour an equilibrium scour hole was never observed accurately, because in these type of tests an equilibrium is reached after a rather long time.
The characteristic time $t_1$ was expressed, on the basis of more than 250 tests with a hydraulic smooth, medium and rough bed protection, as analysed by Breusers and others, see figure 2.7:

$$t_1 = 250 \cdot \Delta^{1.7} \cdot y_o^2 \cdot \left[ \alpha \, \bar{U} - \bar{U}_{cr} \right]^{-4.3} \qquad (2.6)$$

in which:

$t_1$      =   time at which $y_{s,max} = y_o$                      (hours)

$\Delta$      =   relative density,

           $(\rho_s - \rho) / (\rho)$                                  (-)

$\rho_s$      = density of bed material                    (kg/m³)

$\rho$      = density of water                           (kg/m³)

$\alpha$      = a flow factor, which depends on the geometry or on the    (-)
           relative turbulence intensity

$\bar{U}$      = average velocity at end of bed protection (x = 0)      (m/s)

$\bar{U}_{cr}$      = critical mean velocity evaluated from Shields' curve      (m/s)

For geometries, which have an hydraulically rough bed protection, like the bed protection of the Eastern Scheldt Storm Surge Barrier, the constant 250 can be replaced by 330. From the analysis of 150 to 200 tests in a scale model the accuracy of the calculated $t_1$ has been determined at a relative standard deviation of 31 %., see de Graauw, lit.[2.10]. The accuracy of the calculated scour depth, which has been compared with the prototype scour depth in the Eastern Scheldt Storm Surge barrier, is characterised by a relative standard deviation of 10 %, see de Graauw, lit[2.11] and Driegen, lit.[2.14]. Most differences between the calculated and the measured scour depths in the hindcast calculations can be explained by the assumed critical flow velocity for the initiation of motion of clay layers.

The maximum flow velocity $\hat{u} = \alpha \cdot \bar{U}$ in formula (2.6) determines the emperical factor $\alpha$. The value of this factor is a function of geometric parameters, see section 2.5.2.3. In a more detailed approach this factor seems to be a simple function of the relative turbulence intensity, see section 2.5.2.4. In a next step it is supposed that this relative turbulence intensity is a function of geometric parameters of the structure. This relationship is under development now and for engineering practise the formulas with the empirical $\alpha$-coefficient are recommended.


## 2.5.2.2    The critical velocity

The characteristic time $t_1$ depends according to formula (2.6) also on a critical velocity of the bed material. In this section the method to calculate this critical velocity is described.

The critical velocity of non-cohesive bed material is determined by the Shields-parameter $\psi$, which depends on the Reynolds number $Re_*$, see figure 2.8:

$$\psi_{cr} = U_{cr}{}^2/\{C^2 \cdot \Delta \cdot D\} \tag{2.7}$$

in which

| | | |
|---|---|---|
| C | = Chezy-coefficient | $(m^{0.5}/s)$ |
| $\Delta$ | = relative density of the bed material | (-) |
| D | = representative diameter of the bed material $D_{50}$ | (m) |

The Reynolds number $Re_*$ is defined as:

$$Re_* = U_* \cdot D/\nu \tag{2.8}$$

in which the shear stress velocity is defined as:

$$U_* = (\tau/\rho)^{0.5} \tag{2.9}$$

and

| | | |
|---|---|---|
| $u_{*,cr}$ | = critical shear stress velocity | (m/s) |
| $\rho$ | = density of water | $(kg/m^3)$ |
| $\nu$ | = kinematic viscosity | $(m^2/s)$ |

In the first phase of the systematic research on scouring by DHL the initiation of movement of a bed material has been studied in detail, [2.8]. The initiation of movement has been described by seven qualitative criteria. For the determination of $U_{cr}$ a criterium has been selected, which can be described as the grains move permanent and on every place of the bed, see figure 2.8, dashed line number 5 and 6.

If $D_{50}$ is known of the bed material, then from the Shields graph and criterium 5 or 6 in figure 2.8 $\psi_{cr}$ can be determined. The critical velocity can be calculated from (2.7) if the Chezy-coefficient has been determined for example from the Colebrook-White formula:

$$C = 18 \log \left\{ \frac{12. R_0}{k_s + 0.3 \delta_y} \right\} \tag{2.10}$$

in which

$k_s$ = hydraulic roughness, according to Nikuradse (m)

$\delta_y$ = thickness of the viscous sublayer (m)

$R_0$ = hydraulic radius (m)

The thickness of the viscous sublayer can be estimated with:

$$\delta_y = 11.6 \cdot \nu/U_* \qquad (2.11)$$

The hydraulic radius follows from the wetted cross-section divided by the wetted perimeter.

An important assumption for hydraulic roughness of the bed is $k_s = D_{50}$ of a rather uniform bed material. In the systematic research on scouring all critical velocities have been determined with this assumption. In many prototype situations the physical value of the critical flow velocity will deviate from the calculated value, see appendix 2. Therefore the following values are recommended:

$k_s = 2\ D_{50}$ for a horizontal bed protection, build in a laboratory,

$k_s = 3\ D_{90}$ for a prototype bed protection.

Further, it is recommended to investigate the consequences of these estimations of the hydraulic roughness on the critical flow velocity.

### 2.5.2.3 The factor α as a function of the geometry

The factor α is a function of the geometry of a sill, which is characterized by the relative sill height parameter $y_d/y_0$ and the dimensionless length of the bed protection $L_p/y_0$ ($y_d$ = height of a sill, $y_0$ = water depth, and $L_p$ = lenght of the bed protection). The results, which are presented in graph 2.9, are based on tests in the systematic series [2.8]) with a moderate rough and rough bed protection and sill with $k_s = 0.025\ y_0$ and $k_s = 0.05\ y_0$. From the graph in figure 2.9 the following relation has been deduced:

$$\alpha = 1.5 + 5\ (y_D/y_0)^2 \cdot e^{-0.02 \cdot (y_D/y_0)} \cdot (L_p/y_0)^{1.5} \qquad (2.12)$$

This formula is valid if $y_D/y_0 < 0.8$, and a hydraulic rough bed protection. If $y_D/y_0 > 0.8$ formula (2.12) calculates a too high value of $\alpha$, probably because a very high sill causes a reduction of the discharge, which passes the sill.

If a sill is combined with a horizontal constriction $B_s/B = 0.1$ ($B_s$ = length of the abutment and B = width of the upstream flow) and a vertical head ( or face) of this constriction, then a three dimensional scour hole due to the induced vortex street will develop and $\alpha$ follows from (2.13). If $y_D/y_0 < 0.8$ and a hydraulic rough bed protection:

$$\alpha = 1.5 + \{2.6 + 18.6 \ (y_D/y_0)^2\} \ . \ e^{- \ 0.045 \ L_p/y_0} \qquad (2.13)$$

Formulas (2.12) and (2.13) are both presented in figure 2.10, from which follows that in a given situation of a sill with abutments the three dimensional scour holes have much higher values of $\alpha$ than the value of $\alpha$ for the twodimensional scour holes. It is mentioned that the formulas (2.12) and (2.13) are based on an analysis in which y = 0.38. It is recommended to compare (2.12) or (2.13) with the results, which have been published by Dietz (1969) and with the results of DHL-report M1533 part III with a fixed and a flexible bed protection. It is also recommended to reanalyse the threedimensional scour holes with a variable y, as has been done in the analysis of the threedimensional scour holes near spur dikes.

For a smooth sill, $y_D/y_0 > 0.1$ and/or an hydraulic smooth bed protection with $k_s$ very small, $\alpha$ according to (2.12) should be increased, see also table 2.3:

$$\alpha_{smooth} = \alpha_{rough} + 0.3 \qquad (2.14)$$

in which $\alpha_{rough}$ follows from (2.12). For some background information concerning an older formula refer is made to appendix 3.

For a two-dimensional scour hole indicative values for $\alpha$ including effects of turbulence and velocity profile are listed in table 2.3, according to Breusers and Raudkivi, lit.[6]. These results have been based mainly on a systematic investigation on scour holes.

| $\dfrac{y_D}{y_o}$ | $\dfrac{L_p}{y_o}$ | $\alpha$ | |
|---|---|---|---|
| | | Bed protection | |
| | | Smooth | Rough |
| 0 | 10 | 2.0 | 1.5 |
| 0.3 | 1 to 15 | 2.5 | 2.0 |
| 0.6 | 3 | 3.2 | 3.0 |
| 0.6 | 10 | 2.9 | 2.5 |

*Table 2.3  α as a function of the relative sill height and the length of*
*the bed protection and the roughness of the bed protection and*
*the sill.*

Note: "rough" means that the roughness/depth ratios are greater than 0.02.
A rough bed protection reduces the rate of scouring by modifying the
velocity districbution at x = 0. Increasing the sill height results in
greater turbulence, a greater distortion of the velocity profile, and
consequently a greater value of α up to $y_D/y_0$ = 0.7 to 0.8. It is mentioned
that some of the values of alfa in table 2.3 are somewhat lower than the
values of alfa, which are calculated with formula (2.12).

## 2.5.2.4    α as a function of the turbulence

An alternative approach is to relate α to the relative turbulence intensity
of the main flow. In general the rate of turbulence is enlarged by an
hydraulic structure. Over the length of the bed protection this turbulence
is reduced by dissipation of turbulent energy.
For predicting scour downstream of a rough riprap type bed protection α was
related to the average relative turbulence intensity r.

Recently Jorissen and Vrijling [2.23] have analysed a relation between a
local value of α and the turbulence intensity. This relation has been
based on measurements in a two- and a three-dimensional flow pattern and in
this relation U has been replaced by $U_1$, which is the local depth average
velocity  at the downstream end of the bed protection. The relation between
α and $\alpha_1$ is:

$$\alpha \cdot U = \alpha_1 \cdot U_1 \qquad (2.15)$$

They found the following relation:

$$\alpha_1 = 1.5 + 5 \cdot r \qquad (2.16)$$

if $r > 0.07$ and $\alpha_1 > 1.8$.
In (2.16) the relative turbulence intensity, $r$, has been defined by:

$$r = u'/U, \qquad (2.17)$$

in which
$U$ = time averaged flow velocity $\qquad$ (m/s)
$u'$ = the depth average value of the root mean square value of the turbulent
velocity fluctuations in the main flow direction $\quad$ (m/s)

This velocity fluctuation is defined by:

$$u' = \sqrt{\overline{(u'_x)^2}} \qquad (2.18)$$

in which
$u'_x$ = velocity fluctuation in the x-direction $\qquad$ (m/s)

and $U = Q/(y_0 \cdot B)$, which means that $U$ is the depth averaged flow velocity
in the x-direction.

If a formula of this type (2.16) or one of the other formula, which are
treated in appendix 4, is accepted, then the next step should be the
determination of the turbulence intensity as a function of the main
geometric parameters.

2.5.2.5    The factor $\alpha$ along the width of the canal or river

The structures can be divided into temporarely structures, for example
during the closure of a river branch or a tidal channel, and permanent
structures.

The main methods of a closure can be classified in three groups:

- A vertical constriction with an increasing sill height during the construction period. The factor $\alpha$ can be estimated by the formulas for a two-dimensional scour hole.

- A horizontal closure with increasing the lengths of a horizontal constriction from both banks during the construction period. The factor $\alpha$ of the local scour holes around the head of the horizontal constriction can be estimated by the formulas for a three dimensional scour hole near a spur dike, see chapter 3. If the width of the horizontal constriction is considerable, then the constriction scour can not be neglected in all cases.

- A combination of a vertical and a horizontal constriction. If $B_s/B = 0.1$ then the formula for estimating $\alpha$ near an abutment on a sill can be applied. It is recommended to select by engineering judment the dominant aspect (vertical or horizontal closure) and to apply the formulas for this dominant aspect. It is recommended to develop also formulas for estimating $\alpha$ in all combinations of a vertical and a horizontal constriction.

A vertical closure with a sill is combined often with two abutments near the existing banks of the channel or river. Without abutments the main flow has no eddies with vertical axes and the factor $\alpha$ has a constant value along the downstream end of the bed protection, see figure 2.12.

In a river bend the local scour holes should be combined with socalled bend scour, which generates the typical river cross sections in a bend.

A vertical closure with abutments or a horizontal closure generates a flow pattern with two vortex streets downstream of the separation point on the head of the horizontal constriction, see figure 2.12 according to de Graauw, lit.[2.20]. The ´extrusion´ of the vortex street, which depends on the flow field, determines where along the downward edge of the bed protection the highest values of $\alpha$ can be expected. A rough estimation of angle of ´extrusion´ is:

| low sill | $y_D/y_0 < 0.3$ | angle < 1:1 to 1:2 |
| high sill | $0.3 < y_D/y_0 < 0.6 < 0.6$ | angle = 1:1 to 1:2 |

With spurdikes on one bank this angle can become negative also! More detailed information about the flow field can be obtained from mathematical or scale models.

In this section and the foregoing sections it is supposed that during all construction stages of the closure the main flow is sub-critical, therefore the Froude number is smaller than 1. In an estuary this will be often the case, but in a closure of a river branch super critical flow is possible.

### 2.5.3  Supply of sediment from upstream

The theory in the foregoing sections has been based mainly on the results of physical scale models, in which the upstream supply of sediment is normally absent. However in the prototype a supply of sediment from upstream of the scour hole can be observed in most cases. This supply of sediment will reduce the development of a scour hole, because a part of the sediment transport capacity of the flow has already been used for this upstream supply and is not available for the transport of sediment from the scour hole. An approximate calculation method for this reduction is treated in the following.

The contents of a scour hole can be expressed by:

$$I(t) = b \cdot y_{s,max}^2(t) \tag{2.19}$$

in which

$I(t)$   = size of a scour hole below the original bed level
          = and with a width of 1 m                                    ($m^2$)
$b$       = shape factor of the scour hole                             ($-$)
$y_{s,max}(t)$ = maximum scour depth                                    ($m$)

The contents of a scour hole depends on the time from the beginning of the development of a scour hole.

The upstream sediment supply, $q_s$, is defined as the volume of the sediment particles including the porosity per m width and per unit of time (hours, or seconds). The contents of the scour hole is reduced by $q_s$:

$$I_{red}(t) = I(t) - q_s \cdot t \tag{2.20}$$

in which

q$_s$ = sediment transport per m width           (m³/(m.s) or m³/(m.hour))
t   = time                                        (s or hour)
I$_{red}$= reduced contents of a scour hole       (m²)

If t is expressed in days then also q$_s$ should be expressed in m³/(m.day).
The substitution of (2.19) in the latest formula (2.20) results in:

$$y_{max, red} = [y_{max}(t)^2 - q_s \cdot t/b]^{0.5} \qquad (2.21)$$

This formula cannot be applied in case of an initial scour hole, which has
a content of I(0) and which has been developed earlier under different
flow conditions. Then the following approximation should be used, see DHL-
report M1657 by Driegen, lit.[2.13]:

$$(\frac{d I,red}{d t}) = (\frac{d I}{d t}) - q_s \qquad (2.22)$$

It is recommended to apply formula (2.22) at different moments with the
same content I of the scour hole. The advantage is that then the initial
scour hole has no influence on the calculation of the reduced scour hole.
As a consequence it is difficult to fix the absolute time of the scour
process with this formula, this is illustrated in figure 2.13.

The value of q$_s$(t) can determined in different ways:
- calculations, based on sediment transport theories,
- direct prototype measurements, or
- from the substitution of y$_{max}$, which is measured in a model test
  without sediment supply, and y$_{max, red}$, which is measured in the
  prototype, in (2.21), in an early construction phase.

The latest method has been applied succesfully during the construction of
the Eastern Scheldt Storm Surge Barrier, see lit. [2.14]. In this
application q$_s$ has been calculated from (2.21) in different cross sections
in a closure gap, and it was necessary to determine a smoothed distribution
of q$_s$ along the end of the bed protection.
In the final stages of the construction of the Eastern Scheldt Storm Surge
Barrier (2.22) has been applied successfully.

## 2.5.4 Non-steady flow

In general, a scour hole will develop under non-steady flow conditions and therefore, an extension has been elaborated of the treated formulas for steady flow conditions to unsteady flow conditions.

Formula (2.3) can be written as:

$$\frac{y_{max}(t)}{y_0(0)} = f\ (t/t_{1,unsteady}) \qquad (2.23)$$

in which $y_0(0)$ = average original water depth         (m)

And $t_{1,unsteady}$ is defined as:

$$t_{1,unsteady} = 250\ .\ \Delta^{1.7}\ .\ y_0(0)/x \qquad (2.24)$$

in which

$$x = \frac{1}{T}\ \int_{T_1}^{T_2} (\alpha\ .\ U(t) - U_{cr})^{4.3}/y_0(t)\ \ dt \qquad (2.25)$$

in which

T    period of unsteady flow                                              (s,day)

$T_1$    begin of this period, at the moment $\alpha\ .\ U - U_{cr}$ changes
      from positive to negative or opposite from negative to positive
                                                                           (s,day)

$T_2$    end of this period, at the moment $\alpha\ .\ U - U_{cr}$ changes from negative
      to positive or opposite                                             (s,day)

In formulas (2.24) and (2.25) $y_0(t)$ and $U(t)$ are the only variables which depend on the time. If $y_0(t)$ and $U(t)$ are given as a function of time, then $t_{1,unsteady}$ can be calculated by numerical integration. In tidal areas with a dominant tidal period of 12 hours a time step of 0.5 hour is recommended for the numerical integration.

In rather deep water the variations in $y_0(t)$ are limited as a percentage of $y_0$. However the variations in $u(t)$ can be quite important.

In tidal areas the following aspects should be studied:

- the frequency distribution of this tide-difference,
  and the relation between tide-difference - average flow velocity $u_{max}$
  during a tide,

or

- the frequency distribution of the discharge, and the relation between
  discharge - average flow velocity,
- the effects of a series of tides on the development of a scour hole.

or

- the effect of one tide schematized with a constant flow velocity.

These relations have been tested in the prototype verification in the Brouwersluis, see figure 2.14.

An example is given of a tidal motion in which the velocity varies as a sine function:

$$U = U_{max} \cdot \sin (\omega \cdot t) \qquad\qquad (2.26)$$

in which

$\omega \quad = 2\ \pi/T$ $\qquad\qquad$ (s-1)

$U_{max}$ = maximum flow velocity during a tide $\qquad$ (m/s)

Formula (2.26) has been substituted in a simple sediment transport formula:

$$S = a_1 \cdot U^{b}1 \qquad\qquad (2.27)$$

in which $a_1$ and $b_1$ are constants.

As a first estimation it is assumed $b_1 = 4$ to 5. This results in, as shown by de Graauw, $U_{scour} = 0.8\ U_{max}$ and $U_{scour}$ is almost independent from the type of sediment transport formula.

### 2.5.5 Equilibrium maximum scour depth

After some time a scour hole will reach an equilibrium shape and the maximum scour depth will obtain a constant value. In terms of the classification of different phases in the development of a scour hole, see section 2.5.2, this equilibrium defines phase 4, see figure 2.5. In scale model tests with alluvial sand and clear water scour it will take sometimes a long time before this equilibrium is reached, see for example figure

2.15.  Therefore,  the definition of equilibrium maximum scour depth is not always clear in the reports of scale model tests with clear water scour. In general,  in  a  prototype some upstream supply of sediment, $q_s$, exists, by which this equilibrium will be reached in a relatively short time.

In  case  of  clear water scour a first estimation of the equilibrium scour depth in a scour hole near a sill with a bed  protection  can  be  obtained with (according to Dietz, [2.16], see also figure 2.16):

$$\frac{y_{max,e}}{y_0} = \{U_{max} - U_{cr}\}/U_{cr} \qquad (2.28)$$

in which $U_{max} = c \cdot \alpha \cdot \bar{U}$

$c$ = coefficient $\qquad (-)$

It can be concluded from appendix 5 that $c$ is also a function of time: during the development phase of the scouring process:  $c$ = 0.4 to  0.5  and in the final phase of equilibrium scour depth:  $c$ = 1.

The first applications of (2.28)  on  prototype  situations  indicate  that (2.28)  gives  reasonable  results  if  $\alpha$  is  relatively  small,  as first estimation $\alpha < 3$.

In  case  of  upstream  supply  of  sediment  (2.28)  calculates  too  deep equilibrium scour depths. No proved calculation  method  is  available  for this  situation.  A  tentative formula has been suggested by de Graauw, see appendix 5.

### Broad-crested  sill without a bed protection, supercritical flow, submerged jet

For  a  sill  without  a bed protection, as can be observed many times with grade control structures, the equilibrium scour  depth  can  be  calculated with  the  formulas of Bormann, [2.1] and [2.2]. The flow downstream of the sill is like a diving submerged jet with a drowned hydraulic jump.  At  the edge  of  the  sill the main flow separates from the downstream face of the sill, where a small eddy is generated.

The  path of the jet through the tailwater is characterized by the angle of impingement, angle $\beta'$, at the sediment boundary in case of a submerged jet. For  a  free  jet  angle  $\beta'$ is considered to be equal to the angle the jet makes with the tailwater surface. The angle  $\beta'$,  can  be  calculated  with (2.29), see definition sketch in figure 2.17 or 2.2.

$$\beta' = 0.15 \cdot \ln\{(y_D + Y_t)/Y_t\} + 0.13 \cdot \ln\{Y_0/Y_t\}$$

$$+ 0.136 \cdot \sin(\lambda) - 0.05 \cdot \ln\{U_t/(g \cdot Y_t)^{0.5}\} \qquad (2.29)$$

in which

| | | |
|---|---|---|
| $y_D$ | = height of the sill, or vertical distance between the crest of the sill to the original bed level in the tailwater | (m) |
| $Y_0$ | = water depth at the tailwater | (m) |
| $Y_t$ | = local water depth at the downstream crest of the sill | (m) |
| $U_t$ | = average flow velocity at the downstream end of the crest of the sill | (m/s) |
| $\beta'$ | = angle a free jet makes with tailwater surface, measured from the horizontal | (radians) |
| $\lambda$ | = angle of the downstream face of the sill, measured downward from horizontal | (degrees, or radians)) |

The prediction of angle $\beta'$ for a submerged jet is made with a mean square error of approximately 5 degrees.

The maximum scour depth is calculated with (2.30):

$$c_2 = C_d^2 \cdot K^{-1} \cdot g^{-1} \cdot \Delta^{-1} \cdot U_t^2 \cdot Y_t^1 \cdot Y_b^{0.5} \cdot D_{90}^{-1.5} \cdot \frac{\sin\beta' \cdot \tan\lambda}{\cos\lambda \cdot c_3}$$

$$c3 = \tan\phi + \tan\lambda$$

$$y_{s,max} = c_2 - y_D \qquad (2.30)$$

in which:

| | | |
|---|---|---|
| $C_d$ | = diffusion constant for inlet conditions | (-) |
| K | = coefficient, K = 2.3 | (-) |
| $\phi$ | = angle of repose of a submerged sediment particle | (degrees) |

Some recommended values of $C_d$ are:

| condition | $C_d$ |
|---|---|
| flow over a crest | 1.8 |
| an average nozzle | 2.0 |
| a well formed nozzle | 2.3 |

Bormann used $\phi$ = 25 degrees for all cases in the verification of these formulas. Therefore this value is recommended.

The calculated scour depths have been compared with the some measurements published by Tarapore, Rajaratnam, Yuen and Akashi and Saitou, in total more then 200 test-results have been used. The results show deviations up to + 100 % and - 90 % from the calculated values, which vary between 0.03 to 2.5 m, see figure 2.18. In around 30 % of the test negative scour depths have been calculated. Because this is impossible, the results of these tests were omitted in the final verification. In these tests a maximum scour depth has been observed up to 2.5 m, which is almost a prototype value. Therefore with the application of this formula no severe scale effects should be expected.

It is recommended to estimate the equilibrium scour depth by a submerged jet with the formulas of Bormann, if $U_{max} \gg U_c$, else the formula (2.28) of Dietz should be considered as a first approximation.

## 2.5.6   Short-crested spillway/sill, with bed protection

The scouring process downstream of a hydraulic jump has been studied by Fahroudi and Smith,[2.17 [2.18]. The hydraulic jump was created by a flow directed over a standard ogee crest and then down a glacis on to a horizontal apron. The crest can be considered as a special case of a sharp crested sill. The length of the apron was about equal to the length of the hydraulic jump. A plain apron without appurtenances was used, see the sketch in figure 2.19. Three tailwater categories were tested: a drowned hydraulic jump, a balanced hydraulic jump and a downstream moved hydraulic jump.

The formula, which was tested to determine the maximum scour depth, is the same as Breusers had used:

$$y_{s,max}/y_0 = (t/t_1)^y \tag{2.5}$$

From the measurements the value of the exponent y in formula (2.2) has been determined: y = 0.19 rounded off to 0.2, see figure 2.19. This value was scarcely affected by the tailwater conditions.

$$t_1 = 110 \cdot \Delta^{1.4} \cdot Fr^{0.9} \cdot [U_{max} - U_{cr}]^{-3} \tag{2.31}$$

in which

Δ     = relative density                                    (-)
Fr    = Froude number based on U, y and g
        just upstream of the hydraulic jump                  (-)

$$U_{max} = c_v \ (1 + 3 \ . \ r') \ U_{ave} \qquad\qquad (2.32)$$

in which

$c_v$     = emperical velocity distribution coefficient   (-)
$r'$      = mean relative turbulence intensity             (-)
$U_{ave}$ = mean velocity at the end of the protective apron   (m/s)

This formula for $t_1$ shows some similarity with the formula (2.6) of Breusers, in which however $y_0$ is replaced by a Froude number. The value of the constant, 110, has been estimated from the published graphs in lit.[2.17]. This formula can be applied for the situation with a balanced tailwater. No information is given about the value of $c_v$, and therefore as a first approximation $c_v = 1$ is recommended.
The presentation of the results in the papers by Fahroudi and Smith suggests that these formulas (2.31) and (2.32) should be considered as preliminary results, which need further confirmation.

For the prediction of the time dependent development of the maximum scour depth in medium or fine sands just under an hydraulic jump or a relatively short bed protection Popova, lit.[2.25], proposed an empirical formula:

$$y_{s,max} = -\frac{U_{max} \ . \ y_{cr}}{U_{cr}} \ \{0.33 \ \log \frac{U_{max} \ . \ t}{y} - 1 \} \qquad\qquad (2.33)$$

in which

$U_{max} = U_{ave} + 3 \ . \ r$                (m/s)
$y_{cr}$ = critical water depth                 (m)
$y$      = maximum scour depth                  (m)
 s,max
$r$      = relative turbulence intensity        (-)

The critical flow velocity, $U,_{cr}$, should be calculated with Goncharov's formula:

$$U,cr = \{ 1.14 \ . \ g \ . \ delta \ . \ D50 \}^{0.5} \ . \ \log \{ \frac{8.8 \ . \ h}{D_{50}} \} \qquad\qquad (2.34)$$

Formula (2.33) is valid for:

$4 < t < 200$ hours, $\quad 30,000 \leq U_{max} \cdot t/y \leq 3,000,000$

$0.05 \leq r/U \leq 0.5, \quad 0.05 \leq U \cdot U/(g \cdot y) \leq 0.31$

Blazejewski, lit.[2.3], has presented the results of the verification of (2.33) on the data of Dabkowski, Skibinski and Zbikowski of local scour depth under an hydraulic jump and in non-cohesive sand with $D_{50} = 0.400$ mm. In this verification (2.33) underestimated the measured scour depth 0 to 30 %. It is recommended to test the new formula of Blazejewski, because that formula performs good in this verification.

Below an hydraulic jump the Breusers formula underestimates the maximum scour depth (the calculated scour depth is only 10 to 30 % of the measured scour depth), therefore Popova's formula can be recommended in these situations.


## 2.5.7  Initial slope of a scour hole

The initial slope of a scour hole is a characteristic parameter, which determines also the stability of the upstream part of the scour hole and the adjacent part of the structure, that is the bed protection, see section 2.4 on the soil mechanical stability.

The results of the measured initial slope $\beta$ according to the definition in figure 2.20 in the systematic tests of DELFT HYDRAULICS, [2.9] are presented as a function of the geometric parameters $L_p/y_0$ and the sill height $y_D/y_0$, see figures 2.21 and 2.22. From these figures it seems that in a mainly two-dimensional flow along a sill with a bed protection:

$$
\begin{array}{ll}
2.4 < \cot \beta < 4.0 & \text{if } L_p/y_0 > 4 \text{ and} \\
& \text{if } y_D/y_0 > 0.4, \\
4.0 < \cot \beta < 7.5 & \text{if } L_p/y_0 < 4 \text{ and} \\
& \text{if } y_D/y_0 < 0.4.
\end{array}
$$

- These values can be compared with the results of Dietz [2.16]:

$$
\begin{array}{ll}
3.8 < \cot \beta < 4.4 & \text{if } L_p/y_0 > 8 \text{ and} \\
& \text{if } y_D/y_0 > 0.4, \\
4.0 < \cot \beta < 5.2 & \text{if } L_p/y_0 < 8 \text{ and} \\
& \text{if } y_D/y_0 < 0.4
\end{array}
$$

With a bed protection which is inclined in the direction of the flow: (Dietz, [2.16]):

$3.8 < \cot \beta < 5.0$   if $L_p/y_0 > 8$

Therefore, an inclined bed protection has no significant influence on the initial slope, if compared with a horizontal bed protection.

These results of Dietz confirm the mentioned general tendency, which is observed in the systematic test serie of Delft Hydraulics.

- In case of clear water scour the angle $\beta$ of the most upstream slope of the scour hole with a horizontal, can be estimated with a tentative relationship (de Graauw, [2.20]):

$$\cot \beta = 2.3 + (\alpha - 1.3)^{-1} \quad \text{for } \alpha > 1.5 \qquad (2.36)$$

in which

$\beta$ = initial slope of a scour hole, measured with the horizontal, see figure 2.20 (degrees)

$\alpha$ = a flow parameter to in Breusers scour formula, to determine the maximum flow velocity (-)

If $5.10^{-6} < W \cdot D < 1.2 \cdot 10^{-4}$ with W = fall velocity of the sediment particles (m/s) and D = mean diameter of bottom material (m), then the accuracy of $\beta$ calculated with (2.36) is expressed in a relative standard deviation of 20% from the comparison with the measured slopes in the systematic test series [2.9].

A smooth bed protection results in a steeper initial uptream slope because the higher velocities near the bed have more momentum and cause a more rapid expansion of the flow in the scour hole. This tendency is illustrated by Dietz, who presented a graph with $\cot \beta$ as a function of $k_s/y_0$ in which $k_s$ is the roughness according to Nikuradse, see figure 2.23 [2.16]: if $k_s/y_0 > 0.01$ then $\cot \beta$ does not depend on $k_s$.

If only a very short section downstream of the sill is protected, the strong eddy generated by the sill structure transports material back towards the sill and a flatter slope results. Intermediate values of $L_p/y_o$ are associated with steeper slopes because the protection ends approximately where the eddy terminates, and consequently large scale turbulence attacks the first part of the scour hole.

Equation (2.36) is a simplification from the original formula: which should be applied if $W.D < 5.10^{-6}$ and $W.D > 1.2 . 10^{-4}$ and in case of clear water scour [2.11][2.24]:

$$\cot \beta = 5.5 . W/D . \{\frac{\nu}{\Delta^2 g^2}\}^{0.33} [2.5 + 0.75/(\alpha - 1.32)]$$

$$(2.37)$$

in which

| | | |
|---|---|---|
| D | mean diameter of bottom material | (m) |
| $\nu$ | kinematic viscosity | (m²/s) |
| $\Delta$ | relative density | (-) |
| g | acceleration due to gravity | (m/s²) |
| w | fall velocity of bottom material | (m/s) |

The accuracy of the initial slope calculated with (2.37) is expressed in a relative standard deviation of 19 % from the comparison with the measured slopes in the systematic test series lit. [2.8].

If $5.10^{-6} < W.D < 1.2 . 10^{-4}$ then $W/(D . \Delta^{0.67}) = 90$ . This constant value has been substituted in formula (2.37) to derive (2.36).

For a first approximation, if no data about alfa is available, or in a situation with considerable supply of sediment from upstream, the following schematized values can be used, see de Graauw, lit.[2.20]:

| situation | initial slope of a scour hole | downstream slope of a scour hole |
|---|---|---|
| clear water scour | 1 : 2 | 1 : 8 |
| supply of sediment from upstream | 1 : 4 | 1 : 40 |

If required for a special project, these estimations of the initial and downstream slopes can be improved with the results of a scale model investigation.

Three dimensional case:

Initial slopes in three-dimensional situations are generally much steeper, than calculated with (2.36) and (2.37), as has been measured in a prototype test in the Brouwerssluis, see figure 2.24 [2.12]. A problem for a good comparison of the initial slopes in the scale model and in the prototype is the fixed bed protection, which does not represent in a scale model the flexible bed protection, which can follow settlements of the subsoil in the prototype.

A formula for the calculation of $\beta$ in a three-dimensional case is missing. Only measurements in a scale model are available.
Initial slopes measured along a flow line through the point of maximum scour depth are generally steeper than for the two-dimensional case due to the erosive action of vortices with vertical axis.


## 2.6 Research needs

Review of the distinguished cases covered by the presented formulas:

broad-crested weir - with bed protection - subcritical flow.
   The time dependent development (with and without sediment supply) of
   the maximum scour depth can be calcutated with the Breusers approach.
   The equilibrium scour depths can be estimated with the formulas of
   Dietz and Zanke.

broad-crested weir - without bed protection - subcritical flow
   The Breusers method can be applied.

sharp-crested weir - with bed protection - supercritical flow.
   The maximum time dependent scour depth can be calculated with the
   Fahroudi and Smith formulas, and the Popova formule..

sharp-crested weir - without bed protection - supercritical flow
   equilibrium scour depths, without upstream sediment supply,
      Bormann formula. The maximum equilibrium scour depth can be calculated
      with the Bormann-formula.

      missing: time development of geometric maximum scour depth

A general description of specific research needs:

a1  the relation between the scour depth and sediment transport formula especially in case of upstream supply of sediment, improvement of the reduction method.

a2  equilibrium formulas of Bormann can be extended with upstream supply of sediment

b   extension of the formula $\alpha$ as a function of the relative turbulence intensity to a hydraulic jump

c   extension of the Bormann formulas for equilibrium scour depth to the two dimensional case with and without a sill and with a bed protection (Breusers formula)-and comparison with the formula of Dietz and Zanke.

d   extension of the formula for the initial slope for the case of three-dimensional flow.

## 2.7  References

2.1   BORMANN, N.C.
      Equilibrium local scour downstream of grade-control structures
      Colorado State University, Fort Collins, Colorado, United States, 1988

2.2   BORMANN, N.C.
      Predicting local scour for design of hydraulic structures in alluvial channels
      in Design of hydraulic structures 89
      A.A. Balkema, Rotterdam, 1989

2.3   BLAZEJEWSKI, R.
      Time evolution of two-dimensional local scour in cohesionless bed material below a horizontal apron

2.4    BREUSERS, H.N.C.
       Conformity and time scale in two-dimensional
       local scour.
       Proc.Symp. on model and prototype conformity,
       Hydr. Res. Lab., Poona, India, 1966, pp. 1-8


2.5    BREUSERS, H.N.C.
       Time scale of two-dimensional local scour,
       Proc. 12th IAHR Congress Ft. Collins, 3, 1967, pp. 275-282


2.6    BREUSERS, H.N.C. AND A.J. RAUDKIVI
       Scouring
       IAHR hydraulic structures design manual
       A.A.Balkema, Rotterdam/Brookfield, 1991


2.7    COLARIC, PICHON AND SANANES
       Etude des affouillements a l'aval d'un seuil deversant
       Proceedings of the Twelfth Congress of the IAHR,
       Fort Collins, Colorado, United States, Vol. 3, C37, pp 322 - 329


2.8    DELFT HYDRAULICS, W.H.P. Schukking
       Systematisch onderzoek naar twee- en driedimensionale ontgrondingen
       DHL-report M648 / M863, Band I en II
       Delft, 1972 (in Dutch, not available)


2.9    DELFT HYDRAULICS, R. Adihardjo
       Systematisch onderzoek bodembescherming
       part I   : Invloed geometrie en aard van de verdediging bij twee-
                  dimensionale ontgrondingen
       part II  : Invloed ruwheid bestorting
       part III: Invloed geometrie en aard van de verdediging bij drie
                  dimensionale ontgrondingen
       DHL-report M 847 part I, II en III
       Delft, 1972 (in Dutch, not available)


2.10   DELFT HYDRAULICS, A.F.F. de GRAAUW
       Ontgrondingen
       M 1001, Nota II
       Delft, june 1981 (in Dutch, not available)

2.11    DELFT HYDRAULICS, A.F.F. de GRAAUW
Stormvloedkering Oosterschelde
M 1001-12
Delft,        (in Dutch not available)


2.12    DELFT HYDRAULICS, A.F.F. de Graauw en J.J. Taat
Sluis Brouwersdam, twee-dimensionale ontgrondingsproeven
DHL-report M1533, deel I, II, III en IV,
Delft, 1982 (in Dutch not available)


2.13    DELFT HYDRAULICS, J. Driegen
Stormvloedkering Oosterschelde, detailmodel stroomgeulen; reduktie
van de ontgrondingen ten gevolge van aanvoer van bodemmateriaal
DHL-report M1657,
Delft, november 1982 (in Dutch, not available)


2.14    DELFT HYDRAULICS, J. Driegen
Stormvloedkering Oosterschelde, een overzicht en bewaking van
ontgrondingen langs de rand bodembescherming, evaluatie
ontgrondingsonderzoek
DHL-report Q635,
Delft, 1988 (in Dutch, not available)


2.15    DELFT HYDRAULICS, M. v.d. Wal
Onderzoek naar de ontgronding bij een horizonale vernauwing
DHL-rapport Q935
Delft, 1990 (in Dutch, not available)


2.16    DIETZ, J.W.
Kolkbildung im feinen oder leichter Sohlmaterialen bei strömenden
Abfluss,
Mitteilungen Theodor Rehbock Flussbaulaboratorium., Universitat
Fridericiana, Karlsruhe.
Heft 155, 1969, pp. 1 -119


2.17    FAHROUDI, J. and K.V.H. SMITH
Time scale for scour downstream of hydraulic jump
Proc. ASCE 108, HY10, 1982, pp. 1147 - 1161

2.18    FAHROUDI, J. and K.V.H. SMITH
        Local scour profiles downstream of a hydraulic jump
        Journal of Hydr. Research  23 (4) 1985, pp. 343- 358

2.19    GRAAUW, A.F.F. de  and K.W.  PILARCZYK
        Model-prototype conformity of local scour in non-cohesive sediments
        beneath overflow dams.
        Proc. 19th IAHR Congress New Delhi, India, 1981

2.20    GRAAUW, A.F.F. de
        A review of research on scour. Delft Hydraulics
        DHL-report S 562 (in Dutch, not available).
        Delft, 1983

2.20    Grondmechanica Delft, F. SILVIS
        Orienterende    studie    naar    grondmechanische    aspecten    bij
        ontgrondingskuilen
        Report CO-291720/12
        Delft, maart 1988 (in Dutch, not available)

2.21    KONTER, J.L.M. and T. VAN DER MEULEN
        Influence of upstream sand transport on local scour.
        Proc.  IAHR Symposium on scale effects in modelling sediment
        transport phenomena, Toronto, Canada, August 1986, p. 208-220

2.22    KONTER, J.L.M. and R.E. JORISSEN
        Prediction of time development of local scour

2.23    JORISSEN, R.E. and J.K. VRIJLING
        Local scour downstream hydraulic constructions
        23th Congress of IAHR, Ottawa, Canada, August 1989
        p.p. B-433 - B-440

2.24    PILARCZYK, K.W.
        Interaction water motion and closing elements, Local scour
        in: The closure of tidal basins
        Delft University Press,
        Delft, 1984 and 1987, pp 387 - 405

2.25    POPOVA,K.S.

        Computation for time evaluation of local scour depth below dams
        (in Russian)

        Izvestia VNIIG, vol. 119, 1985, pp.66-73


2.26    RAUDKIVI, A.J.

        Study of sediment ripple formation.

        Proc. ASCE  89, (1976), p. 15-33


2.27    RAUDKIVI, A.J.

        Loose boundary hydraulics.

        Oxford, Pergamon Press. second edition 1976


2.28    RESH, T.J. and H. Leutheuser

        Le  ressant  hydraulique:  mesures  de  turbulence  dans  la  region
        diphasique

        La Houille Blanche, Vol. 27, 1972 No. 4, pp. 279 - 293


2.29    RIJN, L.C. van

        Equivalent roughness of alluvial bed

        Journal of the Hydraulics Division ASCE

        Vol. 108, No. HY10, 1982.


2.30    ZANKE, U.

        Zusammenhange zwischen Stromung und Sedimenttransport, Teil 2:
        Berechnung     des     Sedimentstransportes     hinter     befestigten
        Sohlenstrecken Sonderfall zweidimensionaler Kolk

        Franzius Institut, Mitteillungen, Heft 48, Hannover, Germany, 1978


2.31    ZANKE, U.

        Grundlagen der Sedimentbewegung

        Springer Verlag

        Berlin, 1982

## 3. Spurdikes and abutments

### 3.1 Introduction

Spurdikes

The geometry of a spurdike in rivers or estuaries can be schematized to some basic types of geometries, which are described in section 3.2.1. For example in scale models a spurdike is sometimes schematized to a vertical plate with a vertical head. Such a geometry will be found in the prototype only in exceptional cases. A short description of the flow pattern around a spurdike is given in section 3.2.2. A scour hole just downstream of the head of the spurdike can endanger the stability of the structure, see section 3.2.3. In the Netherlands a lot of experience is obtained with additional protection of the scourhole to prevent too deep scouring and undermining of the spurdikes along the rivers Rhine, Meuse and IJssel. The methods to calculate the maximum scour depth near a spurdike are treated in section 3.2.4. The scour depth near one, isolated spurdike with a flow attack due to a more or less uniform and steady approach flow, is considered in this chapter. This means that the possible interaction between a number of spurdikes in a row along a bank on the development of scour holes, is not treated. In section 3.2.5 some suggestions to expand this chapter are given.

Abutments

The definition of an abutment is important because in some situations an abutment is comparable with a spurdike or a local constriction of the cross section of the waterway (section 3.3.1).

In the flow pattern one or two separation points can be distinguished. From these points vortex streets start which can cause serious scour holes in the bed (section 3.3.2).

The stability of the wing walls and the head of an abutment can be endangered by scour holes near the abutment. In section 3.3.3 a detailed description of an abutment failure is given.

The principle of the calculation of the maximum scour depth is described in section 3.3.4. Some general tendencies for the maximum scour depth can be found in section 3.3.5. Finally some research topics are mentioned (section 3.3.6).

The references for this chapter are listed in section 3.4.

## 3.2  Spurdikes

### 3.2.1  Characteristic geometric parameters

The geometry and the shape of a straight spurdike can be characterised by the following geometric parameters, see the definition sketch in figure 3.1:

- length l, or the dimensionless reduction of the flow width $B_s/B_c$
- width at the water level b (b is measured in the main flow direction)
- angle ($\alpha_1$) between the axis of the spurdike and the bank,
- side slope (angle $\beta_1$) and the slope of the head of the spurdike (angle $\beta_2$),
- height of the crest, and the slope of the crest along the spur axis.

In general a straight spurdike is characterised by:
- the ratio length/width:  l/b > 2,
- angles $\beta_1$ and $\beta_2$: in general between 1:10 and 1:0 (vertical).

If this length/width ratio is smaller than 1 to 2 then the structure can be schematized to an abutment, see section 3.3. If these angles are smaller than 1:10 the local constriction scour will dominate the scour due to the vortex street downstream of the separation point.

The crest of the spurdike in a river has a gentle slope of 1:100 to 1:200 along the spur axis to divert the overflowing flow from the bank to the centre of the flow. In an estuary however a horizontal crest has been applied often.

The foundation of a spurdike can be strengthened by a bed protection to prevent the formation of a scour hole in the direct vicinity of the spurdike. However in that situation a reduced scour hole will be generated just downstream of the bed protection.

More complicated shapes of a spurdike are:
- a spurdike with a T-head,
- a spurdike with a L-head,
- a curved spurdike with a shape like a hockey-stick, or an inverted hockey stick,
- a permeable spurdike,
- a submerged spurdike.

If a strong flow attack on the head is expected, then the head of a spurdike is strengthened with extra size.

In this manual no attention is paid to these more complicated shapes. In general the scour near these complicated spurdikes should be investigated in a scale model.


### 3.2.2  Characteristic flow pattern

The flow field around a spurdike is characterised by an acceleration from upstream to the most contracted cross section somewhere in or just downstream of the head of the spurdike, followed by a deceleration of the flow. A separation point of the flow is located at the head of the spurdike. Downstream of the spur dike the main flow is separated from a large eddy by a vortex street. Downstream of the reattachment point normal flow will be established again.

In an extreme situation (depending on angle $\alpha_1$) just upstream from the spur dike a separation point and a small eddy can exist. Then on the upstream side of the spurdike there is a reattachment point.

The down flow at the spurdike with vertical walls can generate a strong spiral motion near the bed.

If a spurdike is submerged then a rather complex three dimensional flow pattern can be observed, sometimes with a hydraulic jump just downstream of the spurdike, see figure 3.1.


### 3.2.3  Failure mechanism

In general the stability of the not-submerged spurdike is endangered by a scourhole due to the strong vortices just downstream of the separation point at the head of the spurdike. A too steep scour hole can induce a sliding of a part of the head into the scour hole or undermining of this head.

The crest of a submerged spurdike can be damaged by a supercritical flow and a hydraulic jump. In that situation special attention has to be paid to the design of a crest protection.

The soil mechanical aspects of a failure by a too steep scour hole, and the consequent damage to the structure, are treated by Silvis, lit.[3.11].

## 3.2.4    Calculation methods

### 3.2.4.1    Introduction

The formulas for the estimation of the maximum scour depth are treated in two sections. During the developing phase of a scour hole the time dependent maximum scour depth can be calculated with the Breusers approach in some basic geometries, section 3.2.4.2. In the equilibrium phase the maximum scour depth can be estimated with a number of semi-empirical formulas. A selection of this type of formulas is given in section 3.2.4.3. A start has been made with the determination of a formula, which has a more general validity.

The initial slope of a scour hole near a spurdike cannot be estimated with the aid of some formulas up to now. Data of the measured initial slope in scale model tests are available however, for example from the systematic research tests, see DHL-report M847, lit.[3.4], and also from DHL-report Q935, lit.[3.7]. Therefore it is recommended to analyse these data and to derive some formulas for the estimation of the initial slope of a scour hole.

### 3.2.4.2    Breusers formula

The Breusers method has been treated in chapter 2 about sills, therefore in this section only the value of the factors $\alpha$ and $\gamma$ in the Breusers formula are described. The method has been developed for a cohesionless bed material with a uniform gradation. Therefore it is recommended to extend this method for bed material as graded sands and cohesive materials (clays).

$\alpha$ factor:

Consider $\alpha_c \cdot U_c$ in which $U_c$ is the average velocity in the contraction due to the spurdike:

$$U_c = Q / \{y_0 \cdot (B - B_s)\} \tag{3.1}$$

From the results of a scale model investigation Q935, lit.[3.7], with $L_p/y_0$ = 0 and $L_p/y_0$ = 5 the following relation between $\alpha$, $B_s/B$ and $L_p/y_0$ has been determined, see figure 3.2:

$$\alpha_c = 1.5 + \{ 2.7 + 18 (B_s / B)^2 \} \cdot e^{- 0.1 L_p / y_0} \qquad (3.2)$$

Formula (3.2) can be applied if
- $B_s/B < 0.7$,
- the spurdike is not combined with a sill,
- the spurdike has a vertical head and
- the bed protection is rough, that means $k_s > 0.025\ y_0$.

If $B_s/B > 0.7$ the extrapolation of formula (3.2) calculates a further increase of the value of $\alpha_c$, which is not realistic because through the reduced opening, left by the spurdike, the discharge will be reduced strongly. This is observed in a few tests of the systematic research on scouring of DHL, for example DHL-report M1533, part III, [3.6]

If the bed protection is smooth, $\alpha_c$ which is calculated with (3.2), will increase from 0 to 0.5 (see also chapter 2 about sills).

If the head of the spurdike has a slope then the combination of the formulas (3.2) and (3.3) can be estimated with an extension according to Muromov and Papasvili (lit.[3.20] and [3.21]).

$$y_{s,max}/y_0 = \{1 - 0.285\ \beta_2\} \cdot \{\alpha\ U - U_{cr}\}^{1.7} \cdot k^{-0.4} \cdot \Delta^{-0.68} \cdot y_0^{-0.8}\ t^{0.4}$$

$$(3.3)$$

in which $\beta_2$ = slope of the head of the spurdike $1:\beta_2$ $\qquad$ (-)

A preliminary verification of this factor is the comparison of test T7, $\beta_2$= 0, with test T11, $\beta_2$ = 1.5, of a scale model research Q935, lit.[3.7]:

$$\frac{y_{s,max}\ /y_0\ \{T11\}}{y_{s,max}\ /y_0\ \{T7\}} \qquad : \qquad \begin{array}{l}\text{calculated with (3.3):} \\ 0.57 \end{array} \qquad \begin{array}{l}\text{measured:} \\ 0.46\ \text{to}\ 0.51\end{array}$$

This is an acceptable result of a first, preliminary verification.

The reduction factor $\{1-0.285\ \beta_2\}$ is valid if $0 < \beta_2 < 2.5$. If $\beta_2 > 3.5$ this reduction factor becomes negative which is physically impossible. Therefore, the reduction factor can be approximated by:

$$1-0.285\ \beta_2 \approx e^{-0.4\ \beta_2}$$

This factor is probably valid for $0 < \beta_2 < 7$, see figure 3.3. A more extensive verification of this factor is recommended. For example, the results of the scale model M1533 part III, lit.[3.6], for a combination with a sill can be used for this verification. According to the Breusers method a more consistent result should be obtained if the influence of the slope of the head of the spurdike can be expressed directly in the value of $\alpha$, which is the geometric parameter. An alternative is to express the influence in the relative turbulence intensity and to consider $\alpha$ as a function of this relative turbulence intensity, see Jorissen lit.[3.15].

An expression for the influence of the side slopes of the spurdike on $y_{s,max}$ is missing. Probably this influence is of secondary importance.

y-factor

By Driegen lit.[3.5] and Jorissen lit.[3.15] a formula has been deduced to represent the variation of y during the development of a scour hole, see also figure 3.4.

$$y = 10^{(p\ \cdot\ y_{s,max}\ /y_0\ +\ v)} \tag{3.4}$$

in which

p = constant         (-)
v = constant         (-)

In case of a spurdike without a bed protection p = -0.30 and
                     with     a bed protection p = -0.10.
In both cases v = -0.30, see DHL-report Q935, lit.[3.7].

In a publication at the IAHR Congress of 1975 L.V. Cunha, lit.[3.3], paid some attention to the time evolution of local scour near vertically headed spurdikes or groynes.

From his figures can be concluded:

$y_{s,max}/y_0 < 0.5$ to $1$  :             $\gamma > 0.2$, probably near $0.4$

$y_{s,max}/y_0 > 0.5$ to $1$  :             $\gamma = 0.16$
                                                up to equilibrium scour depth

This result confirms the variation in $\gamma$ according to (3.4) and figure 3.5 with different values of $\gamma$.

The combination of a spurdike with a sill

A first estimation of the value of $\alpha$ has been obtained from an analysis of the test results of the systematic research of DHL on local scour downstream of a combination of a spurdike and a sill, see DHL-report M847 lit.[3.4] and van der Meulen and Vinje, lit.[3.19, p 7]:

| vertical constriction $y_D/y_0$ | $\alpha$ |
|---|---|
| 0 | 3.0 |
| 0.3 | 4.0 to 4.7 |
| 0.6 | 6.5 to 8.2. |

Table 3.1: Value of α as a fucntion of the vertical constriction.

This first estimation can be refined with the following formula, if the bed protection is hydraulically rough and $B_s/B = 0.1$:

$$\alpha = 1.5 + ( \ 2.6 + 18.6 \ \{ \ y_D/y_0 \}^2 \ ) \ e^{- 0,045 \ . \ L_p/y_0} \tag{3.5}$$

In this formula $\alpha$ is related to the cross section averaged upstream flow velocity. If $y_D/y_0 = 0$ then $\alpha$ with (3.5) can be compared with $\alpha_c$ with (3.2) and $B_s/B = 0.1$, see figure 3.6. The differences in the values of $\alpha$ and $\alpha_c$ are partly due to different definitions of $\alpha$ and $\alpha_c$, that is the average upstream flow velocity and the average flow velocity in the constriction. The calculated $\alpha$ according to (3.5) have been compared with the values of $\alpha$, which are determined from the tests of the systematic research on scouring, see figure 3.7 which is based on figure 42 of DHL-report M847 part III, lit.[3.4]. It is mentioned that the vertical scale in that figure should be multiplied with 2 to correct an error in the original figure. From figure 3.6. it can be concluded that formula (3.5) fits very well to the test results for a rough bed protection.

The comparison of (3.5) with (3.2) shows that the influence of a width reduction, $B_s/B$, on $\alpha$ is almost the same as the influence of a sill height reduction, $y_D/y_0$, on $\alpha_c$. Probably this can be explained by the conclusion that a horizontal or a vertical constriction has almost the same influence on the generation of the turbulence, which forms an important contribution to the development of the downstream scourhole.

### 3.2.4.3 Equilibrium scour depth

A review of some selected semi-empirical formulas to estimate the maximum equilibrium scour depth is given in the following.

Inglis (1949), lit.[3.12], analysed field data on the maxium scour depth observed near spurdikes and the noses of guide banks in India and Pakistan. He compared the total scoured depth $(y_0 + y_s)$ with the three-dimensional Lacey regime depth $y_{3r}$ which can be obtained from the equation $y_{3r}=0.47(Q/f)^{0.33}$.

$$y_0 + y_s = 0.47 \cdot K \cdot f^{-0.33} \cdot B^{0.33} \cdot y_0^{0.33} U_0^{0.33} \tag{3.6}$$

in which

| | | |
|---|---|---|
| f = | silt factor equal to 1.76 $\sqrt{d}$ | $(m^{0.5})$ |
| D = | diameter of bed material | $(m)$ |
| K = | factor for flow and geometric conditions | $(-)$ |

Formula (3.6) can be compared with a general expression for the maximum scour depth:

$$y_0 + y_s = C_1 \cdot (\frac{B}{B-B_s})^x \cdot y_0^y \cdot U_0^z \tag{3.7}$$

in which

C1 $= 0.47 \cdot K \cdot f^{-0.33}$
x $= 0.33$
y $= 0.33$
z $= 0.33$

Field data gave a value of 1.6 to 3.9 for the ratio $(y_0+y_s)/y_{3r}$. The recommended values for K are:

| Scour at straight spurs facing upstream, with steeply sloping | K (-) |
|---|---|
| heads ( 1.5 V : 1 H)<br>Same with long sloping heads (1 V : 20 H)<br>Scour at noses of large-radius guidebanks<br>Scour at spurs along river banks, depending<br>on severity of attack | 3.8<br>2.25<br>2.75<br><br>1.7 - 3.8 |

Table 3.2  Value of k as a function of the hydraulic and geometric condi-
tions

Ahmad (1953), lit.[3.1], performed scouring studies on single spurs in vertically sided channels. He used as a basis for the total scoured depth $(y_0 + y_s)$. It is mentioned that this formula is similar to the formula for the dimensional Lacey regime depth:

$$y_0 + y_s = K (\alpha_1) \cdot q_c^{2/3} \qquad (3.8)$$

Formula (3.8) can be written as:

$$y_0 + y_s = C_1 \cdot (B/(B-B_s))^x \cdot y_0^y \cdot U_0^z \qquad (3.7)$$

with
$C_1 = K(\alpha_1)$
$x = 0.67$
$y = 0.67$
$z = 0.67$

| $\alpha_1$ | units | 30° | 45° | 60° | 90° | 120° | 150° |
|---|---|---|---|---|---|---|---|
| $K(\alpha_1)$ | metric | 1.8 | 2.0 | 2.15 | 2.25 | 2.4 | 2.45 |

Table 3.3  Values of K as a function of spur angle $\alpha_1$

An a-symmetry in the velocity distribution due to a bend was found to in-
crease the total scoured depth roughly in proportion to the ratio of the velocity in the river section adjacent to the spur and the average velo-
city.  Ahmad recommends the following values for K (metric units).

| Spur geometry | K (metric units) |
|---|---|
| Spur below a bend on the concave side with swirl behind the bend | 3.0 - 3.35 |
| Spur in moderate bend no swirl | 2.2 - 2.6 |
| Spur in straight channel $\alpha_1$ = 30° - 90° | 1.8 - 2.2 |
| Same $\alpha_1$ = 90° - 150° | 2.2 - 2.6 |

*Table 3.4   K as a function of the spur geometry*

Ahmad detected no influence of grain size but his tests were limited to d = 0.35 and 0.70 mm. Tests with the finer sand attained equilibrium more quickly. The shape of the end of the spur ( T-shape, hockey spur) only affected $(y_o + y_s)$ moderately; less than 10% variation in the result was attributable to this.

Liu, Chang and Skinner (1961) lit [3.18] performed extensive investigations on vertical wall-type spurs and some abutments in two flumes, with B = 4.2 and 2.4 m and with sands $d_{50}$ = 0.56 mm and 0.65 mm.

Tests with spurdikes having vertical heads (boards having virtually zero thickness) and flow velocities above the critical were used to derive an empirical relation:

$$\frac{y_{se}}{y_0} = 2.15 \left[\frac{B_s}{y_0}\right]^{0.4} Fr^{1/3} \tag{3.9}$$

in which Fr is the Froude number:
$$Fr = U_0 / ( g \cdot y_0 )^{0.5}$$
The analysis of field data from spurs along the Mississippi River confirmed (3.9) and shows an upper limit of $B_s/y_0$, according to Richardson et al. (1975), lit.[3.22]:

$B_s/y_0 \leq 25$     formula (3.9)
$B_s/y_0 > 25$     formula (3.9) with $B_s/y_0$ = 25:
$$y_{se}/y_0 = 7.8 \ Fr^{0.33}$$

Formula (3.9) can be written as:

$$y_s = C_1 \cdot B_s^x \cdot y_0^y \cdot U_0^z \tag{3.10}$$

with

$C_1$    =    $2.15 \cdot g^{-0.167}$

$x$    =    $0.4$

$y$    =    $0.44$

$z$    =    $0.33$

For conditions with dunes, $y_s$ fluctuates around the average value of $y_{se}$. The maximum value $y_{sm}$ is found by adding $0.3\ y_o$ to $y_{se}$.

The resulting expression according to Laursen, lit.[3.16, 3.17], for sediment transporting flow $(U > U_c)$ can be approximated for $2 < B_s/y_0 < 100$ by:

$$\frac{y_s}{y_0} = 1.6 \left[\frac{B_s}{y_o}\right]^{0.47} \tag{3.11}$$

Formula (3.10) can also be written as:

$$y_s = C_1 \cdot B_s{}^x \cdot y_0{}^y \cdot U_0{}^z \tag{3.10}$$

with

$C_1$    =    $1.6$

$x$    =    $0.47$

$y$    =    $0.53$

$z$    =    $0$

These relationships are not supported by experiments!

C.V. da Cunha (1971), lit.[3.2], performed a large number of tests with various vertical sided headed groynes, and water depths in the range 0.04 to 0.14 m. Velocities were varied from 1.0 to 1.4 $U_c$.
Maximum scour depths around the head of the groyne follow from:

$$\frac{y_s}{y_0} = 1.65 \left[\frac{b}{y_0}\right]^{0.3} \left[\frac{h}{y_0}\right]^{0.95} \left[\frac{w}{u_*}\right]^{0.15} \tag{3.12}$$

in which

$w$   = fall velocity of a grain of the bed material      (m/s)

$u_*$ = shear velocity      (m/s)

Formula (3.12) can be used if $B_s/y_o$ = 1.5 to 12 and $\alpha_1$ = 90°, and this formula can be written as:

$$y_s = C_1 \cdot B_s^x \cdot y_0^y \cdot u_*^z \qquad (3.13)$$

with
$$C_1 = 1.65 \cdot w^{0.15} \; (h/y_0)^{0.95}$$
$$x = 0.3$$
$$y = 0.7$$
$$z = -0.15$$

where h is the height of the groyne relative to the original bed level. The shear velocity $u_*$ was not systematically varied, this explains the deviating negative value of the exponent of $u_*$.

The relations derived from the different investigations on spur dike (or groyne) scour models can be subdivided into three groups :

a) those for which $U_o > U_c$ , and which give $y_s$ as a function of the geometry of the obstruction

b) relations giving $y_s$ as a function of flow velocity as well as the geometry of the obstruction,

c) relations considering the discharge intensity in the contracted flow section as well as geometrical properties.

Type a) and b) relations have the disadvantage that they are derived from small-scale experiments; extrapolation to practical conditions has a consequent risk.

Type c) relations, however, have been shown to be applicable in natural conditions.

A general expression for $y_0 + y_s$:

$$y_s = B_s^x \cdot y_0^y \cdot U_0^z \qquad (3.10)$$

with
$$x = 0.33 \text{ to } 0.8$$
$$y = 0.33 \text{ to } 0.7$$
$$z = 0.33 \text{ to } 0.75$$

This variation in the value of the exponents is illustrated in figure 3.8, from this graph it can be concluded that

- in a scale model with $y_0 < 1$ and $U_0 < 1$ the difference between $y_0^y$ or $U_0^z$ with different values of the exponent is relatively small,

- in the prototype with $y_0 > 1$ and $U_0 > 1$ the difference between $y_0^y$ or $U_0^z$ with different values of the exponent is increasing.

This explains the difference between $y_s$ calculated with different formulas for prototype conditions. Consequently, the best estimation for maximum scour depth is given by:

$$(y_0 + y_s) = K \cdot (B/(B-B_s))^{0.6} \cdot y_0^{0.6} \cdot U_0^{0.6} = K \cdot q_c^{0.67} \qquad (3.14)$$

in which $q_c = B/(B-B_s) \cdot y_0 \cdot U_0$

$y_s$ = equilibrium scour depth of the deepest point of a scour hole (m)
$K$ = coefficient                                                    (-)
$q_c$ = specific discharge in the constriction                       (m²/s)

$$q_c = Q / (B-B_s) = y_0 \cdot U_c \qquad (3.15)$$

This coefficient K depends on many different influences. Some K values are given in table 3.5 for a first estimation of $y_s$.

| Structure and location | K |
|---|---|
| Groynes in straight channels $\alpha_1 = 90°$ | 1.8 - 2.4 |
| Spur in moderated bend ; no swirl | 2.2 - 2.4 |
| Spur below a bend on the concave side with swirl behind the bend | 3.0 - 3.3 |

Table 3.5  Factor K as a function of different structures

The equilibrium maximum scour depth can be estimated with the Dietz formula:

$$\frac{y_{s,max}}{y_0} = \frac{c \cdot \alpha_c \cdot u_o}{u_{cr}} - 1 \qquad (3.16)$$

in which

c = coefficient

The verification of (3.16) with physical model tests, see lit. [3.7] resulted in C = 0.6 to 0.7. The accuracy of the formula is about 30%. This accuracy is better than the accuracy of the foregoing formules, and therefore (3.16) is recommended.


### 3.2.5   Research needs

For abutments and spurdikes with moderate slopes a reduction of scour depth of up to 20% may be applied. Therefore it is expected that K depends on the slope of the head of the spurdike; and also that K depends on the erodibility of the bed material, for example expressed in w or $D_{50}$. It is recommended to analyse the available information to determine a design formula for a relation between K and these parameters.

It is also recommended to include in this review of formulas for the calculation of the maximum scour depth the formulas of Garde [3.9], Izzard and Bradley, and other investigators, such as Blench, Straub-Gill, Kennedy. It is recommended to include the results of Sastry, see Gill lit.[3.10], who published a relation between the angle of the spurdike with the bank and the reduction in scour depth, expressed in $y_s$(angle degrees)/ $y_s$(90 degrees).

This chapter should be completed with design rules for the spacing of spur dikes and the elevation of spurdikes along rivers. Some information about these aspects has been given by Richardson et al. lit.[3.22].


### 3.3   **Abutments**

### 3.3.1   Characteristic geometric parameters

An abutment along a bank of a canal, a river or a tidal channel can be characterised by the following geometric parameters:
-       length l, width b, the angles of the wing walls $\alpha_1$ and $\alpha_2$, see for the definition of these angles figure 3.9,
-       the slope of the side wall $\beta$ and the slope of the wing walls,

-       the  form of the edges between the side wall and the wing wall can be
        sharp or rounded, see figure 3.9. A special case is an abutment  with
        a completely rounded head.

In general an abutment can be distinguished from other structures by:
-       the ratio length/width;  l / b > 1 to 2, and
-       the angles $\alpha_1$ and $\alpha_2$ > about 10 degrees.
If  this  length/width ratio is smaller than 1 to 2, then the structure can
be schematised to a spurdike. And if  these  angles  are  smaller  than  10
degrees  the  structure  can  be  schematized  to  a local constriction. An
abutment can be placed on one bank or symmetrically  on  both  banks  of  a
canal.  The  bed  between  two  abutments  is supposed to be horizontal. In
practice, a combination of abutments with a sill is designed frequently.

An abutment can be protected by an adjacent bed protection; however in this
chapter only abutments without a bed protection  are  considered.  A  scour
hole  downstream  of  a  bed  protection  is  comparable  with a scour hole
downstream of a bed protection near a spurdike, see section 3.2.


3.3.2   Characteristic flow pattern

The pattern of the flow through an abutment is characterised by an   accele-
ration  from  upstream  to a cross section somewhere in the constriction of
the abutment, followed by a deceleration of the flow.
This  pattern  can  be  more detailed by the number and the position of the
separation points of the flow,  see  figure  3.9.  Two  situations  can  be
distinguished:
-       one separation point in cross section 2,
-       two  separation  points;  one  in  cross  section  2 and one in cross
        section 4.

If  angle  $\alpha_1$  is  near  90 degrees also just upstream of cross section 2 a
separation point can exist with small vortices in the  corner  between  the
bank  and  the wing wall, see figure 3.9. Near this corner a surface roller
can be generated. A vortex street forms the  separation  between  the  main
flow and one or more eddies (depending on the geometry). A vortex street is
an important part of the flow pattern because a  vortex  street  can  cause
serious scour holes in the bed.

### 3.3.3   Failure mechanism

The stability of the side wall of an abutment without an adjacent bed protection is endangered by the scour hole due to general acceleration of the flow and the vortex street downstream of separation point, see figure 3.10. Especially in the case the side wall consists of a vertical sheet piling this scour hole can have a considerable depth. This depth will be reduced by a sloped side wall of an abutment. A bed protection can prevent such a scour hole.

A frequent mode of abutment failure is outflanking, i.e., erosion of the causeway while the abutment structure remains intact. This results from the causeway material sliding into the scour hole and thus creating a cove in the causeway behind the abutment. Progressively an eddy develops in that recess, which draws the interface to the stagnation region back from the head of the abutment, more of the flow impinges, downflow strength increases and the scour depth increases. The final result can be a breakthrough behind the abutment head.
In exceptional cases the scour hole due to the vortex street downstream of cross section 4 and the deceleration of the flow can endanger the stability of the downstream wing wall. This scour hole can be prevented by an extended bed protection, or by an increase of angle $\alpha_2$. Or the stability of the wing wall can be guaranteed by an increase of the foundation depth of this wing wall. Further the undermining of wing walls can be repaired with the same measures as mentioned in the chapter about bridge piers.

### 3.3.4   Calculation methods

The maximum depth of the scour hole near the side wall can be calculated by the superposition of the scour depth due to the acceleration of the flow and the scour depth due to the vortex street downstream of the separation point in cross section 2, see figure 3.10.
In the same way the maximum depth of the scour hole near the downstream wing wall can be calculated by superposition of the scour depth due to the deceleration of the flow and the scour depth due to the vortex street downstream of the separation point in cross section 4.

The scour depth due to the acceleration and the deceleration of the flow can be estimated by a one-dimensional model. In most cases the scour depth

due to the vortex street can be estimated with the Breusers method in which the factor α should have a value for three dimensional flow, see section 3.2 about spurdikes.


### 3.3.5   General tendencies and data

If the water depth is much smaller than the width b, then the scour depth depends mainly on this width. This follows also from a model for general constriction scour.
If the length of an abutment increases also the maximum scour depth will increase, because normally abutments are rather short. Also this tendency can be simulated with a model for general constriction scour.
Near abutments relatively large scour depths, of the order of 2 to 5 times the water depth or 1.0 to 1.5 times the abutment length have to be expected as an upper limit for the maximum scour depth.


### 3.3.6   Research needs

This chapter should be extended with some formulas for the maximum scour depth due to constriction scour. These formulas are an alternative for a more complex mathematical model of a flood routing model.

For an estimation of the stability of wing walls more attention should be paid to the soil mechanical aspects.

Data and formulas for the slopes of a scour hole near an abutment are missing in this draft version of the manual. Kwan, lit.[3.14], gives some data, but most data of his report is related to the maximum scour depth. Therefore a continued search in the literature or some tests in a physical scale model are recommended.


### 3.4   References

3.1   M. AHMAD
       Experiments on design and behaviour of spur dikes.
       Proc. IAHR Conf. Minnesota, USA, 1953, pp. 145 - 159

3.2   L.V. CUNHA
      Erosöes    lokalizadas    junta   de   obstaculos   salientes   de margens.
      (Local scour at  obstacles  protruding from river banks).
      Thesis presented to the University of Lisbon, LNEC, Lisboa, Portugal,
      1971.


3.3   L.V. Cunha
      Time evolution of local scour
      16th Congress of International Association for Hydraulic Research,
      Volume 2, subject B.a B36,  pp 285 to 299
      Sao Paulo, Brasil, 1975


3.4   DELFT HYDRAULICS, R. ADIHARDJO
      Systematisch onderzoek bodembescherming, invloed geometrie en aard
      van de verdediging bij driedimensionale ontgrondingen
      DHL-report M847 part III
      Delft, 1972 (in Dutch, not available)


3.5   DELFT HYDRAULICS, J. DRIEGEN
      Stormvloedkering  Oosterschelde,  evaluatie  ontgrondingen,  voorstel
      aanpassing verwerkingsprocedure
      DHL-report Q496,.
      Delft, April 1987 (in Dutch, not available)


3.6   DELFT HYDRAULICS, J.J. TAAT and A.F.F. de GRAAUW
      Sluis Brouwersdam, twee-dimensionale ontgrondingsproeven
      DHL-report M1533 part III
      Delft, 1982 (in Dutch, not available)


3.7   DELFT HYDRAULICS, M. v.d. WAL
      Onderzoek naar de ontgronding bij een horizontale vernauwing
      DHL-report Q935
      Delft, 1990 (in Dutch, not available)


3.8   DELFT HYDRAULICS
      Documentation WENDY
      Delft, 1990

3.9   R.J. GARDE, et al.
      Study of scour around spur-dikes.
      ASCE Proceedings Vol. 87, HY6, November 1961.


3.10  M.A. GILL
      Research for river regulation dike design
      ASCE Proceedings, Vol. 94, no. WW2, 1968


3.11  GRONDMECHANICA DELFT, F. SILVIS
      Orienterende    studie    naar    grondmechanische    aspecten    bij
      ontgrondingskuilen
      Report CO-291720/12
      Delft, maart 1988 (in Dutch, not available)


3.12  C.C. INGLIS
      The behaviour and control of rivers and canals.
      C.W.I.N.R.S. Poona, Res. Publication No. 13, 1949


3.13  C.F. IZZARD and J.N. BRADLEY
      Field  verification of  model test on flow through highway bridge and
      culverts.
      IOWA, USA, 1958.


3.14  KWAN, T.F.
      Study of abutment scour
      University of Auckland, Department of Civil Engineering,
      report no. 328, Auckland, New Zealand, 1984


3.15  R.E. JORISSEN AND J.K. VRIJLING
      Local scour downstream hydraulic constructions
      23th Congress of IAHR, Ottawa, Canada, August 1989


3.16  E.M. LAURSEN
      Scour at bridge crossings
      Iowa Highway Res, board, Bull. NO. 8, 1958


3.17  E.M. LAURSEN
      An analysis of bridge relief scour
      Proc. ASCE 89, HY3, 1963, pp. 93 -117

3.18    LIU, H.K., CHANG, F.M. AND SKINNER, M.M.
        Effect of Bridge Construction on Scour and Backwater
        Colorado State University, Department of Civil Engineering,
        report no CER60-HKL22, 1961.


3.19    T. VAN DER MEULEN AND J.J. VINJE
        Three dimensional local scour in non-cohesive sediments
        16th Congress of IAHR, Vol. 2, subject B.a, pp. 263 - 270
        Sao Paulo, Brasil, 1975


3.20    V.S. MUROMOV et al.
        Deformacii podmostovykh rusil (in Russian)
        Deformations of beds under bridges
        Transport, Moscow, Russia, 1970


3.21    A.G.PAPASHVILI
        Investigations on local scour at transversal training structures.
        (in Russian)
        Ph. D. Thesis, Tbilisi, Russia, 1973


3.22    E.V. RICHARDSON, M.A. STEVENS AND D.B. SIMONS
        The design of spurs for river training
        Proceedings of 16th IAHR-congress, Volume 2,
        Sao Paulo, Brazil, 1975, pp. 382 - 388


3.23    TEY, C.B.
        Local scour at bridge abutments
        University of Auckland, Department of Civil Engineering,
        Report no. 329
        Auckland, New Zealand, 1984.


3.24    WONG, H.H.
        Scour at bridge abutments
        University of Auckland, Department of Civil Engineering
        Report no. 275
        Auckland, New Zealand, 1982.

## 4. <u>Bridge piers</u>

### 4.1 Introduction

The local scour around bridge piers depends strongly on the geometry of the pier. The characteristic geometric parameters are described in section 4.2. Secondly a complicated interaction exists between this local scour and the flow pattern around a pier. A summary of the main parts of this flow pattern can be found in section 4.3. Different failure mechanisms of bridge piers are illustrated with a few experiences from practise ( section 4.4 ) and also some methods to prevent local scour are mentioned (section 4.5). In general, the local scour around a bridge pier is a relatively rapid process, therefore, most investigators are interested in the maximum scour depth in the equilibrium phase of this scour process (section 4.6.3). Similar to the other chapters some aspects of the time dependent development phase of this scour process have been treated in detail, section 4.6.2, with the purpose to extend the applicability of the Breusers method. The schematized shape of a local scour is determined by the maximum scour depth and the side slopes of the scour hole, section 4.6.4. Specially about the local scour near bridge piers many publications are available. It is out of the scope of this manual to give a more or less complete review of all these publications.

Finally some research needs are mentioned in section 4.7 and a list of references is given in section 4.8.

### 4.2 Characteristic geometric parameters

The process of local scour is influenced by some geometric parameters of a bridge pier. These parameters are listed below, see the definition sketch in figure 4.1:

* $B_p$ = the pier projected width, this width includes the alignment that is characterised by the angle of attack,
* $y_0$ = flow depth upstream of the pier,
* shape in a horizontal cross section:
    - circular, squared, rectangular, elliptic, and other shapes,

*   shape in a vertical cross section:
    -   in elevation a constant shape (prismatic pier),
    -   in elevation tapered piers,
    -   or piers with a increased width at the base,
*   piers composed of different elements:
    -   a pier with a ringlike footing to prevent scouring,
    -   a pier based on a foundation cap or a footing, which is  supported
        by foundation piles,
    -   a caisson with a flat bottom based directly on the subsoil,
    -   a caisson without a bottom, penetrated into the subsoil.
*   a group of separated piers, without a footing.

Most studies have been focused to local scour near one circular prismatic
pier in a non-cohesive sand bed. The local scour is caused by a constant
uniform flow. This situation is a reference case for other geometries.

The foundation of a prismatic pier is normally a continuation of  the  pier
for at least a few pier diameters into the subsoil. If the pier has a large
diameter compared with the height of the pier then the pier can be  founded
as a caisson.

## 4.3  Characteristic flow pattern

The flow pattern near a pier is in detail rather  complicated,  see  figure
4.2.  The  main  parts  are  the  wake vortices and the horse shoe vortices
combined with the downflow. For the local scour  near  a  bridge  pier  the
interaction between the wake vortices is important, see table 4.1, in which
$y_0$ is the undisturbed water depth (m) and $B_p$ the width of the  bridge  pier
(m), and figure 4.3:

| pier geometry | interaction |
|---|---|
| $B_p / y_0 < 0.5$ | a strong interaction, intermittantly vortices are generated from a separation point at the left and the right side of the cylinder |
| $0.5 < B_p / y_0 < 1.5$ | a weak interaction |
| $B_p / y_0 > 1.5$ | no interaction, the vortices are generated independently from a point at the left and the right side of a cylinder |

Table 4.1 Flow characteristics around a circular pier

The most simple flow pattern is generated by a steady, uniform approach flow, which is characterized by the following parameters:

    U  depth averaged flow velocity,

    $U_*$  shear stress velocity,

    v  kinematic viscosity, which represents the influence of the temperature of the water,

      and additionally the relative turbulence intensity, which varies from place to place in the flow field around the pier.

Some special conditions for the flow pattern can be mentioned:
- An accelerated flow of a local contraction or a river bend with well developed bend flow,
- Supercritical flow, (normally the flow is subcritical),
- In an unsteady flow as in a tidal estuary, a scour hole will be generated by each main flow direction.
- An ice cover can divert the flow to the bed near the pier and therefore an ice cover can cause additional increase of local scour.

In this report only some information is given about local scour in a tidal flow. Furthermore subcritical flow is considered in this report, if not mentioned differently.

The complex flow pattern in the scour hole has been described in detail by several authors, for example by Dargahi, lit.[4.9], or the IAHR-manual on Scouring, lit.[4.6]. The waterdepth reduces the local scour depth if the surface roller on the upstream side of the pier interferes with the horse-shoe vortices near the bottom.

## 4.4  Failure mechanism

The scour near bridge piers in rivers can be considered as a composition of bed scour by different processes, like:
- general bed scour occurring from the natural changes in the stream,
- constriction scour caused by the narrowing of the waterway at the bridge site,
- local scour near the pier, that results from flow disturbances introduced by the presence of the bridge pier.

As a first estimation the scour, which is caused by each process separately, may be added linearly to obtain the resulting scour. In this report only the local scour near bridge piers is treated. In a report of a field survey to bridge pier scour which is executed by the West Virginia University, lit.[4.27], it is concluded that the most significant contribution to total scour at a bridge pier comes from general scour or contraction scour, and probably local scour accounts for less than 20 % of the total scour depth.

The local scour process depends on the following properties of the bed material:

-   a representative diameter of the bed material: $D_{50}$, $D_{84}$, $D_{16}$, and the gradation of the bed material, which determines the formation of an armour layer,
-   the density and the relative density of the bed material.

In most studies the local scour of non-cohesive bed material has been tested, therefore $D_{50}$ > 100 micron.

Some additional properties of the bed material are:

-   shape of the grains,
-   surface packing of the grains,
-   homogeneity of the bed material,
-   multi layers of different bed materials.

The influence of these additional properties on the scour hole is of secondary importance and these properties are not treated in this manual. Also the local scour through damaged bed protection layers around a pier is not treated in detail.

The local scour hole is characterised by

-   maximum scour depth (sections 4.6.2 and 4.6.3),
-   volume of the scour hole(section 4.6.4),
-   initial slope, and side slopes of the scour hole (section 4.6.4).

The slope of a scour hole around a bridge pier can be divided in three regions, see sketch in figure 4.1 (according to Dargahi, lit.[4.9]): upper and lower region and in the deepest part of a scour hole a concave region.

The maximum scour depth of a scour hole is decisive for a failure of a bridge pier. The volume and the initial slope of a scour hole have no direct influence on the stability of a bridge pier.

In general the design of wall-type bridge piers is based on the assumption that the length axis of a wall-type pier is parallel to the direction of the flow. Over time, a meandering river can cause a change in the angle of attack of the flow on the pier. If the direction of the flow is not parallel to the pier axis, then the local scour depth can increase considerably. To prevent such an increase in the scour depth it is advised to design circular piers, where the local scour depth is insensitive for the angle of attack, see Davis, Case histories of scour problems at bridges, lit.[4.11].

Davis concludes that in general it is cost effective to protect foundations from scour for events with greater recurrence intervals than are used in the design of the waterway openings. Then damage to bridge and road elements (e.g. spurdikes, riprap protection, roadway approaches) from rare flood events can usually be repaired rather quickly as long as the structure itself is not damaged.

Based on practical experience Blodgett, lit.[4.3], advises as a general guideline that no bridge maintenance problems associated with general scour and lateral erosion should be expected as long as the bridge piers occupy less than 5 % of the wet cross section of the original waterway. Although the local scour process around bridge piers is a rapid process, the constriction scour and the general scour process may continue for decades, see the case of a bridge crossing the Sacramento River, Blodgett, lit.[4.3].

With a summary of some case histories in Canada some measures to prevent the failure of a bridge pier due to scour, have been described by Neill and Morris, lit.[4.23]. The railway bridges of these cases were constructed in 1913 and are located in the Thompson River Valley in Canada.

One pier had a concrete footing directly placed on hard clay with sufficient bearing capacity, but sensitive to erosion by the river. Two piers were strengthened by foundation piles to support the original footing. At the same time a guiding dike and a riprap protection for two piers were constructed.

A few decades later the erosive action of the river had been shifted to another pier of this bridge, where the angle of attack was around 20 degrees. The rather high water level differences near this pier during floods induce pressure differences in the alluvium sublayers. The river bed scour near this pier could be caused by piping through voids in the alluvium. To strenghten this pier the following measures were considered:

-       further placement of riprap as in the past,
-       more closely controlled local scour protection,
-       river training works,
-       structural upgrading of the foundations by sheet piling.

The first mentioned measure was executed by placing a layer of rip rap on the existing bed level. This protection requires regular inspection and maintenance.

Another variant to place the riprap in a dredged trench below the actual bed level was rejected for reason of costs.

The failure of a pier in another bridge has been due to

-       the high angle of attack up to about 40 degrees under certain flow conditions,
-       and a foundation of the concrete footing on a 5 to 6 m thick layer of gravel.

To prevent a failure of this pier in the future a hydraulic scale model study has been executed and the following measures were considered:

-       sheet piling around the existing foundation block,
-       closely spaced steel pipe piling around the existing foundation block and grouting of the material under the foundation block,
-       load-bearing pipe piles connected to the existing foundation block (for this connection three alternatives were studied),
-       a scour protection apron around the nose and the exposed side of the pier.

The last mentioned measure was the cheapest solution, with on top a mat of interlinked concrete blocks from 1.1 m width, 1.1 m length and 0.8 m height.

These descriptions of case histories of bridge pier failures are a good introduction to the measures to prevent local scour near bridge piers.

## 4.5 Measures to prevent local scour

The measures to prevent or to reduce the local scour around a bridge pier can be summarised as follows:

-a       riprap protection around a bridge pier,

-b       a mattress protection around a bridge pier,

-c       a horizontal deflector fixed to a pier at the bed level,

-d       a separated horizontal deflector around a pier,

-e       a vertical deflector ring around a pier,

-f       stone bags fixed to the footing or grouted gravel or hinged plates with riprap,

-g       guide vanes,

-h       group of smaller piles upstream of the main piers.

Some of these measures are described more in detail in the following.

### Rip rap protection around a bridge pier

The size of the rip rap can be calculated with stability criteria as Isbash or Shields, if the maximum decisive flow velocity is known. With a potential flow theory the maximum shear stress and the maximum flow velocity near a cylinder type pier can be calculated: $\tau_{max} = 4 \tau_{undisturbed}$ and $U_{max} = 2 U_{undisturbed}$.
In this calculation the increase in turbulence intensity around a pier is not included.

The minimum layer thickness is 2 $D_{50}$, but often a larger thickness will be advantageous. Especially the connection between the riprap layer and the footing of the pier needs extra attention. Some qualitative information is given in Ettema (1980), lit.[4.8].

For the length of the protection layer (or the diameter of the protection layer) some preliminary design rules are available from the literature: Bonasoundas, lit.[4.4], gives the length of bed protection $L_p$ = 2.5 $B_p$ upstream and $L_p$ = 4 $B_p$ downstream a circular pile in a uniform current and Hjorth, lit.[4.16], gives $L_p$ = 0.75 $B_p$ upstream and $L_p$ = 5 $B_p$ downstream for the region with strong wake vortices.
Carstens, lit.[4.7], found that $L_p$ not only depends on $B_p$ but also on $y_0$: hypothetically:

$$L_p = c_s \cdot y_{s,max} / \tan(\phi) \tag{4.1}$$

in which

$c_s$      = safety factor      (-)

$y_{s,max}$      = maximum scour depth measured from the original bed level    (m)

$\phi$      = angle of repose      (degrees)

The angle of repose depends on the type of soil and the compaction of the soil, therefore the angle of repose varies between $20 < \phi < 50$ degrees; assume $\phi = 35$ degrees as an average value, and $c_s = 1.5$ then:

$$L_p = 2.1 \ y_{s,max} \tag{4.2}$$

More information about the shape of a local scour hole can be found in section 4.6.4. If one assumes an upper limit of $y_{s,max} = 3 \ B_p$ then $L_p = 6.3 \ B_p$ and this confirms the protection length or protection diameter according to Bonasoundas and Hjorth. It is mentioned that if waves cause a scour hole the slope of the scour hole is less than the angle of repose and therefore a larger bed protection is needed then compared with scour by a current only.

**Mattress protection around a bridge pier**

For a local protection around a big, circular pier in a bed of fine sand an artificial protection has been proposed as a new concept. This protection consists of numerous bundles of polyester filaments which can be suspended under a frame cantilevered from a pier. A first prototype test shows promising results, see Carstens, lit.[4.7]. In general special attention has to be given to a tight connection between the mattress and the pier, because through a small gap the downflow can induce severe erosion, which extends under the mattress.

**A fixed horizontal defelctor of the downflow or collar**

The downflow near the pier can be deflected by a deflector, see Carstens , lit.[4.7], and Dargahi, lit.[4.9].
For the determination of the width and the height of the deflector, which is fixed to the pier, no design rules are available. Carstens published some results for the height of the deflector in only one situation.
Dargahi investigated the shape of the collar and the position of the collar relative to the original bed level.

The shape varied from circular collars to so called Joukowski collars (egg-shaped). No significant difference in the maximum scour depth was found between these two shapes. A collar at or just below the original bed level gives the highest reduction of the maximum scour depth and a slower development of the scour hole.

**A separated horizontal deflector of the downflow**

For a preliminary design of the piers of the Eastern Scheldt Storm Surge Barrier the effectiveness of a separated deflector around a prismatic pier has been studied in a scale model, see DHL-report M1402, lit.[4.14]. With a open space of 0.3 m between the deflector and the pier the maximum scour depth was reduced by about 25 %.

**A separated vertical deflector of the approach current**

As an alternative in the preliminary design stage of the Eastern Schaldt Storm Surge barrrier the effectiveness of a separated vertical deflector around a prismatic pier has also been tested in a scale model, see DHL-report M1402, lit.[4.14]. This deflector has been placed on the bed protection mattress. The distance between deflector and pier was around 4 m and the gap between the mattress and the pier was around 0.3 m. Other data are $B_p$ = 18 m and $y_0$ = 15 m. This deflector did not reduce the erosion depth noticeable.

**Stone bags around a pier**

This type of protection guarantees a flexible connection of the riprap with the pier and therefore good results have been obtained with this type of protection (Eastern Scheldt Storm Surge Barrier and Ekofisk offshore construction).

Grouted gravel or sand has been used as a repair method for scour under the bottom of a caisson.

## 4.6    Calculation methods

### 4.6.1    Introduction

The local scour process around a bridge pier is divided into several
phases:

1      initiation of the scour process,
2      developing phase,
3      equilibrium phase.

The time dependent growth of the maximum depth of a scour hole in the
developing phase is described with the Breusers method, section 4.6.2.

In the equilibrium phase the shape and the maximum depth of a scour hole
are constant and do not depend on time. For the maximum scour depth in the
equilibrium phase many semi-empirical formulas have been published, see
section 4.6.3. For a first estimation of the shape of a schematized scour
hole some information is given in section 4.6.4.

Local scour around a bridge pier is a relatively rapid process, therefore
mainly formulas for the equilibrium phase have been developed.

### 4.6.2    Time dependent maximum scour depth

### 4.6.2.1    Introduction

The Breusers method has been developed first for sills with a bed
protection, see chapter 4. Recently some successfull attempts to apply
these same approach to the scour process around a bridge pier have been
published. In this section the results of these efforts are summarised. The
dimensionless scour depth is an empirical power-function of time:

$$\frac{y_{max}}{y_0} = \{\frac{t}{t_1}\}^\gamma \tag{4.3}$$

in which

$y_{max}$ =    time dependent maximum scour depth in the scour hole around the
          pier                                                           (m)
$y_0$  =    original water depth just upstream of the pier              (m)
$t$    =    time                                                         (s)
$t_1$  =    time at which $y_{max} = y_0$                                (s)
$\gamma$    =    empirical constant                                      (-)

The exponent in formula 4.3 is analysed in section 4.6.2.2. In section 4.6.2.3 the formulas to estimate the time $t_1$ in (4.3) are analysed.

4.6.2.2    The exponent y

The time dependent development of the maximum scour depth near a bridge pier can be described in analogy of the Breusers method with formula (4.3).

For a rectangular pier Nakawaga et al, lit.[4.21], measured $y_{max}$ at a corner of this pier. The type of scour is probably clear water scour because the upstream bed consists of fixed sand layer, see fig 7 of lit.[4.21]. Also from the data in publications from Davies, Ninomiya and Delft Hydraulics it was possible to determine a value for  . For a squared pier Ninomiya et al, lit.[4.24], measured the results for clear water scour, shown in table 4.2.

| $B_p$ / $y_0$ | $y_{max}/y_0$ | y | author |
|---|---|---|---|
| 1 | 0.002 to 0.15<br>0.15 to 0.55 | 0.8<br>0.22 | Nakawaga et al.<br>Nakawaga et al. |
| 0.4 | 0.02 to 0.10<br>0.10 to 0.60 | 0.8<br>0.22 | Nakawaga et al.<br>Nakawaga et al. |
| 0.3 to 0.5 | 0.2 to 0.8 | 0.1 | Davies et al. |
| 0.8 | 0.04 to 0.7 | 0.36 | Ninomiya et al. |
| 1.2 to 1.9 | 0.6 to 1.5 | 0.23 | DHL-report M1841 |

*Table 4.2 The exponent  y for different bridge piers*

From these references it seems to be that the exponent  is not sensitive to the angle between the main direction of the approach flow and the longest axis of the rectangular pier.

Davies et al, lit.[4.10] determined  y = 0.10, but this result needs further verification, because of viscosity effects in the scouring around the small circular piers where $B_p$ = 0.016, 0.019 and 0.025 m and $y_0$ = 0.05 m.

Dargahi, lit.[4.9], determined from one detailed scour test, y = 0.38. This test concerns a circular cylinder with $B_p$ = 0.15 m, $y_0$ = 0.20 m and $y_{max}$ = 0.12 m.

Dargahi used a formula, which is similar to formula (4.3):

$$\frac{y_{max}}{y_{max,e}} = c_A \cdot \left\{ \frac{t}{t_e} \right\}^y \tag{4.4}$$

in which

$y_{max,e}$     = equilibrium scour depth which is the local maximum     (m)

$t_e$     = time after which the equilibrium scour depth is reached (s, days)

$c_A$     = coefficient, approximately equal to 1     (-)

Formula (4.4) can be written as:

$$\frac{y_{max}}{B_p} = \frac{y_{max,e}}{B_p} \cdot \left\{ \frac{t_1}{t_e} \right\}^y \cdot c_A \cdot \left\{ \frac{t}{t_1} \right\}^y \tag{4.5}$$

In a two dimensional flow pattern, for example at the edge of a bed protection the maximum scour depth follows from (4.3) with $y$ = constant, 0.38. Laboratory tests with groynes and abutments showed that in a strongly three-dimensional flow field the scour process cannot be described by $y$ = constant, but with a variable exponent according to (4.6):

$$y = 10^{p \cdot y_{max} / y_0 + v} \tag{4.6}$$

in which

p     = empirical constant     (-)

v     = empirical constant     (-)

From the results of a test in a scale model of a pier of a preliminary design of the Eastern Scheldt Storm Surge Barrier, with $B_p/y_0$ = 1.2 and $y_{max}/y_0$ = 0.3 to 2.0 (see DHL-report M1385, lit [4.13]), the following values of p and v have been determined, see DHL-report Q647, lit.[6.16]: p = -0.34, v = -0.10 (see also figure 4.4). These values apply to clear water scour.

In case of live bed scour a lower value of will be obtained if $y_{max}/y_0 > 1$.

The results of a test in a scale model of a circular caisson of an offshore construction with $y$ = 0.23, see DHL-report M1841, lit.[4.15], imply that p = 0 and v = -0.64.

All these results have been plotted in the graph with $y$ as a function of $y_{max}/y_0$, see figure 4.4. In the initiation phase of the scour process rather high values of $y = 0.8$ have been measured.

In the development phase the results show a considerable scatter, which is partly caused by the influence of the water depth. In the equilibrium phase the water depth reduces the maximum scour depth, if $B_p/y_0 > 0.3$, according to Melville and Sutherland, lit.[4.20]. In the present report the limit is choosen to be $B_p/y_0 > 1$ for a first estimation. The scatter in figure 4.4 can be reduced by the following refinement, see figure 4.5:

$B_p/y_0 \geq 1$ then:

$$\frac{y_{max}}{y_0} = \{\frac{t}{t_1}\}^y \qquad\qquad (4.3)$$

$B_p/y_0 < 1$ then:

$$\frac{y_{max}}{B_p} = \{\frac{t}{t_1}\}^y \qquad\qquad (4.7)$$

It seems reasonable that if $B_p < y_0$ the maximum scour depth is more determined by $B_p$ than by $y_0$. The remaining scatter is caused by the different geometries and possibly by the difference between live bed scour and clear water scour. The analysis of more published results of scale model tests is recommended.

For a very first estimation the following values can be recommended, see figure 4.5:
- clear water scour :    $p = -0.3$ and $v = -0.1$
- live bed scour
    if $y_{max}/y_0 < 1.5$ :  $p = -0.3$ and $v = -0.3$
    else                    $y = 0.2$

The most important differences between $y_{max} / y_0$ according to these values of $y$ can be observed in the first part of the developing phase as $t/t_1 < 0.5$. For the maximum scour depth in the last part of the developing phase, as $t > t_1$, these differences are rather small.

Clear water scour starts slowly relative to live bed scour, but after $t > t_1$ clear water scour reaches a deeper scour depth than live bed scour, see figure 4.6. This is confirmed by figure 5.1 of the Scouring-manual, lit.[4.6], see figure 4.7.

4.6.2.3    The reference time $t_1$

Nakawaga and Suzuki, lit.[4.21], used a slightly different definition of (4.3), $y_0$ has been replaced by $B_p$ as in (4.7). Then they found from the experimental results:

$$t_1 = 37.5 \cdot B_p^{2.9} \cdot y_0^0 \cdot (\alpha \cdot U_0 - U_{cr})^{-3} \tag{4.8}$$

in which $\alpha = 1.4$

From theoretical considerations Nakawaga et al supposed that the constant 37.5 should also depend on the relative density $\Delta$ of the bed material:
$$37.5 = 29.2 \, \Delta^{0.5}$$

in which    $\Delta = (\rho_s - \rho)/\rho$.

The relative density of sand is 1.65 as an average value.
In the test program only sand has been used as bed material, and therefore no verification of their theoretical consideration has been obtained.
It is mentioned that in their experiments $B_p/y_0 = 1$ and 0.4, therefore it can be concluded that if $B_p/y_0 < 1$ then $t_1$ does not depend on $y_0$ but on $B_p$.

From tests with a squared pier Ninomiya et al, lit.[4.24], found in the developing phase of the scouring process, if
$0.1 < y_{max}/y_0 < 0.5$:

$$t_1 = C \cdot g \cdot y_0^2 \cdot U^{-3} \tag{4.9}$$

in which
C    = constant                                                              (-)

In the tests $B_p/y_0 = 0.8$ and $B_p/y_0$ is smaller than 1, therefore, it should be preferred to replace $y_0$ in (4.9) by $B_p$. In all their tests they kept $B_p/y_0 = 0.8$, therefore, this replacement affects only the constant C.

The formula (4.8) and (4.9) can be compared with the Breusers formula for $t_1$:

$$t_1 = 250 \cdot \Delta^{1.7} \cdot y_0^2 \cdot [\alpha \cdot U - U_{cr}]^{-4.3} \tag{4.10}$$

The exponent -4.3 in (4.10) has been confirmed in a scale model study of a pier for the Eastern Scheldt Storm Surge Barrier, lit.[4.13]. Nakawaga et al found -3 instead of -4.3. This result of the study of Nakawaga has been confirmed by Ninomiya (only if $U > U_{cr}$).

The geometry factor $\alpha$ has the following values:

| pier geometry | flow | $B_p/y_0$ | study | $\alpha$ |
|---|---|---|---|---|
| rectangular pier | current | 0.4 to 1 | Nakawaga | 1.4 |
| elongated pier | current | 1.2 | DHL-M1385 | 7.15 |
| cylindrical pier | current | 1.2 to 1.9 | DHL-M1841 | 7.8 |
| | waves | | DHL-M1841 | 5.8 to 6.3 |

*Table 4.3   Parameter $\alpha$ as a function of the geometry*

The difference between a rectangular pier and an elongated or circular pier can probably be explained by the value of $B_p/y_0$.

Finally the following tendency for the reference time $t_1$ is recommended for the scour around bridge piers in the developing phase:

- $B_p/y_0 < 1$

$$t_1 = B_p^x \cdot [\, \alpha \cdot U - U_{cr} \,]^y \tag{4.11}$$

   with
   x = 2 to 2.9
   y = -3 to -4.3
   $\alpha$ depends on the geometry, see table 4.3.

- $B_p/y_0 > 1$ then $B_p$ in (4.11) should be replaced by $y_0$.

The presented formules for $t_1$ can be summarized in the following general expression:

$$t_1 = C \cdot \Delta^w \, p^x \cdot (\alpha U - U_{cr})^y \tag{4.12}$$

with

$P = B_p$ if $B_p / y_0 < 1$

$P = y_0$ if $B_p / y_0 \geq 1$

$2 \leq x \leq 2.9$

$-3 \leq y \leq -4.3$

and $\alpha$ according to table 4.3

## 4.6.3   **Equilibrium maximum scour depth**

The maximum scour depth can be written as a dimensionless parameter $y_{s,max}/B_p$ or $y_{s,max} / y_0$, in which $B_p$ is the width of the pier and $y_0$ is the waterdepth. In case of a single cylindrical pier, which is placed in an uniform approach flow and an uniform sand, this parameter is a function of:

- the waterdept: $B_p / y_0$, expressed in factor $K_{y0}$;
- the approach flow velocity, either is divided by the critical flow velocity for the initiation of motion: $U / U_{cr}$ or expressed in a dimensionless Froude number, $Fr = U / (g . y_0)^{0.5}$. Normally only subcritical flow is considered, therefore $Fr < 1$.

This most simple case has been used as a reference for all other cases and the deviations with respect to this simple case are expressed in socalled K-factors:

- pier shape, which is expressed in factor $K_s$;
- the orientation of the pier to the flow, which is expressed in the factor $K_\omega$;

- the distance between the piers: a separated pier with no influence of the other piers, or a group of piers close to each other with some interference of the water motion and the local scour holes, factor $K_{gr}$;
- the gradation of the bed material, which is expressed in the factor $K_g$;
- the grain diameter and the density of the material, which are expressed in the critical flow velocity for the initiation of sediment motion.

The influence of the flow velocity can be described as follows:

- if $U/U_{cr} > 1$ then socalled live bed scour occurs; which means that sediment motion upstream of the pier results in a supply of sediment in the local scour hole. An decrease of the approach flow velocity will result in a modest increase or even a reduction of the maximum scour depth, because of the sharp increase of the sediment supply from upstream.

- if $U/U_{cr} < 1$ then socalled clear water scour occurs; which means that the local scour hole is not filled with sediment from upstream of the pier. The maximum scour depth strongly increases with an increase of the flow velocity.

The critical flow velocity $U_{cr}$ can be determined as follows:
- from the Shields graph, for the upstream approach conditions,
  $U_{cr} = c. u_{*,cr}$ and $u_{*,cr} / \{g \Delta D_{50}\} = $ constant
  the constant c depends on the vertical velocity profile,
- eventually from the formula of Hincu for sand.

For sand near a pier the critical flow velocity is about 0.5 of the critical flow velocity in the upstream approach conditions.

ripple forming (coarse material) and non-ripple forming (fine material)

The influence of different factors on the maximum scour depth is treated in the following by comparing this influence relative to the case of a circular cylinder founded in uniform sand as bed material.
As a general formula for the maximum depth of the local scour hole around a bridge pier a combination of the formula of Breusers, lit.[4.5], the formula of the IAHR-manual on scouring, lit.[4.6], and the formula of Shen, lit.[4.6], is proposed.

With Breusers formula (1977) the maximum scour depth around a single cylindrical pier in a uniform flow and placed on a bed of uniform sand can be calculated:

$$\frac{y_{s,max}}{B_p} = 1.5 . f(U/U_{cr}) . \tanh(y/B_0)_p \qquad (4.13)$$

The $f(U/U_{cr})$ is defined as:

If $\quad U/U_{cr} \leq 0.5$ no local scour: $\qquad\qquad f(U/U_{cr}) = 0$

$0.5 < U/U_{cr} \leq 1.0$ clear water scour: $\qquad f(U/U_{cr}) = 2 . U/U_{cr} - 1$

$\qquad U/U_{cr} > 1.0$ live bed scour: $\qquad\qquad f(U/U_{cr}) = 1$

The constant 1.5 gives the best fit with measured scour depths. However, if (4.13) is applied as a design formula, then 1.5 should be replaced by 2.0, which means a safety factor of 1.3 with respect to the maximum measured scour depths. This gives an impression of the accuracy of (4.13), and the standard deviation of the normal distribution is estimated at $0.1\ y_{s,max}/B_p$

For other situations than a single cylindrical pier in a uniform flow and placed in a uniform sand formula (4.13) can be extended to a more general form:

$$\frac{y_{s,max}}{B_p} = 1.5 . f(U/U_{cr}) . \tanh(y_0/B_p) . K_s . K_\omega . K_g . K_{gr} K_{size} \qquad (4.14)$$

in which

| | | |
|---|---|---|
| $K_s$ | = factor for the influence of the pier shape | (-) |
| $K_\omega$ | = factor for the influence of the alignment of the pier | |
| | to the flow | (-) |
| $K_g$ | = factor for the influence of the gradation of the bed | |
| | material | (-) |
| $K_{gr}$ | = factor for the influence of a group of piers instead of | |
| | a single pier | (-) |
| $K_{size}$ | = factor for the influence of the relative size of the pier | |
| | and the sediment | (-) |

It is remarked that in (6.13) $\tanh (y_0/B_p)$ is the factor for the influence of the water depth.
In the basic situation of one single pier which has a cylinder-shape and has been placed into uniform bed material: $K_s = 1$, $K_\omega = 1$, $K_g = 1$ and $K_{gr} = 1$.

For a first order estimate of the local scour depth formula (4.15) is given in the IAHR-manual on Scouring (1991):

$$\frac{y_{s,max}}{B_p} = 2.3 \cdot K_s \cdot K_\omega \cdot K_g \cdot K_{gr} \cdot K_{y0} K_{size} \qquad (4.15)$$

In practice, live bed scour is far more important than clear water scour, therefore formula (4.15) is based on live bed scour. This formula can be compared with formula (4.14) and the main difference is the value of the constant 2.6 instead of 2.0 (when applied as a design formula). That means that (4.15) can be used as a design formula with a safety factor of 1.30 with respect to the maximum measured scour depths.

This formula shows some similarity with the design formula of Melville and Sutherland, lit.[4.20], for live bed scour. They replaced the constant 2.6 by 2.4 and for uniform sediments this design formula with constant 2.3 includes a safety factor of 1.15 to 1.30.

In the United States Shen (1969), lit.[4.6], has developed the socalled Colorado State University formula:

$$\frac{y_{s,max}}{B_p} = (2.2 \text{ to } 3.4) \ Fr^{0.43 \text{ to } 0.67} \cdot \{ Y_0/B_p \}^{0.33 \text{ to } 0.35} \qquad (4.16)$$

in which:

$$Fr = U / \sqrt{(g \cdot y_0)}$$

The influence of the flow velocity in (4.15) can be compared with this influence in (4.13).
It is remarked that in (4.15) $K_{y0} = \{ y_0/B_p \}^{0.33 \text{ to } 0.35}$ is the factor for the influence of the water depth.
This relation has been confirmed by A-Han Chen, lit.[4.17] only with some minor changes in the constant and the exponents. In his report he includes also tables with data from his tests, which concern a circular pier in two bed materials, one uniform and one graded.

**Water depth**

The water depth does not influence the maximum scour depth if
$y_0 / B_p > 2.6$. However if $0.5 < y_0/B_p < 2.6$ then this influence follows from, see Melville and Sutherland, lit.[4.20]:

$$K_y = 0.78 \ ( \ y_0/B_p)^{0.255} \tag{4.17}$$

This formula gives the minimum reduction compared with the data. For the extreme case with $y_0 < 0.5 \ B_p$ no data are available.

**Pier shape**

The influence of the shape of a horizontal cross section of the pier has been investigated by Laursen and Toch (1956), lit.[4.19], Neill (1973), lit.[4.22] and Dietz (1972), lit.[4.12]. These results confirm each other, therefore one table with recommended values of $K_s$ can be composed:

| form of horizontal cross- section | $K_{s(-)}$ |
|---|---|
| lenticular | 0.7  to 0.8 |
| elliptic | 0.61 to 0.83 |
| circular | 1.0 |
| rectangular | 1.0  to 1.2 |
| rectangular with semi-circular nose | 0.90 |
| rectangular with chamferred corners | 1.01 |
| rectangular nose with wedge-shaped tail | 0.86 |
| rectangular with sharp nose 1:2 to 1:4 | 0.65 to 0.76 |

Table 4.4    Shape factor $K_s$ for the influence of the shape of a horizontal cross section of the pier.

The shape of a vertical cross section can also be expressed in the value of $K_s$. The basic case is a pier with a prismatic shape and $K_{s,v} = 1.0$.
A pier with a circular horizontal cross section and in elevation tapered:

| form of vertical cross section | $K_{s,v}$ (-) |
|---|---|
| pyramid like (upwards narrowing) | 0.76 |
| pyramid up-side down (upwards broadening) | 1.2 |

Table 4.5  Shape factor $K_{s,v}$ for the influence of the shape of  a  vertical cross section of the pier.

For piers with a foundation footing or a pile-cap no data for the shape factor were found in the mentioned references.

**Alignment of the pier to the flow**

For cylindrical piers no influence of the angle of flow attack on the maximum equilibrium scour depth has to be considered, if the spacing between the piers is more than $3 B_p$ to $11 B_p$

For piers with a rectangular horizontal cross section this influence has been studied by Laursen and Toch, lit.[4.19]. If the angle of attack is zero (that means the angle between the main axis of the horizontal cross section of the pier with the direction of the approach flow) then $K_\omega$ = 1. Their empirical relationship in figure 4.8 has been confirmed roughly by data of Chabert and Engeldinger and Varzeliotis.

Nakagawa and Suzuki, lit.[4.21], have presented some results of scour around a rectangular cross section with $L_s/B_p$ = 1.75 and the angle of attack $\omega$ = 0, 30 and 45 degrees. They found that the final scour for 30 degrees is almost equal to that for 45 degrees, but it is much larger than that for zero degrees: $K_\omega$ = 1.3 to 1.8. This confirms the graph of Laursen and Toch roughly.

Frohlich has given a formula for $K_\omega$ which confirms also this graph roughly.

**Gradation of bed material**

The gradation of bed material can be characterised by the geometric standard deviation $\sigma_s$, see Vanoni, lit.[4.26]:

$$\sigma_s = \{ D_{84} / D_{16} \}^{0.5} \tag{4.18}$$

For illustration of this parameter some values of $\sigma_s/D_{50}$ are given:

natural river sand $\qquad\qquad\qquad$ $\sigma_s/D_{50}$ = 0.8
uniform sand $\qquad\qquad\qquad\qquad$ $\sigma_s/D_{50}$ = 0.3

In the basic case the bed material consists of uniform sand with $K_g$ = 1.

The effect of the grain size distribution on $y_{s,max}$ was reported by Raudkivi and Ettema, lit.[..]. The relation between $K_g$ and $\sigma_s/D_{50}$ is given in figure 4.9. These results are only valid if $u_* = u_{*,cr}$. Figure 4.9 is replotted in figure 4.10 showing $K_\sigma$ as a function of $\sigma_g$.

A more general method to determine the effect of the gradation has been published by Melville and Sutherland, lit.[4.20]. This method is summarised below with some adjustments.

They used an approximation of the geometric standard deviation of the particle size distribution:

$\sigma_s \approx D_{84} / D_{50}$

natural river sand $\qquad\qquad \sigma_s$ = around 1.3

uniform sand $\qquad\qquad\qquad \sigma_s < 1.3$

If $\sigma_s < 1.3$ no effect of the gradation, therefore $K_g = 1$.

If $\sigma_s > 1.3$ a representative diameter of the armour layer is calculated with:

$$D_{50,a} = 0.55 \cdot \sigma_s^{2.28} \cdot D_{50} \qquad\qquad (4.19)$$

The critical flow velocities for $D_{50}$ and $D_{50,a}$ can be calculated with the Shields graph and the modification of this graph according to van Rijn:

$$D_* = D_{50} [ \Delta \cdot g / \nu^2 ]^{0.33} \qquad\qquad (4.20)$$

$$D_{*,a} = D_{50,a} [\Delta \cdot g / \nu^2 ]^{0.33} \qquad\qquad (4.21)$$

The Shields parameter $\theta_{cr}$ follows from:

$$D_* \leq 4 \qquad \theta_{cr} = 0.24 \, D_*^{-1}$$

$$4 < D_* \leq 10 \qquad \theta_{cr} = 0.14 \, D_*^{-0.64}$$

$$10 < D_* \leq 20 \qquad \theta_{cr} = 0.04 \, D_*^{-0.10}$$

$$20 < D_* \leq 150 \qquad \theta_{cr} = 0.013 \, D_*^{0.29}$$

$$D_* \geq 150 \qquad \theta_{cr} = 0.055$$

If in the above formulas $D_*$ is replaced by $D_{*,a}$ then $\theta_{cr,a}$ is calculated with these formulas. The critical shear velocity follows from the definition of the Shields parameter:

$$u_{*,cr} = \sqrt{\theta_{cr} \cdot \Delta \cdot g \, D_{50}} \qquad\qquad (4.22)$$

$$u_{*,cr,a} = \sqrt{\theta_{cr,a} \cdot \Delta \cdot g \, D_{50}} \qquad\qquad (4.23)$$

With the assumed logarithmic velocity distribution the critical approach flow velocities can be calculated:

$$U_{cr} = 5.75 \ u_{*,cr} \cdot \log \left[ \frac{12Y_0}{3.D_{50} + \delta/4} \right] \tag{4.24}$$

$$U_{cr,a} = 5.75 \ u_{*,cr,a} \cdot \log \left[ \frac{12Y_0}{3.D_{50,a} + \delta/4} \right] \tag{4.25}$$

in which $\delta$ is the thickness of the sublayer:

$$\delta = 11.6 \quad / \ u_{*,cr} \tag{4.26}$$

$$\text{or } \delta = 11.6 \quad / \ u_{*,cr,a}$$

$$\text{If } U < U_{cr} \quad : U_a = U_{cr,a} \tag{4.27}$$

$$\text{If } U > U_{cr} \quad : U_a = 0.8 \ U_{cr,a}$$

If $U_a < U_{cr}$ then Melville and Sutherland recommend $U_a = U_{cr}$ as a first approximation.

$$\text{If } \frac{U - (U_a - U_{cr})}{U_{cr}} \leq 1 \quad \text{then } K_g = 2.4 \ \left| \frac{U - (U_a - U_{cr})}{U_{cr}} \right|$$

$$\text{If } \frac{U - (U_a - U_{cr})}{U_{cr}} \geq 1 \quad \text{then } K_g = 2.4$$

In general this method is on the safe side and in the publication of Melville and Sutherland this method has been tested on quite a few measured data.

## Group of piers

As the most simple case a group of only 2 piers is considered:

- 2 piers, with a circular cross section, in a line parallel to the flow direction:

  The maximum scour depth around the front pier will increase by a maximum 15 % if the pier spacing is 2 to 3 $B_p$. The influence of the second pier on the front pier scour disappears if the pier spacing > 15 $B_p$. The maximum scour depth of the rear pier is reduced by 10 to 20 %. This reduction is almost independent of the pier spacing.

- 2 piers, with a circular cross section, in a line perpendicular to the flow direction:

  The mutual influence of both piers on the maximum scour depth disappears if the pier spacing > 10 $B_p$.
  If the pier spacing is very small < 1.5 $B_p$ both piers have almost the same effect as one pier with a diameter of 2 $B_p$ of a single pier. Therefore, the maximum increase in maximum scour depth is 100 %.

- 2 piers, with a circular cross section, with a variable angle ω between the line through the piers and the flow direction (angle of attack)
  If the pier spacing is 5 $B_p$, then the maximum scour depth around the upstream pier (the front pier) is not sensitive for the angle of attack: the maximum increase is 15 % at an angle of attack of 45 degrees.
  The maximum scour depth around the downstream pier (the rear pier) is sensitive for the angle of attack: the maximum increase is 20 % at an angle of attack of 45 degrees.

These results for 2 circular piers are summarised in table 4.6:

| angle of attack (degrees) | pier spacing (B_p) | front pier $K_{gr}$ (-) | rear pier $K_{gr}$ (-) |
|---|---|---|---|
| 0 | 1 | 1.0 | 0.9 |
| 0 | 2 to 3 | 1.15 | 0.9 |
| 0 | > 15 | 1.0 | 0.8 |
| 45 | 1 | 1.9 | 1.9 |
| 45 | 5 | 1.15 | 1.2 |
| 45 | > 8 | 1.0 | 1.0 |
| 90 | 1 | 1.9 | 1.9 |
| 90 | 2 to 3 | 1.2 | 1.2 |
| 90 | > 8 | 1.0 | 1.0 |

Table 4.6   The factor $K_{gr}$ for a group of 2 circular piers

The results for 2 piers in table 4.6 are a confirmation of the general rule
that the resulting scour hole of a group of piers  can be considered as the
superposition of the separated scour holes of the individual piers.

### 4.6.4   Shape of a local scour hole

The shape, the slopes of a scour hole and the maximum scour depth determine
the  volume  of a scour hole, and the minimum extend of a bed protection to
prevent a local scour. First the shape of  a  local  scour  hole  around  a
cylindrical  pier is treated and next the local scour hole around all other
types of piers.

**A single cylindrical pier**

The reference case of a single pier in a uniform flow and  founded  into  a
uniform  bed  material  has  been  studied in detail. For example, Dargahi,
lit.[4.9], gives a detailed description of  the  development  of  the  side
slopes  of  a  local scour hole around a single cylindrical pier during the
scouring process, see figure..

For  that situation the shape of local scour hole in a horizontal cross
section has been schematized into a half circle at the upstream  side;  and
at  the  downstream  side this half circle is connected with the half of an
elongated ellipse. Bonasoundas, lit. [4.4], used  this  schematization  for
the bed protection around a cylindrical pier.

The upstream part of the scour hole has an upper part slope and a slope for the deepest part of the scour hole. This slope in deepest part of the scour hole is gouverned by the horseshoe vortex. For simplicity these two slopes, which differ only two degrees in the experiments of Dargahi, are averaged into one side slope of 0.90 of the angle of internal friction or the angle of the natural slope $\epsilon$.

In the same way the downstream part has a steeper lower part slope than the upper slope of a scour hole. The difference between these slopes is about 4 degrees. Therefore both are averaged into a slope of 0.47 $\epsilon$.

These side slopes are expressed in the angle of repose because the angle of repose is an upper limit for the side slope in a two dimensional geometry. In a local scour hole the concave three dimensional surface can result in some sideway support by which a steeper stable slope can be obtained than the angle of repose. However this effect has been observed only in sand with some cohesion by clay particles, for example in the prototype tests in the Brouwerssluice, but not in pure non-cohesive sand, for example in laboratory tests.

The angle of repose depends on the type of soil and also on the compaction of the soil, see table 4.7 for some characteristic values.

| soil type | | angle of repose (degrees) |
|---|---|---|
| coarse sand, | compact | 45 |
| sand and gravel | firm | 38 |
| | loose | 32 |
| | | |
| medium sand | compact | 40 |
| | firm | 34 |
| | loose | 30 |
| | | |
| fine sand | compact | 34 |
| | firm | 30 |
| | loose | 28 |
| | | |
| fine silty sand | compact | 32 |
| sandy silt | firm | 30 |
| | loose | 28 |
| | | |
| fine uniform silt | compact | 30 |
| | firm | 28 |
| | loose | 26 |
| | | |
| day (saturated) | medium | 10-20 |
| | soft | 0-20 |

*Table 4.7  The angle of repose for different soils.*

The schematized shape of a local scour hole is a function of the side slopes, the radius of the upstream half circle and the length of the axis of the downstream half ellipse.

The top radius of a local scour hole is measured from the center of the cilindrical pier, see figure...:

upstream   :  radius of a circle          $2 B_p$
downstream:  longest axis of an ellipse   $5 B_p$
             shortest axis of an ellipse  $2 B_p$

The downstream value is not a radius, but the half length of the longest axis of the ellipse, and the length of the shortest axis is equal to two times the upstream radius. The radius of the bottom of a local scour hole is measured also from the center of a cylindrical pier:

upstream   : radius of a cirle            $0.6 B_p$
downstream : longest axis of an ellipse   $0.8 B_p$
             shortest axis of an ellipse  $0.6 B_p$

With these data of slopes and widths of the schematized scour hole the volume and the minimum extend of a bed protection, to prevent a local scour hole, can be determined, if the water depth $> 3 B_p$. It is remarked that no difference is observed between the shape of the local scour hole in clear water scour or in live bed scour. The gradation can have some minor influence on the shape of a scour hole, because by segragation in the scour hole the coarse fraction will form a layer on the bottom of the scour hole.

**Other types of piers**

With respect to the shape of local scour holes around non-cylindrical piers in a non uniform flow no systematic data about this shape have been found in the used references. By combining some data from different sources average values have been assessed.

The characteristic values of the side slopes of a local scour hole have been measured from graphs and figures from different publications, see table 4.8 In all these publications no information about the angle of repose has been included, therefore this angle has been estimated. For these estimations it is assumed that in laboratory tests the sand had a loose compaction and that in prototype situations the soil had a firm compaction after many years of consolidation.

In some situations the water depth is less than $3 B_\rho$, therefore the water depth reduces the maximum scour depth to some extend, but it is supposed that this influence does not affect the shape of the scour hole.

| research / author | pier | flow | $\epsilon$ | side slopes | |
|---|---|---|---|---|---|
| | | | | upstream $\epsilon$ | downstream $\epsilon$ |
| Dargahi | 1 | a | 32 | 0.90 | 0.47 |
| Nakawaga / Suzuki | 1 | b | 35 | 0.07 | 0.03 |
| Delft Hydr. M1841 | 1 | a | 30 | 0.92 | - |
| Delft Hydr. | 1+1 | a | 35 | 0.90 | 0.45 |
| Nakawaga/ Suzuki | 2 | a | 32 | 0.80 to 0.90 | 0.70 |
| Delft Hydr. M1385 | 3 | a | 28 | 0.95 | 0.50 |
| | 3 | b | 28 | 0.78 | 0.30 |
| Average values | | a | | 0.90 | 0.50 |
| | | b | | 0.70 | 0.25 |

pier:    1 = cylindrical pier
         2 = rectangular pier
         3 = rectangular pier with circular nose

flow:    a = unidirectional flow
         b = tidal flow

*Table 4.8    Side slopes in a local scour holes of different piers.*

From table 4.8 the following conclusions can be formulated:
-   The shape of the pier has probably no influence on the maximum upstream side slope of the local scour hole.
-   In an estuary tidal flow will reduce the side slopes of a local scour hole:

|                      | upstream side | downstream side |
|----------------------|---------------|-----------------|
| unidirectional flow  | 0.9 $\epsilon$ | 0.5 $\epsilon$  |
| tidal flow           | 0.7 $\epsilon$ | 0.25 $\epsilon$ |

In case of tidal flow the upstream side of a pier or the downstream side is defined relative to the highest flow velocity during ebb or flood flow.

These conclusions are based on a limited number of references and need further confirmation from other studies. This holds also for the assumption regarding the neglectable influence of the water depth on the shape of the scour hole. The influence of gradation of the subsoil and the flow direction ω relative to the pier axis on this side slope of a local scour hole can not be assessed from this limited number of references.

## 4.7  Research needs

In this section not only research needs are described, but also aspects, which are missing in this draft version of the manual and which are proposed to be included in a final version.

In this draft version of the manual only the local scour near a bridge pier is treated, and it is recommended to include the constriction scour. Also some general aspects of the influence of bridge piers and bridge abutments on the flow pattern and the morphology of a river should be included.

In the developing phase of a scour hole the preliminary expression for tl needs further confirmation and development.

The methods, which are mentioned in this manual to prevent bridge pier scour, are not complete. Specially the effectiveness of these methods to reduce the maximum scour depth should be included in this manual.
The interaction between an ice cover and a bridge pier scour hole is not treated in this manual. Ice can increase the effective size of a pier and therefore the local scour. It is recommended to expand the manual with this interaction.

The influence of waves and the combination of waves and currents on bridge pier scour is not included in this manual. It is recommended to include this influence.

For the equilibrium phase of the scour process a general formula for the maximum scour depth is missing. The proposed formula and the existing formulas need more verification on data from scale models and from the prototype. For verification purposes a representative and complete data base of bridge pier scour measurements would be advantageous.

## 4.8 References

4.1    C.J. Baker
New design equations for scour around bridge piers
Journal of the Hydraulics Division of the ASCE, HY4,
April 1981, pp507 - 511

4.2    C.J. Baker
Theoretical approach to the prediction of scour around bridge piers
Journal of Hydraulics Research, Vol. 18, No.1, 1980, pp 1 - 12

4.3    J.C. BLODGETT
Effect of bridge piers on streamflow and channel geometry
Transportation Research Record 950
Committee on Hydrology, Hydraulics and Water Quality,
USA, 198.., pp. 172 - 183

4.4    M. BONASOUNDAS
Stromungsvorgang und kolkproblem am runden Bruckenpfeiler
Versuchsanstalt fur Wasserbau, Bericht No 28
Techn. Universitat Munchen, Munchen, Germany, 1973

4.5    H.N.C. BREUSERS, G.NICOLET AND H.W. SHEN
Local scour around cylindrical piers
Journal of Hydraulic Research 15, no 3, 1977, pp 211 - 252

4.6    H.N.C. BREUSERS AND  A.J. RAUDKIVI
Hydraulic structures design manual, Scouring
A.A. Balkema
Rotterdam / Brookfield, 1991.

4.7    T. CARSTENS
Seabed scour by currents near platforms
Third international conference on port and ocean engineering
under artic conditions
University of Alaska, 19.., pp 131 - 145

4.8   R. ETTEMA
      Scour at bridge piers
      University of Auckland, report no. 216
      Auckland, New Zealand, 1980


4.9   B. DARGAHI
      Flow field and local scouring around a cylinder
      Bulletin No. TRITA - VBI - 137
      Department  of Hydraulics Engineering, Royal Institute of Technology,
      Stockholm, Sweden, 1987


4.10  S.K. DAVIES AND G. DE VAHL DAVIS
      Erosion of the sand bed near piers
      7th Australasian Hydraulics and Fluid Mechanics Conference,
      Brisbane, Australia, August 1980, pp. 220 - 224


4.11  S.R. DAVIS
      Case histories of scour problems at bridges
      Transportation Research Record 950,
      Committee on Hydrology, Hydraulics and Water quality   USA,   1984   of
      later, pp. 149 - 155


4.12  J.W. DIETZ
      Ausbildung von langen Pfeilern bei Schraganstromung am
      Beispeil der BAB-Mainbrucke Eddersheim
      Mitt. blatt der bundesanstalt fur Wasserbau, Karlsruhe,  Germany,  No
      31, 1972, pp 79 - 94


4.13  DELFT HYDRAULICS,
      Stormvloedkering   Oosterschelde,   werkgroep   8,   Vormgeving   en
      konstruktie van sluitgaten, WL8-44 Ontgrondingen bij de putten van de
      pijleroplossing
      DHL-report M1385, Delft, April 1976


4.14  DELFT HYDRAULICS, G.J. AKKERMAN
      Stormvloedkering Oosterschelde, Werkgroep 8,
      Vormgeving  en  konstruktie van sluitgaten, WL8-59 Ontgrondingen rond
      putten bij gedeeltelijk verdedigde bodem
      DHL-report M1402, Delft, July 1976

4.15  DELFT HYDRAULICS, J.L.M. KONTER

Texaco Mittleplate Platforms, scour and bed protection

DHL-report M1841, Delft, January 1982


4.16  DELFT HYDRAULICS, J.DRIEGEN

Handboek ontgrondingen, analyse geometriefaktor alfa in een extreem driedimensionaal geval.

DHL-report Q647, Delft, December 1987


4.17  A. HAN CHEN

Local scour around circular piers

Thesis, Asian Institute of Technology, Bangkok, Thailand, 1980


4.18  P. HJORTH

Studies on the nature of local scour

Bull. Ser. A No 46

Department of Water Resources Engineering, Lund Institute of Technology, Lund Sweden, 1975


4.19  E.M. LAURSEN AND A. TOCH

Scour around bridge piers and abutments

Bull. No 4, Iowa Highway Res. Board, 1956


4.20  B.W. MELVILLE AND A.J. SUTHERLAND

Design method for local scour at bridge piers

Journal of the Hydraulics Division of the ASCE, Vol.114, No.10, 1988, pp 1210 - 1226


4.21  H. NAKAWAGA AND K. SUZUKI

Local scour around bridge pier in tidal current

Coastal engineering in Japan, Vol. 19, 1976, pp 89 - 100


4.22  C.R. NEILL

Guide to bridge hydraulics

University of Toronto Press, 1973


4.23  C.R. NEILL AND L.R.MORRIS

Scour problems at railway bridges on the Thompson River Canadien Journal of civil Engineering 7, 1980, pp.357 - 372

4.24 K. NINOMIYA, K. TAGAYA AND Y. MURASE
A study on suction and scouring of sit-on-bottom type
offshore structures
Offshore technology conference, Dallas, Texas, United States,
1972, pp I-870 to I-878

4.25 H.W. SHEN, V.R.SCHNEIDER AND S. KARAKI
Local scour around bridge piers
Proceedings ASCE, vol. 95, (HY6), 1969, pp. 1919 - 1940

4.26 V.A. VANONI (EDITOR)
Sedimentation engineering
American Society of Civil Engineers, New York, USA, 1977
Chapter 6 Bridge piers

4.27 WEST VIRGINIA UNIVERSITY
Scour around bridge piers
Morgantown, West Virginia, United States, February 1980

## 5. <u>Outlets</u>

### 5.1 **Introduction**

In general, an outlet is positioned downstream of a hydraulic structure, such as sluices, outlets of low head hydropower stations, weirs or the outlet of cooling water of thermal power stations. Therefore many different types of outlets exist, here only some types of outlets with rectangular cross sections are considered. An important class of circular pipe outlets is missing in this draft version of the manual. The main geometric parameters of an outlet are defined in section 5.2.

The main features of the flow pattern in and downstream of an outlet are treated in section 5.3. This flow pattern causes scour holes in the bed downstream of the structure and these scour holes can induce a failure of the structure, section 5.4.

Methods to calculate the main dimensions of these scour holes are treated in section 5.5. Some data on scour holes downstream of outlets are collected in section 5.6. Finally the most important research needs for the calculation methods are summarised (section 5.7) and a list of references is given in section 5.8.

### 5.2 **Characteristic geometric dimensions**

The shape of some types of outlets with a rectangular cross section can be characterised by a horizontal or gentle sloped bed protection (hydraulic rough or flat), which is bordered by two diverging wing walls. In most cases the bed protection is longer than the length of the wing walls, see figure 5.1. In general the rate of divergence of the wing walls is less than 1:8 to prevent a separation of the flow. Such a separation will result in an a-symmetric flow pattern at the downstream end of the bed protection, and an increase in the size of the scour hole. With a sill, energy-dissipaters or other devices, this separation can also be prevented and then the slope of divergence can be increased to for example 1:4.

As a special case, the prototype tests in the Brouwersluis are considered with a sill in the bed protection. These results have confirmed the results of three-dimensional scour holes in a systematic model investigation in a flume.

The following characteristic dimensions are determined:

-       the length of the bed protection $L_p$ and the dimensionless parameter $L_p /y_0$,

-       the sill height $y_D$ and the dimensionless parameter $y_D /y_0$,

-       the length of the vertical constriction on the sill $B_{s,c}$ and the dimensionless parameter $B_{s,c} / B_s$, in which $B_s$ = width of the sill.

The length of the bed protection Lp is measured from the structure to the nearest edge of the bed protection in the direction of the flow.


Some types of outlets with rectangular cross sections are not considered in this chapter, because no information is available in the literature in section 5.8 on these outlets, such as:

- an outlet without a bed protection,

- an outlet with non-symmetric wing walls, or with submerged wing walls,

- an outlet with the flow direction of the discharge not parallel to the flow direction of the receiving river or estuary. This affects the shape of the scour hole and can often be observed in outlets of cooling water circulation systems of power plants.


## 5.3  Characteristic flow pattern

The type of structure determines the main flow pattern and the turbulence intensity at the downstream edge of the bed protection.

After the most constricted cross section of the structure the flow decelerates above a bed protection. Normally the flow is sub-critical with a rather low turbulence intensity after an outfall with, for example, some tubes, see figure 5.2. Downstream of some hydropower turbines a much higher turbulence intensity should be expected. High turbulence intensities can be expected if the flow is super-critical followed by a hydraulic jump above the bed protection and sub-critical flow at the downstream end of the bed protection. If the bed protection consists of a concrete plate, then in general this bed protection is equipped with energy dissipaters.

The vortex street downstream of the separation point at the end of the wing wall can be decisive for a three-dimensional scour hole. If this vortex street is weak compared with the main discharge through the outlet, this main discharge causes a more or less two-dimensional scour hole.

If the direction of the discharge of the outlet is perpendicular to the flow direction of the receiving river or estuary, the described flow pattern is inclined to the direction of the flow in the river. This will also influence the shape of the scour hole.

The detailed flow pattern in the scour hole has been described in chapter 2. If the flow characteristics at the end of the bed protection show a good similarity with the flow characteristics at the end of a bed protection near a sill or a spurdike, then the formulas and the theory given in the chapters about sills and spurdikes can be applied.


## 5.4 Failure mechanism

The failure mechanism of the bed protection and the structure by too deep scour holes with too steep initial slopes is almost the same as described in the chapter about sills.
If the bed protection consists of a concrete plate with energy dissipaters then undermining of this plate by the downstream scour hole should be prevented.
An important difference is that in general the bed protection should be continued some distance downstream of the end of the wing walls. The vortex street downstream of the wing wall ending can cause a strong three dimensional scour hole. This scour hole endangers the stability of the wing wall. The soil mechanical aspects of the stability of the wing walls are similar as mentioned in the chapter about abutments. It is recommended to treat these aspects more in detail.


## 5.5 Calculation methods

### 5.5.1 <u>Introduction</u>

The following calculation methods of the maximum scour depth are treated:
The maximum scour depth during the development phase of the scour hole can be calculated with the Breusers-formula, in which the coefficient $\alpha$ is related to the geometry and the flow pattern of an outlet, (section 5.5.2). An alternative approach should be a relation between $\alpha$ and the turbulence intensity at the edge of the bed protection, see Jorissen and Vrijling, lit.[5.10]; this is not treated here. It is recommended to develop such an

approach, if sufficient data from scale models or from prototypes are available, see chapter 2 about sills, section 2.5.2.4.

The maximum scour depth in the equilibrium phase is estimated with some empirical formulas from Dietz and Zanke, see chapter 2.

For the initial slope of a scour hole no calculation method is included in this draft version of the manual. In DHL-reports M1533, lit.[5.3, 5.4, 5.5], some data about measured slopes in scale models and the prototype can be found.

### 5.5.2 Maximum scour depth according to the Breusers-formula

The maximum scour depth can be calculated with the Breusers-formula, see chapter 2, if a fair estimation of the value of the coefficient $\alpha$ in that formula can be made. In this section most attention is paid to the determination of the value of $\alpha$.

First the value of $\alpha$ depends on the definition of average flow velocity U. The definition of U in the Breusers formula is in case of an outlet as follows:

$$U = Q / ( y_0 \cdot B_{s,b})$$ (5.1)

in which

| | | |
|---|---|---|
| Q | = discharge | $(m^3/s)$ |
| $B_{s,b}$= | width of the bed protection between the | |
| | end of the wing walls | (m) |
| $y_0$ = | water depth above the bed protection | |
| | between the end of the wing walls | (m) |

or

$$U = Q / ( y_0 \cdot B_s)$$ (5.2)

in which

| | | |
|---|---|---|
| $B_s$ = | width between the wing walls just upstream | |
| | of the sill on the bed protection | (m) |
| $y_0$ = | water depth above the bed protection just | |
| | upstream of the sill | (m) |

With three-dimensional scour holes the coefficient γ is not constant (0.38 to 0.40) but varies, see chapter 3 about spurdikes. In the earliest investigations α has been determined from the measurements, with the supposition of a constant γ. It is recommended to re-analyse these data with a variable gamma. It is expected that the general relationship will not change by this re-analysis, possibly only the equilibrium scour depth will reduce.

The value of α is independent of the flexibility of the bed protection (especially the downstream end of the bed protection), see DHL-report M1533- part III, lit.[5.4]. The roughness of the bed protection has a relatively small influence on the value of α, see also DHL-report M1533 part III.

**The length of the bed protection**

In a vortex street with a high turbulence level the coefficient α in the Breusers-formula can be estimated as a function of the dimensionless length of the bed protection $L_p/y_0$, in a geometry with $y_D/y_0 = 0$ with a formula from chapter 5 about spurdikes:

$$\alpha(L_p/y_0) = 1.5 + (1.55 \; \alpha_{10} - 2.35) \; . \; e \qquad\qquad (5.3)$$

From figure 5.3 it is indicated that with formula (5.3) and $\alpha_{10} = 3.5$ to 5 a fair estimation of α can be obtained.

Probably this formula can be used also if $L_p/y_0 < 5$, because a short bed protection will not cause a deviation in the flow pattern near the scour hole as can be observed after sills, when a bottom eddy just behind the sill can protect the scour hole, see also chapter 2 about sills.

In figure 5.3 the results of different investigations with complex geometries are presented, therefore the value of $L_p/y_0$ is not very accurate, see also table 5.1. However the general tendency according to (5.3) is not sensitive for this inaccuracy. Also the calculation of α from $\alpha_{local}$ is not very accurate.

It is recommended to extend this figure with the results of the Grevelingen-discharge structure, DHL-report M1321.

This result which is presented in figure 5.3, means that the $\alpha$ of a scour hole downstream of an outlet has the same value of $\alpha$ of

- a vertical constriction of $y_D/y_0$ = 0.6 combined with a horizontal constriction $B_s/B$ = 0.1, and U = Q / ( B . $y_0$ ) in which $y_0$ = water depth upstream of the vertical constriction, or
- a horizontal constriction of $B_s/B$ = 0.1 to 0.5 only, y = variable, $L_p/y_0$ = 5 and U = Q / ($y_0$ . ($B_s/B_s$)), in which U is related to the most constricted cross section, the socalled throat of the structure.

The scour hole due to a vortex street downstream of a wing wall is almost the same as the scour hole due to a small spur dike.

These kind of comparisons are complicated by the different definitions of the velocity and the length of the bed protection.

It is recommended to use the data of scale model tests in DHL-reports M1533 - I, III and IV, lit.[5.3, 5.4, 5.5], to investigate the interaction between horizontal constrictions and vertical constrictions.

### 5.5.3   Equilibrium scour depth

The equilibrium scour depth can be approximated with the formula, which Zanke lit.[5.11] has published for a two-dimensional flow pattern:

$$T = 6 . y_{s,max}^2 . w^4 . \theta^4 \left[ \{ (U_m . \frac{c_4}{1 + y_{s,max}} )^2 . - U_{cr}^2 \} \right.$$

$$\left. D*^4 . \nu . c_5 . 10^{-7} . ( U_b / U_m )^4 / p \right] \qquad (5.4)$$

in which

| | | |
|---|---|---|
| T | = time in which the maximum scour will be realized | (s) |
| w | = fall velocity of bed material | (m/s) |
| $\theta$ | = shape factor depending on the geometry | (-) |
| $U_m$ | = average velocity above the bed protection | (m/s) |
| $U_{cr}$ | = critical, average velocity | (m/s) |
| D* | = diameter of the bed material, defined (9.  ) | (m) |
| D* | = $(\Delta . g . \nu^{-2})^{0.33} . D$ | |
| $U_b$ | = velocity at y = $0.05y_0$ from the bottom | (m/s) |
| p | = 1 - porosity | (-) |

It is necessary to determine the value of $\theta$, $c_4$ and $c_5$ from a previous measured development of a scour hole. The parameter $c_4$ depends on $y_{s,max}/y_0$ and therefore varies during one test. At this moment no recommended values for theta, $c_4$ and $c_5$ are available for different structures with a strong three dimensional flow pattern.

In M1533 part III, lit.[5.4], this formula has been compared with the measured equilibrium scour depth. This comparison showed a reasonable result, see figure 5.5.


## 5.6 Data

The maximum scour depth downstream of an outlet has been determined in different scale model investigations by DHL recently. In all these investigations outlets with rectangular cross sections, diverging wing walls and a bed protection of riprap were tested. From the measured scour depths the value of $\alpha$ has been determined. In table 5.1 the geometric parameters of the most important tests and the values of $\alpha$ are listed. In the first column the number of the DHL-reports is given. This table can be the start of a more extensive data-base of scale model data.

| lit. | $y_0$ m | $L_p$ m | $y_D$ m | $B_{s,c}$ m | $B_s$ m | $L_p/y_0$ | $y_D/y_0$ | $B_{s,c}/B_s$ | $\alpha$ - |
|---|---|---|---|---|---|---|---|---|---|
| Q77 | 4,5 | 270 | 0 | 0 | 0 | 60 | 0 0 | 0 | 2,4 |
| M2110 | 4 | 70 | 0 | 0 | 0 | 17 | 0 | 0 | 2.9 |
|  | 4 | 130 | 0 | 0 | 0 | 32 | 0 | 0 | 3.2 |
|  | 4 | 70 | 0 | 0 | 0 | 17 | 0 | 0 | 3.4 |
| Q243 | 5 | 140 | 0 | 0 | 0 | 28 | 0 | 0 | 2.9 |
| Q965 | 18 | 200 | 0 | 0 | 0 | 11 | 0 | 0 | locally 2.9-3.2 |
|  | 18 | 100 | 0 | 0 | 0 | 5.5 | 0 | 0 | locally 3.1 |
| | estimation of $\alpha = 1.5\ \alpha_{local}$ | | | | | | $\alpha$: 4.4-4.8 $\alpha$: 4.6 | | |
| M1533 part I | 10.8 10.8 | 65 65 | 5.4 3.6 | 5 5 | 50 50 | 6 6 | 0.5 0.33 | 0.1 0.1 | 6.1 4.2 |

Table 5.1  *Data of geometry parameters and $\alpha$ in a vortex street with a high relative turbulence intensity*

## 5.7 Research needs

This chapter about outlets with a rectangular cross section and a low head difference between the inflow and the outflow of the structure should be extended with a review of pipe outlets with a circular cross section. The scour holes due to these outlets with a relatively high head difference are similar to the scour holes due to free falling jets.

It is recommended to investigate the relation according to Jorissen and Vrijling between $\alpha$ and the relative turbulence intensity at the downstream end of the bed protection, because in the outflow of the considered type of outlet the turbulence intensities are rather high.

In addition of the outlets with a rectangular cross section the following geometries should be included:
- an outlet without a bed protection,
- an outlet with non-symmetric wing walls, or with submerged wing walls
- an outlet with the flow direction of the discharge not parallel to the flow direction of the receiving river or estuary.

The formula for the equilibrium scour depth should be tested on more scale model data. Probably the formula of Zanke can be reduced to a more simple formula.


## 5.8 References

5.1    DELFT HYDRAULICS
       Systematisch onderzoek naar twee- en driedimensionale ontgrondingen,
       DHL-report   M648 / M863, Band I
       Delft, 1972


5.2    DELFT HYDRAULICS
       Systematisch onderzoek bodembescherming, invloed geometrie en aard
       van de verdediging bij driedimensionale ontgrondingen,
       DHL-report M847 - III.
       Delft, 1972

5.3    DELFT HYDRAULICS
       Sluis Brouwersdam
       DHL-report M1533, deel I,
       Delft, 1982

5.4    DELFT HYDRAULICS
       Sluis Brouwersdam
       DHL-rapport M1533 part III
       Delft

5.5    DELFT HYDRAULICS
       Sluis Brouwersdam
       DHL-report M1533, deel IV,
       Delft, 1982

5.6    DELFT HYDRAULICS
       Waterkrachtcentrale Maurik
       DHL-report M2110
       Delft, 1986

5.7    DELFT HYDRAULICS
       Waterkrachtcentrale Linne
       DHL-report Q243
       Delft, 1986

5.8    DELFT HYDRAULICS
       Waterkrachtcentrale Alphen
       DHL-report Q77
       Delft, 1987

5.9    DELFT HYDRAULICS
       Stormvloedkering Oosterschelde
       Een  overzicht  van  methodieken  voor  voorspelling  en bewaking van
       ontgrondingen langs de rand bodembescherming
       DHL-report Q635
       Delft, 1988

5.10  R.E. JORISSEN AND J.K. VRIJLING
      Local scour downstream hydraulic constructions
      23th Congress of IAHR, Ottawa, Canada, August 1989
      pp. B-433 - B-440

5.11  U. ZANKE
      Zusammenhange zwischen Stromung und Sedimenttransport, Teil  2:
      Berechnung     des     Sedimentstransportes     hinter     befestigten
      Sohlenstrecken- Sonderfall zweidimensionaler Kolk
      Franzius Institut, Mitteilungen, Heft 48, Hannover, Germany,  1978

# 6. Jets

## 6.1 Introduction

Jets can occur as a result of flow under, through or over hydraulic structures, such as reservoirs, weirs and culverts. In this chapter only scour will be discussed as a result of jets occurring at high-head structures. The jets can be divided in submerged and free ones. Scour downstream of culvert outlets can be considered as a special case of submerged jets and is discussed in chapter 5. The scour due to flow over and under low-head structures such as gates, weirs and low dams can with respect to the underflow situation be compared with the submerged jet to be treated in this chapter, while refer is made to chapter 2 with respect to the overflow situation.

The main geometric parameters of submerged and free jets are defined in section 6.2. The flow pattern in a jet is discussed in section 6.3. The failure mechanism will be treated in section 6.4. Section 6.5 summarizes the available calculation methods which can be applied for design purposes. Finally, the most important research needs and a list of references are summarized in section 6.6 and 6.7 respectively.

## 6.2 Characteristic geometric parameters

A distortion has to be made between submerged and free or plunging jets. Both jet types can be two dimensional (circular) or three dimensional (plane). Furthermore, submerged jets can be divided into horizontal and vertical jets and plunging jets into vertically or obliquely impinging jets. In figure 6.1 examples of the different jet types are shown.

The important parameters with respect to jet scour (figure 7.2) are:
- the equilibrium scour depth $y_{s,max}$,
- the length $L_s$ of the scour hole,
- the width $B_s$ of the scour hole for two dimensional jets, and
- the length $L$ of a fixed (protected) bed.

For design purposes it is not relevant to deal with the development of the scour with time, because the final scour depth is attained in a few hours. Stilling basins are sometimes applied as energy dissipation structure or area in order to protect the region of intensive scour. Design methods for these structures will not be presented in this chapter.

## 6.3 Characteristic flow pattern

The parameters that determines submerged jet flow are (figure 6.3):
- the efflux velocity $u_o$,
- the efflux parameters $D_u$ or $2 B_u$ for three dimensional (circular) or two dimensional (plane) jets respectively,
- the distance x for the efflux opening, and
- the radial distance r to the centre line of the jet.

The submerged jet flow can be characterised by a linear increase in width and a Gaussion velocity distribution in the fully developed part of the jet. The first part of the jet, the flow establishment zone, has a core of diminishing width and length $L_k$. In the core the velocity is equal to the efflux velocity.

In the fully developed part of the jet the velocities can be calculated with [6.1]:

$$3D\text{-jet and } x > 6 D_u : \qquad \frac{U_m}{U_o} = 6 \frac{D_u}{x} \tag{6.1}$$

$$\frac{U}{U_m} \exp \left[-72(\frac{r}{x})^2\right] \tag{6.2}$$

$$3D\text{-jet and } x > 12 B_u: \qquad \frac{U_m}{U_o} = (\frac{12 B_u}{x})0.5 \tag{6.3}$$

$$\frac{U}{U_m} \exp \left[-56(\frac{r}{x})^2\right] \tag{6.4}$$

Submerged vertical jets will offen strike the river bed perpendicularly. A wall jet (figure 6.3) will be the result. Refer is made to [6.1] with respect to the special velocity equations for this type as well as for more details about the presented equations.

Plunging jet flow can be characterised by (figure 6.3):
- the efflux or overfall velocity $u_o$ or the specific discharge $q_o$,
- the difference H in upstream and downstream water level,
- the velocity $u_o'$, dimension Du (or 2 Bu) and the angle $\beta$ at the impact location of the free jet with the tailwater level.

The equations (6.1) up to (6.4) can be applied for determining the jet velocity and dimensions if the values at the moment of impact are taken as initial values. These values can be calculated with:

$$b_1 = \frac{q}{(u_o^2+v_1^2)^{0.5}} = \frac{q}{(u_o^2+2gy\phi^2)^{0.5}} \qquad (6.5)$$

in which:
| | | |
|---|---|---|
| $q$ = specific discharge | $(m^2/s)$ |
| $u_o$ = initial velocity | $(m/s)$ |
| $v_1$ = vertical component of jet velocity at entry point | $(m/s)$ |
| $y$ = downstream energy height | $(m)$ |
| $\phi$ = velocity coefficient | $(-)$ |

For $\phi$ the following values can be applied:

| $y$ (m) | 1 | 2 | 3 | 4 | 5 |
|---|---|---|---|---|---|
| $\phi$ (-) | 0.965 | 0.930 | 0.895 | 0.870 | 0.855 |

The angle $\beta_1$ can be determined with:

$$\beta_1 = \{\tan (v_1/u_o)\}^{-1} = \{ \tan (\phi(2gy)^{0.5}/u_o)\}^{-1} \qquad (6.6)$$

The depth of jet penetration may be taken as 20 $D_u$ for circular jets and 80 $B_u$ for plane jets.
The jet velocity is during its flight in air affected by aeration. However, it is recommended to ignore this influence for design purposes. [6.2]

### 6.4 Failure mechanism

The relative high velocities in jet flow together with the high turbulence level will result in scouring of the river bed if no stilling basin is provided. This holds particularly in the case of submerged vertical jets and impinging plunging jets, which strike the bed perpendicularly or obliquely. In that situation a stagnation zone with increased pressure is formed (figure 6.3).

The erosion process itself is quite complex and depends upon the interaction of hydraulic and morphological factors. Scouring can have the following effects:

- The endangering of the stability of the structure itself by scour holes with too steep initial slopes,
- The endangering of the stability of the downstream river bed and banks,
- The formation of a mound of eroded material which can raise the tailwater level at high-head structures (only in the case of plunging jets).

If a stilling basin is applied, scour will occur downstream of this basin. The scour depth depends on the length of the stilling basin. Information about the design of stilling basins is presented in [6.3] and will not be given in the report.

## 6.5 Calculation methods

### 6.5.1 Introduction

In general, the available calculation methods give an indication of scour to be expected. For most situations the various methods result in rather large differences in predicted scour dept. Therefore, it is recommended to perform detailed physical model studies for each particular design. This holds especially for plunging jets, but also for submerged jets.

In this section generally applicable calculation methods if available will be presented for submerged horizontal and vertical jets (section 6.5.2) and plunging jets (section 6.5.3). All methods will be related to the equilibrium scour depth. An overview of the calculation methods is presented in [6.3] and [6.4].

### 6.5.2 Submerged jets

The functional relationship for the equilibrium scour depth $Y_{s,max}$ for both horizontal and vertical jets reads:

$$Y_{s,max} = f(D_u, U_0, U_{*c}) \tag{6.7}$$

in which:

| | | |
|---|---|---|
| $D_u$ | = efflux opening | (m) |
| $U_o$ | = efflux velocity | (m/s) |
| $U_{*c}$ | = critical shear stress velocity for the given bed material | (m/s) |

Note, that equation (6.7) is for circular (3D) jets. In the case of plane (2D) jets, the parameter $D_u$ should be replaced by $2B_u$.

Furthermore, some experiments mentioned in literature give also other parameters, such as the bed material diameter D, the upstream and downstream water level difference H and the fall velocity w of bed material. These parameters are not included is equation (6.5) because they do not appear generally in the different methods.

The available experimental data have been replotted using the parameters in equation (6.5). This resulted in the figures 6.4 and 6.5. From these figure the following equations could be derived [6.4]:

submerged horizontal jet (figure 6.4):

$$\text{circular jet:}\quad \frac{Y_{s,max}}{D_u} = 0.08 \, \frac{U_o}{U_{*c}} \tag{6.8}$$

$$\text{plane jet:}\quad \frac{Y_{s,max}}{2B_u} = 0.008 \, (\frac{U_o}{U_{*c}})^2 \tag{6.9}$$

submerged vertical jet (figure 6.5):

$$\text{circular jet:}\quad \frac{Y_{s,max}}{D_u} = 0.75 \, \frac{U_o}{U_{*c}} \qquad \text{for} \quad \frac{U_o}{U_{*c}} < 100 \tag{6.10}$$

$$\frac{Y_{s,max}}{D_u} = 0.35 \, (\frac{U_o}{U_{*c}})^{2/3} \qquad \text{for} \quad \frac{U_o}{U_{*c}} > 100 \tag{6.11}$$

$$\text{plane jet:}\quad \frac{Y_{s,max}}{2B_u} = 0.05 \, (\frac{U_o}{U_{*c}})^{4/3} \tag{6.12}$$

The length $L_s$ of the scour hole due to a horizontal jet can be approximated with:

$$L_s = 7 \cdot Y_{s,max} \tag{6.13}$$

The diameter $D_c$ of the scour hole due to a vertical jet can be approximated with:

$$D_c = 5 \cdot Y_{s,max} \tag{6.14}$$

A remark should be made about $Y_{s,max}$ for the vertical jets. The value resulting from the above given equations is the one related to the static scour, viz. after the jet flow ceased. From the experiments it proved that the dynamic scour depth can be 1.3 times larger. Some researchers even found values up the two times the static scour depth.

## 6.5.3  Plunging jets

A general applicable calculation method for determining the scour depth due the plunging jets is not available. Most equations are of the form:

$$Y_s + Y_o = f (q, H, D) \tag{6.15}$$

In [6.3] a comparison is made between the various scour prediction equations for a practical case. The results were that most relations predict a scour depth in the right order, although the differences are large (factor 1.5 compared to measured prototype scour depth).

One equation will be presented here because it is based on 47 model data sets and 26 prototype data sets. This equation reads [6.5] [6.6]:

$$Y_s + Y_o = (6.42 - 3.1H^{0.1}) \cdot q^{0.6 - 0.0033H} \cdot H^{0.05 + 0.005H} Y_o^{0.15} g^{-0.3} D_{50}^{-0.1} \tag{6.16}$$

The equation is based on the assumption of $D_{50} = 0.25$ m for the prototype data. The accuracy of equation (6.16) is about 25%.

## 6.6  Research needs

Many of the available calculation methods are based on small-scale experiments resulting in prediction equations that show great variation in the form of the equations and the coefficients. Furthermore, the influence of some parameters on the scour depth is not clear, for instance the distance H and the effect of aeration in the case of plunging jets.

On the basis of the fore going, it is recommended to carry out research onto the following subjects:
- the determination of the influence of the water level difference H,
- the influence of the bed material diameter D on scour depth and length of the scour hole,
- the ratio between static and dynamic scour depth,
- the verification of the available methods with prototype data, and
- the influence of stilling basins on the scour downstream.

## 6.7 References

6.1    N. RAJARATNAM
       Turbulent jets
       Elsevier, Amsterdam, 1976

6.2    E. HAUSLER
       Spillways and outlets with high energy concentrations,
       Trans. Int. Symp. on the lay-out of dams in narrow gorges, ICOLD, Rio de Janeiro II, 1983.

6.3    J.G. WHITTAKER AND A. SCHLEISS
       Scour related to energy dissipators for high-head structures.
       Mitt. nr. 73, VAW/ETH, Zurich, 1984.

6.4    H.N.C. BREUSERS AND A.J. RAUDKIVI
       Scouring, Hydraulic structures design manual no 8
       A.A  Balkema, Rotterdam, 1991

6.5    P.J. MASON
       Erosion  of plunge pools downstream of dams due to the action of free trajectory jets
       Proc. Inst. Civ. Engrs, Part 1, 76, 1984

6.6    P.J. MASON AND K. ARUMUGAM
       Free jet scour below dams and flip buckets
       J. Hydr. Eng., ASCE 111(2), 1985

# 7. Waves

## 7.1 Introduction

Wave (and current) velocities often increase in the neighbourhood of coastal structures, which increases the scour near the structure. By studying the influence of a structure on the local hydrodynamics, an estimate can be made of the likelihood and possible extent of scour induced by waves and currents. The main effects of a structure on the local hydrodynamics are:

(i) The local peak orbital velocities in front of the structure are increased, as a result of combined incident and reflected waves. The increased orbital velocities and the induced scour can be related to a reflection coefficient $C_r$ of the structure.

(ii) Waves and tidal currents concentrate along or close to the structure. Since these effects can not be accounted for as with (i), they should be obtained from site-specific studies.

Simple prediction methods are available at present which relate the scour depth to the incident wave conditions, the local water depth, the structure geometry and/or the reflection coefficient. No effects of angled wave attack, tidal or wave induced currents are accounted for.

This chapter deals with the scour induced by wave and current actions near seawalls, breakwaters, pipelines, piles and submerged structures.

## 7.2 Pipelines

### 7.2.1 Calculation methods

Scour around pipelines may be caused by currents and/or waves. In shallow water storm waves can produce large velocities in both horizontal and vertical directions. If the sea bed is composed of erodible materials, the dynamic equilibrium of granular sediments may be disturbed and scouring occurs. Kjeldsen et al [7.3]. Proposed the following relation for the equilibrium scour depth, based on experiments with pipes with diameters of 0.06 to 0.50 m and sediment grain size of 0.074 mm:

$$S = 0.972(U^2/g)^{0.2} D^{0.8} \tag{7.1}$$

where  S = equilibrium scour depth below the bottom of the pipeline    (m)
       U = flow velocity                                              ($m^2$/s)
       g = gravitational acceleration, g = 9.81                       (m/$s^2$)
       D = pipe diameter                                              (m)

The scour depth is not influenced if the ratio of water depth to pipe diameter is greater than 3 to 5.

Chao and Hennessy provide an order-of-magnitude estimation of the maximum scour depth under offshore pipelines due to currents.

Herbich [7.3] reports on experiments to study the effects of storm waves on buried pipelines approaching the shoreline. A tentative conclusion of two- and three-dimensional tests is that the presence of the pipe does not appreciably affect the equilibrium beach profile.

There is a clear difference between pipes submerged in intermediate or deep water, and pipes submerged in shallow water. In the latter situation the wave-induced drag and lift forces on the pipe and the water particle velocities are much higher than in intermediate or deep water. This results in fundamentally different soil properties, whence different design approaches and considerations apply for both situations.

7.2.2   <u>Measures to mitigate scour</u>

Protection of pipelines can be established by several methods. One method is to bury pipelines by dumping rocks on them. A more expensive method uses flexible mat-shaped membranes filled with mortar to cover pipelines. An economic method is the use of longitudal sausage-shaped mats which are only partly filled with mortar. Two of them are positioned on either side of the pipeline and one on top of them.

7.3  **Piles**

7.3.1   <u>Calculation methods</u>

Zanke [7.1] introduced the parameter A/b, where A=H/sin kh is the double amplitude of the orbital motion of water at the bed and b is the diameter or width of the structure. Steady flow conditions are approached for

A/b > 100. With decreasing A/b the net local scour depth decreases rapidly and the maximum depth moves to the flanks. With waves superimposed on a current the net local scour depth approaches the values due to the current only.

**Currents**

Turbulence is the main cause of scour near piles. The scouring force is dominated by primary vortices developing in front of the pile.
Herbich [7.3] recognizes that up till now no satisfactory theoretical model exists to predict scour around piles caused by currents. One has to resort to results obtained from experiments in order to predict this phenomenon. Ref. 7.3 describes two empirical models for prediction of scour induced by currents.

Jain and Fischer derived the following relations from open-channel experiments with uni-directional flow:

$$S_p / D_p = C_1 (h / D_p)^{0.5} (Fr - Fr_*)^{0.25} \qquad \text{(live bed)} \qquad (7.2)$$

and

$$S_p / D_p = C_2 (h / D_p)^{0.3} Fr_*^{0.25} \qquad \text{(clear water)} \quad (7.3)$$

where   $S_p$ = scour depth
$D_p$ = pile diameter perpendicular to the flow
$Fr = U/(gh)^{1/2}$   (Froude number)
$Fr_* = U_*/(gh)^{1/2}$ (critical Froude number)
$U$ = mean flow velocity
$U_*$ = critical velocity for initiating sediment movement
$h$ = mean flow depth
$g$ = gravitational acceleration

The coefficients $C_1$ and $C_2$ in these formulas are 1.86 , respectively 1.41. However, for design purposes it is recommended to use 2.0 (if (Fr - $Fr_*$ >= 0.2), respectively 1.84.

Results for local scour around piles from several researchers are summarized by Imberger, see fig. (7.1). He proposes the best fitting line to predict scour:

$$S_p / D_p = K (u_* / u_{*cr} - 0.374) \qquad (7.4)$$

where   $S_p$ = scour depth
       $D_p$ = pile diameter perpendicular to the flow
       $K$ = coefficient = 2.18
       $u_*$ = shear velocity
       $u_{*c}$ = critical shear velocity

Probably the upper limit for the ratio $S_p / D_p$ is 2.5.

**Waves**

Laboratory and field studies of scour around cylindrical piles due to waves show that initially scour develops at the sides of the pile. In this phase some bed material is deposited at the upstream and downsteam sides of the pile, but in the equilibrium phase these depositions are removed and the resulting scour hole has the shape of an inverted cone. The side slopes of the scour hole are equal to the sediment´s angle of repose.

The parameters which are characteristic for the description of scour around piles in wave action are:

| | | |
|---|---|---|
| $h$ | = still water depth | [m] |
| $L$ | = wave length | [m] |
| $H$ | = wave height | [m] |
| $T$ | = wave period | [s] |
| $d_{50}$ | = median grain diameter | [m] |
| $\rho_s$ | = density of sand | [kg/m$^3$] |
| $\rho$ | = density of water | [kg/m$^3$] |
| $\phi$ | = angle of repose of sand particles | [degrees] |
| $g$ | = gravitational acceleration | [m/s$^2$] |
| $D$ | = pile diameter | [m] |
| $C_s$ | = span between piles | [m] |
| $U$ | = free stream velocity | [m/s] |
| $S_u$ | = ultimate scour depth | [m] |
| $t$ | = elapsed time | [s] |

The functional relation between these variables for scour is:

$$S_u/H = f(H/gT^2, H/L, h/L, R_p, S_s, S_u/d, t/T, \phi, D/C_s) \qquad (7.5)$$

where $\quad R_p \quad = UD/\nu \quad$ (pile Reynolds number)

$\qquad \nu \qquad$ = kinematic viscosity

$\qquad S_s \quad = U/((g_s -1)gd)^{1/2}$ (sediment number)

$\qquad g_s \quad$ = specific gravity of sand

$\qquad d \quad$ = grain diameter

Equation (7.5) is not further specified in the used references.
Studies for scour around structures with more than one pile indicate that the formation of ripples is an important phenomenon. The wave height of the ripples should be added to the local scour depth in order to obtain the ultimate scour depth.

**Waves and currents**

Dimensional analysis gives the following functional relation for the scour depth $S_u$ at a cylindrical pile due to the combined wave and current motion:

$$S_u/D = f(h/L,H/L,UL(\rho_s-\rho)/\mu,(\rho_s-\rho)/\rho,U^2(\rho_s-\rho)/\tau,S_s,\tau',Re,S) \qquad (7.6)$$

where

| | |
|---|---|
| $S_u$ = ultimate scour depth | [m] |
| $D$ = pile diameter | [m] |
| $h$ = water depth | [m] |
| $L$ = wave length | [m] |
| $H$ = wave height | [m] |
| $U$ = mean fluid velocity | [m/s] |
| $\rho_s$ = density of sand | [kg/m$^3$] |
| $\rho$ = density of water | [kg/m$^3$] |
| $\mu$ =dynamic viscosity | [Ns/m$^2$] |
| $\tau'$ = time-averaged shear stress | [N/m$^2$] |
| $\tau$ = dimensionless shear stress | [-] |
| $S_s = U/((g_s -1)gd)^{1/2}$ (sediment number) | [-] |
| $g_s$ = specific gravity of sand | [-] |
| $d$ = grain diameter | [m] |
| $g$ = gravitational acceleration | [m/s$^2$] |
| $S = 0.316/Re^{1/4}$ D/U | [-] |

$$Re = UR/\nu \quad \text{(Reynolds number)} \qquad [-]$$

R   = hydraulic radius                                      [m]

$\nu$   = kinematic viscosity                               $[m^2/s]$

Equation (7.6) is not specified in the used references.

Experiments by Machemelh and Abad show that scour at a cylindrical pile due to a combination of waves and currents is dominated by the effect of currents. Eadie and Herbich conducted experiments to study the effects on scour near a cylindrical pile due to combined random waves and currents. Their main conclusions are:

- After an initially rapid scour development the scour rate decreased until an equilibrium scour depth was reached,
- Scour development due to current-wave interaction is faster than the development due to only steady current,
- The equilibrium scour depth due to current-wave interaction is about 10% geater than the depth due to only steady current, but the shapes of the scour holes are identical,
- The type of wave train (mono-chromatic or random) appears to insignificant for predicting the scour depth, but of importance for predicting the geometry of the scour hole.

### 7.3.2  Large diameter piles

Table 7.1. shows the scour depth and the extent of the scour hole for several piles with diameter $D_p$ larger than a tenth of the wavelength in a wave-current flow. These results are found by Rance during laboratory experiments.

| Pile shape | Scour depth | Scour extent |
|---|---|---|
| Circular | $0.06D_p$ | $0.75D_p$ |
| Hexagonal with side facing the flow | $0.07D_p$ | $1.00D_p$ |
| Hexagonal with corner facing the flow | $0.04D_p$ | $1.00D_p$ |
| Square with side facing the flow | $0.13D_p$ | $0.75D_p$ |
| Square with corner facing the flow | $0.18D_p$ | $1.00D_p$ |

*Table 7.1. Scour depth and extent for several pile shapes*

## 7.4 Seawalls

Seawalls can be divided into two types: seawalls which reflect waves and seawalls on which waves break. Seawalls which reflect waves as well break waves will cause serious erosion of the seabed in front of the seawall. On the other hand erosion has also been observed at locations where waves do not break.

### 7.4.1 Calculation methods

Reference [7.2] suggests the following relation for scour near vertical or steeply sloping structures, resulting from only wave action:

$$S_d = H_{max} \qquad (7.7)$$

with:

$S_d$ = maximum scour depth relative to the initial bed level

$H_{max}$ = height of the maximum unbroken wave that can be supported by the original water depth at the toe of the structure

In some cases however, this relation may under-estimate scour.
Some general rules suggested by several studies are:
- for $0.02 < s < 0.04$, the scour depth is approximately equal to the incident unbroken wave height. s is a factor for the structure geometry,
- maximum scour occurs when the structure is located around the plunge point of breaking waves,
- the scour depth is proportional to the structure reflection coefficient.

These methods apply for scour on sandy beaches; up till now little attention is paid to scour on shingle beaches.

The following expression is given in [7.3] for the asymptotic value of the scour depth:

$$S = (D-A/2) * \{(1-C_r)u_*[3/4C_d\rho \, \cot\theta/(d(y_s-y))]^{1/2} - 1\} \qquad (7.8)$$

where

$S$ = ultimate scour depth [m]

$D$ = still water level [m]

$A$ = $H_1 + H_r$ [m]

$H_1$ = loop height [m]

$H_r$ = node height [m]

$C_r$ = reflection coefficient [-]

$u_*$ = local fluid velocity parallel to bottom [m/s]

$C_d$ = drag coefficient [-]

$\theta$ = seawall angle [degr]

$d$ = water depth [m]

$\gamma_s$ = specific sediment weight [-]

$\gamma$ = specific fluid weight [-]

Experiments to scour in front of seawalls due to waves and currents lead to the following conclusions:

- Soon after the start of the experiments a very regular, sinusoidal-shaped pattern of ripples occurred.
- There is a limit to the scour depth in front of seawalls which is reached asymptotically; initially the scour depth develops rapidly. The scour depth is mainly determined by the local velocity parallel to the bottom.
- Scouring of natural flat sand beaches occurs in a narrow range of the ratio wave height H to water depth d. This range is between the boundary limits of wave breaking and incipient sand movement.
- For wave conditions in this range the scour depth initially increases with increasing number of waves acting on the bed; after obtaining its ultimate value the scour depth became independent of the number of waves.
- The scour wavelength (the distance between two crests) showed to be equal to half the wavelength and the extent of scour eqaul to one-fourth of the wavelength.
- The ultimate scour depth depends on the reflection coefficient which, of all seawalls studied, is lowest for $15^0$ seawalls. The scour depth increases with increasing reflection coefficient. For $45^0$, $67.5^0$ and $90^0$ seawalls little difference is found between the reflection coefficients, whence the measured relative ultimate scour depths were almost the same.

## 7.4.2   Measures to mitigate scour

Scour near coastal structures resulting from wave and current actions can be reduced or even prevented by the following measures:

- reducing the wave reflections will reduce the forces. This can be achieved by flattening the revetment slope by e.g. an energy-dissipating revetment face, or an almost horizontal berm on the revetment face,
- a scour control blanket may isolate the problem area close to the structure,
- the bed foundation material may be reinforced by grouting.

In many cases large stones or pre-cast concrete units of different shapes have been placed in front of seawalls. Although reflection of waves has not decreased and erosion continued the depth of erosion has been limited. Furthermore these units may serve as a foundation for additional units.

## 7.5   Breakwaters

For scour near breakwaters due to waves it is important whether waves arrive normally or obliquely. In the first case standing or partially standing waves are generated causing mounds and troughs at half, respectively quarter wavelengths distances from the breakwater. Obliquely arriving waves generate short-crested waves with complex orbital motions, such as vortices. Oblique waves are reflected almost completely; at the intersection of the incident and reflected waves island crests are formed. The mass-transport within the short-crested waves exceeds the mass-transport in the progressive incident waves and is maximal along the path of the island crests. Erosion caused by obliquely arriving waves occurs over a greater width of the bed than erosion by normally arriving waves; it is most severe adjacent to the face of the breakwater.
The effects of scouring in case of spectral waves are less than those of monochromatic waves.

## 7.5.1  Calculation methods

Flume tests described in [7.4] with bed slopes of 1:5 and 1:10 and with normally approaching flow lead to the following relation:

$$S/d_w = C \ (HL/dd_w)^2 \qquad\qquad (7.9)$$

where

|   |   |   |
|---|---|---|
| S = scour depth | [m] |
| d = water depth | [m] |
| $d_w$= water depth adjacent to the wall | [m] |
| H = wave height at d = 0.9 | [m] |
| L = wave length at d = 0.9 | [m] |
| C = 0.011 for the 1:10 slope | [-] |
|     0.033 for the 1:5 slope | [-] |

No relations are found for waves arriving obliquely.

## 7.5.2  Measures to mitigate scour

As with seawalls massive blocks can be positioned at the foot of breakwaters. It was found that this solution prevents scour from extending more than about 4 m.

## 7.6  Submerged structures

This section deals with offshore platforms and gravity structures. Little literature is available on these topics, which highlights the need for a continued research in this field.

## 7.6.1  Offshore platforms

Scour near an offshore platform can occur either in the form of local scour around each leg, or more widely around the whole complex. Both types can be caused by waves and/or currents. The scour hole due to currents alone takes the shape of an inverted cone of which the base is a few times the diameter of a leg of the platform. A combination of waves and currents however leads

to a scour hole with a width of one or two times the width of the whole structure.

No methods for calculating scour was found in the used references.

## 7.6.2 Gravity structures

The shape of the structure is an important parameter influencing scour. At the corners of square structure vortices may be formed due to waves or currents, resulting in an increase of scour. Oblique waves can cause trenches adjacent to the walls of the structure. Long-period effects may be more important than short duration storm waves.

Although for a combination of waves and currents the rate of scour development is faster than for only waves or only currents, the maximum scour depth is equal to or less than scour due to currents alone.

### 7.6.2.1 Calculation methods

The following relation is suggested by Torsethangen:

$$S/D = 1.8(U/U_{cr} - 0.54)d/D \qquad (7.10)$$

where

| | | |
|---|---|---|
| S | = scour depth | [m] |
| D | = structure diameter | [m] |
| U | = mean velocity | [m/s] |
| $U_{cr}$ | = incipient sediment motion velocity | [m/s] |
| d | = water depth | [m] |

Other studies simply suggest:

$$S = 1.5 D$$

Breusers found ratios of S/D between 1.3 and 1.75, whereas other researchers concluded that the size of the scour hole does not depend on sediment size, erodability and transport rate.

## 7.6.2.2   Measures to mitigate scour

Several methods exist for mitigating the effects of scour near gravity structures, such as hinged concrete slabs, clusters of sand bags, artificial seaweed and colcrete mats (flexible mats filled with mortar). The latter solution seems to be most promising due to its ease of installation.

## 7.7  Uncertainties in scour predictions

Several uncertainties are involved in the prediction of scour due to waves and currents. First it is difficult to obtain reliable information on soil characteristics of a dynamically active area as the ocean bottom. Also wave and current characteristics such as magnitude and frequency at a specific site may be hard or expensive to obtain. Furthermore the interaction (forces) between waves and a specific structure is very complicated and not yet described adequately. Another uncertainty stems from the fact that most results presented in this chapter are obtained from small-scale models in laboratories and not from field tests.

## 7.8  References

7.1   H.N.C. BREUSERS AND A.J. RAUDKIVI
      Scouring, Hydraulic structures design manual no 8
      Published by the Int. Ass. for Hydr. Research
      A.A. Balkema, Rotterdam, 1991

7.2   CUR/CIRIA
      Manual on the use of rock in coastal and shoreline engineering
      Gouda, 1991 (draft)

7.3   J.B. HERBICH
      Scour around pipelines, piles and seawalls
      Handbook of Coastal and Ocean Engineering, vol. 2, ch. 18
      Gulf Publishing Company

7.4    R. SILVESTER
       Scour around breakwaters and submerged structures
       Handbook of Coastal and Ocean Engineering, vol. 2, ch. 19
       Gulf Publishing Company

# 8. <u>Cohesive soils</u>

## 8.1  Introduction

The physico-chemical properties of cohesive sediments play a significant role in the resistance of cohesive soils against currents and waves. these properties depend strongly on the granulometric, mineralogical and chemical characteristics of the sediment involved. Up to now, direct quantitative relations between the physico-chemical properties and the erosion resistance have not been established. Nevertheless, design engineers require information to predict scour in cohesive soils, because these soils are the most widely spread sedimentary deposits in nature.

This chapter will give a few approaches which enable to predict scour depths as a first indication. The governing parameters of erosion of cohesive soils will be discussed in section 8.2. The calculation methods in section 8.3. Finally, the research needs will be summarized in section 8.4. A list of references is presented in section 8.5.

## 8.2  Governing parameters

The initiation of motion and the transport of non-cohesive sediments are both determined by the submerged weight of the particles. For cohesive sediments relative large forces are necessary to break the aggregates within the bed and relative small forces to transport the material. Experiments [8.1] [8.2] have shown that the scour of clay soils with natural structure (in a water saturated state) by water flows occurs in several stages. In the initial stage, elementary dispersed loosened particles and aggregates (separates) and those with weakened bonds are washed away. This process leads to a rougher surface with increased drag and lift forces on elements for further increase of flow velocity. Higher pulsating drag and lift forces increase the vibration and dynamic action on the protruding aggregates. As a result the bonds between aggregates are destroyed little by little until the aggregate is instantaneously torn out of the surface and carried away by the flow. Parameters that influence the above mentioned scour process are [8.3]:

- cohesion
- cation exchange capacity CEC
- salinity
- sodium adsorption ratio SAR
- pH-level of pore water
- temperature
- sand
- organic content
- porosity

In the following table the various effects on erosion are summarized. the strength of a bed of cohesive sediments increases for an:

| Pore water properties | | Sediment properties | |
|---|---|---|---|
| increase in | decrease in | increase in | decrease in |
| salinity (<2-10 ppt) | SAR pH T | bed density sediment concentration<br><br>CEC (at low SAR)<br><br><br>sand conc (at high SAR)<br>organic content | particle diameter CEC (at high SAR)<br><br><br><br><br>sand conc (at low SAR) |

*Table 8.1 Various effects on clay erosion*

According to Mirtskhoulava [8.1] the cohesion at saturation water content and the size of the particle diameter appear to be the most significant features among the extensive complex of physico-mechanical and chemical properties of cohesive soils. However, it does not suffice to rely on averaged properties, also the inhomogeneity has to be considered.

## 8.3 Calculation methods

General applicable design equations for the depth of scour holes are not available. Most equations in literature are related to one or two particular parameters influencing the erosion of cohesive soils, moreover, they are often related to a specific sediment. In this section two

approaches will be presented enabling the determination of an indicative value of the scour depth.

permissible nonscouring velocities

In many scour prediction equations a critical velocity $U_{cr}$ is applied. For instance, the Breusers-formula (see chapter 2):

$$y_{s,max} = f (\alpha \bar{U} - U_{cr})$$ (8.1)

As a first estimation the following values may be used for cohesive soils:

- fairly compacted clay (voids ratio 0.50) :  $U_{cr}$ = 0.80 m/s
- stiff clay (voids ratio 0.25)  $U_{cr}$ = 1.50 m/s


Mirtskhoulava presents also an equation to calculate the permissible nonscouring mean velocity [8.1][8.2]:

$$U_{cr} = \log(\frac{8.8 \ h}{D_{50}}). \ [0.0002.m\{(\rho_s-\rho)gD_{50}+1.25 \ C_f\}]^{0.5}$$ (8.2)

in which:

h   = water depth  (m)
$D_{50}$ = sediment diameter (m)
m   = coefficient
$C_f$ = fatigue rupture strength of clay    (Pa)
$\rho_s$ = density sediment  (kg/m$^3$)
$\rho$  = density water (kg/m$^3$)

The value of $C_f$ can be approximated with:

$$C_f = 0.035 \ C$$ (8.3)

in which:
C  = cohesion          (Pa)

In the following table values for C are given.

| type of clay | cohesion ($10^5$. Pa) |
|---|---|
| low compactness | 0.01 |
| medium compactness | 0.05 |
| compact | 0.15 |
| very compact | 0.30 |

*Table 8.2 Cohesion of clay*

The coefficient m accounts for the influence of different factors on canal operation conditions. A safe approximation is to use m= 1.

Based on equation (8.2) Mirtskhoulava presented tables with permissible nonscouring mean velocities(see [8.1]).

Finally, a simplified procedure is recommended in [ 8.2] if only the cohesion and the discharge is known. The equation reads:

$$U_{cr} = K \cdot Q^{0.2} \qquad \text{for Q > 10 m}^3\text{/s} \qquad\qquad (8.4)$$

Values for k can be found in table 8.3.

| soil type | cohesion ($10^5$.Pa) | k |
|---|---|---|
| low density loamy sand and clay | 0.005-0.02 | 0.30-0.40 |
| | 0.02 -0.04 | 0.40-0.50 |
| | 0.04-0.075 | 0.50-0.70 |
| medium density loamy clay | 0.075-0.100 | 0.70-0.75 |
| | 0.100-0.150 | 0.75-0.90 |
| dense loamy clay and clay | 0.150-0.200 | 0.90-1.00 |
| | 0.200-0.300 | 1.00-1.10 |
| | 0.300-0.400 | 1.10-1.40 |
| very dense clay | 0.400-0.500 | 1.40-1.60 |
| | 0.500-0.600 | 1.60-1.70 |

*Table 8.3 Values of k*

More detailed information can be found by Mirtskhoulva [8.1][8.2], Randkivi [8.4], Raudkivi and Tan [8.5] and Ven te Chow [8.6]. However it is recommended to check the approximation with laboratory tests not only for the value of $U_{cr}$ but also for $y_s$.

## equivalent particle diameter

The second approach is based on substituting an equivalent particle diameter into equations for determining the critical velocity (see section 2.5.2.2):

$$U_{cr} = C (\psi \Delta D')^{0.5} \qquad\qquad (8.5)$$

in which:

C = Chezy-coefficient ($m^{0.5}/s$)
$\psi$ = critical value of the Shield parameter (-)
$\Delta$ = relative density (-)
$D'$ = equivalent particle diameter (m)

The calculated value of $U_{cr}$ can be used in equations to determine the scour depth $y_{s,max}$, such as equation (8.1).

Changxi et al [8.7] present values of the equivalent particle diameter originally presented by Mao in 1984. They are summarized in the following table.

| soil type | | equivalent particle diameter [mm] |
|---|---|---|
| sand, gravel, cobble | | actual grain diameter |
| silt very fine sand | | 0.2 to 0.5 |
| silty loam, loess clayey silt | loose<br>tighter<br>much tighter | 0.5 to 1.0<br>1 to 2<br>2 to 4 |
| silty clay, loam with sandy kernels | loose<br>tighter<br>much tighter | 2 to 4<br>4 to 8<br>8 to 12 |
| clay, silty clay with sandy kernels | loose<br>tighter<br>much tighter | 8 to 12<br>12 to 20<br>20 to 40 |
| ultra clay with colloid, weathered rock pieces | | 30 to 50 |

*Table 8.4 Equivalent particle diameter cohesive soils*

The dry unit weight of loose, tight and much tighter soil in table 8.4 is smaller than 1.3, 1.3 to 1.8 and larger than 1.8 respectively. The values are based on literature data and prototype data.

Another possibility is to relate the equivalent particle diameter to the cohesion C or the shear strength $\tau$. In [8.7] equations are presented, but they do not have general applicability.

Changxi et al compared their results with a prototype scour hole and concluded that the results agreed very well (within 20 % of the actual measured scour depth).

## 8.4 Research needs

The erosion characteristics of cohesive soils are not fully understand up to now. For specific sediments at a given location quantitative information is available about the erosion parameters. However, for most situations the designer has to perform an erosion test.

The available knowledge up to now enables to predict indicative values of scour depths using the permissible nonscouring velocities approach or the equivalent particle diameter approach. The first method requires further refinement to be more accurate. Particularly, the influence of the stochastic behaviour of turbulence should be incorporated, because the erosion process seems to be determined largely by bursts-induced accelerations in the turbulent boundary layer. Furthermore, the influence of the homogeneity of the riverbed has to be taken into account.

The second calculation method requires also more refinement. Furthermore, it will be necessary to find a general relationship between the equivalent particle diameter and the cohesion or the shear stress. In principle, methods to determine the cohesion or the shear stress are available.

Finally, it is recommended to investigate whether both calculation methods are related to each other. If this appears, then all the attention can be focussed on the determination of a permissible scouring velocity either by the derivation of a accurate formula or by the development of a simple laboratory test method.

## 8.5 References

8.1    Ts.E. MIRTSKHOULAVA
       Scouring by flowing water of cohesive and noncohesive beds
       Journal of Hydraulic Research, Vol. 29, no 3, 1991

8.2    Ts. E. MIRTSKHOULAVA
       Basic physics and mechanics of channel erosion
       Leningrad, Gidrometeoizdat, 1988.

8.3    RIJKSWATERSTAAT, DELFT HYDRAULICS
       Cohesive sediments, flow induced erosion of cohesive beds,
       Delft, 1989.

8.4    A.J. RAUDKIVI
       Loose boundary hydraulics
       Pergamon Press, Oxford, 1990

8.5    A.J. RAUDKIVI AND S.K. TAN
       Erosion of cohesive soils
       Journal of Hydraulic Research, Vol 22, 1984

8.6    VEN TE CHOW
       Open-channel hydraulics
       McGraw-Hill, 1959

8.7    M.CHANGXI, Z. MINGDE, J. LIANG AND Z.DAN
       Local scour on earth bed below sluice-dams
       7th Congress APD-IAHR, Beijing, 1990

acceleration deceleration
zone zone

$y_0$

$Y_D$

$L$

$\beta_s$

SILL

scour hole

$L_p$

bed protection

transition to
super critical flow

sub critical flow

hydraulic jump

sub critical flow

$y_0$

hydraulic
jump

bed protection

SILL, SHORT−CRESTED

DELFT HYDRAULICS

Q 647

FIG. 2.1

acceleration zone

deceleration zone

eddy

flow separation point

L

scour hole

reattachment point

$y_o$

$Y_D$

$\beta_s$

flow separation point

eddy

L

$L_p$

bed protection

scour hole

edge bed protection

– – – – – flow line

SILL, BROAD–CRESTED

DELFT HYDRAULICS
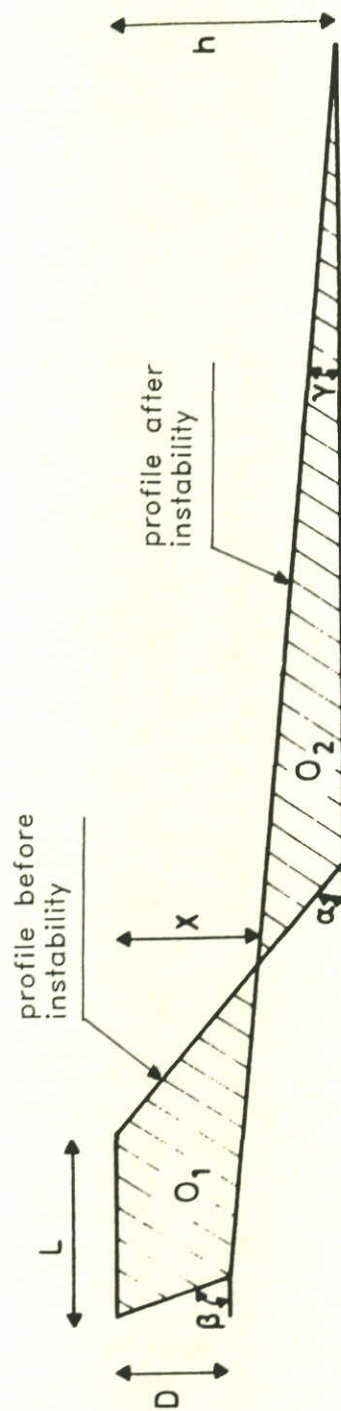
Q 647

FIG. 2.2

TWO DIMENSIONAL SCHEMATIZATION
OF A FLOW SLIDE

DELFT HYDRAULICS

Q 647     FIG. 2.3

THREE DIMENSIONAL SCHEMATIZATION
OF A FLOW SLIDE
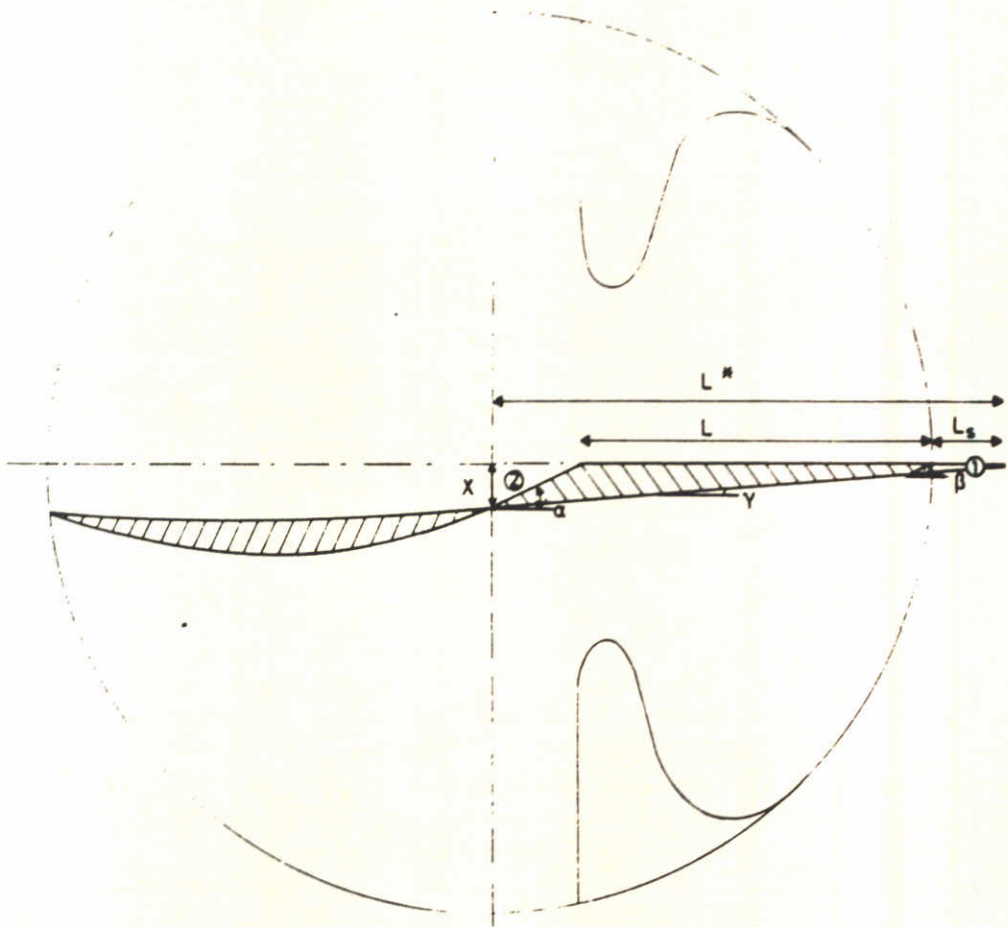
DELFT HYDRAULICS          Q 647          FIG. 2.4
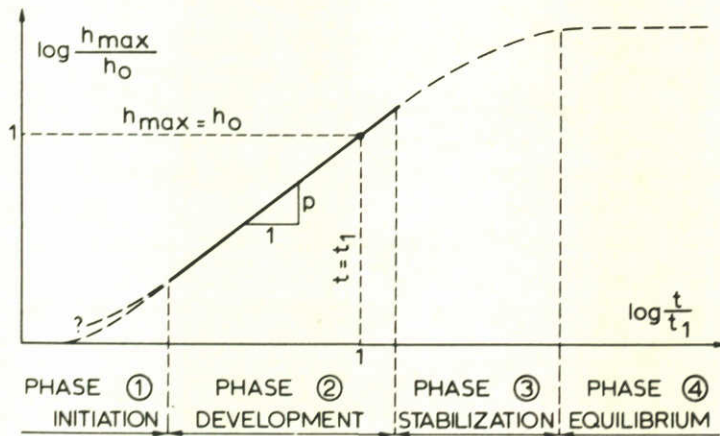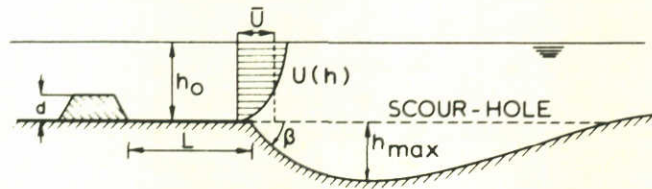
$$\frac{h_{max}}{h_0} = \left(\frac{t}{t_1}\right)^P \; ; \; \begin{array}{l} 2\text{-dim} , p = 0.4 \\ 3\text{-dim} , p \geqslant 0.4 \end{array}$$

| Pilarczyk | manual |
|-----------|--------|
| $h_0$ | $Y_0$ |
| P | $\gamma$ |
| $h_{max}$ | $Y_{max}$ |
| d | $Y_D$ |

| | | |
|---|---|---|
| DIFFERENT PHASES IN THE DEVELOPMENT OF A SCOUR HOLE | | |
| DELFT HYDRAULICS | Q 647 | FIG. 2.5 |
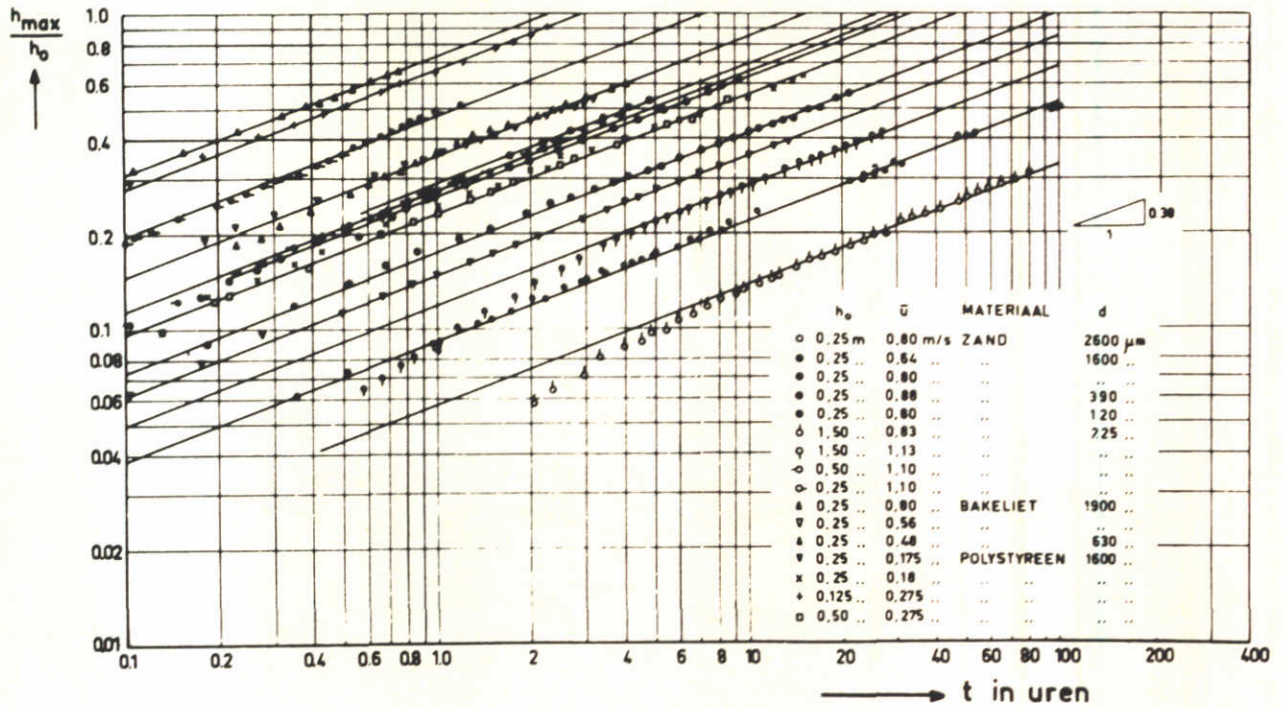
$$\gamma = 0.38$$

DETERMINATION OF EXPONENT $\gamma$
IN BREUSERS FORMULA

| DELFT HYDRAULICS | Q 647 | FIG. 2.6 |

The figure contains the following legend table:

| MATERIAAL | | d | h_o | serie |
|---|---|---|---|---|
| O | POLYSTYREEN | 1600 μ | 0,125 m | 19 |
| ó | ,, | 1600 μ | 0,20 m | 13 |
| Q | ,, | 1600 μ | 0,30 m | 8'' |
| φ | ,, | 1600 μ | 0,40 m | 13 |
| ⊖ | ,, | 1600 μ | 0,60 m | 8'' |
| △ | BAKELIET | 1900 μ | 0,25 m | 15 |
| ▽ | ,, | 630 μ | 0,30 m | 16 A |
| X | ZAND | 840 μ | 0,25 m | 15 |
| + | ,, | 390 μ | 0,30 m | 16B |
| ✳ | ,, | 225 μ | 0,50 m | 19 |
| ✱✱ | ,, | 225 μ | 1,50 m | 19 |

Vertical axis: $(\alpha\bar{u} - u_{kr})$ (m/s)

Horizontal axis: $t_1/\Delta^{1,7}\cdot y_o^2$ (hours/m²)
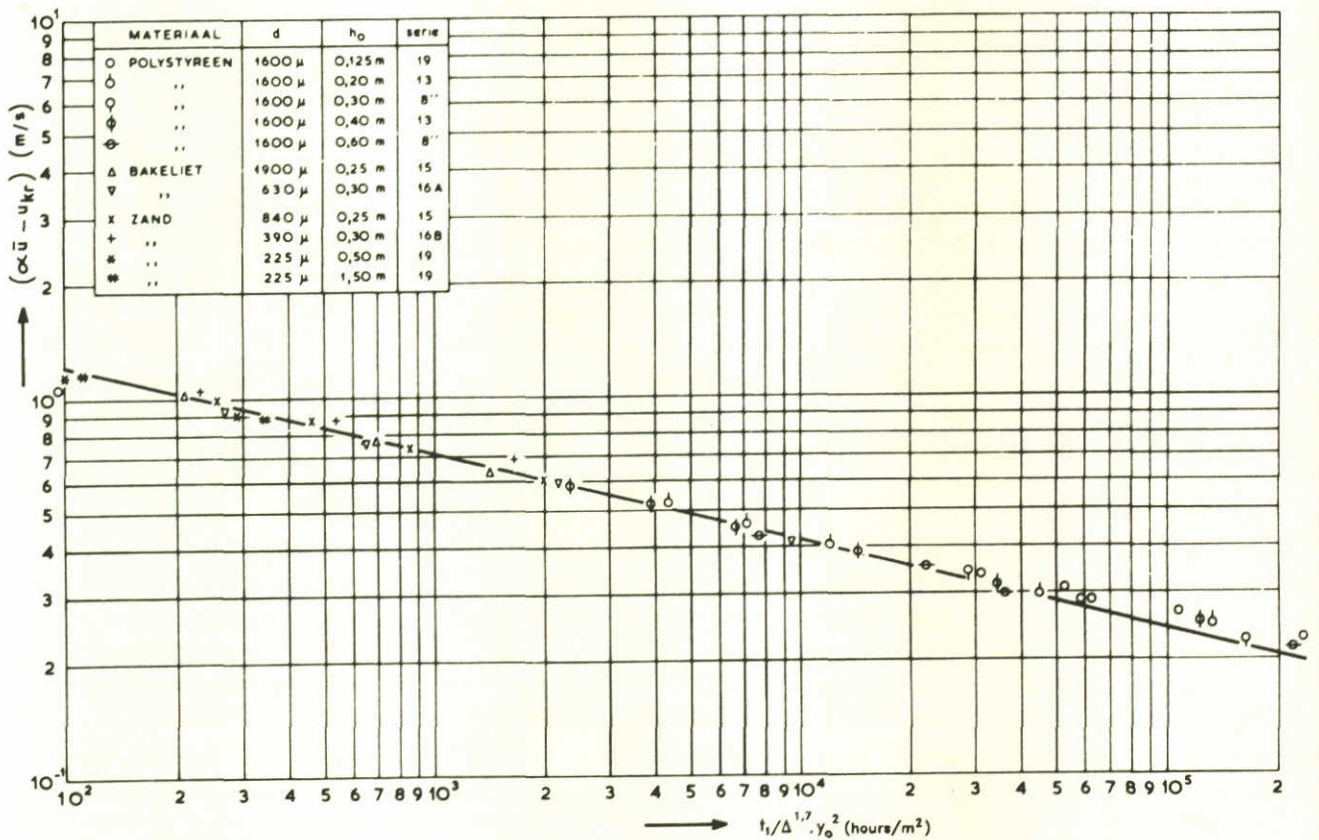
$$t_1 = 250.\Delta^{1,7}.\,y_o^{\,2}.\left[\alpha\bar{u} - \bar{u}_{cr}\right]^{-4.3}$$

DETERMINATION OF EXPONENT AND
COEFFICIENT IN BREUSERS FORMULA

| DELFT HYDRAULICS | Q 647 | FIG. 2.7 |
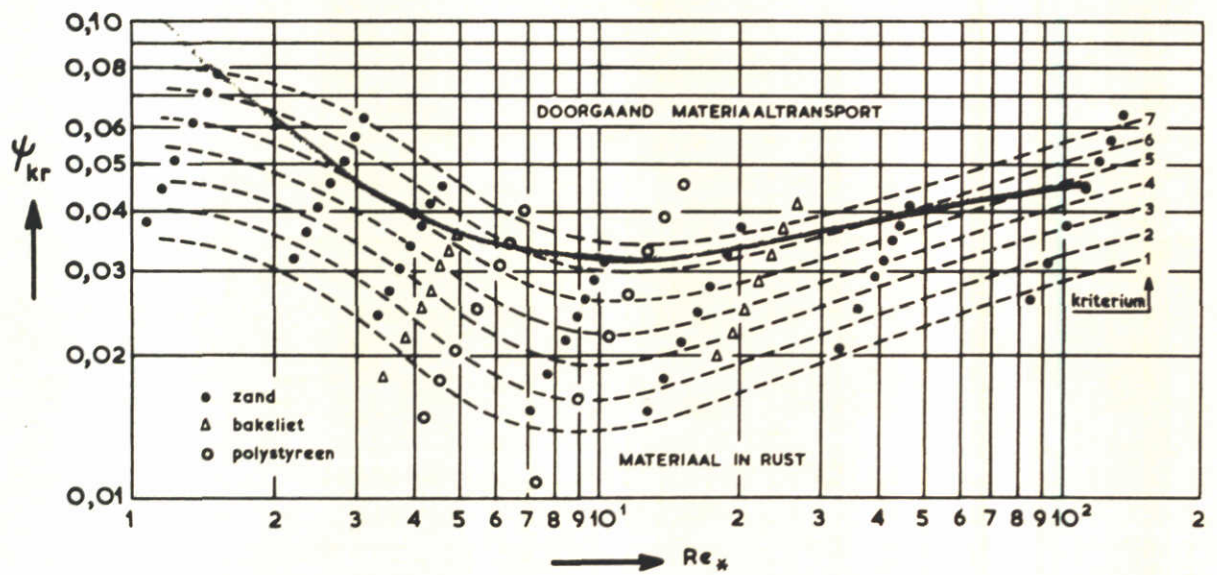
SHIELDS GRAPH ACCORDING TO BREUSERS
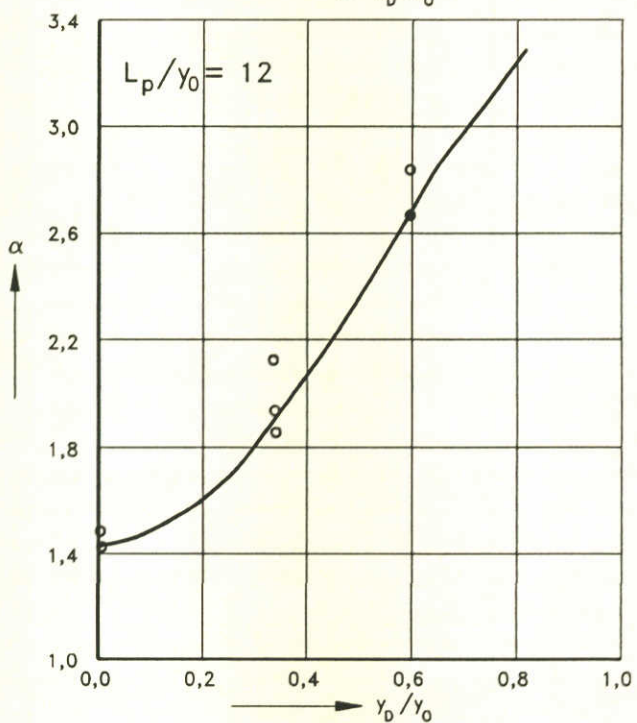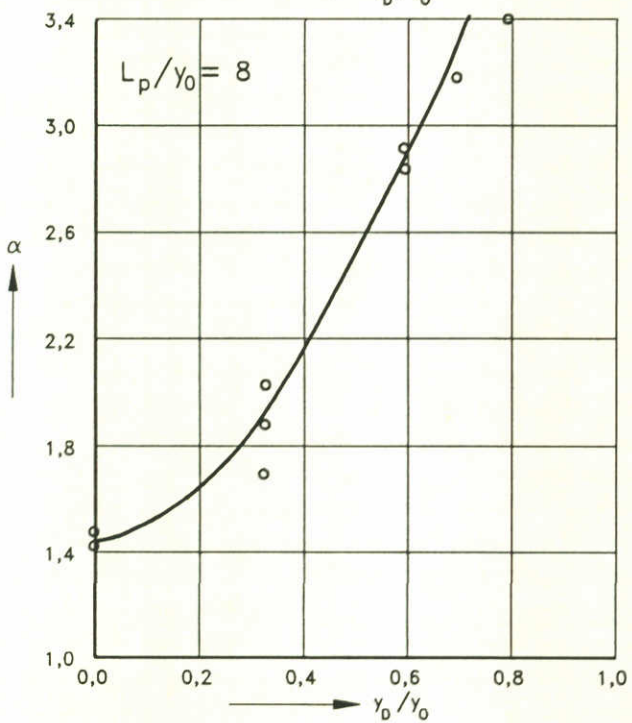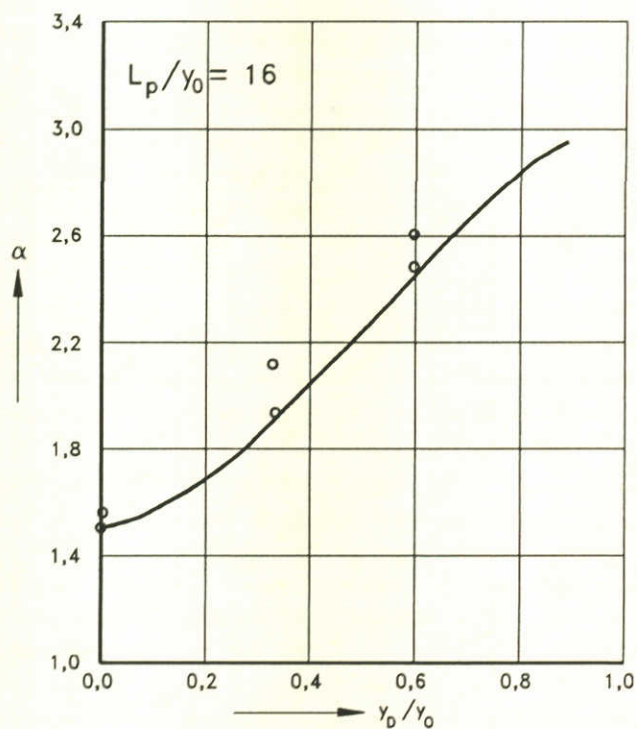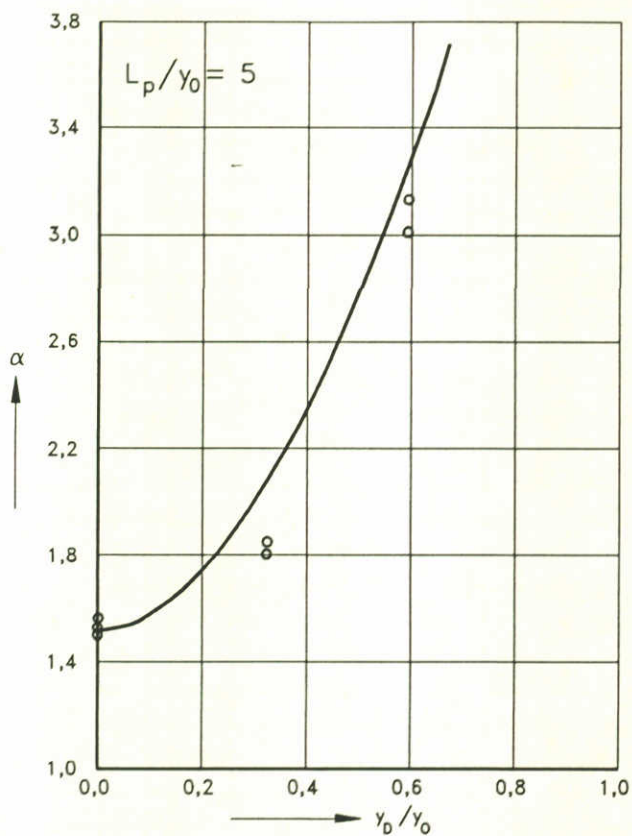
DELFT HYDRAULICS          Q 647          FIG. 2.8

RELATION BETWEEN $\alpha$ AND LENGHT BED
PROTECTION, AND RELATIVE SILL HEIGHT

DELFT HYDRAULICS | Q 647 | FIG. 2.9

$\alpha$ AS A FUNCTION OF $Y_d/Y_o$
2- AND 3- DIMENSIONAL FLOW

DELFT HYDRAULICS · Q 647 · FIG. 2.10

RELATIONSHIP BETWEEN $\alpha$ AND THE
RELATIVE TURBULENCE INTENSITY

DELFT HYDRAULICS

Q 647

FIG. 2.11

Abutments on sill
$Y_D = 0.3$ à $0.6$ $Y_o$

1:1
1:2

Edge bed protection

B

no scour | 3-dim | 2-dim | 3-dim | no scour
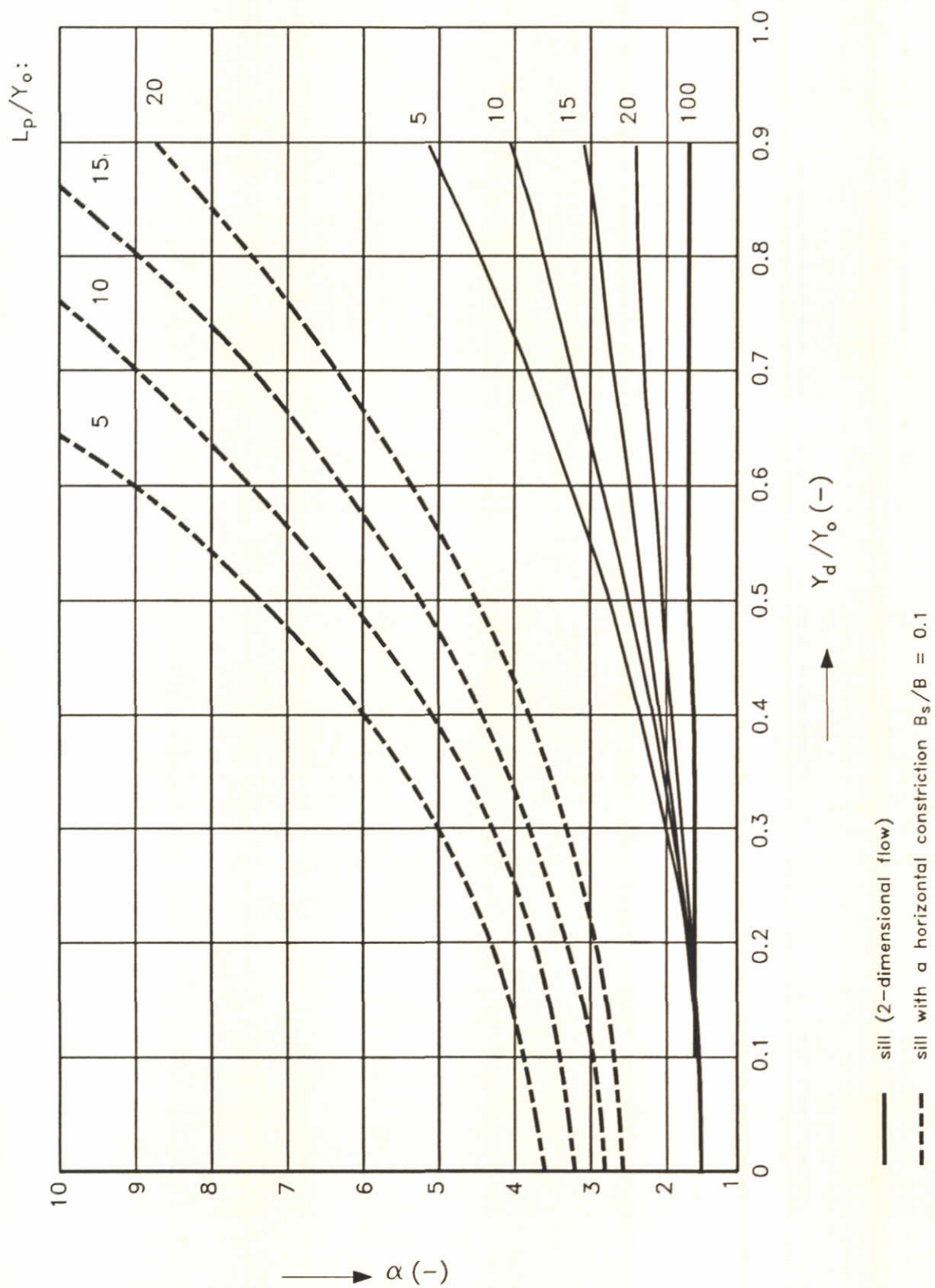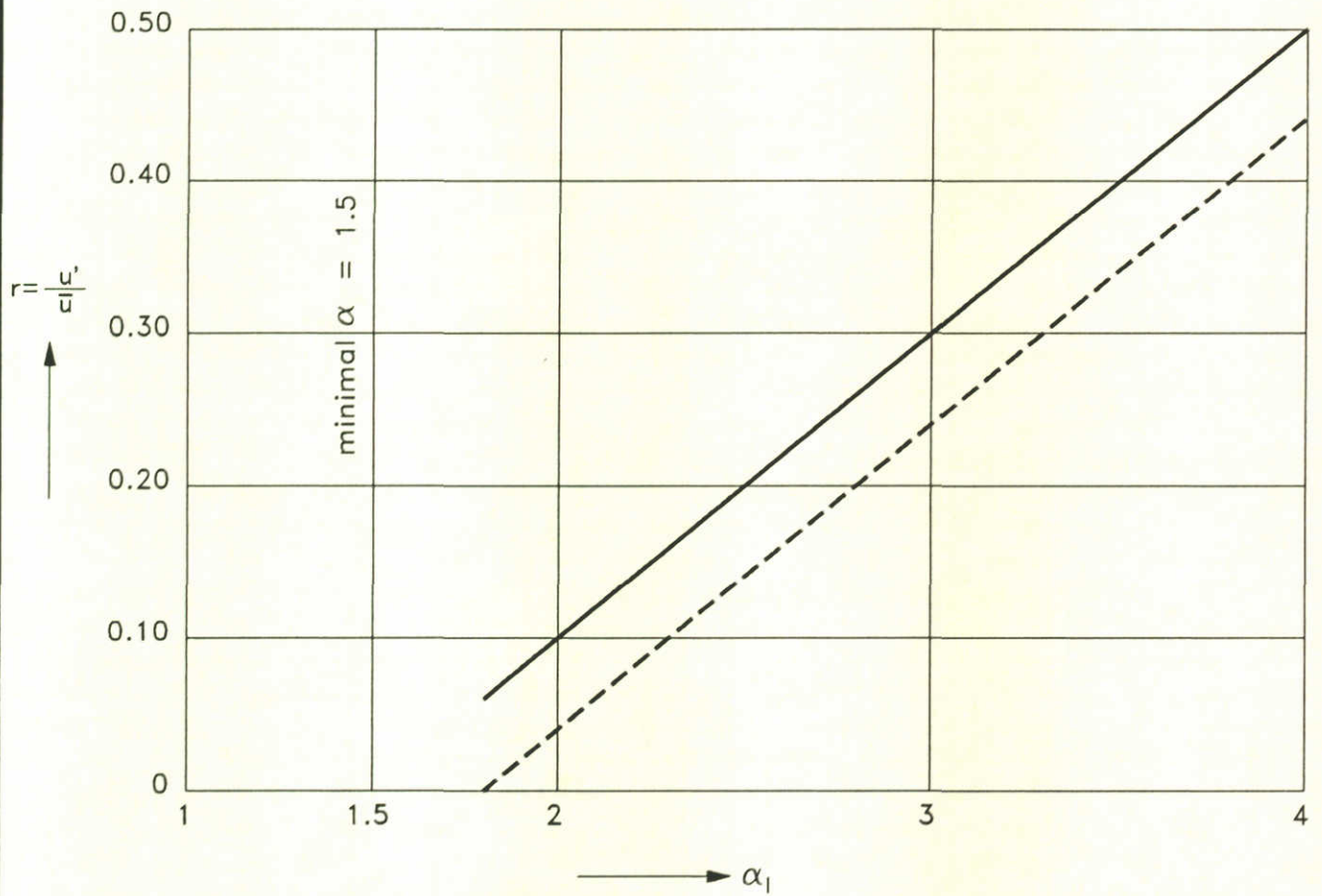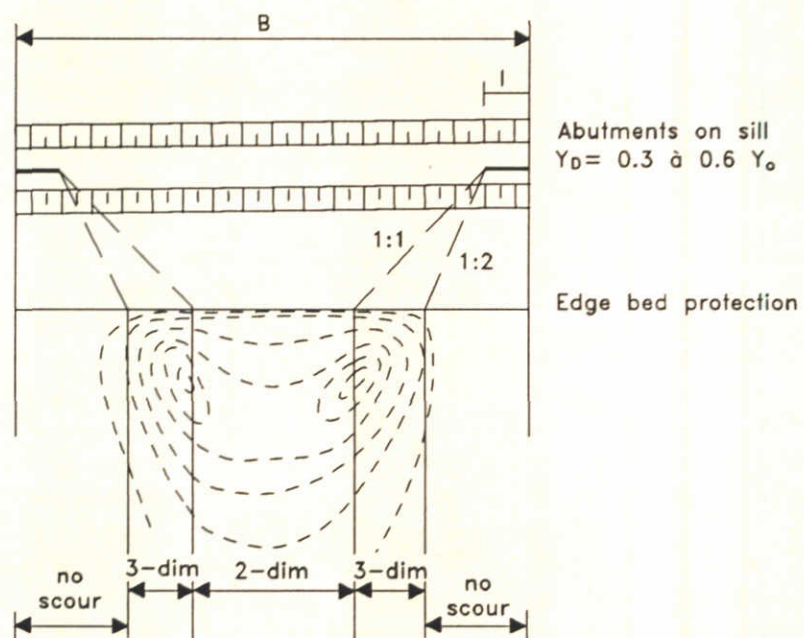
TOP VIEW OF A CLOSURE

| TYPE OF SCOUR HOLE AS A FUNCTION OF THE RIVER WIDTH | | |
|---|---|---|
| DELFT HYDRAULICS | Q 647 | FIG. 2.12 |
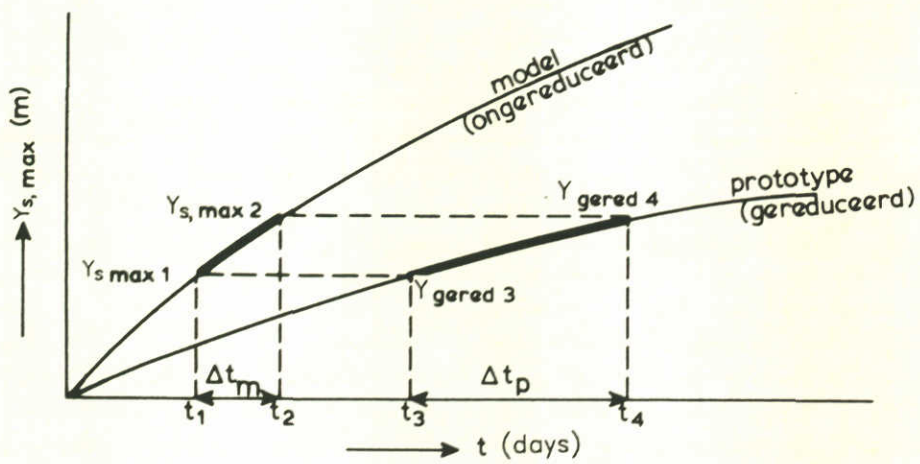
SKETCH TO ILLUSTRATE REDUCTION METHOD

DELFT HYDRAULICS

Q 647

FIG. 2.13

NORTH-SEA                                          GREVELINGEN-LAKE

ELEVATION

TOP-VIEW

PROTOTYPE SITUATION - SITUATION NATURELLE          sizes in m

$Q = \mu A \sqrt{2g\Delta H}$
$\mu \approx 1.4$
$A = 54\,m^2$

model (steady flow):
o   test 1, Q ≅ 404 m²/s
x   test 2, Q ≅ 370 m²/s
△   test 3, Q ≅ 384 m²/s

prototype (tidal flow)

$h_{max} \propto t^{0.4}$
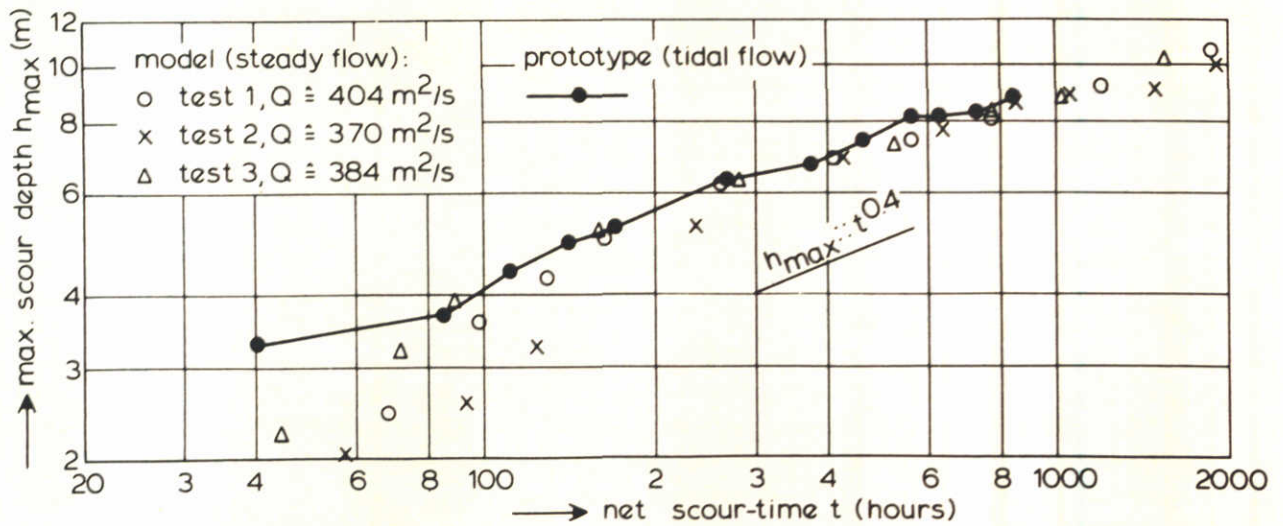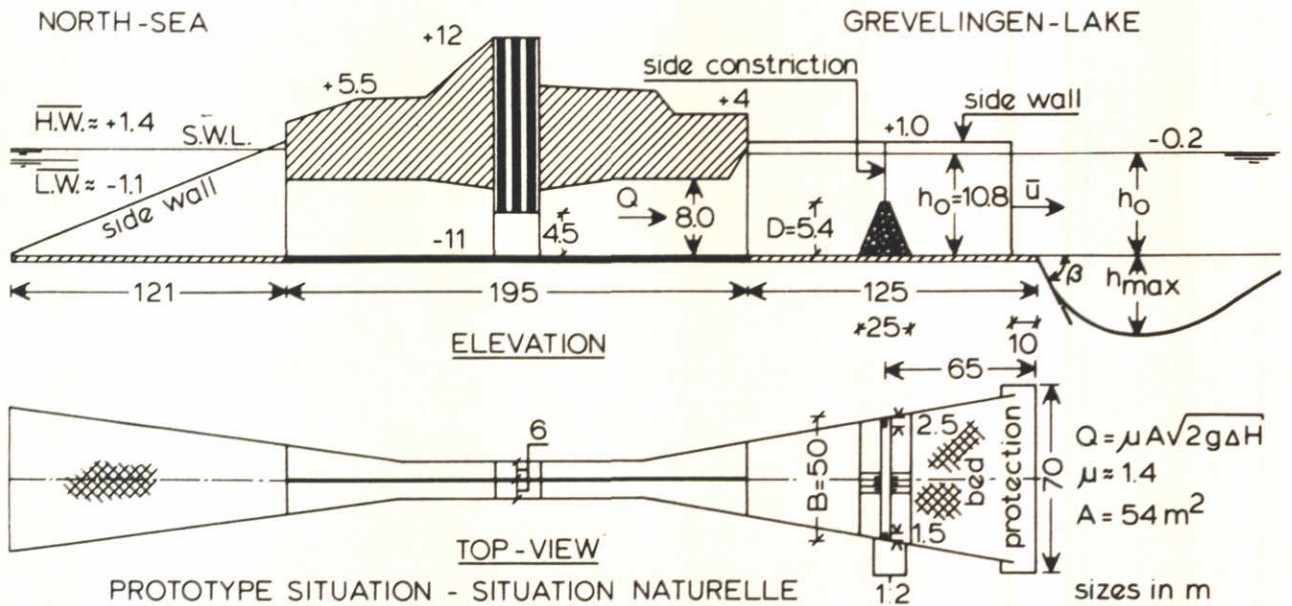
TIME-SCOUR RELATION - RELATION TEMPS-AFFOUILLEMENT

| Dietz: | manual: |
|--------|---------|
| D | $Y_D$ |
| $h_0$ | $Y_0$ |
| $h_{max}$ | $Y_{max}$ |

BROUWERSLUIS PROTOTYPE SCOURING TEST

DELFT HYDRAULICS          Q 647          FIG. 2.14
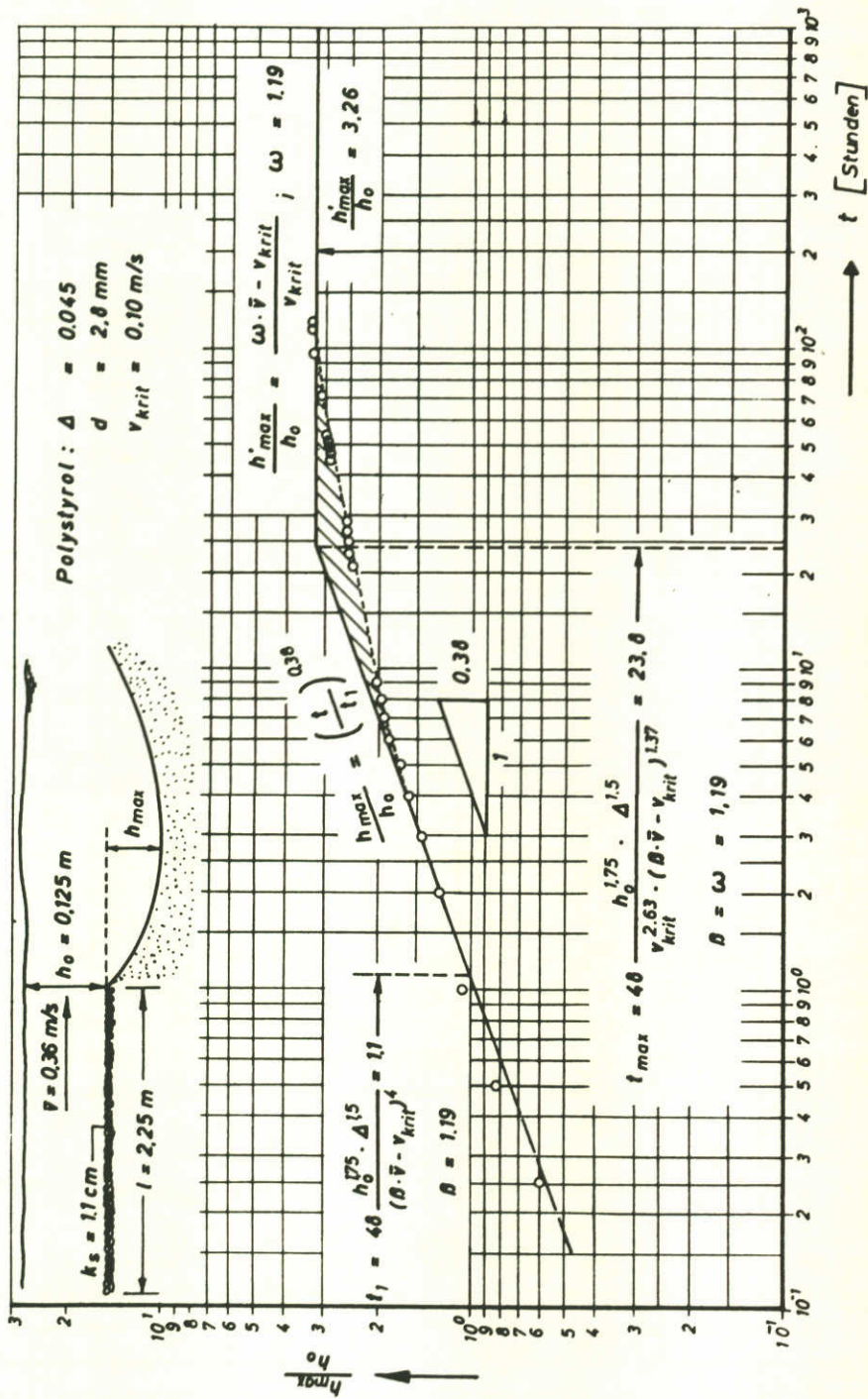
EXAMPLE OF A SCALE MODEL TEST RESULT,
ACCORDING TO DIETZ

DELFT HYDRAULICS

Q 647

FIG. 2.15

| Material | Δ | d [mm] | hₒ [m] | ρ | Signatur |
|---|---|---|---|---|---|
| Feinsand | 1.65 | 0.12 | 0.250 | 1.50 | △ |
| | | | 0.175 | | ▽ |
| | | | 0.125 | | ◁ |
| Braunkohle | 0.37 | 1.1 | 0.200 | 1.50 | ▣ |
| | | | 0.175 | | ▢ |
| | | 3.4 | 0.250 | 1.50 | ◆ |
| | | | 0.200 | bis | ◇ |
| | | | 0.175 | | ◈ |
| | | 7.8 | 0.250 | 2.00 | ╈ |
| | | | 0.200 | | ╈ |
| | | | 0.175 | | ┿ |
| Polystyrol | 0.045 | 1.6 | 0.250 | 1.25 | ◉ |
| | | | 0.175 | | ⊙ |
| | | | 0.125 | | ⊙ |
| | | 2.8 | 0.125 | 1.35 | ● |

$$\frac{h'_{max}}{h_o} = \frac{\omega \cdot \bar{v} - v_{krit}}{v_{krit}}$$

$$t_1 = \frac{48 \cdot h_o^{1.75} \cdot \Delta^{1.5}}{(\rho \cdot \bar{v} - v_{krit})^4}$$

$$\frac{h_{max}}{h_o} = \left(\frac{t}{t_1}\right)^{0.38}$$

0.38
1

manual:
α
c. α
$\frac{1}{c}$

Dietz:
β
ω
$\frac{\beta}{\omega}$

→ time (—)

$\frac{d}{c}$ →

$\frac{1}{c}$ (—) ←

0.5
0.67
1.0
1.1
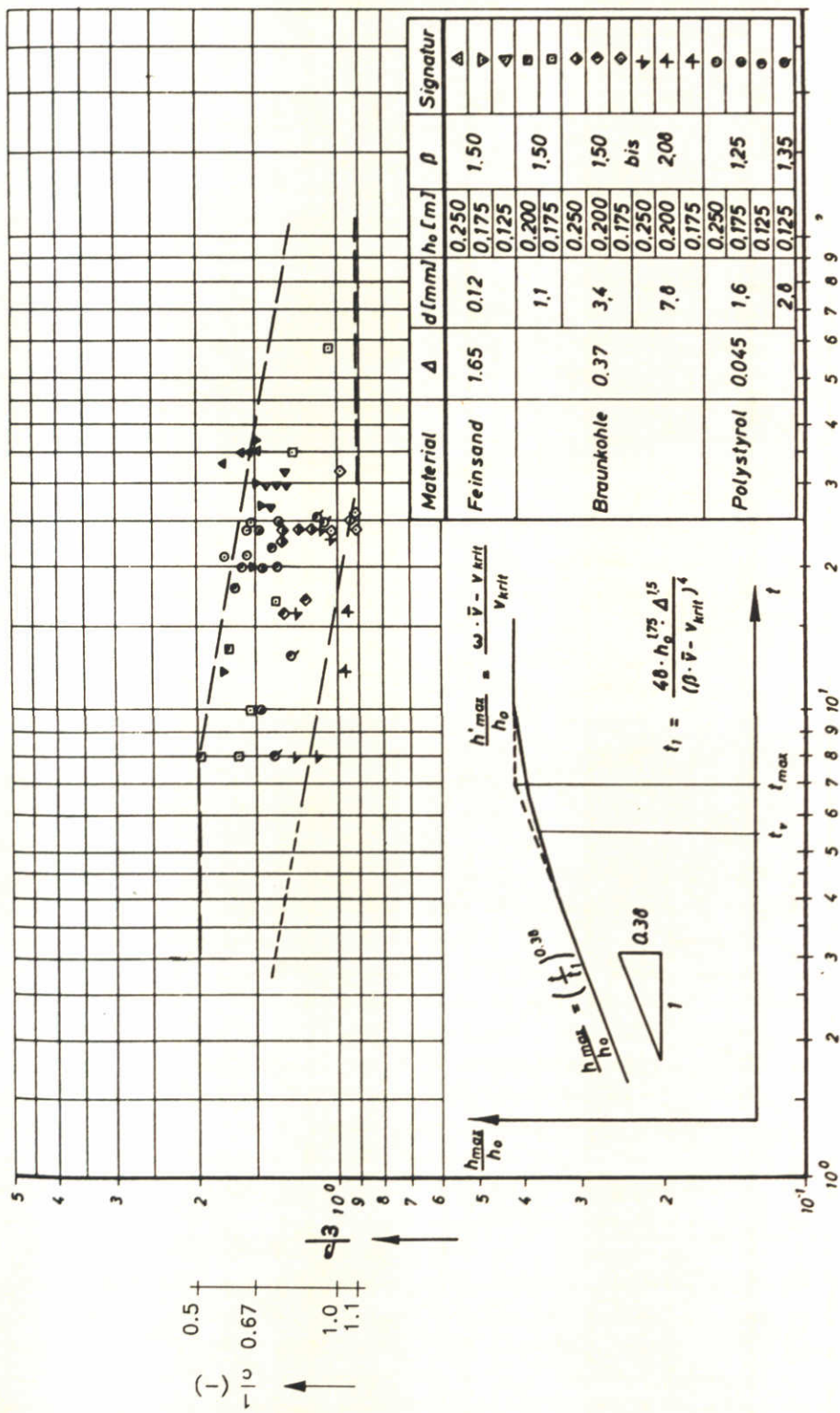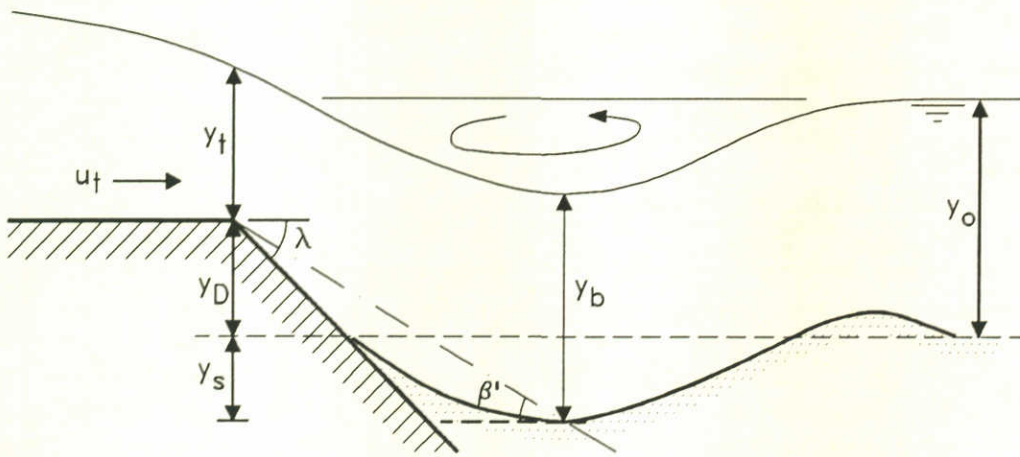
DEFINITION SKETCH OF A SCOUR HOLE
DOWNSTREAM OF A GRADE CONTROL STRUCTURE
ACCORDING TO BORMANN

DELFT HYDRAULICS

Q 647

FIG. 2.17
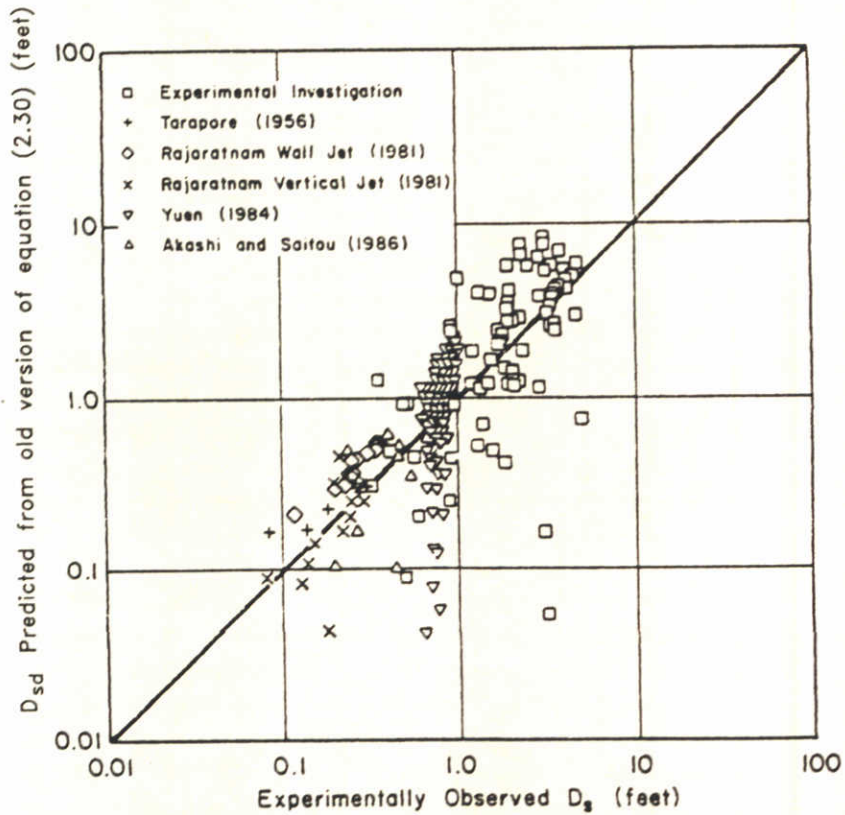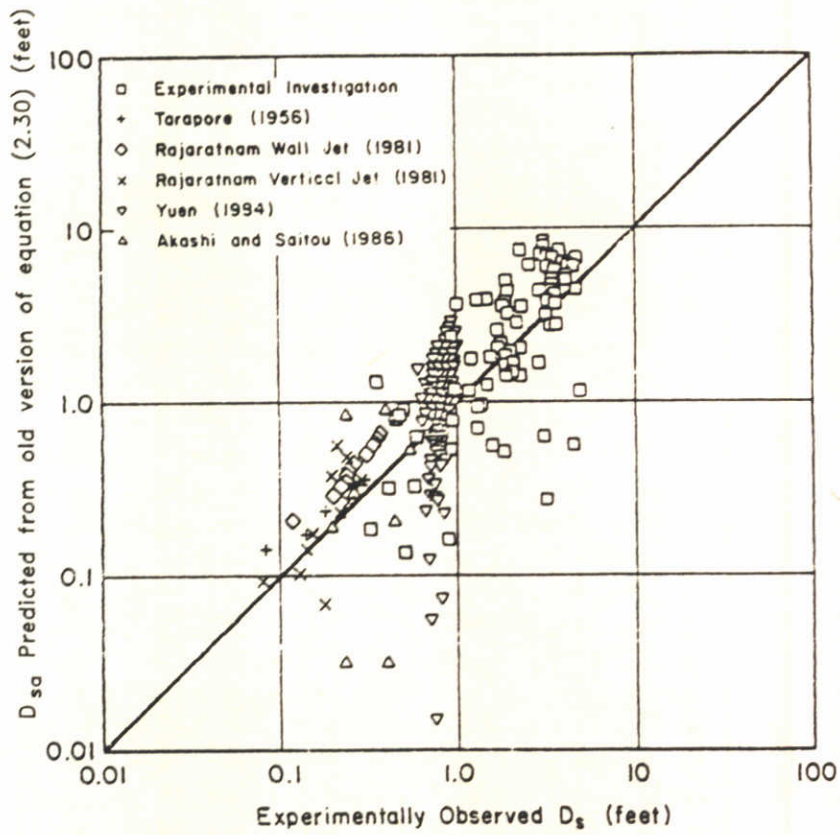
VERIFICATION OF THE MAXIMUM SCOUR
DEPTH ACCORDING TO BORMAN

DELFT HYDRAULICS                      Q 647        FIG. 2.18
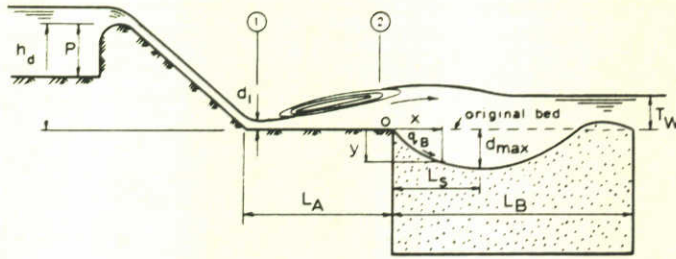
Definition Sketch for Model Tests
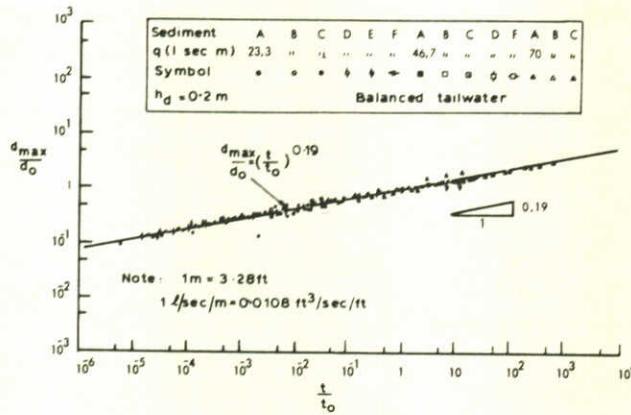


Plot of Dimensionless Scour Depth Against Dimensionless Time for All Runs Listed on this Figure
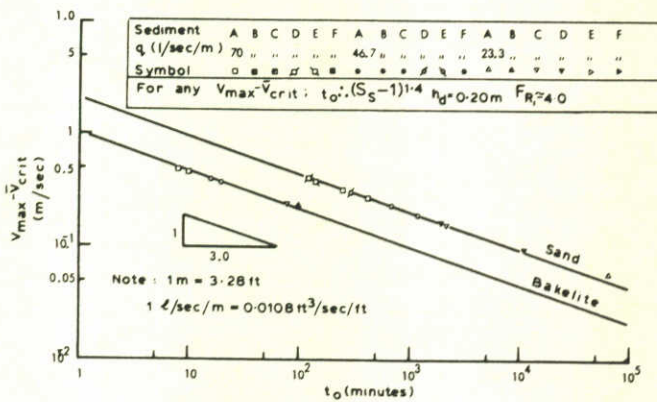


Influence of Velocity and Sediment Density on Time Scale Relationship Under Balanced Tailwater Condition in Medium Size Model

THE MAXIMUM SCOUR DEPTH ACCORDING TO FAHROUKI AND SMITH

DELFT HYDRAULICS

Q 647

FIG. 2.19

PARAMETERS

cotg β        β = EQUILIBRIUM SLOPE

cotg γ        $cotg \, \gamma = x_{max}/h_{max}$

T             $T = O/h_o^2$ MET O = HOEVEELHEID UITGESPOELD MATERIAAL (GEARCEERD)
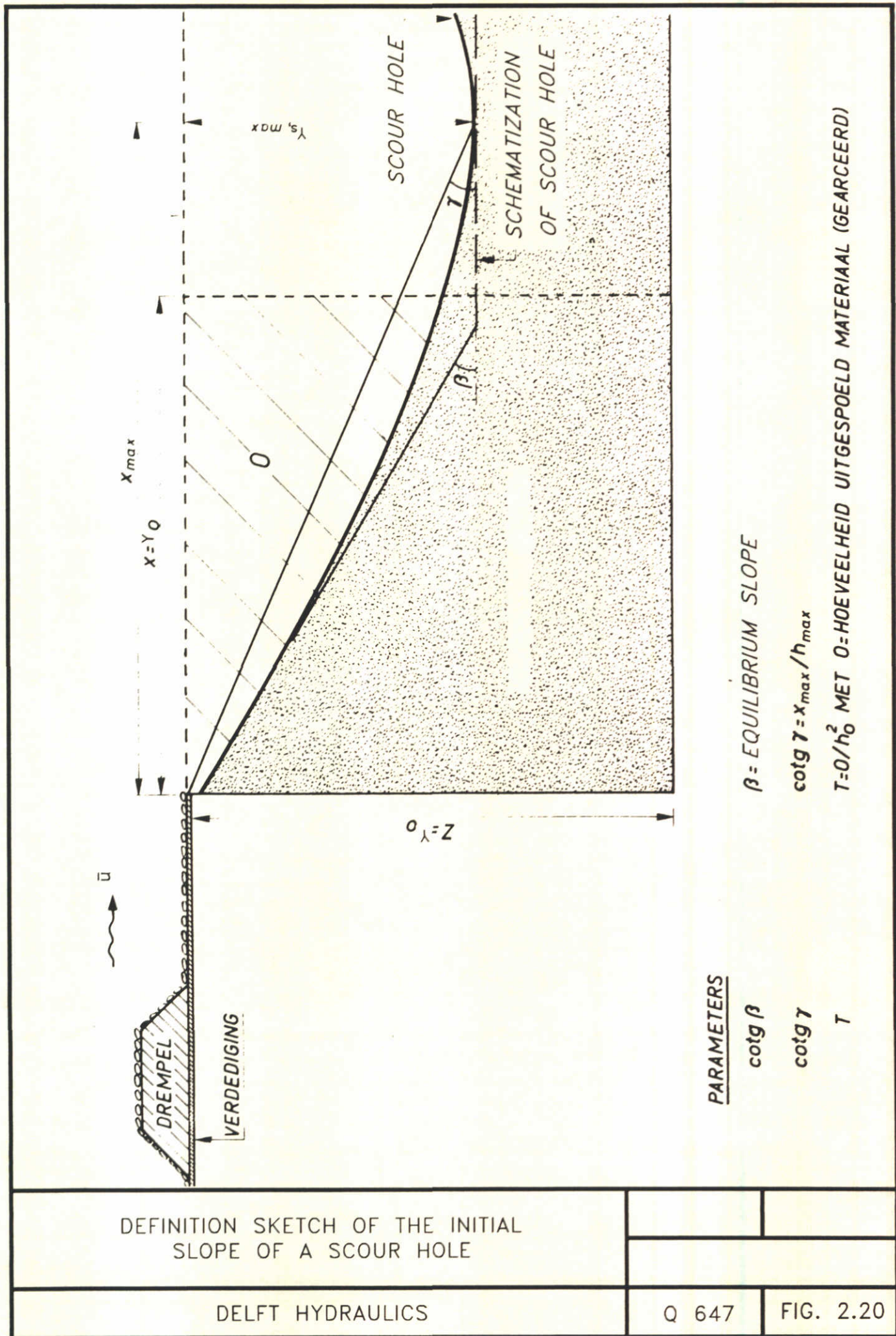
DEFINITION SKETCH OF THE INITIAL
SLOPE OF A SCOUR HOLE

DELFT HYDRAULICS          Q 647          FIG. 2.20

8

cotg $\beta$ (−)

6

4

2

0

0        0.2       0.4       0.6       0.8       1.0

$Y_D/Y_0$ (−)
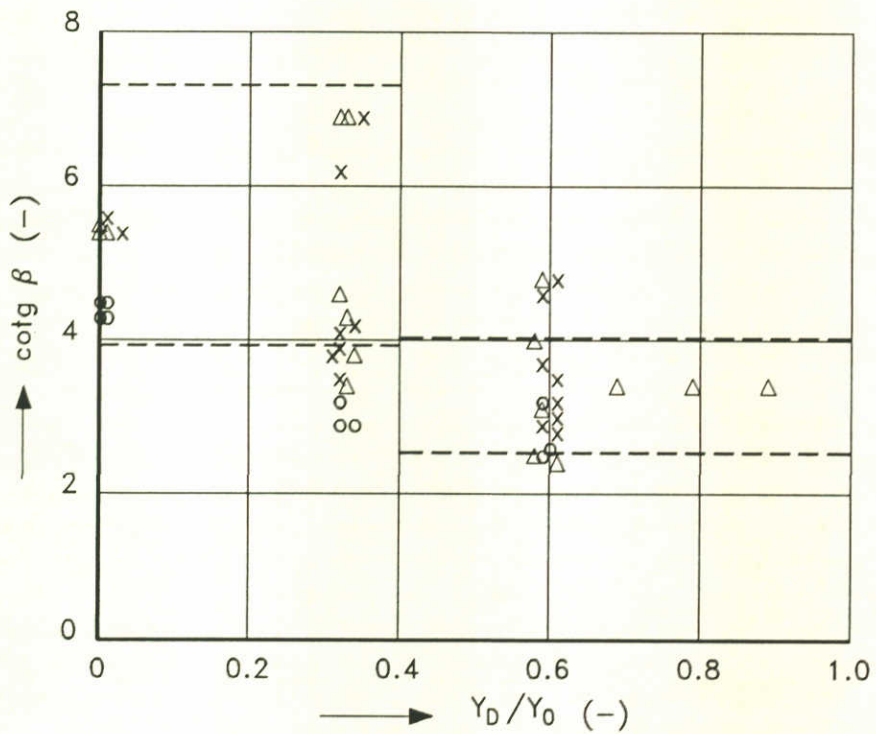
△ = smooth bed protection

x = rough bed protection

o = medium rough bed protection

THE INITIAL SLOPE AS A FUNCTION
OFF THE SILL HEIGHT

DELFT HYDRAULICS        Q 647        FIG. 2.21

THE INITIAL SLOPE AS A FUNCTION
OF THE BED PROTECTION LENGTH

| DELFT HYDRAULICS | Q 647 | FIG. 2.22 |

according to Dietz 1969

| Sign. | $h_0$ [m] | $\bar{v}$ [m/s] | $\delta$ |
|---|---|---|---|
| ⊙ | 0,154 | 0,29 | 90 |
| ▣ | 0,125 | 0,36 | 123 |

Polystyrol.

$\Delta = 0,045$
$d = 2,8\,mm$
$v_{krit} = 0,10\,m/s$
$w = 0,044\,m/s$
$A_\bullet = 1,13 \cdot 10^{-4}$

$$\delta = \frac{\bar{v} - v_{krit}}{w} \cdot \frac{1}{\sqrt[5]{A_\bullet}}$$

$\bar{v}$

$h_0$

$k_s$

$l = 3,75$
und 5,50 m

$\beta$

$\mathrm{ctg}\ \beta$

$\dfrac{k_s}{h_0}\ (-)$

manual:

Dietz:

| manual: | Dietz: |
|---|---|
| $Y_0$ | $h_0$ |
| $u$ | $\bar{v}$ |
| $D$ | $d$ |

THE INITIAL SLOPE AS A FUNCTION OF
THE RELATIVE ROUGNESS

DELFT HYDRAULICS

Q 647

FIG. 2.23

THE INITIAL SLOPE AS A FUNCTION
OF THE BED PROTECTION LENGTH

DELFT HYDRAULICS

Q 647 FIG. 2.24

cotg $\beta$

L/D

$D/h_0 = 0,33$

$D/h_0 = 0,6$
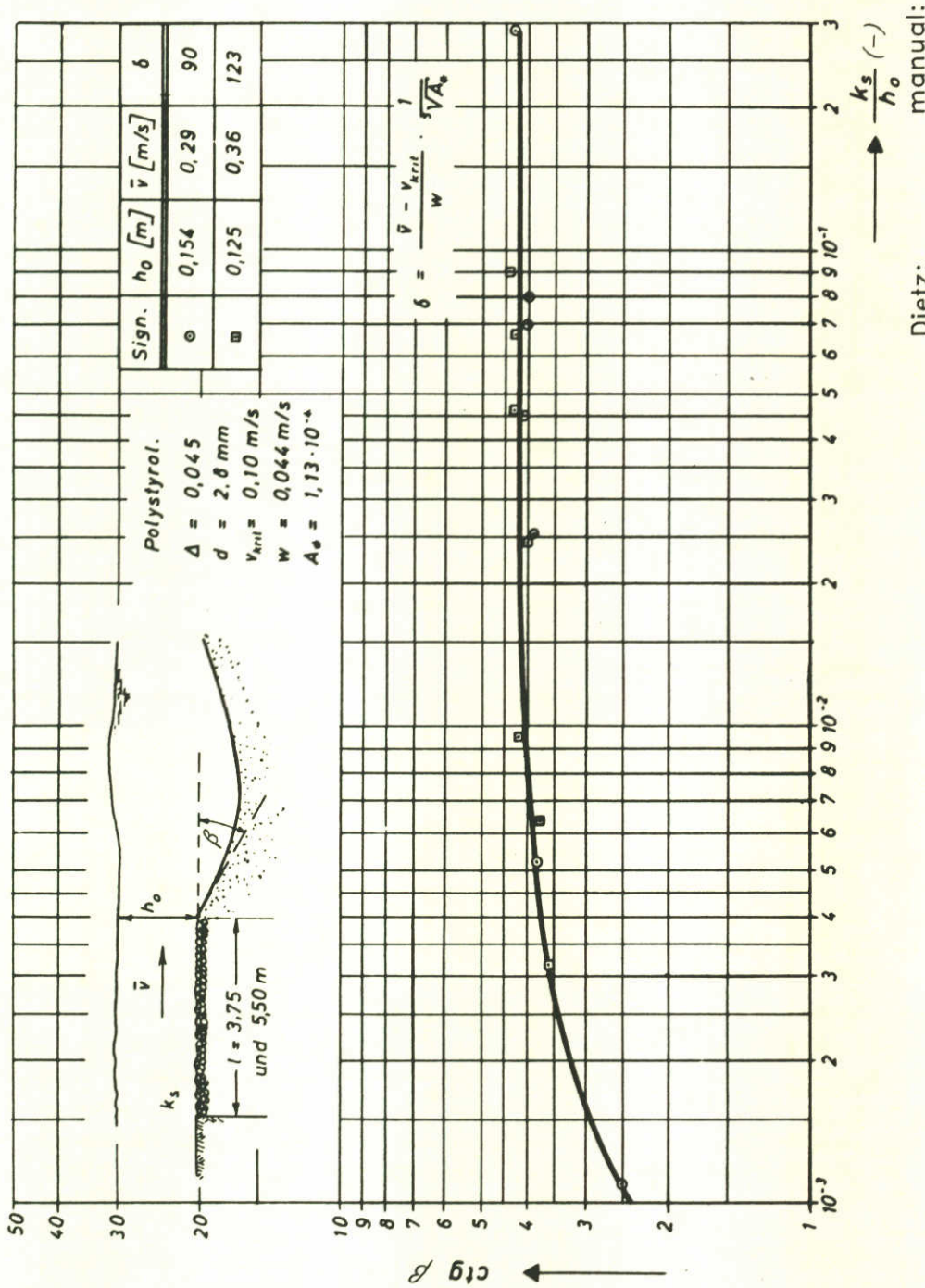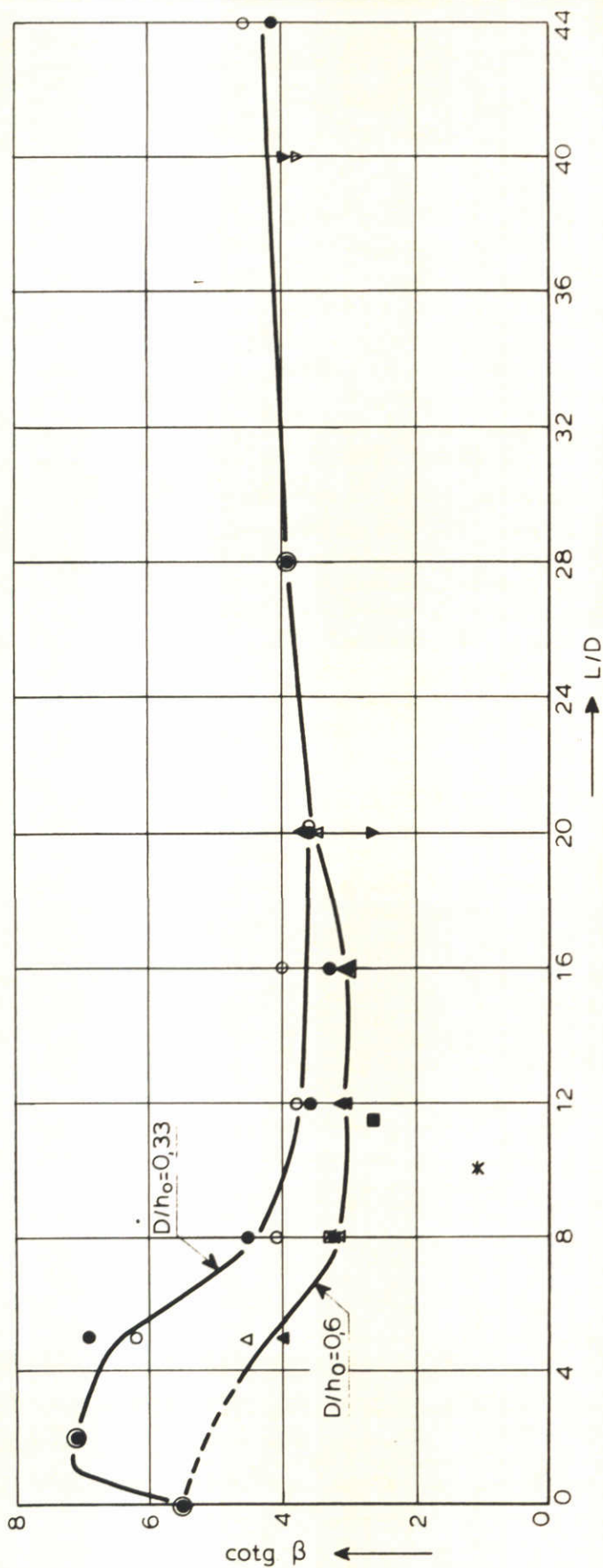
figure :    manual:

L          $L_p$

D          $Y_D$

| | serie | $D/h_0$ | $k_s/h_0$ | |
|---|---|---|---|---|
| x + □ | I | 0,7 0,8 0,9 | 0,025 | M 846-I |
| ● ○ | II | 0,33 | 0,025 0,05 | |
| ◄ ○ | III | 0,6 | 0,025 0,05 | |
| ■ | proef B | 0,66 | 0,03 | M 1533 |
| ▶ | serie1,3 | 0,5 | 0,05 0,10 | |
| ▽ | serie 2 | 0,25 | 0,05 | |
| ✱ | prototype (proef B) | | | |
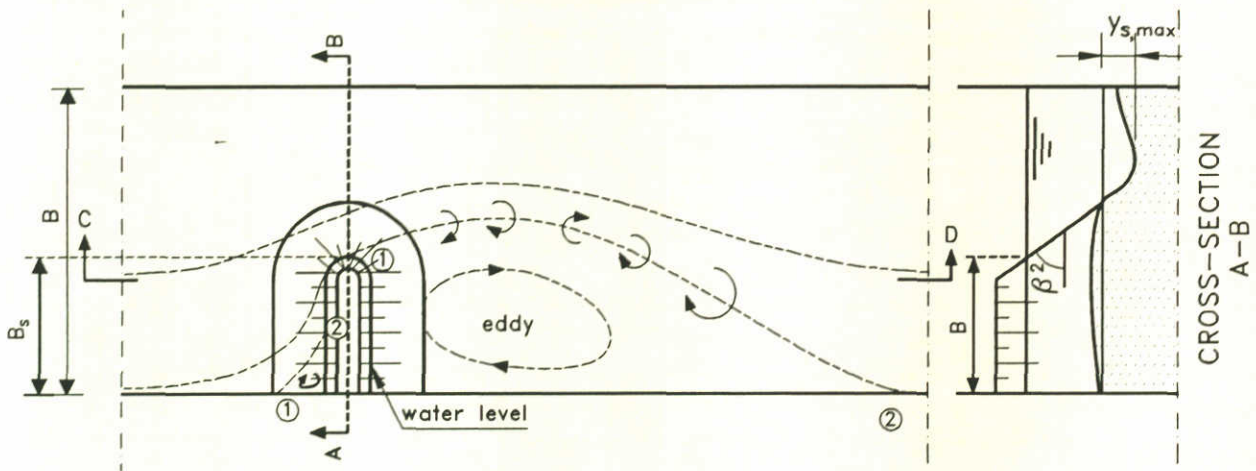
- - - - - - - flow line
① seperation point
② reattachment point

TOP VIEW
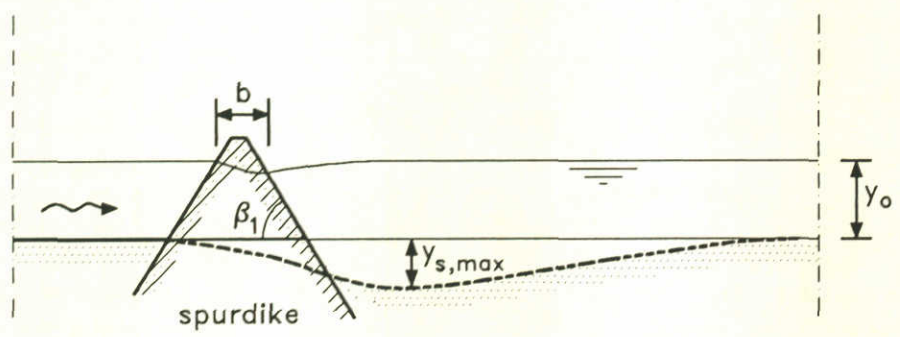
CROSS-SECTION C-D

SPURDIKE, GENERAL LAY-OUT AND FLOW PATTERN

DELFT HYDRAULICS          Q 647          FIG. 3.1

$\alpha = 1.5 + (2.7 + 18(B_s/B_c)^2)_e - 0.1\ L_p/y_0$

results of DHL-research Q 935:

$L_p/y_0=0$    △

$L_p/y_0=5$    □

| Lp/y0=0 |
| Lp/y0=2 |
| Lp/y0=5 |
| Lp/y0=10 |
| Lp/y0=20 |
| Lp/y0=30 |
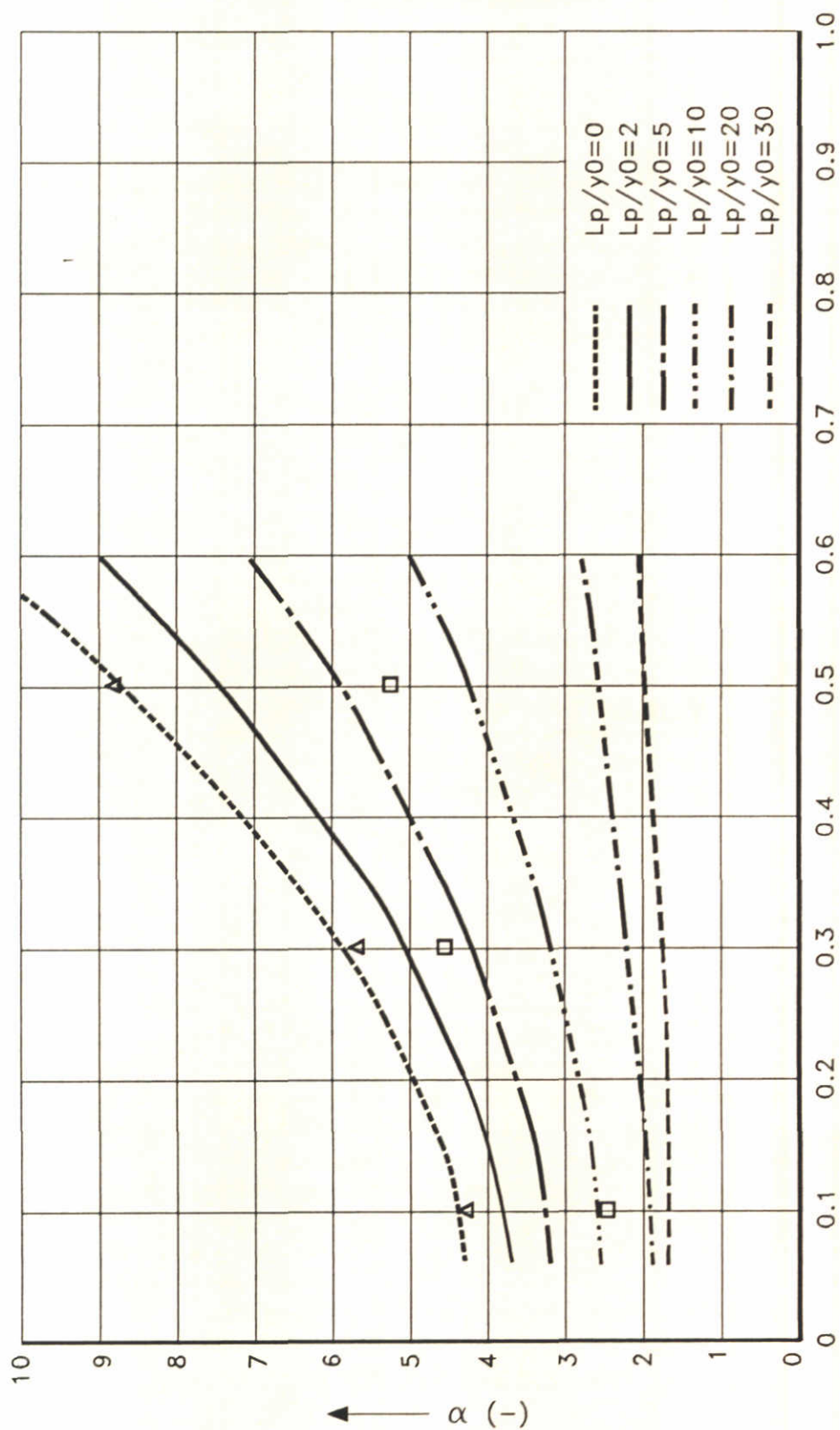
SPURDIKE, $\alpha$ AS A FUNCTION
OF $B_s/B$ AND $L_p/y_0$
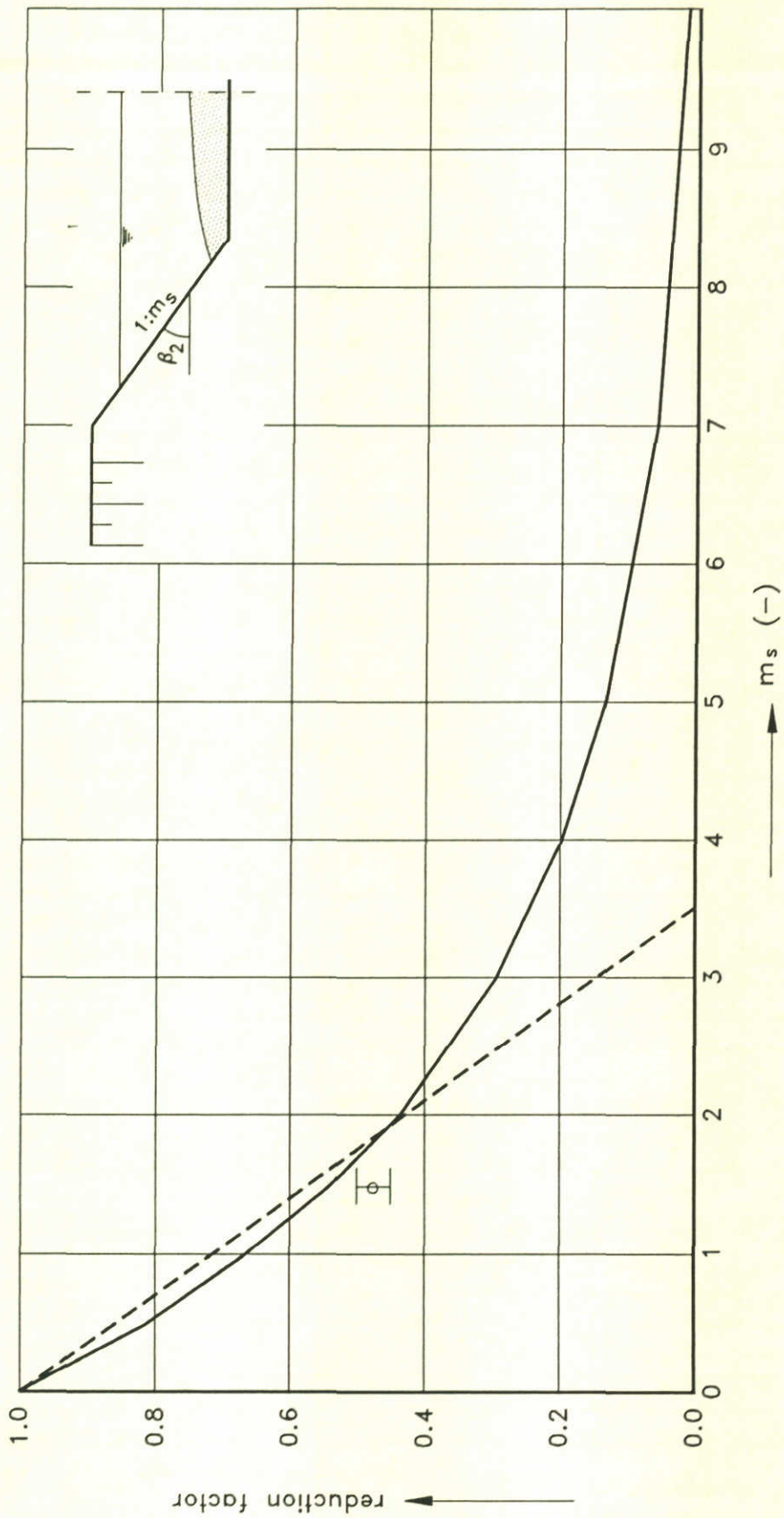
DELFT HYDRAULICS     Q 647     FIG. 3.2

REDUCTION FACTOR AS A FUNCTION OF
THE SLOPE OF THE HEAD OF THE GROYNE
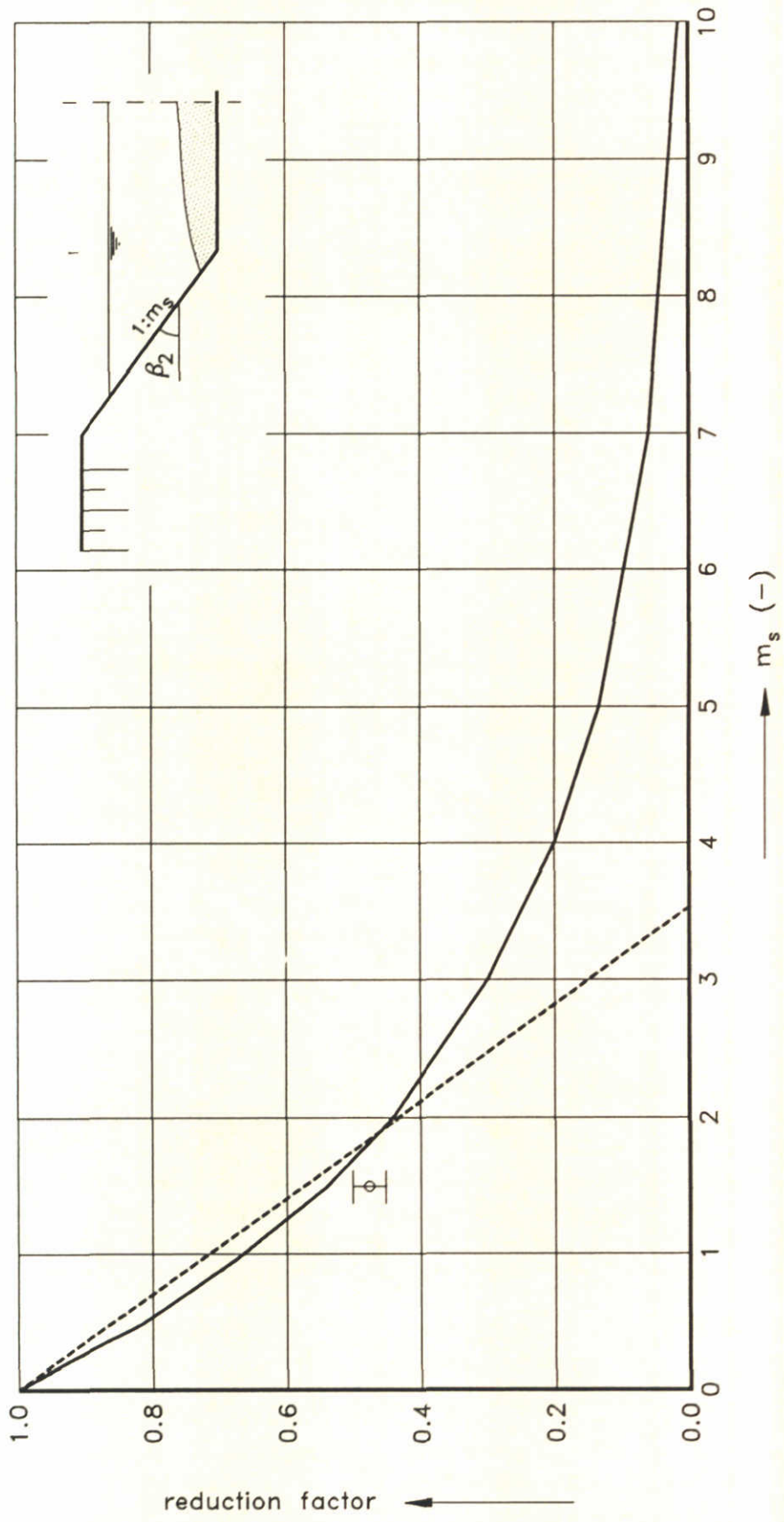
DELFT HYDRAULICS     Q 647     FIG. 3.3

REDUCTION FACTOR AS A FUNCTION OF THE
SLOPE OF THE HEAD OF THE GROYNE

| DELFT HYDRAULICS | Q 647 | FIG. 3.3 |

$$\gamma = 10^{\,P} \frac{y_m}{y_0} + V$$

---- $\gamma = 0.38$

x $\gamma = 0.36$

—— $\gamma = 0.20$

—·— $p = -0.3, \ v = -0.3$

$\frac{y_{max}}{y_0}$ (−)

$t/t_1$ (−)

MAXIMUM SCOUR DEPTH AS A FUNCTION OF $t/t_1$

DELFT HYDRAULICS | Q 647 | FIG. 3.4
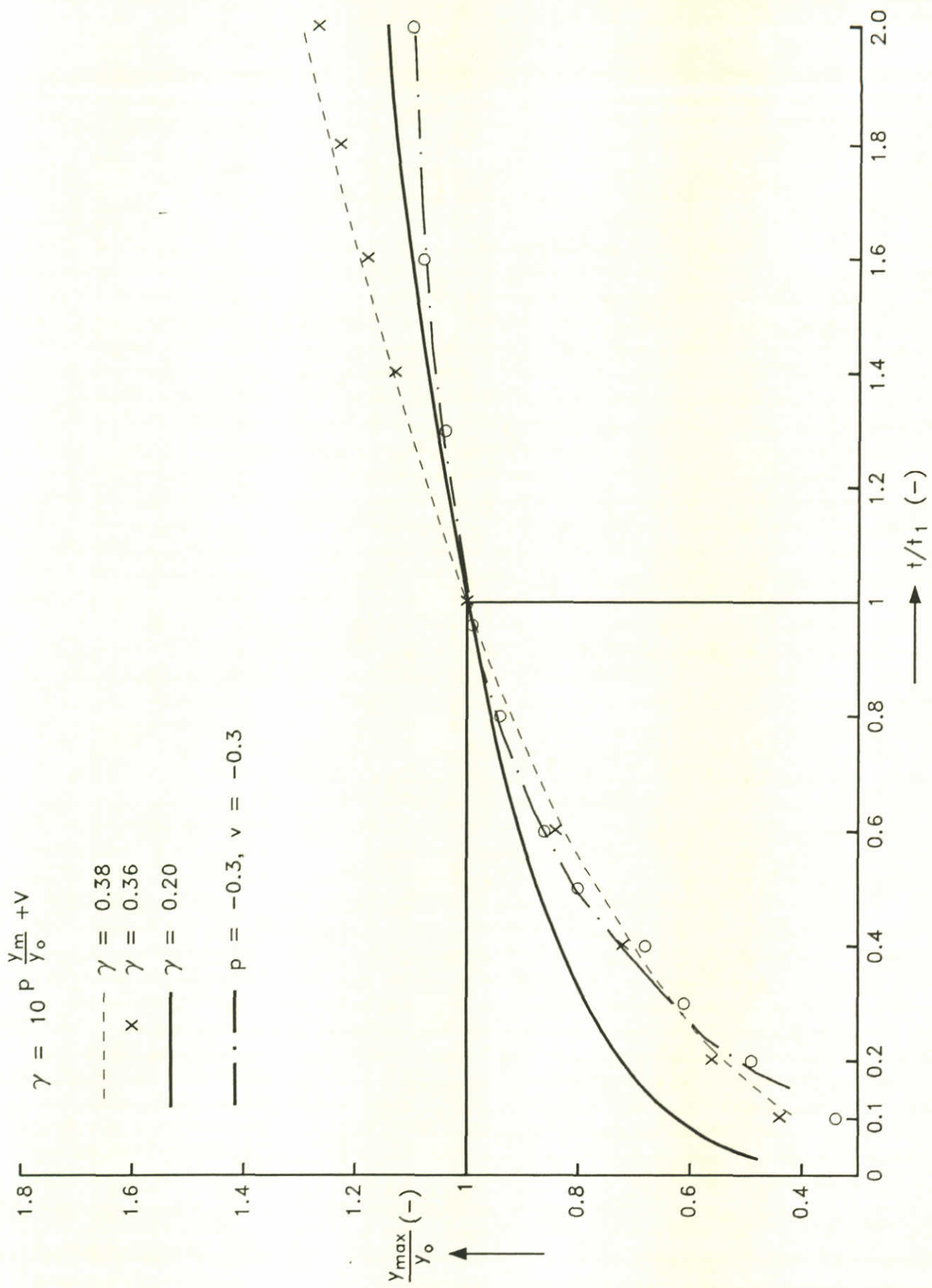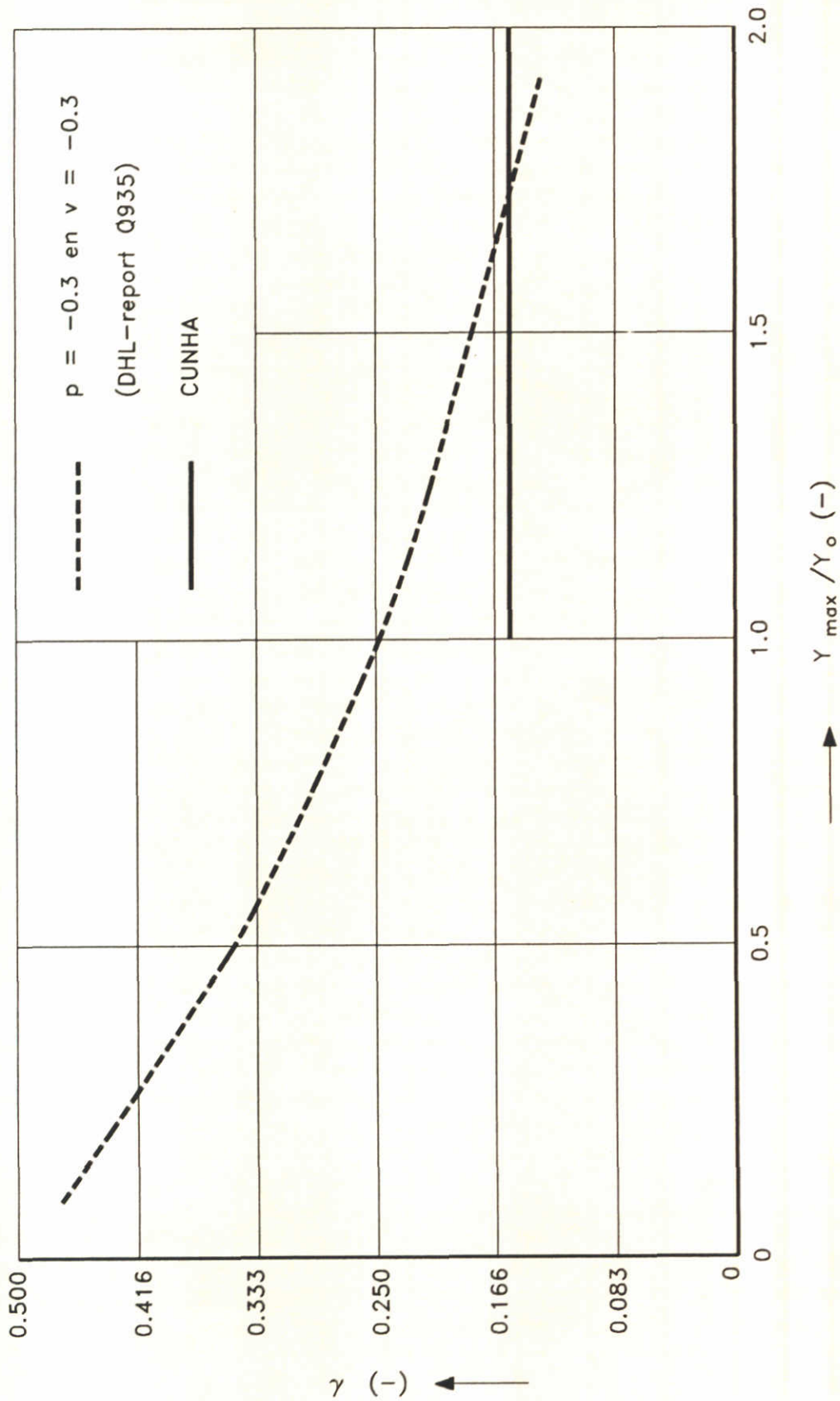
spurdikes without bed protection

Legend:
- $p = -0.3$ en $v = -0.3$ (DHL–report Q935)
- CUNHA

Y-axis (left): $\gamma$ $(-)$ — values: 0.500, 0.416, 0.333, 0.250, 0.166, 0.083, 0

X-axis (bottom): $Y_{max}/Y_o$ $(-)$ — values: 0, 0.5, 1.0, 1.5, 2.0

SPURDIKE, $\gamma$ AS A FUNTION OF $Y_{max}/Y_o$

DELFT HYDRAULICS

Q 647

FIG. 3.5

a combination of a sill and a spurdike

$\alpha$ (-) ◄

$Y_D / Y_o$ (-)

Lp/y0=0
Lp/y0=5
Lp/y0=10
Lp/y0=20
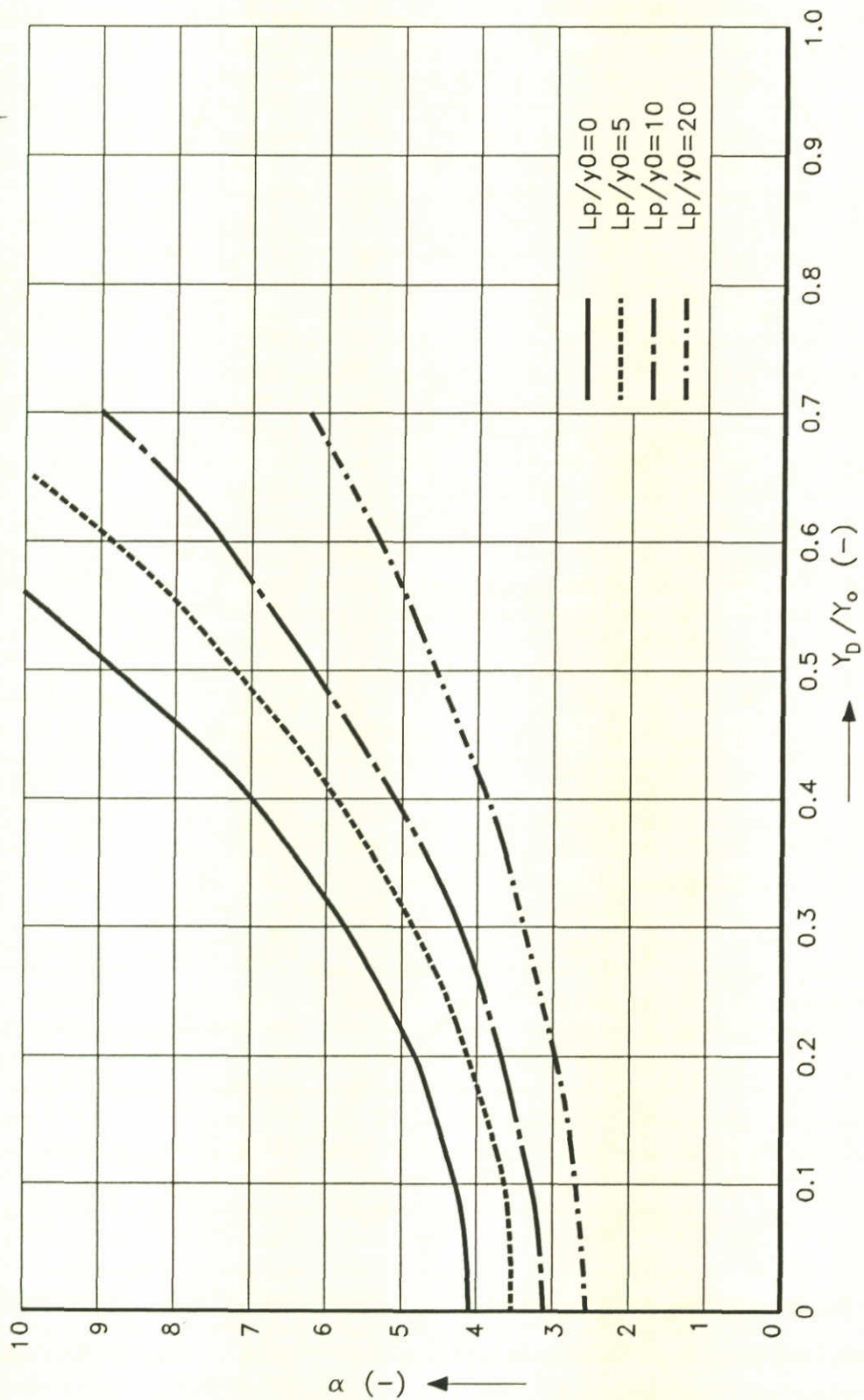
SPURDIKE ON A SILL, $\alpha$ AS A FUNCTION
OF $Y_D / Y_0$ AND $L_p / Y_0$, $B_s / B = 0.1$

DELFT HYDRAULICS

Q 647

FIG. 3.6
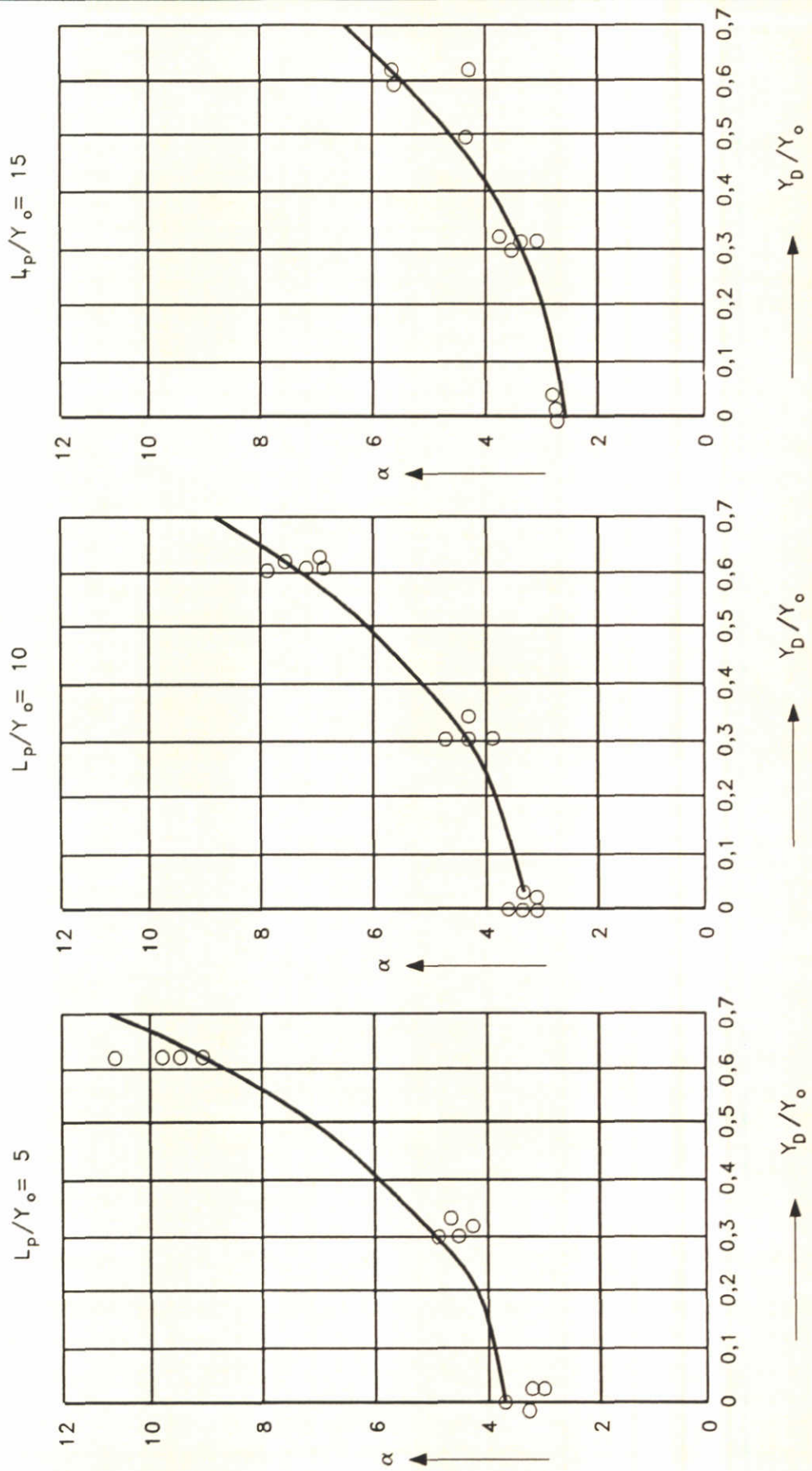
SPURDIKE ON A SILL,

CALIBRATION OF THE CALCULATED $\alpha$

DELFT HYDRAULICS

Q 647

FIG. 3.7
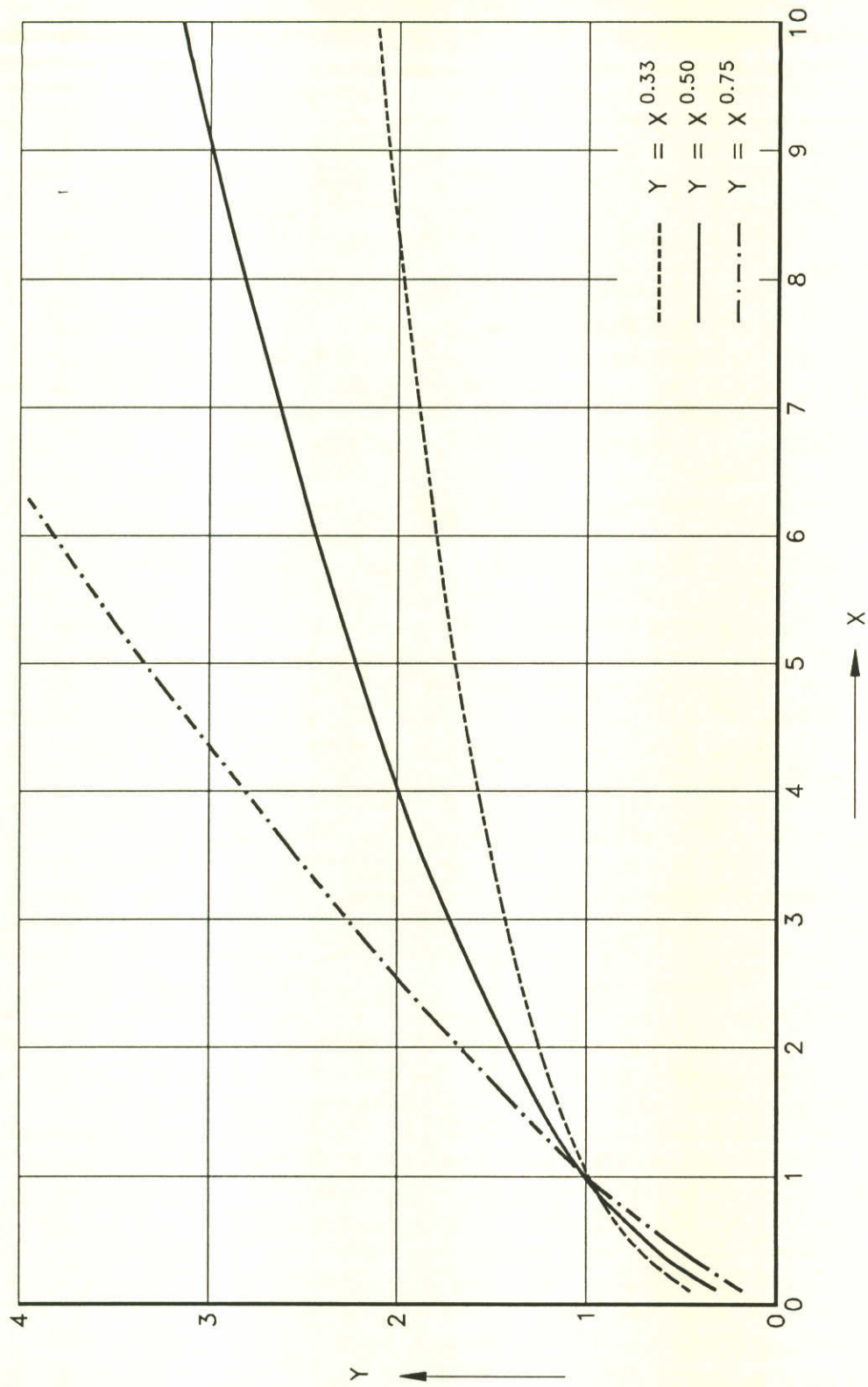
RELATIONSHIPS OF THE TYPE y=x$^\alpha$

DELFT HYDRAULICS          Q 647          FIG. 3.8

without a
bed protection

CROSS-SECTION A-B

TOP VIEW
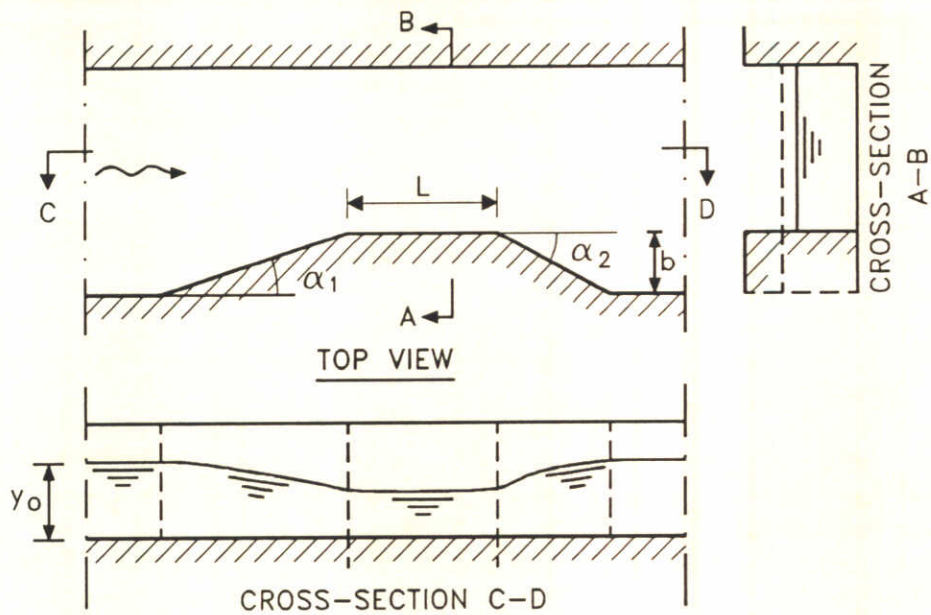
CROSS-SECTION C-D

FLOW PATTERN

one separation point

TOP VIEW

two separation points
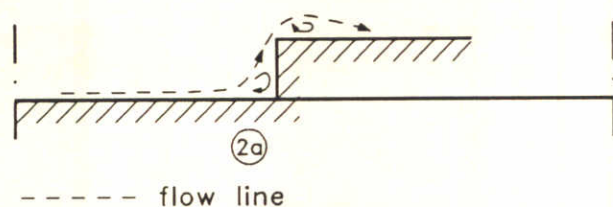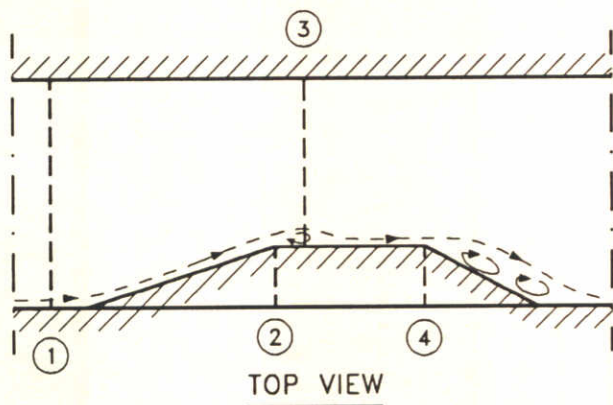
TOP VIEW

- - - - - flow line

ABUTMENT, GENERAL LAY-OUT
AND FLOW PATTERN

DELFT HYDRAULICS

Q 647

FIG. 3.9

flow line

lines of equal
scour depth

TOP VIEW

scour hole due to
general constriction

scour hole due to
vortex street
local scour
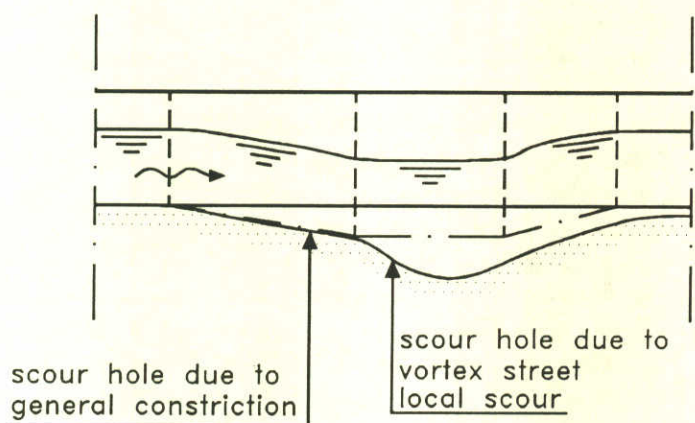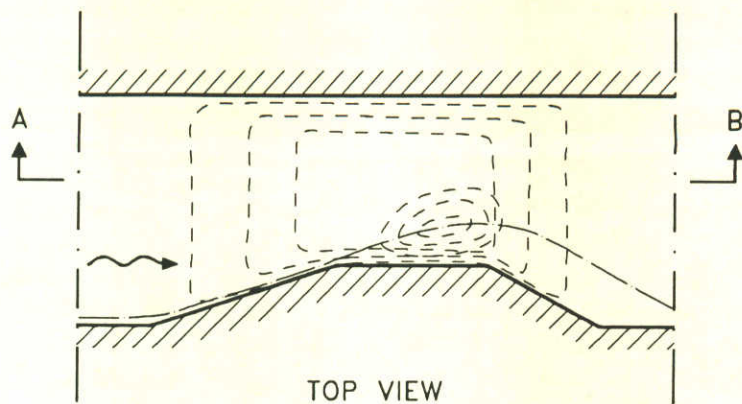
CROSS–SECTION A–B

with a bed protection
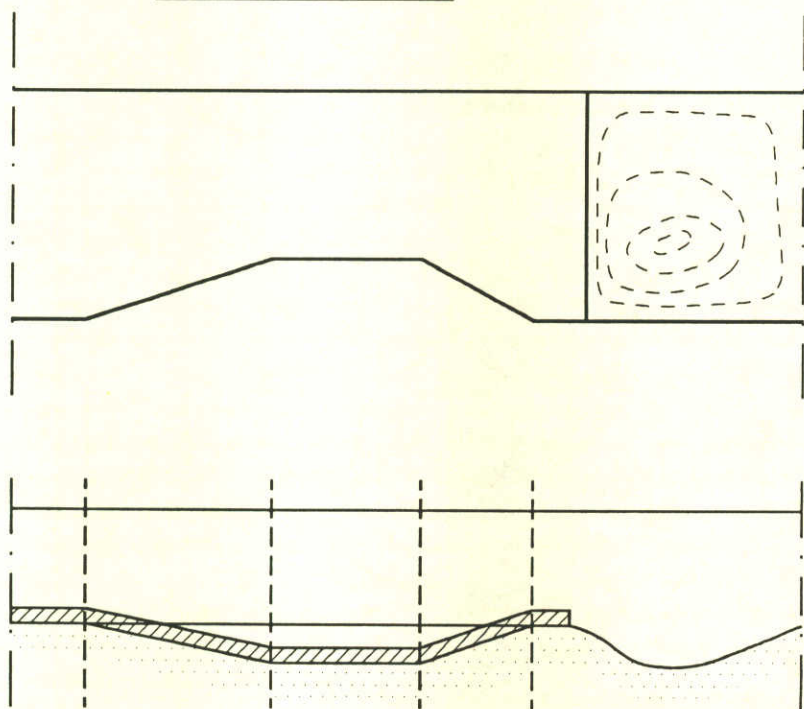
CROSS–SECTION A–B

ABUTMENT, SCOUR HOLE

DELFT HYDRAULICS

Q 647

FIG. 3.10

$B_p$

alternative

$y_0$

$y_{s,max}$

I

II

III

caisson
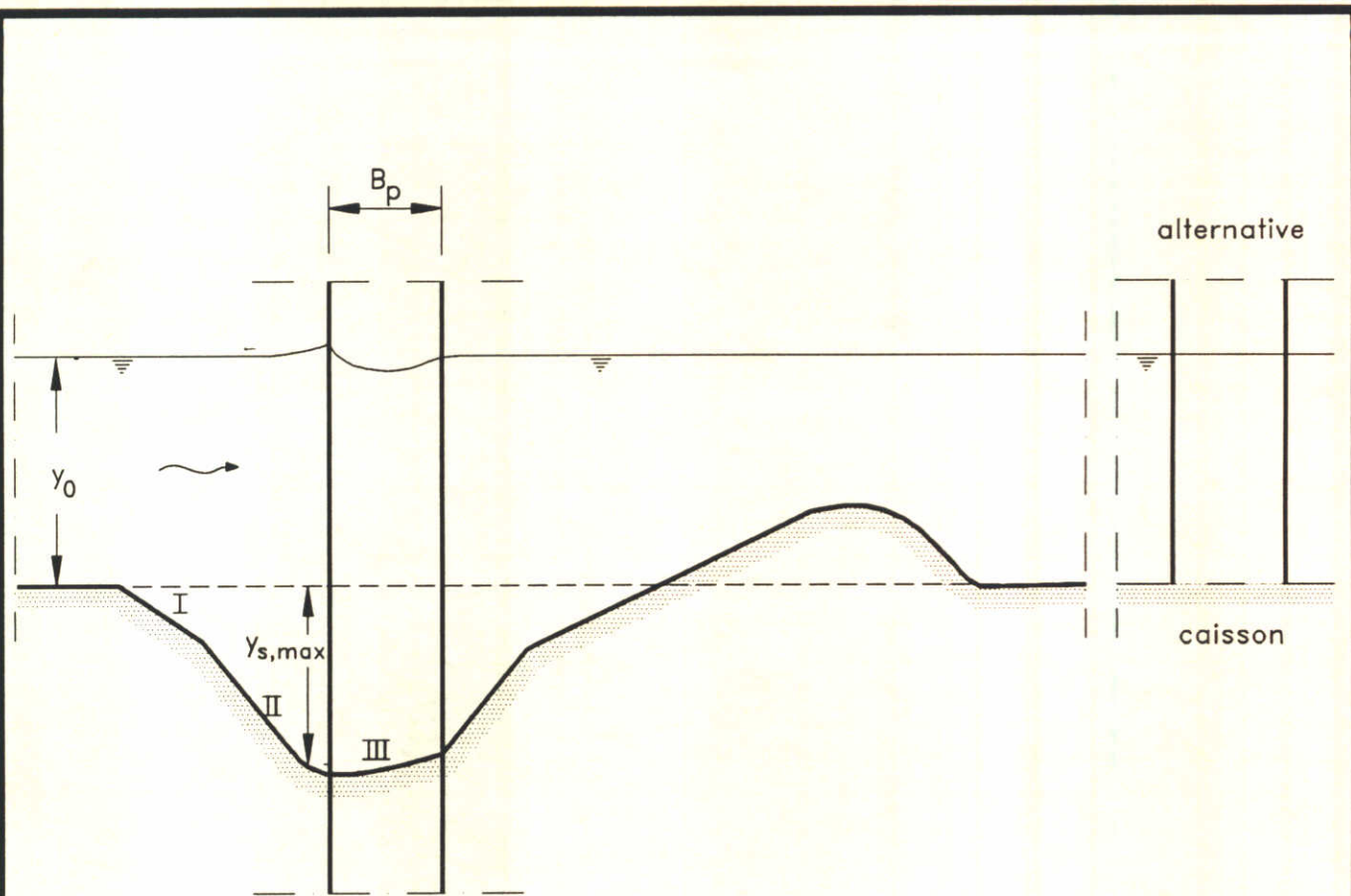
I upper slope
II lower slope
III concave region

CROSS-SECTION A-A

A

A

deposition area

score hole
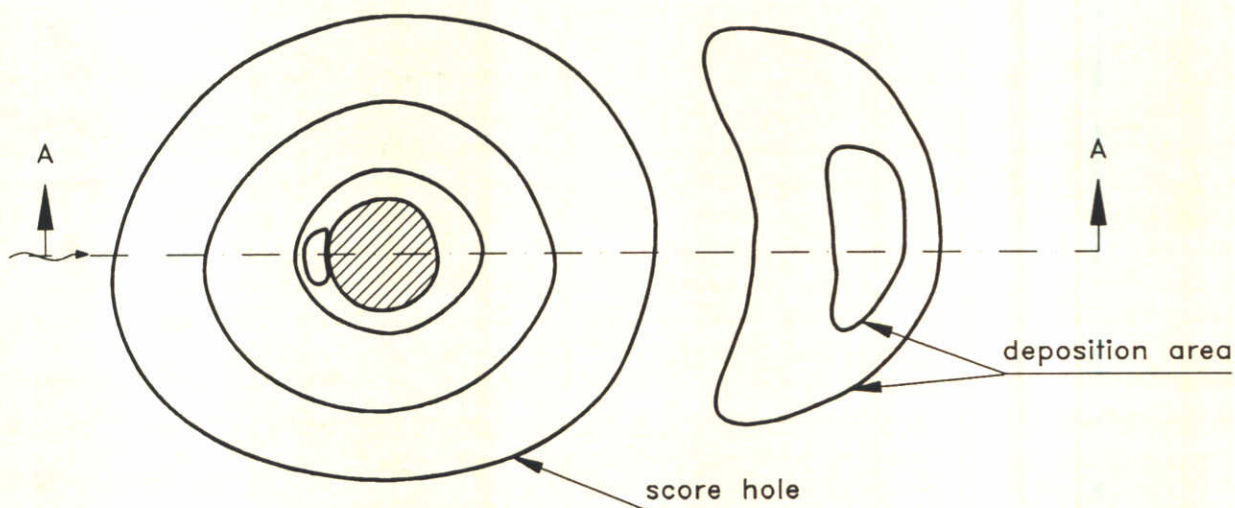
TOP VIEW SCOUR HOLE

DEFINITION SKETCH OF SCOUR AROUND BRIDGE PIERS

DELFT HYDRAULICS

Q 647

FIG. 4.1

Cylinder

Wake vortices

Y

Plane of
symmetry

X

Ordinary separation
line

Skewed velocity
profiles

BOW WAVE

WAKE
SHED VORTICES

DOWNFLOW

HORSESHOE VORTEX
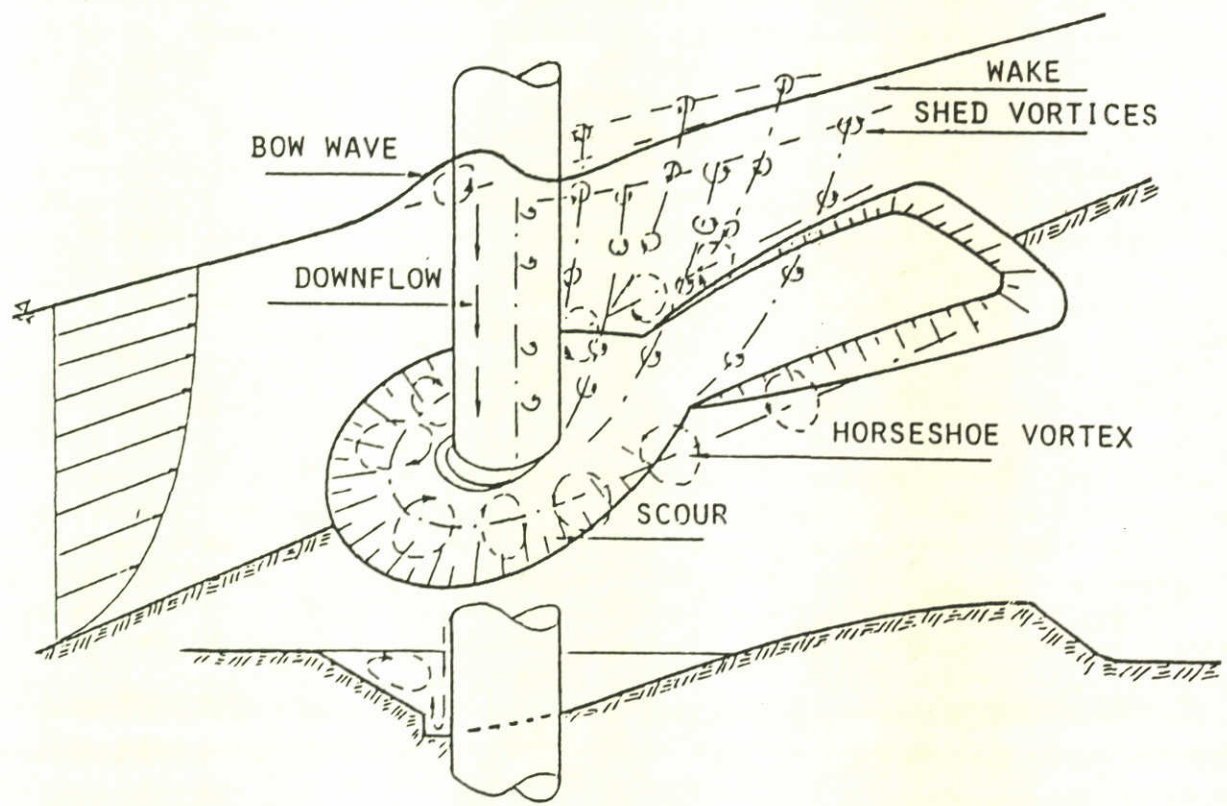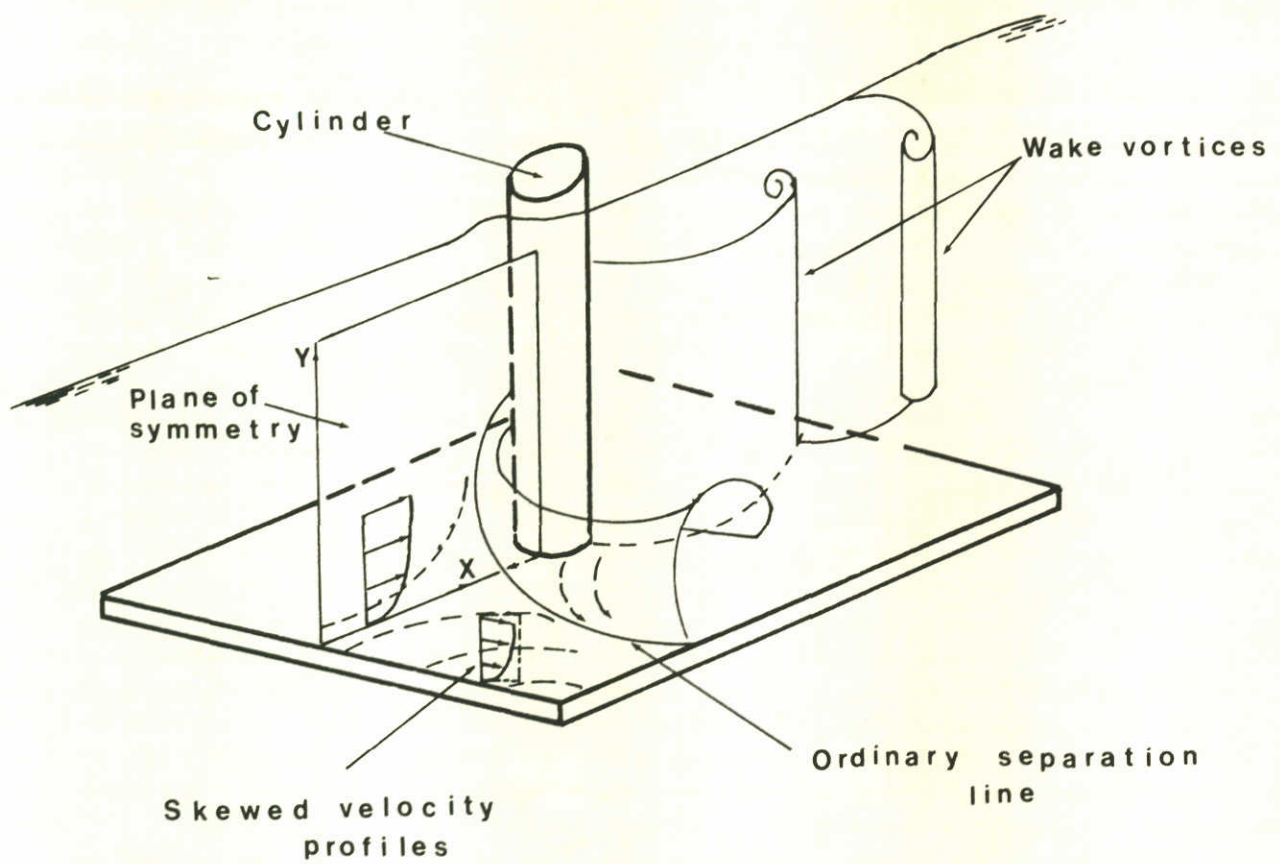
SCOUR

FLOW PATTERN ACCORDING TO DARGAHI

DELFT HYDRAULICS

Q 647

FIG. 4.2
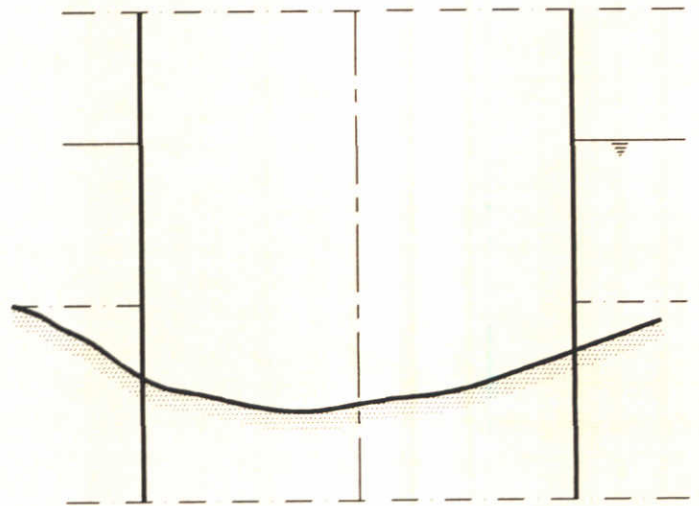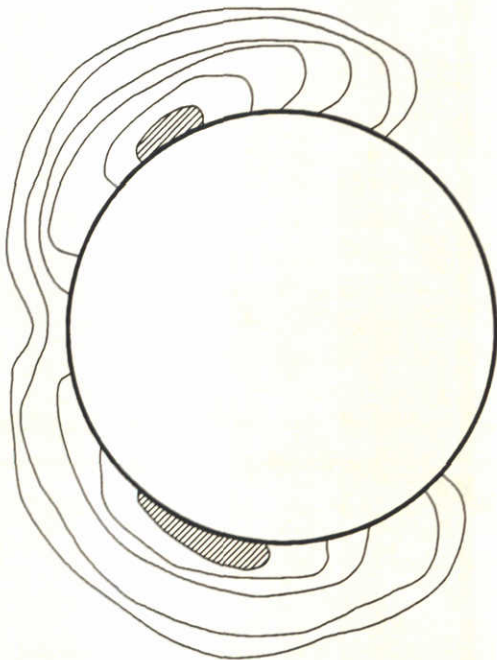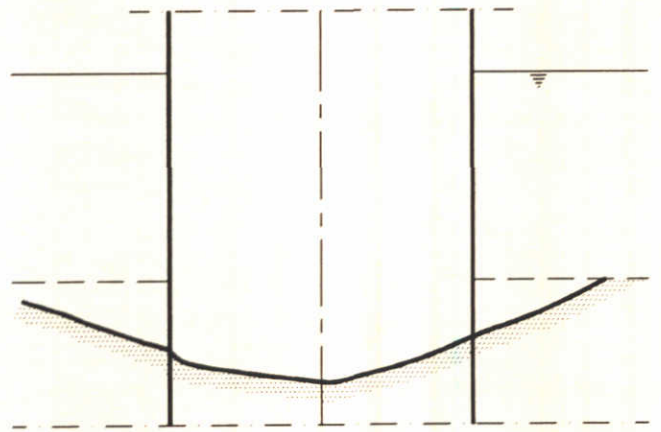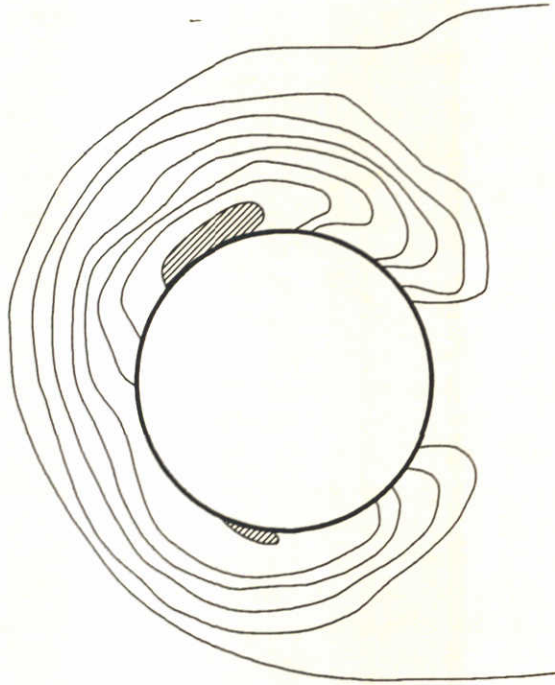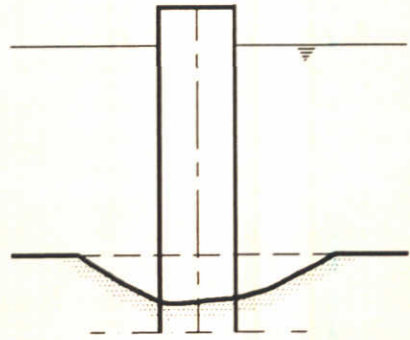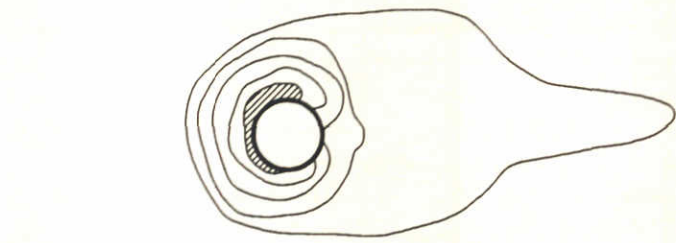
SCOUR PATTERN AND THE PLACE OF
$Y_{s,max}$ ACCORDING TO CARSTENS

DELFT HYDRAULICS          Q 647          FIG. 4.3

initial phase    developing phase    equilibrium phase

shape of pier

$\gamma$ AS A FUNCTION OF $Y_{s,max}/Y_o$

DELFT HYDRAULICS          Q 647          FIG. 4.4
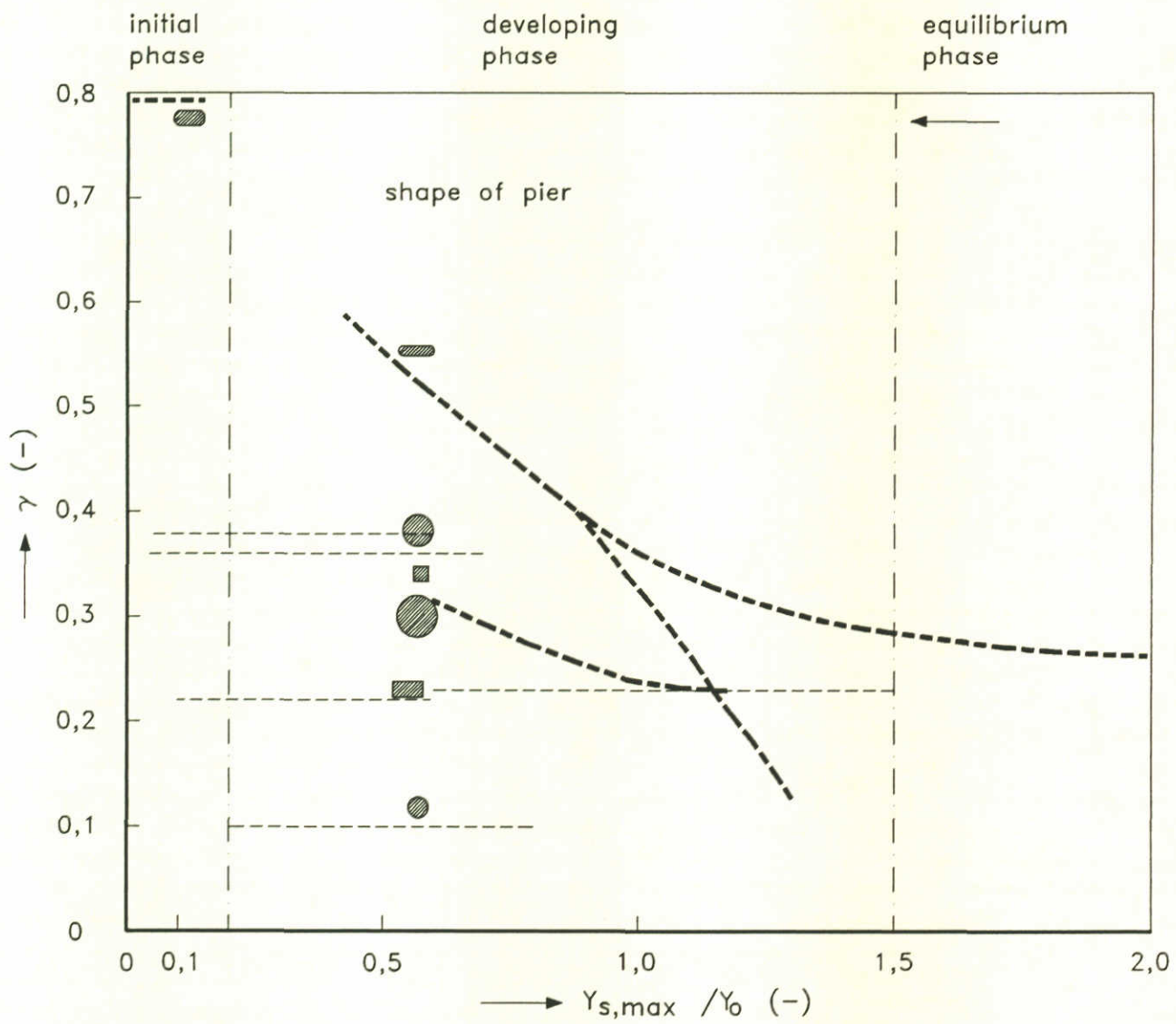
γ AS A FUNCTION OF
$Y_{s,max}/Y_o$ AND $Y_{s,max}/B_p$

DELFT HYDRAULICS          Q 647          FIG. 4.5
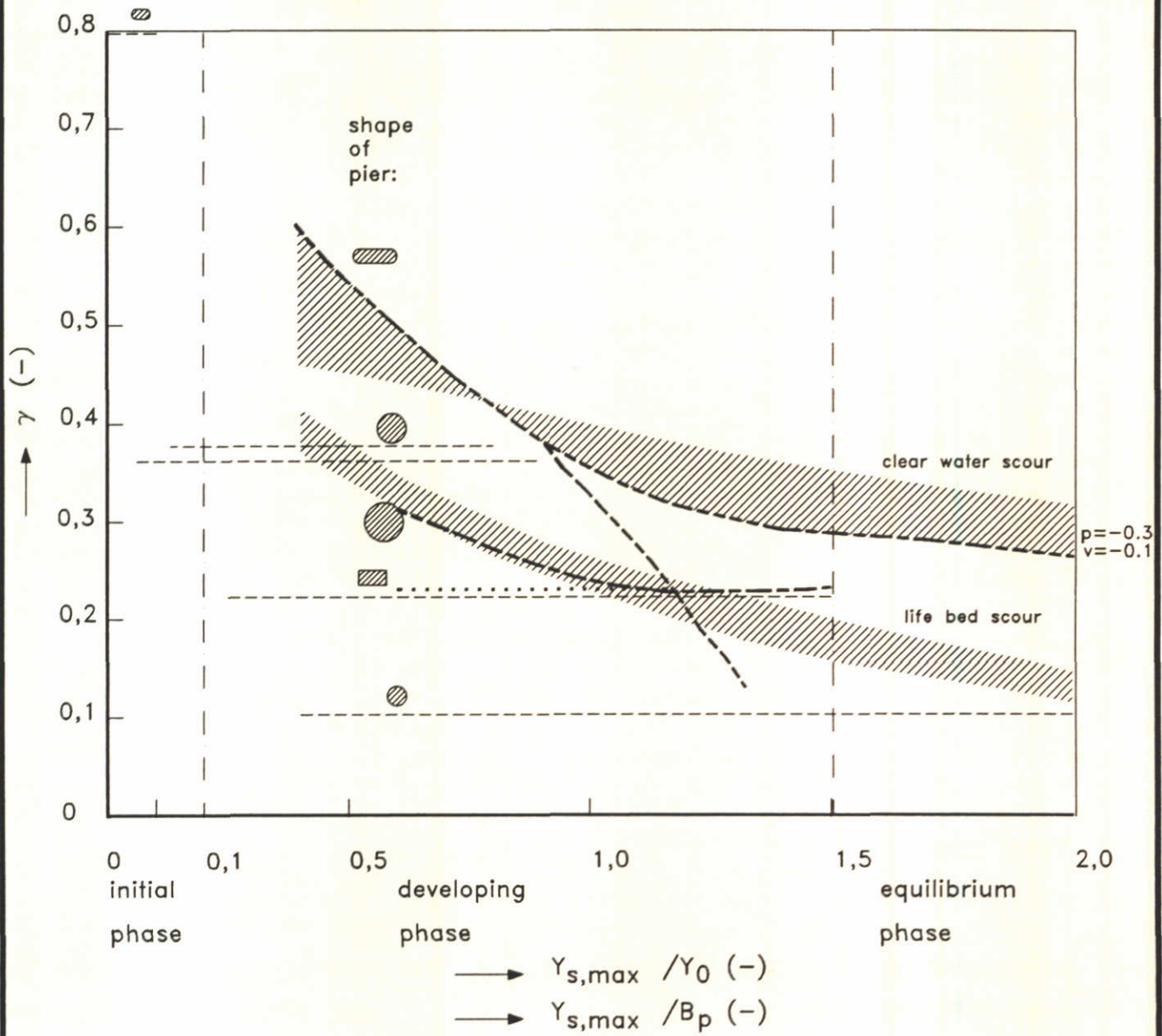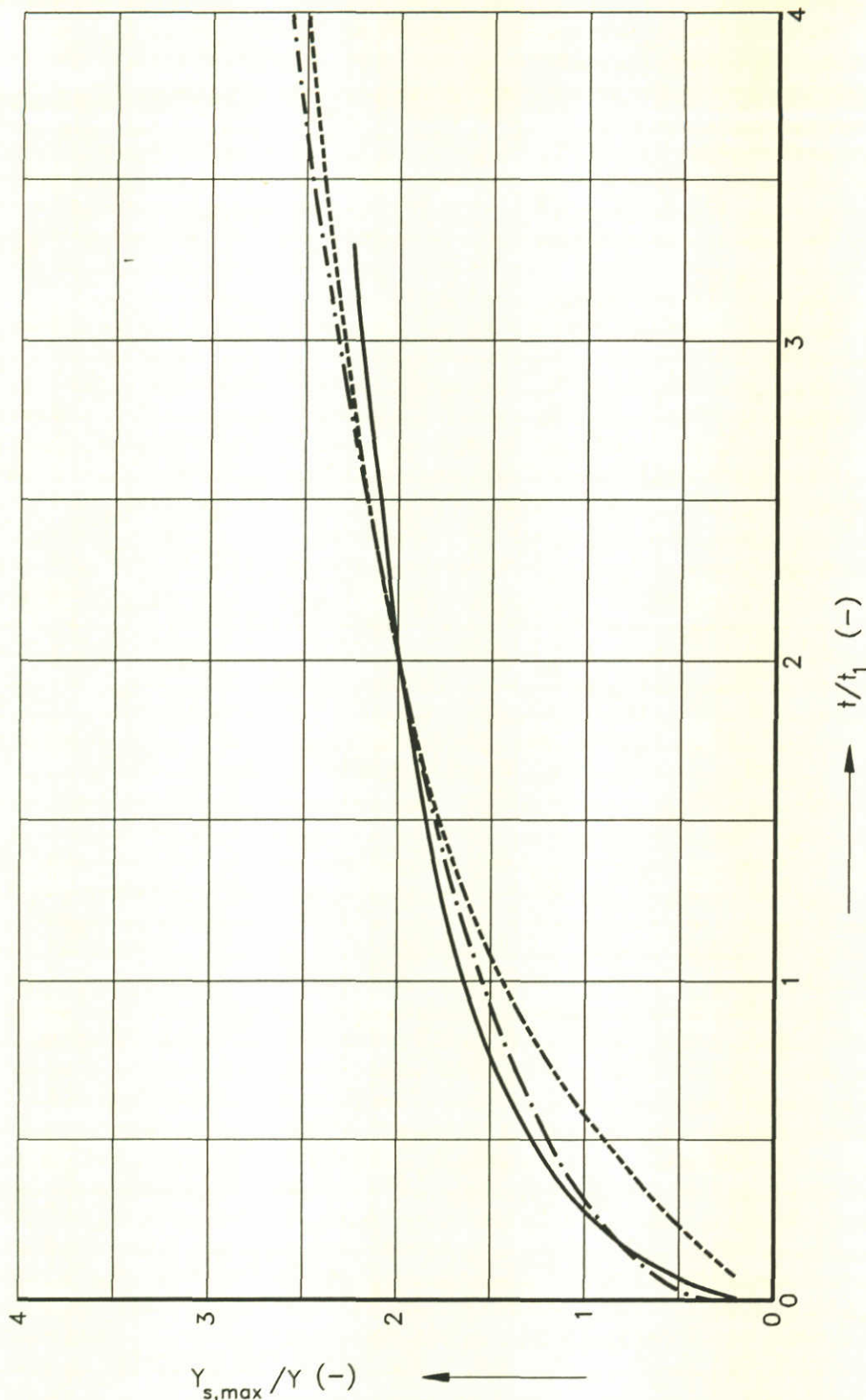
BRIDGE PIER SCOUR:

— $p = 0.30$  $v = -0.30$ life bed scour

---- $p = -0.30$  $v = -0.10$ clear water scour

-·-·- $\gamma = 0.38$  two-dimensional scour
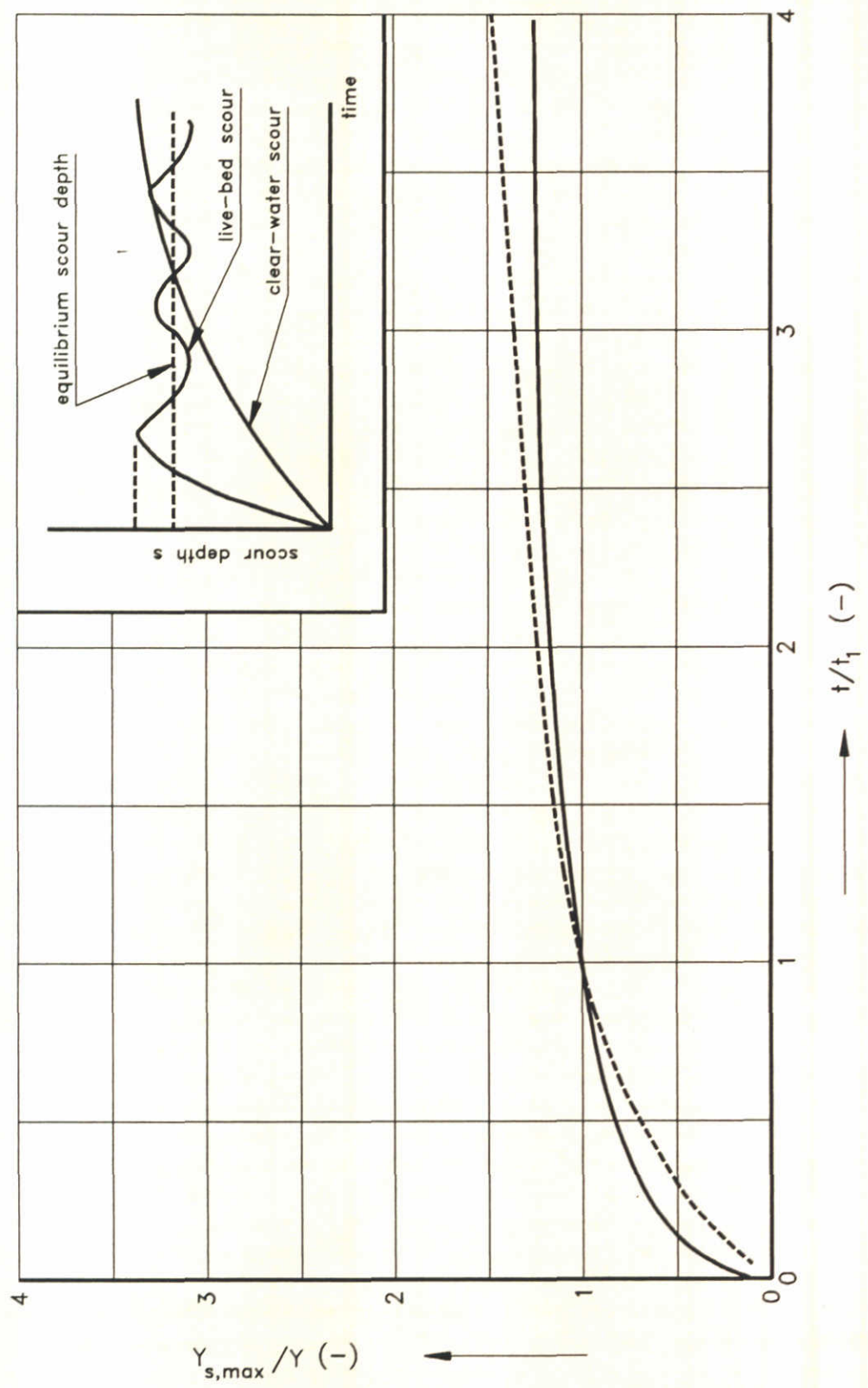
$t/t_1$ $(-)$

$Y_{s,max}/Y$ $(-)$

DIFFERENCE BETWEEN CLEAR WATER
SCOUR AND LIFE BED SCOUR

DELFT HYDRAULICS        Q 647    FIG. 4.6

DIFFERENCE BETWEEN CLEAR WATER
SCOUR AND LIFE BED SCOUR

DELFT HYDRAULICS

Q 647

FIG. 4.7
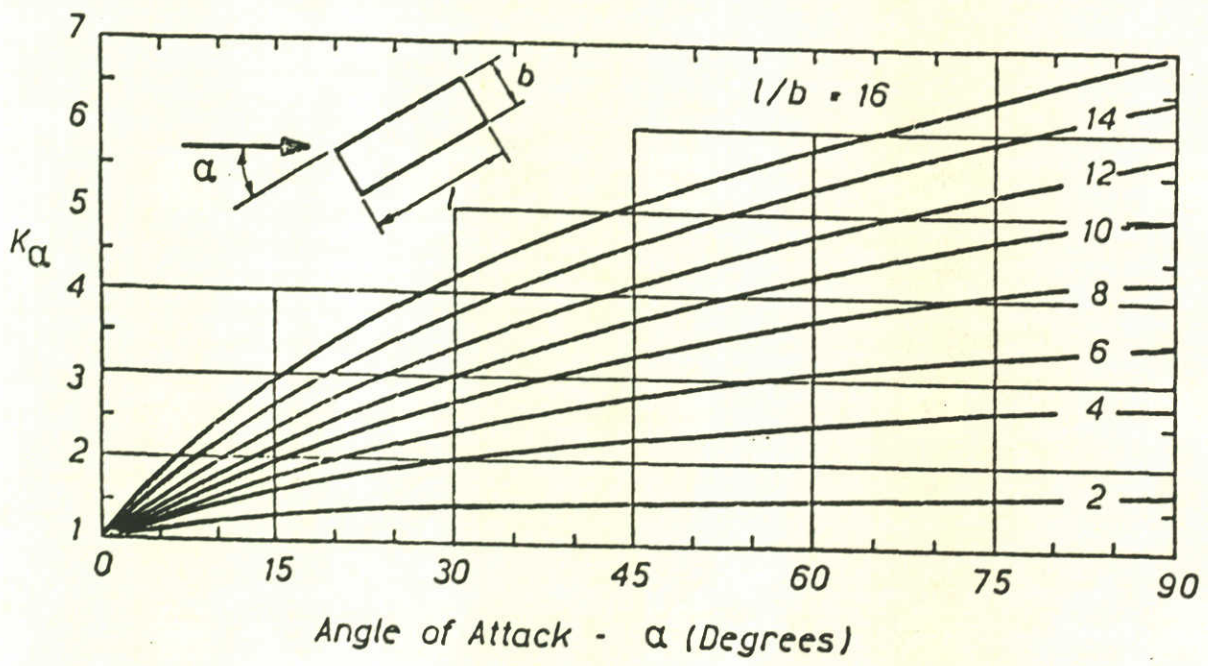
THE INFLUENCE OF THE ALIGNMENT OF THE PIER
TO THE FLOW, ON THE MAXIMUM SCOUR DEPTH

| DELFT HYDRAULICS | Q 647 | FIG. 4.8 |
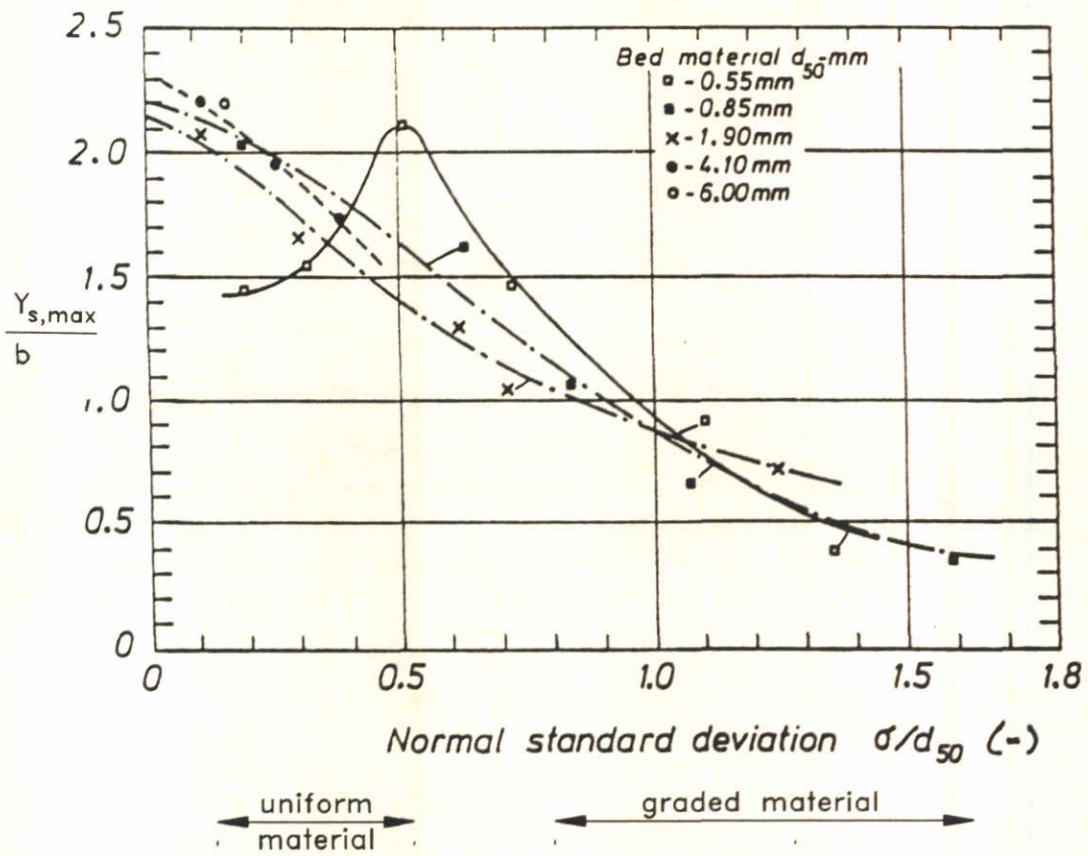
THE INFLUENCE OF THE GRADATION ON
THE MAXIMUM SCOUR DEPTH

DELFT HYDRAULICS          Q 647      FIG. 4.9

THE FACTOR $K_\sigma$ AS A FUNCTION OF $\sigma_g$

DELFT HYDRAULICS          Q 647          FIG. 4.10
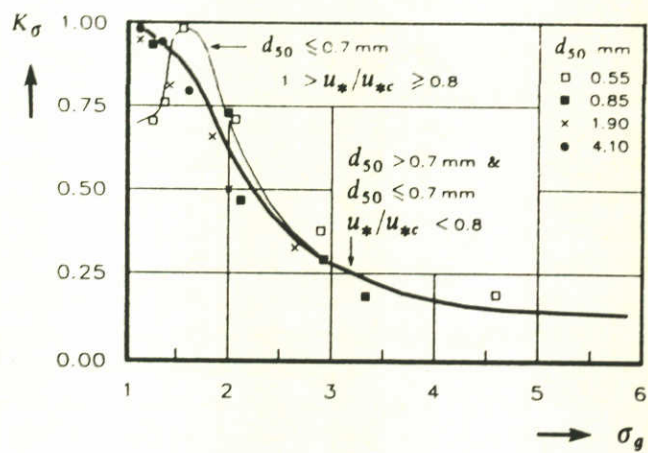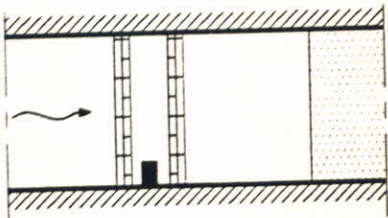
systematic series

TOP VIEW

systematic series
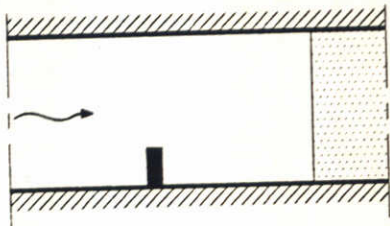
TOP VIEW

CROSS-SECTION
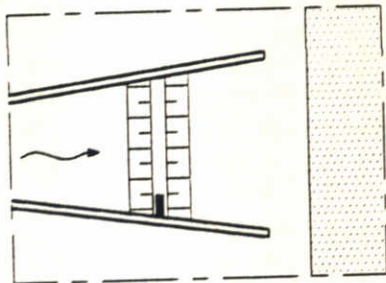
CROSS-SECTION

prototype test

TOP VIEW
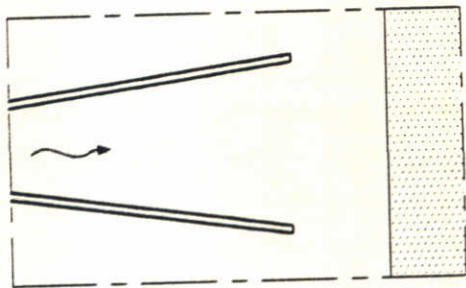
CROSS-SECTION

low head hydro power station

TOP VIEW
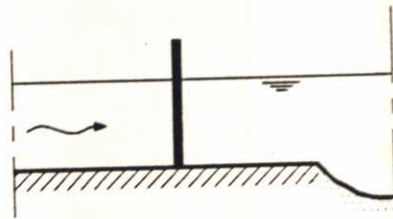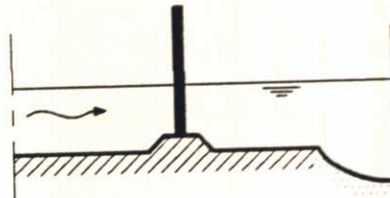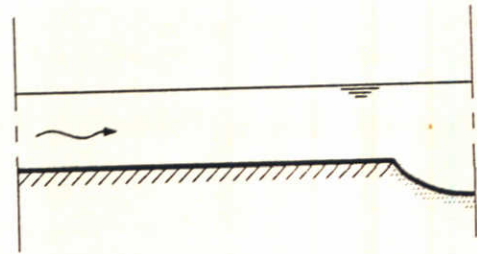
CROSS-SECTION
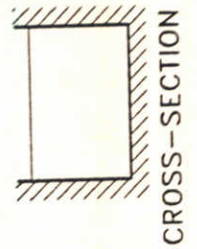
CROSS-SECTION

| TYPES OF OUTLETS AND THE MAIN GEOMETRIC PARAMETERS | | |
|---|---|---|
| DELFT HYDRAULICS | Q 647 | FIG. 5.1 |
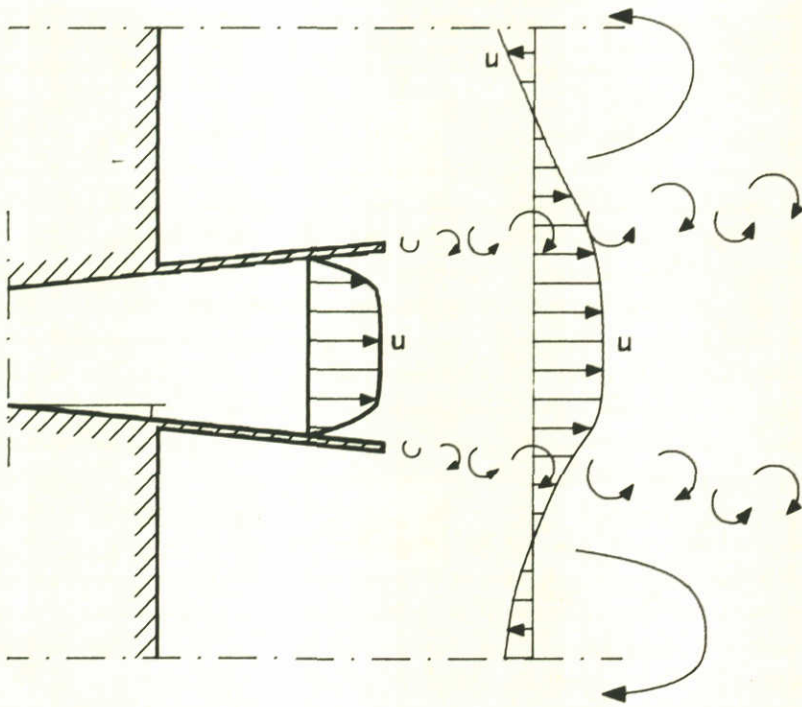
FLOW VELOCITY DISTRIBUTION
AT EDGE OF BED PROTECTION
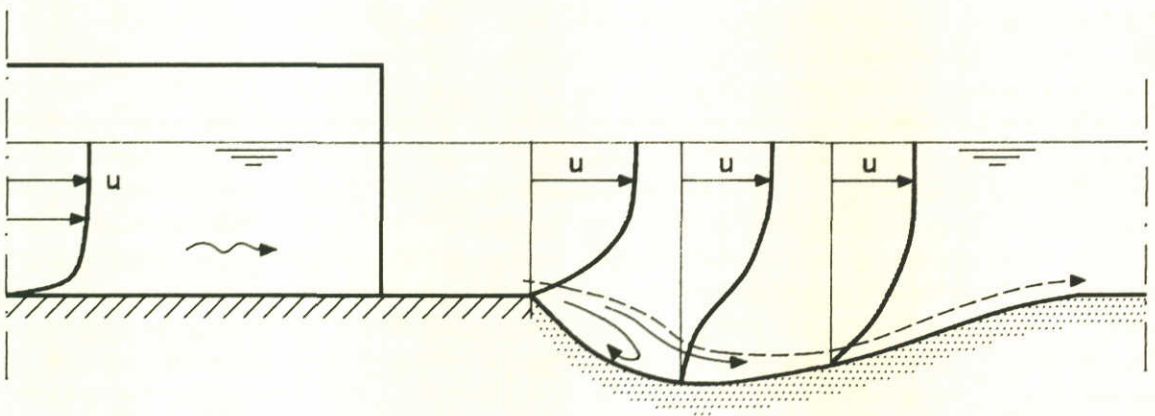
------- flow line

GENERAL FLOW PATTERN NEAR AN OUTLET

DELFT HYDRAULICS     Q 647     FIG. 5.2
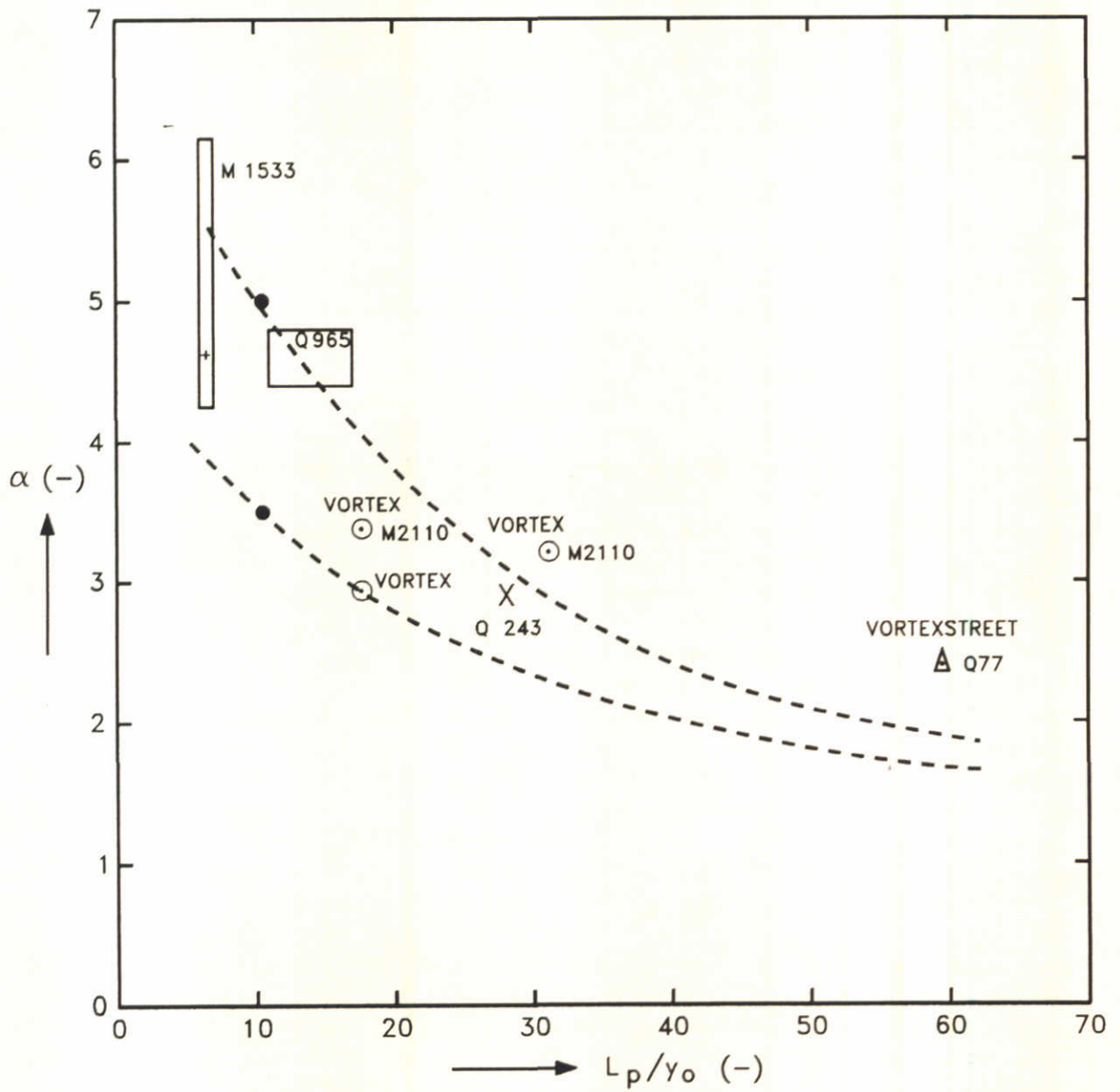
α AS A FUNCTION OF $L_p/y_o$, $Y_D/Y_o=0$,
IN A VORTEX STREET

DELFT HYDRAULICS | Q 647 | FIG. 5.3

influence variabele $B_s$,no (bottom protects scour hole)
no $B_{s,c}$ is so small that vartex street is dissapeared
at the end of protection

$Y_D / Y_0 = 0.5$

$Y_D / Y_0 = 0.3$

$Y_D / Y_0 = 0$

$\alpha$ (−)
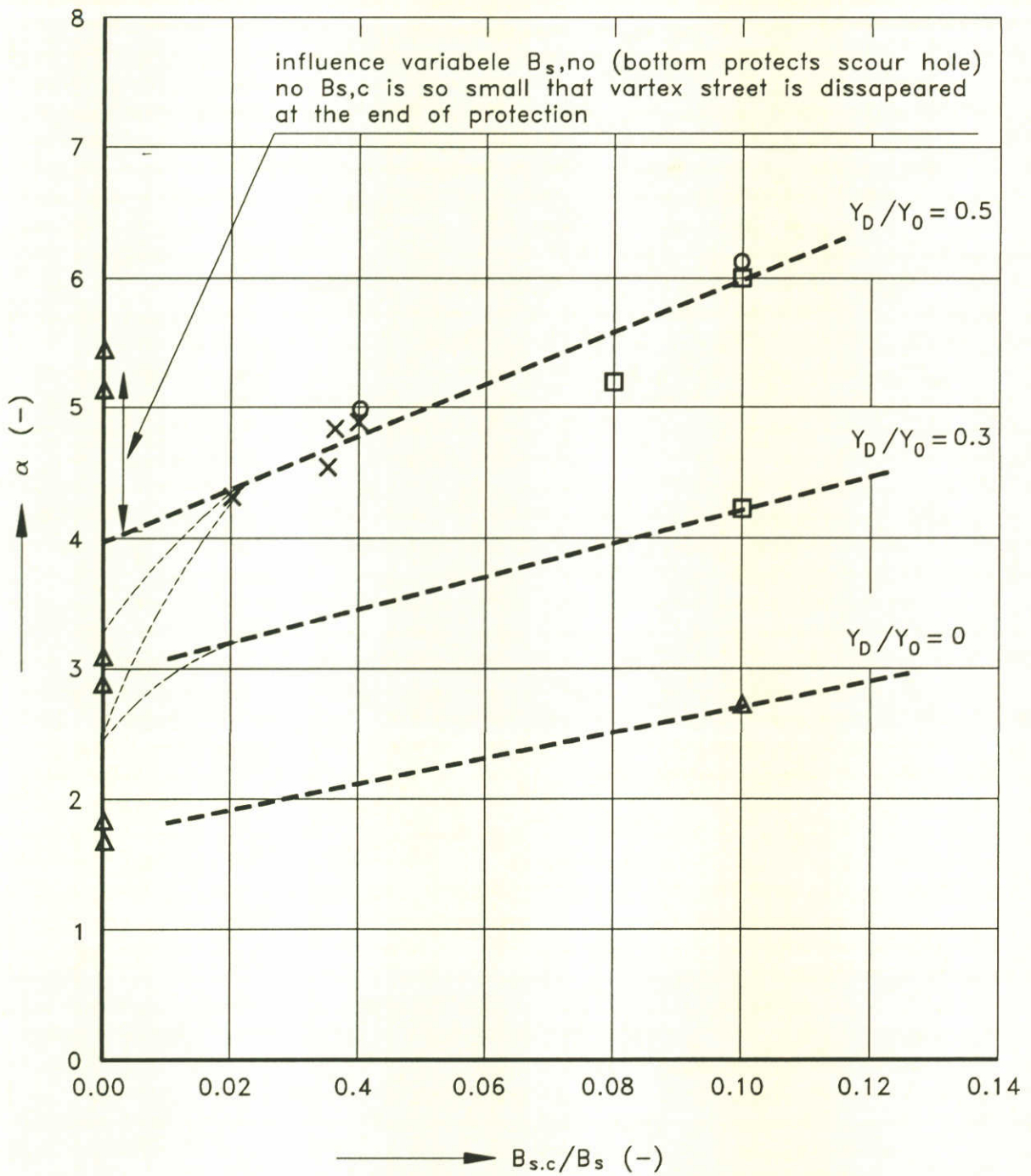
$B_{s.c} / B_s$ (−)

| symbol research | $L_p / Y_0$ |
|---|---|
| ✕, O  M 1533 I | 6−7 |
| □  M 1533 IV | 6−7 |
| △  Jorissen | 6−7 |

$\alpha$ AS A FUNCTION OF $B_{s.c} / B_s$ AND $Y_D / Y_0$

WATERLOOPKUNDIG LABORATORIUM     Q 647,     FIG. 5.4
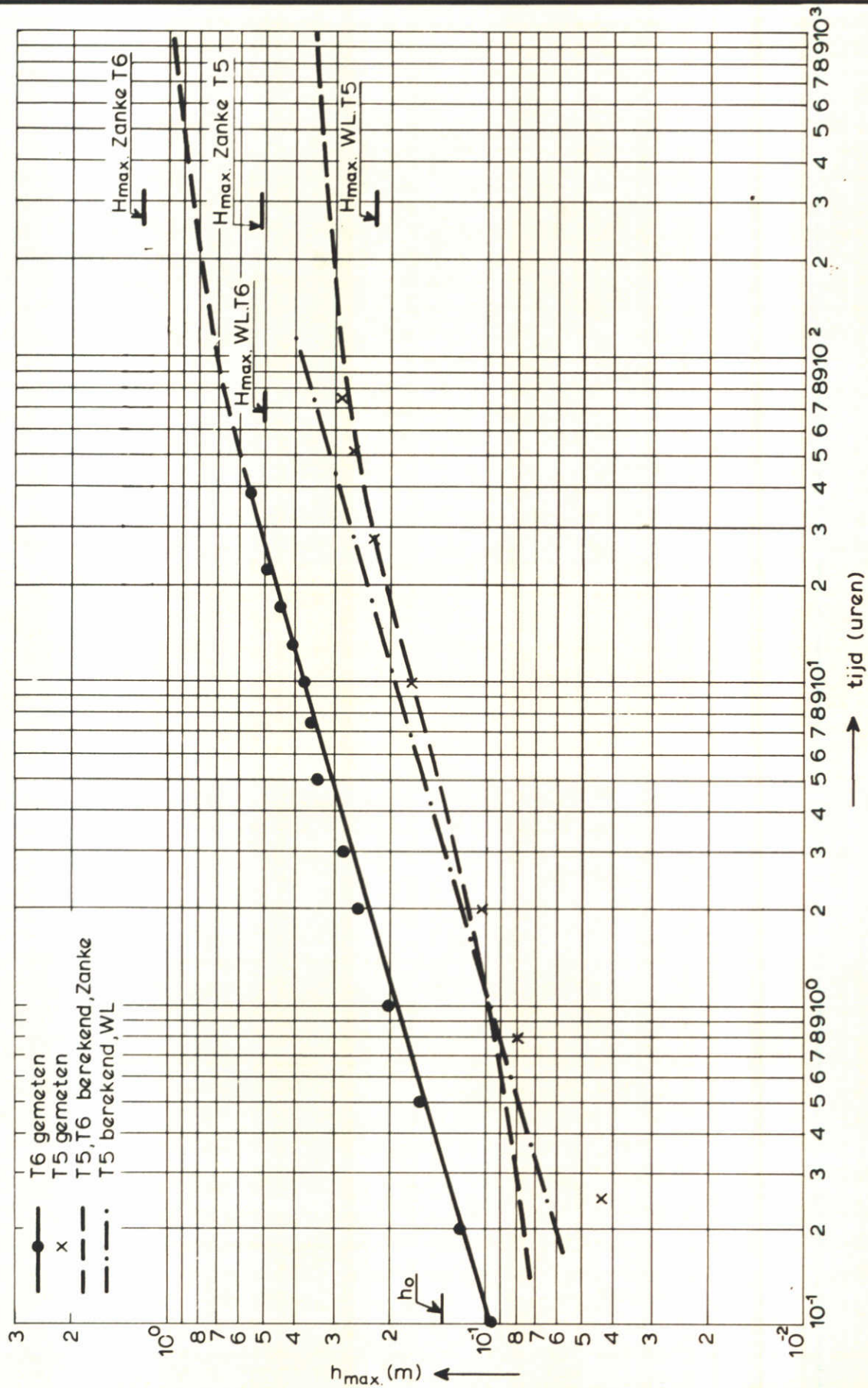
THE EQUILIBRIUM SCOUR DEPTH AND THE
MEASURED SCOUR DEPTH IN 2 TESTS

DELFT HYDRAULICS

Q 647

FIG. 5.5
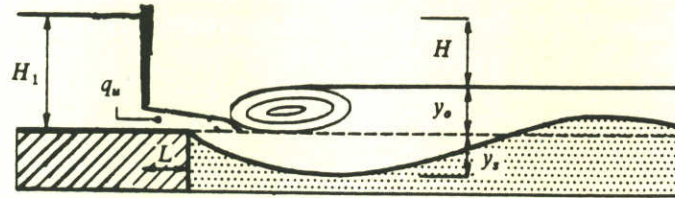
SUBMERGED JETS



FREE OR PLUNGING JETS

a) overfall
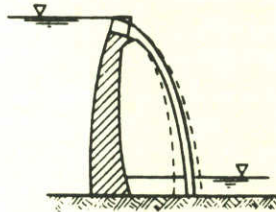


b) outflow under pressure
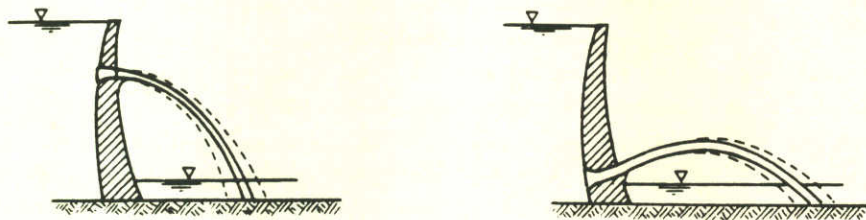


c) ski-jump spillway
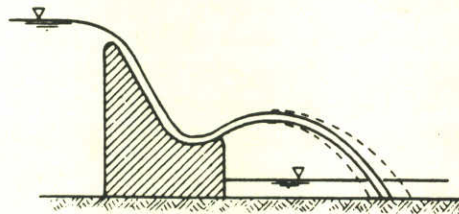


| | | |
|---|---|---|
| TYPES OF JETS | | |
| | | |
| DELFT HYDRAULICS | Q 647 | FIG. 6.1 |

HORIZONTAL JETS

$L_{st}$

$L_s$

$D_u$ or $2B_u$

$U_o$

$y_{sm}$

$B_{sm}$
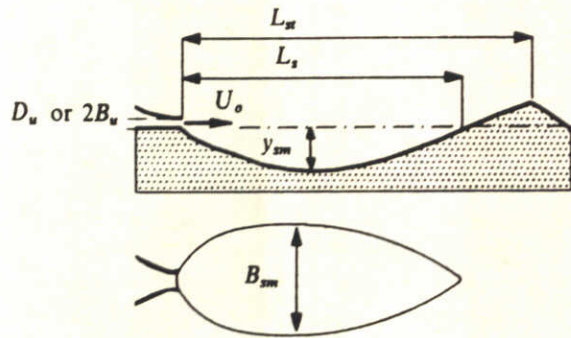
Note: The lower part
of the sketch
is for jets of
finite width.

VERTICAL JETS

$D_c$

$H$

$y_{ss}$

$y_{sd}$

low
velocities

high
velocities

JET SCOUR PARAMETERS

DELFT HYDRAULICS

Q 647

FIG. 6.2
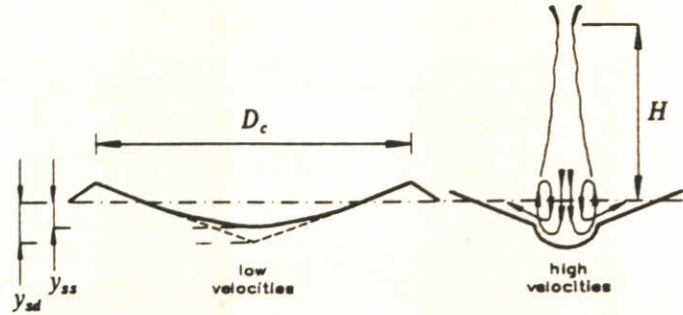
SUBMERGED HORIZONTAL JETS
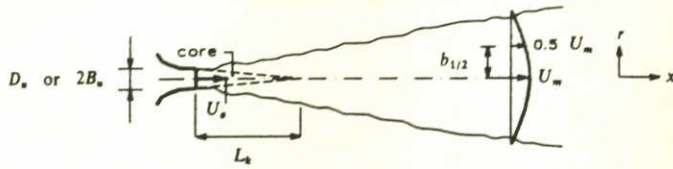
SUBMERGED VERTICAL AND RADIAL WALL JETS
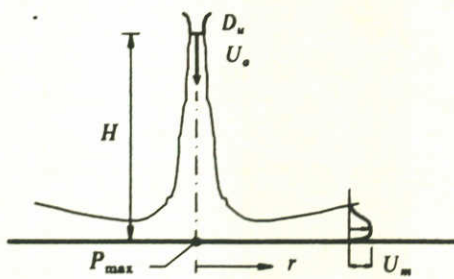
PLUNGING JETS
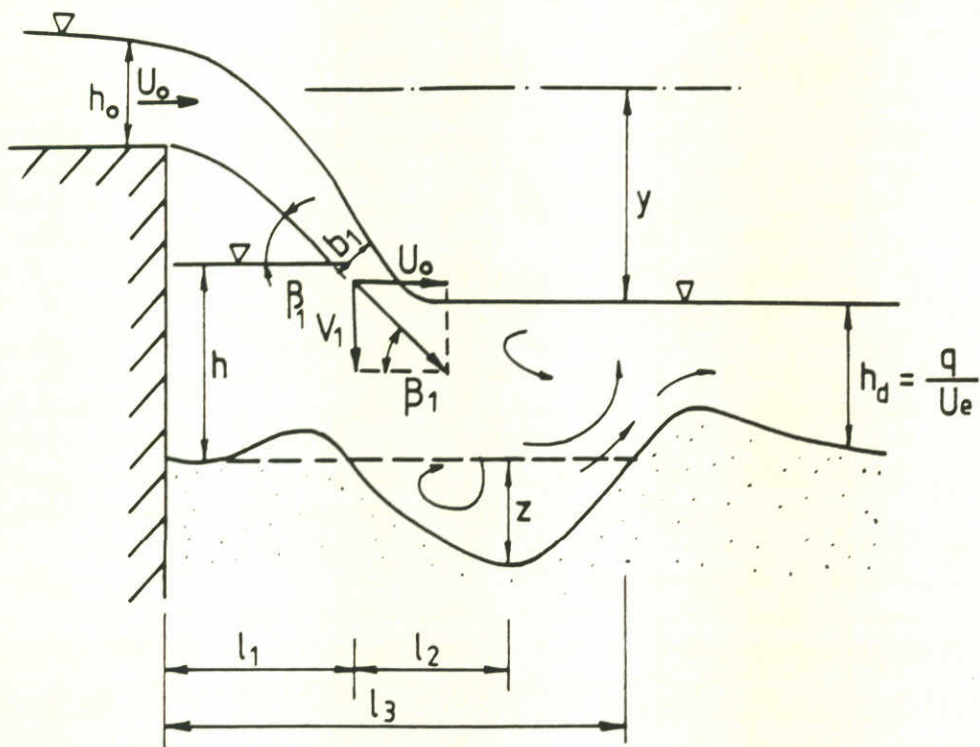
CHARACTERISTICS OF JET FLOW

DELFT HYDRAULICS     Q 647     FIG. 6.3

(a) SUBMERGED PLANE HORIZONTAL JETS

(b) SUBMERGED CIRCULAR HORIZONTAL JETS

$$\text{(a)} \quad \frac{y_s}{2B_u} = 0.008 \left( \frac{U_o}{u_{*c}} \right)^2$$

$$\text{(b)} \quad \frac{y_s}{D} = 0.08 \frac{U_o}{u_{*c}}$$
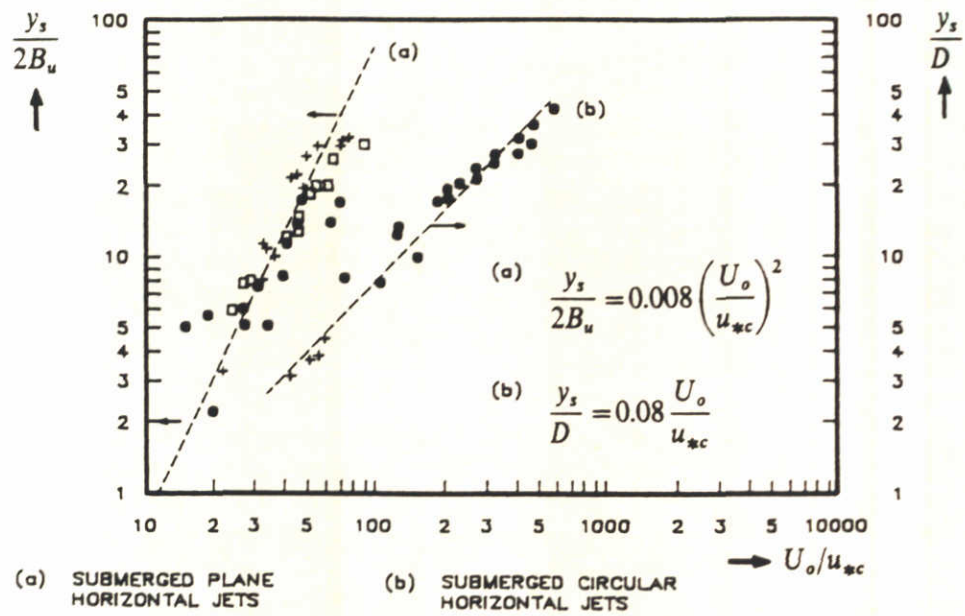
bron: [6.4]

| MAXIMUM SCOUR DEPTH FOR SUBMERGED HORIZONTAL JETS | | |
|---|---|---|
| | | |
| DELFT HYDRAULICS | Q 647 | FIG. 6.4 |

CIRCULAR JETS

$$\frac{y_s}{D_u}$$

$$\frac{y_s}{D_u} = 0.035 \left(\frac{U_o}{u_{*c}}\right)^{2/3}$$

$$\frac{y_s}{D_u} = 0.75 \frac{U_o}{u_{*c}}$$

$$\longrightarrow U_o/u_{*c}$$

PLANE JETS

$$\frac{y_s}{2B_u}$$

$$\frac{y_s}{2B_u} = 0.05 \left(\frac{U_o}{u_{*c}}\right)^{4/3}$$

| $H/2B_u$ | AUTHOR: |
|---|---|
| ● 6,25 | AKASHI/SAITO |
| ■ 12,5 | AKASHI/SAITO |
| ○ 25 | AKASHI/SAITO |
| + 50 | RAJARATNAM |
| × 30 | RAJARATNAM |
| △ 15 | RAJARATNAM |
| □ 5 | RAJARATNAM |

$$\longrightarrow U_o/u_{*c}$$
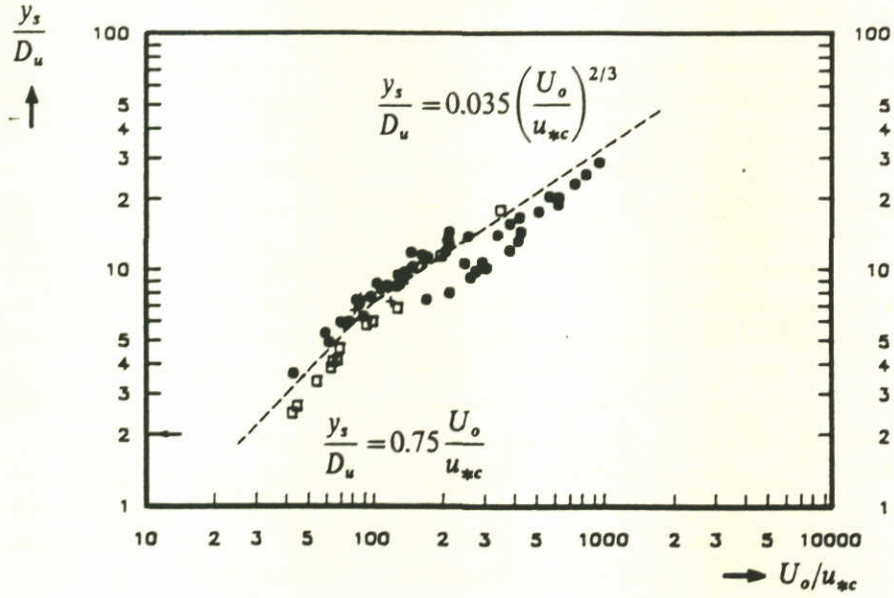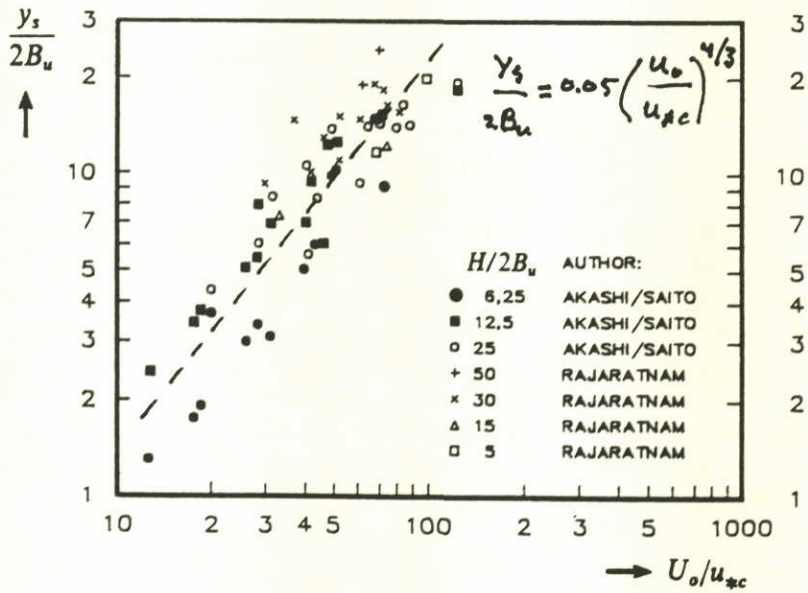
bron: [6.4]

MAXIMUM SCOUR DEPTH FOR
SUBMERGED VERTICAL JETS

| DELFT HYDRAULICS | Q 647 | FIG. 6.5 |
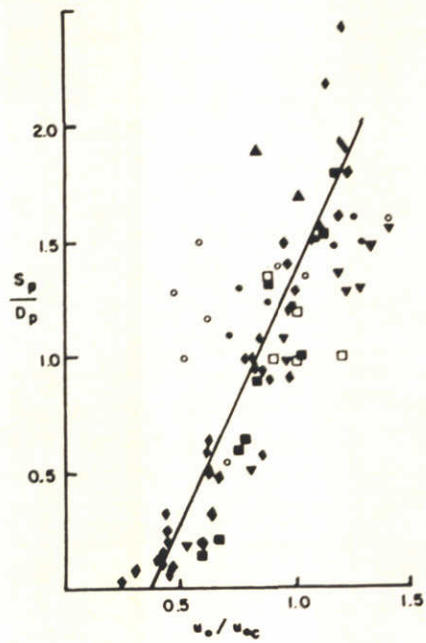
LOCAL SCOUR AROUND PILES

| | | |
|---|---|---|
| DELFT HYDRAULICS | Q 647 | FIG. 7.1 |

Appendix A

## Comparison of Dietz scour formula for tl with Breusers formula

The development of the maximum scour depth as a function of time is characterized by time $t_1$, which is a function of the relative density, the water depth, the flow velocity and the critical flow velocity according to the analysis of more than 250 tests with a hydraulic smooth, medium and rough bed protection, as analysed by Breusers and others:

$$t_1 = 250 \, . \, \Delta^{1.7} . \, y_o^{\,2} \, . \, \left[ \, \alpha \, \bar{U} - \bar{U}_{cr} \, \right]^{-4.3} \tag{A.1}$$

in which:

$t_1$ = time at which $y_{s\,max} = y_o$ (hours)

$\Delta$ = relative density,

$\quad (\rho_s - \rho) \, / \, (\rho) \quad (-)$

$\rho_s$ = density of bed material (kg/m³)

$\rho$ = density of water (kg/m³)

$\alpha$ = a flow factor, which depends on the geometry or on the $\quad$ (-)

$\quad$ relative turbulence intensity

$\bar{U}$ = average velocity at the edge of bed protection (x = 0) $\quad$ (m/s)

$\bar{U}_{cr}$ = critical mean velocity evaluated from Shields´ curve $\quad$ (m/s)

For geometries, which have an hydraulically rough bed protection, like the bed protection of the Eastern Scheldt Storm Surge Barrier, the constant 250 can be replaced by 330.

The analysis by Dietz, lit.[2.16], of systematic model tests on sills with a horizontal bed protection have resulted in a similar formula for $t_1$ as (A.1):

$$t_1 = 48 \, . \, y_0^{1.75} . \, \Delta^{1.5} \, . \, (U_{max} - U_c)^{-4} \tag{A.2}$$

In case of an hydraulic rough bed protection:

$$U_{max} = ( \, 1 + 3 \, r \, ) \, \bar{U} \tag{A.3}$$

in which

$\bar{U}$ = depth averaged flow velocity at the edge of the bed protection (m/s)
$r'$ = relative turbulence intensity                                   (-)

The relative turbulence intensity is defined by (A.4):

$$r' = \{(\Delta u')^2\}^{0.5} \tag{A.4}$$

In case of an hydraulic smooth bed protection:

$$U_{max} = 1.5 \ (1 + 3 \ . \ r') \ \bar{U} \tag{A.5}$$

The comparison of formula (A.2) with (A.1) is demonstrated for a rough bed protection without a sill, see Dietz and Breusers for the used data: $\alpha = 1.5$ substituted in (A.1):

$$t_1 \ :: \ 250 \ . \ 1.5^{-4.3} \ . \ (\bar{U})^{-4.3} \ = 43.7 \ . (\bar{U})^{-4.3} \tag{A.6}$$

and $r' = 0.07$ to 0.09 according to [2.16],
substituted in (A.3) and (A.2) and neglecting the influence of $U_c$:

$$t_1 \ :: \ 48 \ . \ (1.21 \ \text{to} \ 1.27 \ )^{-4}. \ (U)^{-4} \ = (22.4 \ \text{to} \ 18.5) \ .(\bar{U})^{-4} \tag{A.7}$$

From this example it is demonstrated that formula (A.2) confirms formula (A.1), although $t_1$ calculated with (A.2) is about 2 times smaller than $t_1$ calculated with (A.1). The reason for this difference is not complete clear at this moment; possible reasons are:
- Different definitions of $U_{cr}$ by Breusers and Dietz. These differences can be caused by the assumed hydraulic roughness. In Dietz's analysis of a systematic research on scouring he has used the assumption $k_s = D_{90}$ instead of $k_s = D_{50}$ of the bed material.
- A difference in the hydraulic roughness of the bed protection in both researches.
- Small differences in the exponent of the water depth and the relative density.

In one specific geometry the influence of the roughness of the bed protection on the scour depth has been studied [2.12]. However, the results of this study, a very limited influence, have no general validity.

The general conclusion is that the formula of Dietz for the calculation of $t_1$ confirms the formula of Breusers roughly. For engineering practice the formula of Breusers is recommended.

Appendix B

**The determination of the influence of the hydraulic roughness on the critical flow velocity.**

The physical importance of the hydraulic roughness for the calculated critical flow velocity is illustrated with the following remarks.

The assumption $k_s = D_{50}$ for the calculation of the critical flow velocity in the Breusers scour formula is valid during the very first stage of the initiation of movement of fine sands in a flat bed. It is recommended to verify wether the assumption is consistent with the selected criteria for the inititation of movement. Probably $k_s = 2 . D_{50}$ is a better approximation for the hydraulic roughness if the grains move permanent and at every location.

In prototype conditions a natural bed has, in general, a higher hydraulic roughness, with an average value of $k_s = 3 D_{90}$, see van Rijn [2.29]. This increased hydraulic roughness can result in an increase of 3% of $\alpha$.

At the place of a future scour hole downstream of a bed protection the hydraulic roughness of the bed material just before the development of a scour hole is completely determined by the roughness of the upstream bed protection, [2.15]. In general this hydraulic roughness of the rip-rap is much higher then the hydraulic roughness of the bed material (normally sand). The physical critical velocity of the sand is probably determined by this relatively high roughness of the rip-rap.

In some cases the value of $\alpha$ can be reduced by 15 to 20 % if $k_s = 3 D_{90}$ with $D_{90}$ of the rip-rap of the bed-protection is used, instead of $k_s = D_{50}$ of the bed material (sand) as supposed by Breusers.

Appendix C

## Formulas for the estimation of factor α

The values of the factor α, which are presented in figure 2.9, are based on tests in the systematic series [2.9]) with a moderate rough and rough bed protection and sill with $k_s = 0.025\ y_0$ and $k_s = 0.05\ y_0$. From the graph in figure C.1 the following relation has been deduced:

$$\alpha = 1.5 + 5\ (y_D/y_0)^2 .\ e^{-\ 0.02}\ .\ (y_D/y_0)\ .\ (L_p/y_0)^{1.5} \tag{C.1}$$

If a sill is combined with a horizontal constriction $B_s/B = 0.1$ and a vertical head ( or face) of this constriction, then a three dimensional scour hole due to the induced vortex street will develop and α follows from:

$$\alpha = 1.5 + \{2.6 + 18.6\ (y_D/y_0)^2\}\ .\ e^{-\ 0.045\ L_p/y_0} \tag{C.2}$$

Formula (C.2) is an extension of the formula of de Graauw, [2.19] [2.20] and figure C.3 with

$$\alpha_{10} = 3.2 + 12\ (y_D/y_0)^2 \tag{C.3}$$

in which

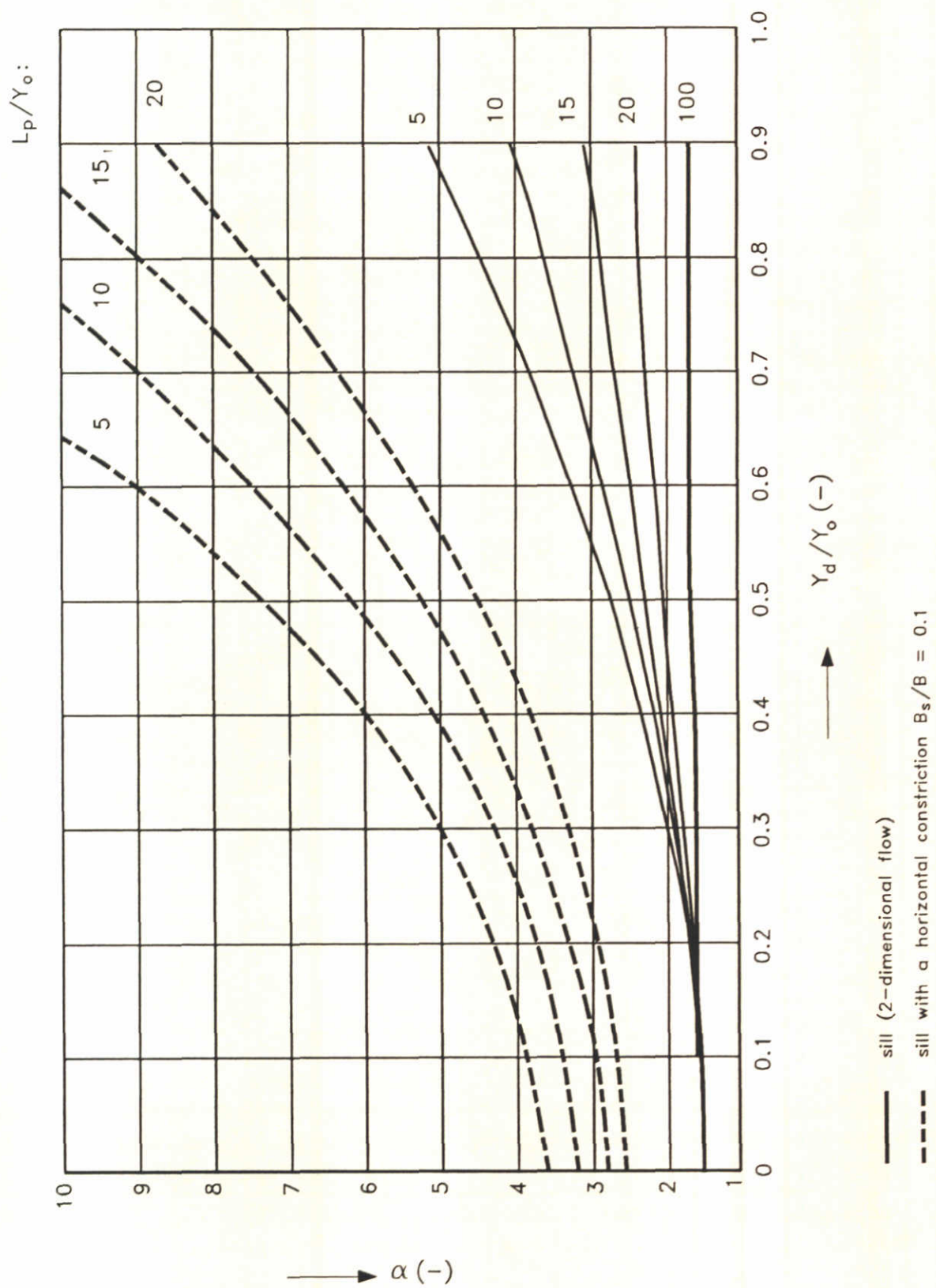$\alpha_{10}$ = value of alfa if $L_p/y_0 = 10$          (-)

It is mentioned that here the most recent version of the formula of de Graauw is used which has been published in 1986. In earlier reports, a different figure has been published, which results in a change in (C.3) (see figure 6.4):

Formulas (C.1) and (C.2) are both represented in figure C.2, and this figure replaces the earlier published figure C.5. The main tendencies in figure C.2 correspond well with the main tendencies in figure C.5, but the relationships in figure C.2 are more detailed and more uniquely defined then in the old figure.
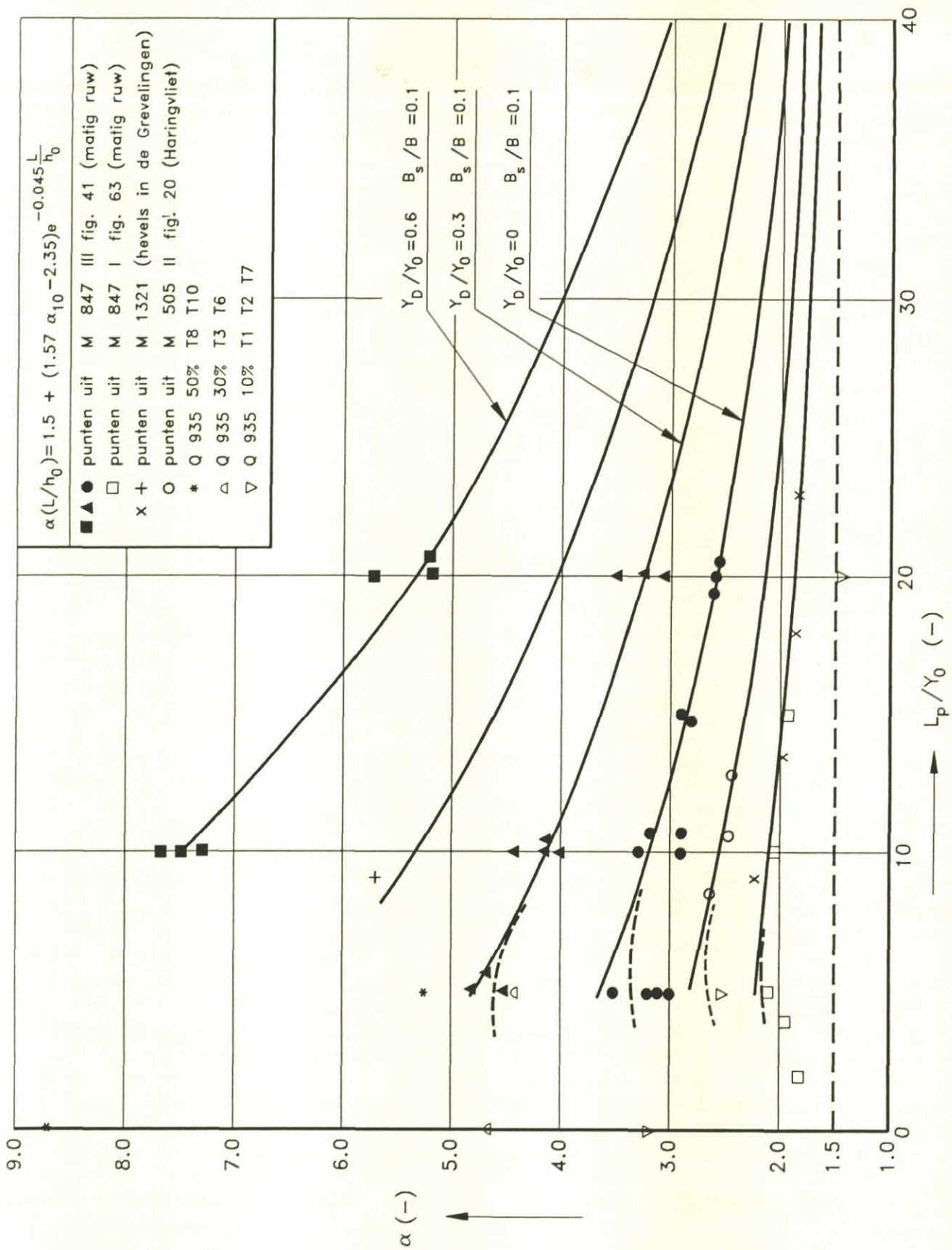
It is recommended to compare (C.2) or (C.3) with the results, which have been published by Dietz [2.16], and with the results of DHL-report M1533 part III, lit. [2.12], with a fixed and a flexible bed protection.
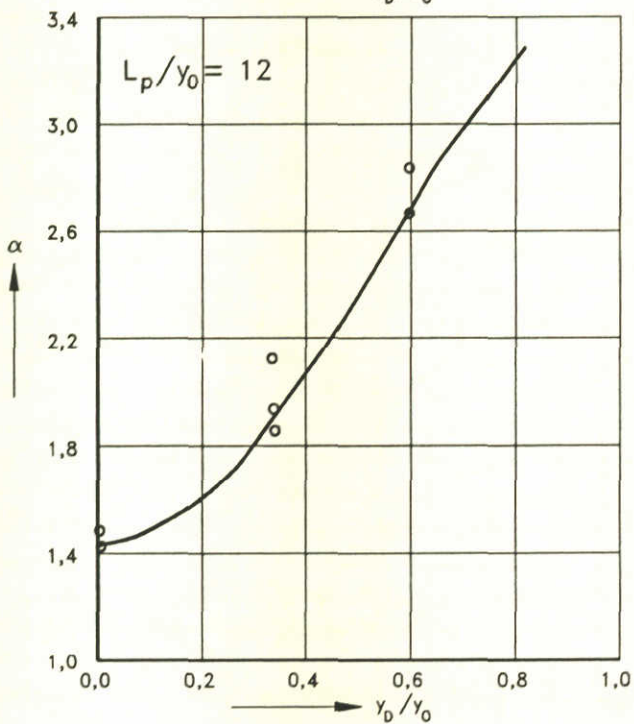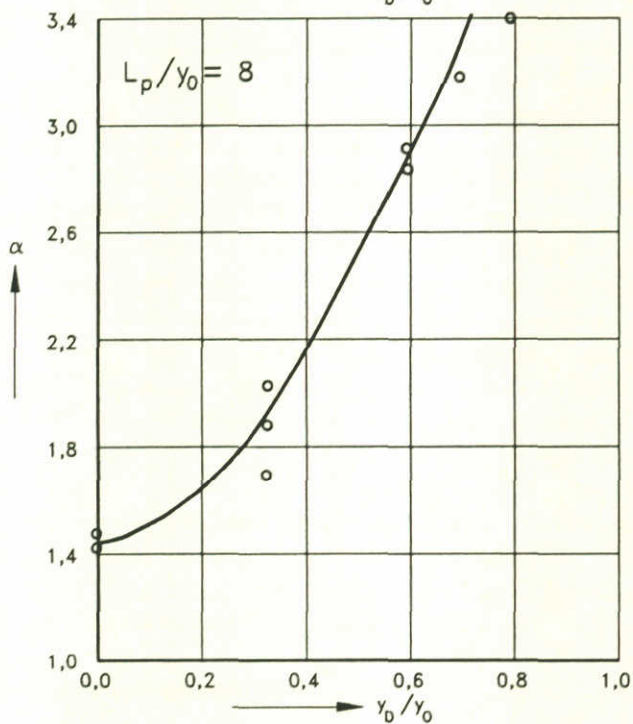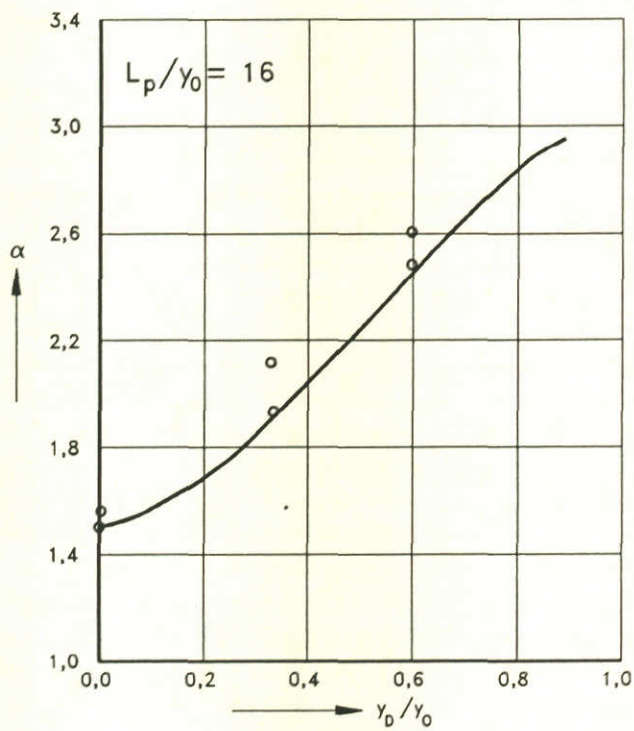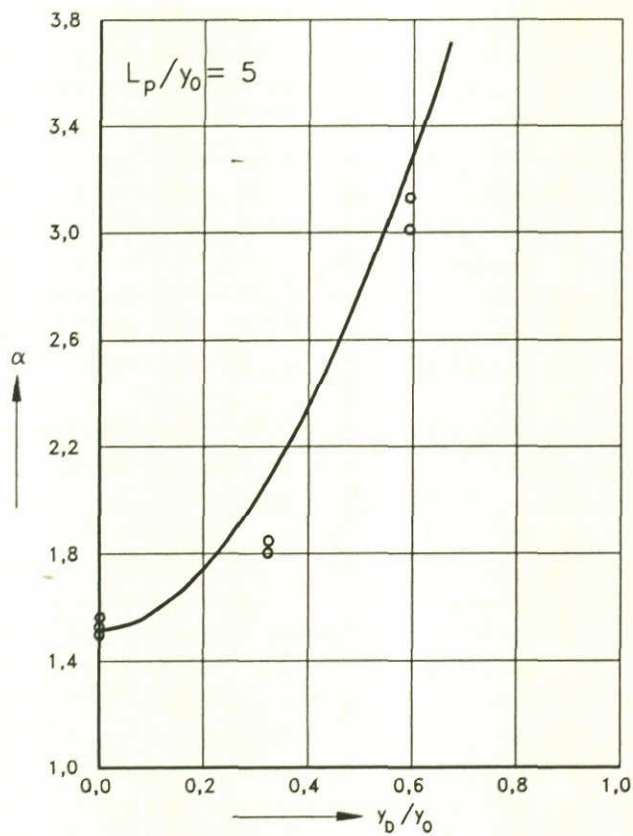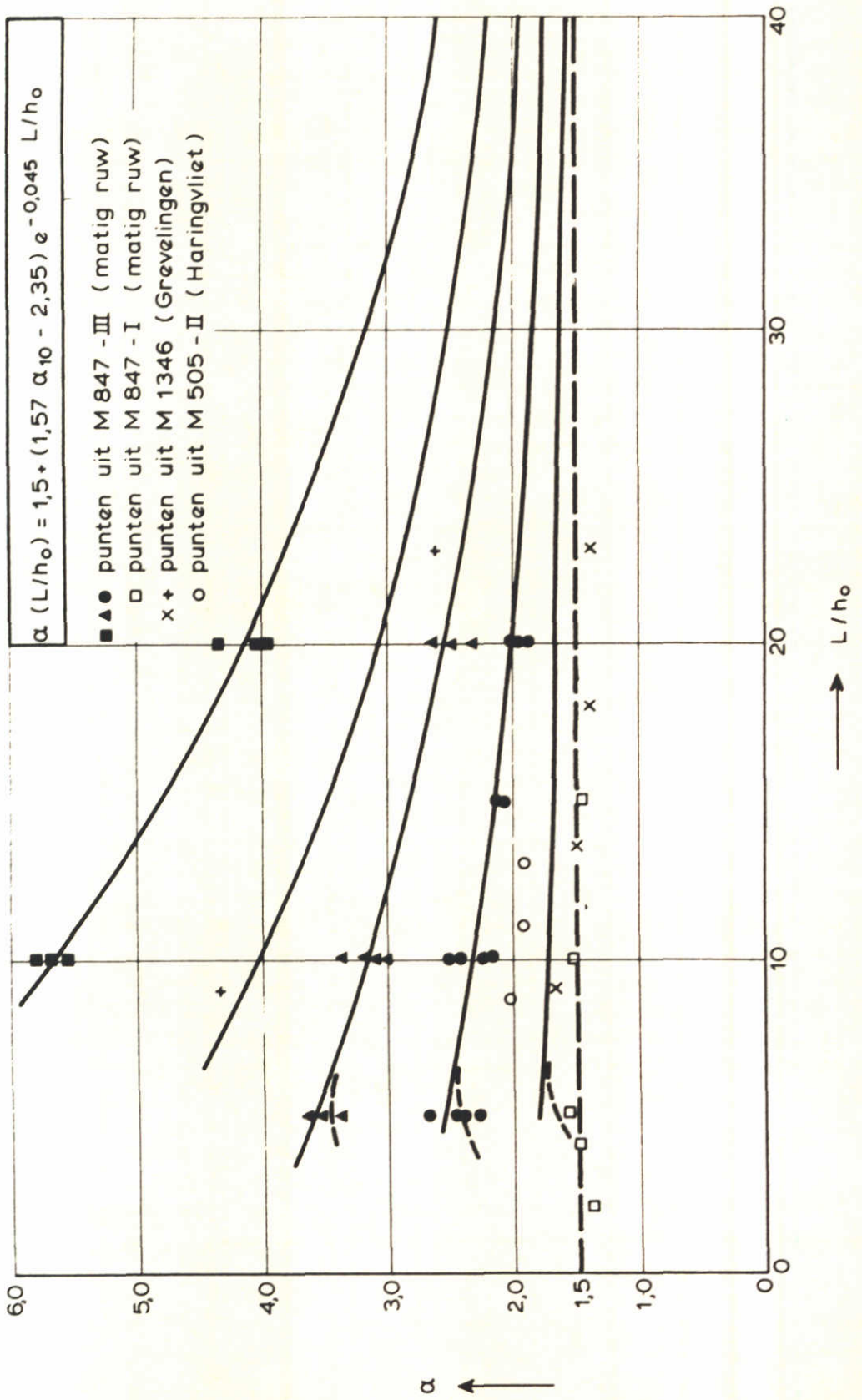
RELATION BETWEEN $\alpha$ AND LENGHT BED
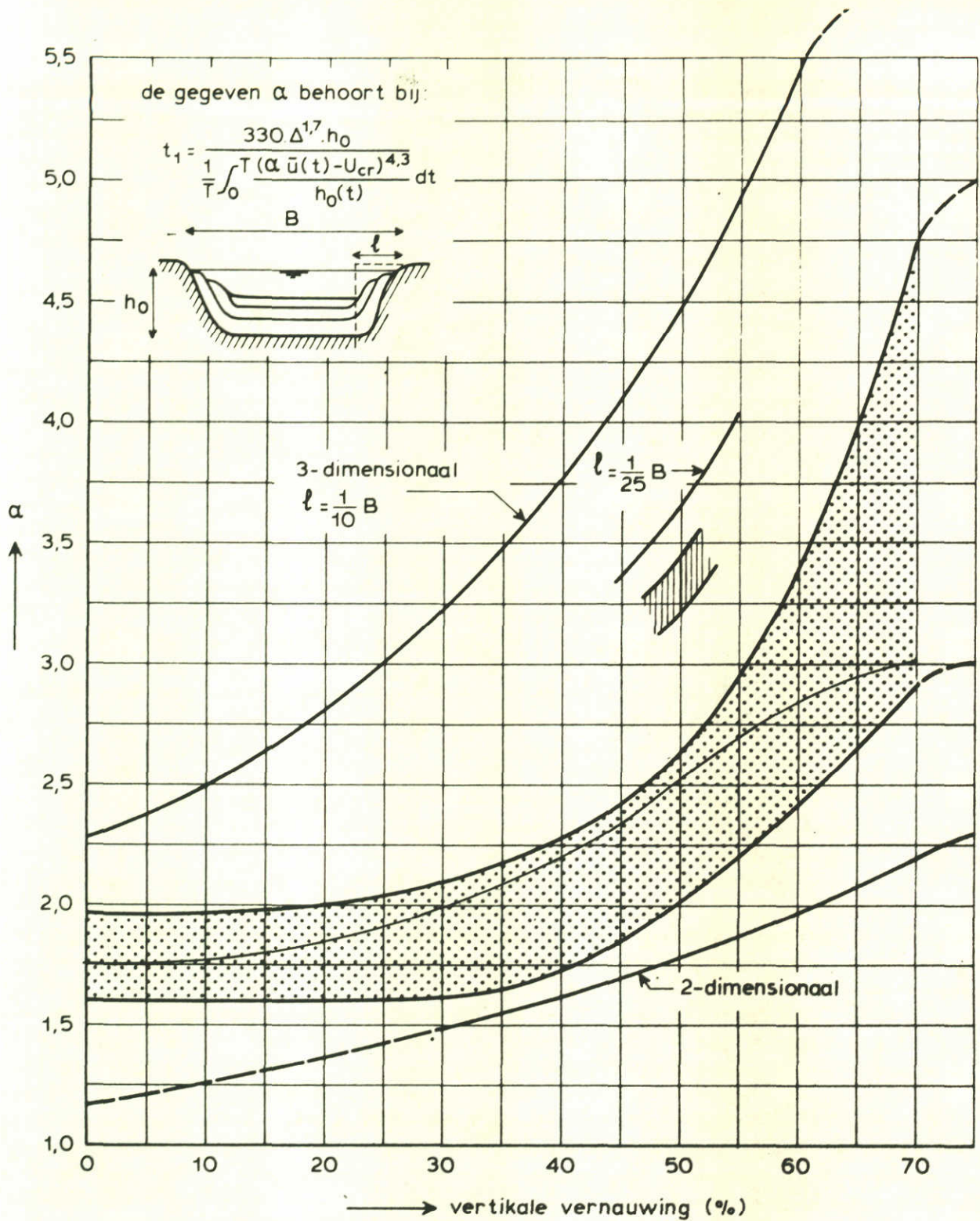PROTECTION, AND RELATIVE SILL HEIGHT

DELFT HYDRAULICS

Q 647

FIG. C.1

α AS A FUNCTION OF $Y_d / Y_o$
2- AND 3- DIMENSIONAL FLOW

| DELFT HYDRAULICS | | Q 647 | FIG. C.2 |

RELATION BETWEEN $\alpha$ AND RELATIVE SILL HEIGHT

DELFT HYDRAULICS

Q 647

FIG. C.3

RELATION BETWEEN α AND L

DELFT HYDRAULICS    Q 647    FIG. C.4

de gegeven $\alpha$ behoort bij:

$$t_1 = \frac{330 \, \Delta^{1.7}.h_0}{\frac{1}{T}\int_0^T \frac{(\alpha \, \bar{u}(t) - U_{cr})^{4.3}}{h_0(t)} dt}$$

3-dimensionaal $\ell = \frac{1}{10} B$

$\ell = \frac{1}{25} B$

2-dimensionaal

$\alpha$

vertikale vernauwing (‰)

▦ samenvallende wervelstraten

▨ normale tweedimensionale situaties in de praktijk

lengte bodembescherming: L = 10 $h_0$ uit drempelteen

RELATIONSHIP BETWEEN $\alpha$ AND THE
RELATIVE SILL HEIGHT, OLD RESULTS

DELFT HYDRAULICS

Q 647

FIG. C.5

Appendix D

**Factor α as a function of the turbulence intensity.**

An alternative approach is to relate α to the relative turbulence intensity of the main flow. In general, the rate of turbulence is enlarged by a hydraulic structure. Over the length of the bed protection this turbulence is reduced by dissipation of turbulent energy.

For predicting scour downstream of a rough riprap type bed protection α was related to the average relative turbulence intensity r as shown in (D.1) according to de Graauw, see lit.[2.20]:

$$\alpha = 0.5 + 10 \cdot r \qquad (D.1)$$

in which

$r = u'/U,$

$U$ = time averaged flow velocity $\qquad (m/s)$

$u'$ = the depth average value of the root mean square value of the turbulent velocity fluctuations in the main flow direction $\qquad (m/s)$

This velocity fluctuation is defined by:

$$u' = \{\overline{(u'_x)^2}\}^{0.5}$$

in which

$u'_x$ = velocity fluctuation in the x-direction $\qquad (m/s)$

and $U = Q/(y_0 \cdot B)$, which means that U is the depth averaged flow velocity in the x-direction.

This relation is also valid for a low sill with a two dimensional flow pattern, (so without abutments). For higher sills or a smooth bed protection (e.g. a concrete apron) where distortion of the velocity profile occurs, a correction factor must be employed, according to Breusers, also mentioned by Dietz, lit.[2.16] (1969):

$$\alpha = \alpha_u (1 + 3 \cdot r) \qquad (D.2)$$

in which

$\alpha_u$ = 1    for a hydraulic rough and horizontal bed protection

$\alpha_u$ = 1.5 for a hydraulic smooth bed protection.


Recently Jorissen and Vrijling [2.23] have refined this relation (D.1) based on more measurements in a two- and a three-dimensional flow pattern and replaced U by $U_1$ which is the local depth average velocity at the downstream end of the bed protection. The relation between $\alpha$ and $\alpha_1$ is:


$$\alpha \cdot U = \alpha_1 \cdot U_1 \qquad\qquad\qquad (D.3)$$


They found the following relation:


$$\alpha_1 = 1.5 + 5 \cdot r \qquad\qquad\qquad (D.4)$$


if $r > 0.07$ and $\alpha_1 > 1.8$.


For a two dimensional flow $U_1$ is approximately equal to U and then (D.4) can be compared with (D.1), [2.20], see figure D.1. Both formulas show a reasonable agreement with the measurements, so (D.4) can be considered as a generalization of (D.1).

If a formula of type (D.2) or (D.4) is accepted, the next step should be the determination of the turbulence intensity as a function of the main geometric parameters. At this moment no formulas are available for the relationship between the relative turbulence intensity and the geometric parameters of an hydraulic structure.
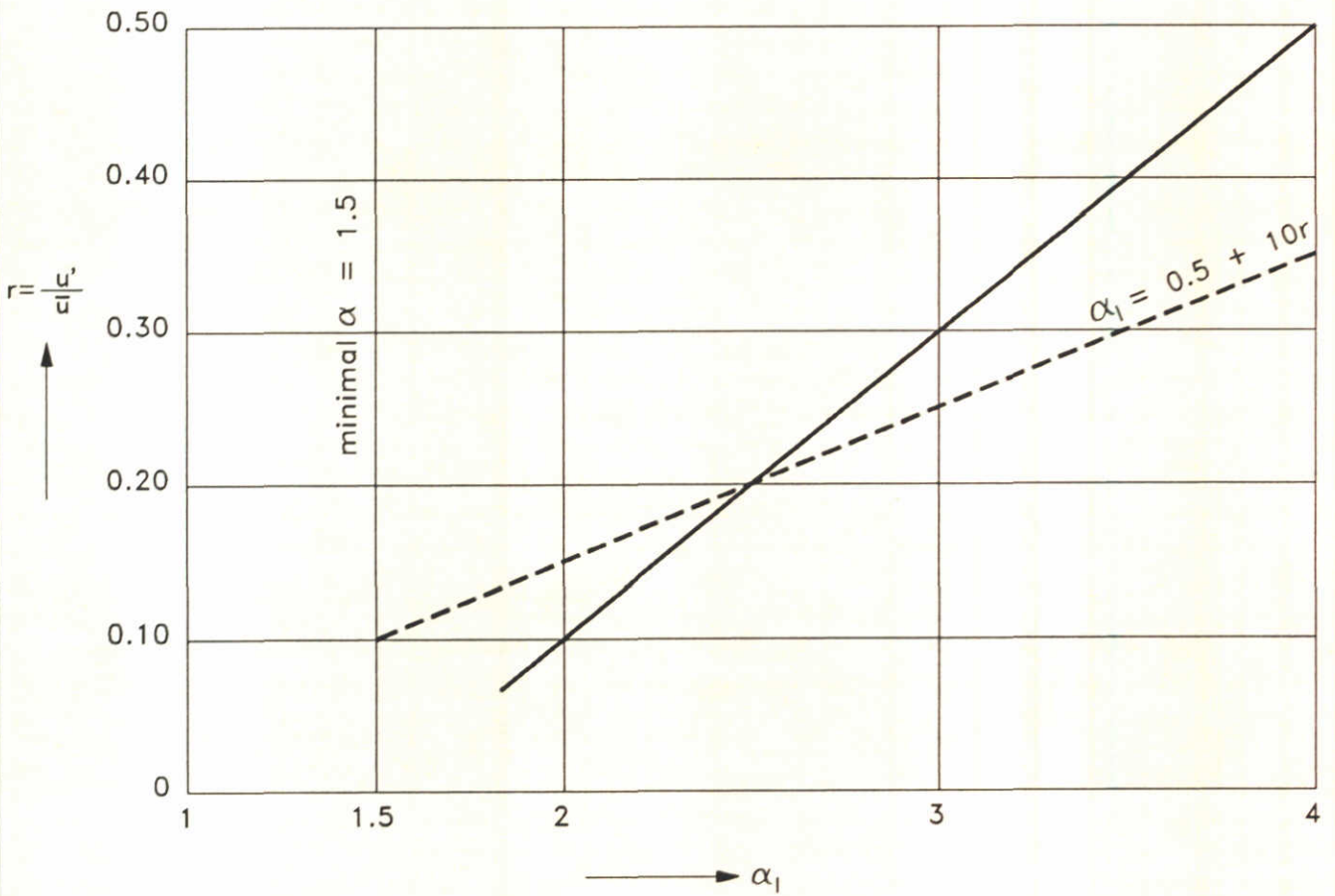
RELATIONSHIP BETWEEN $\alpha$ AND THE
RELATIVE TURBULENCE INTENSITY

DELFT HYDRAULICS

Q 647

FIG. D.1

Appendix E

Equilibrium maximum scour depth

After some time a scour hole will reach an equilibrium shape and the
maximum scour depth will become a constant value. In terms of the
classification of different phases the development of a scour hole, see
section 2.5.2, this equilibrium defines phase 4, see figure 2.5. In scale
model tests with aluvial sand and clear water scour it will take sometimes
a long time before this equilibrium is reached, see for example figure
2.15. Therefore, the definition of equilibrium maximum scour depth is not
always clear in the reports of scale model tests with clear water scour. In
general, in a prototype some upstream supply of sediment, $q_s$, exists, by
which this equilibrium will be reached in a relatively short time.

A first estimation of the equilibrium scour depth $y_{max,e}$ in a scour hole
near a sill with a bed protection can be obtained with (according to Dietz,
[2.16]):

$$\frac{y_{max,e}}{y_0} = \{U_{max} - U_{cr}\}/U_{cr} \qquad (E.1)$$

in which $U_{max} = c \cdot \alpha \cdot \bar{U}$

It can be concluded that c is also a function of time:
during the development phase of the scouring process c = 0.4 to 0.5 and in
the final phase of equilibrium scour depth c = 1.

More specifically the test results were:

0.5 < c < 1  according to Dietz, [2.16] (see also figure 2.16) in two-
dimensional flow, and
0.5 < c < 1  according to Delft Hydraulics, [2.20], and
c = 0.4 to 0.5 in the systematic test series with respect to the
development phase of the scouring process in three-dimensional flow [2.10],
and
c = 1 in the final equilibrium phase of the scouring process [2.12]
These values confirm the formula of Zanke, see lit.[2.30] $U_{cr}$ is determined
from the Shields curve.

The formula of Zanke, lit.[2.30] reads:

$$T = 6 \, y_{max}^2 \cdot w^4 \cdot \theta^4 \cdot c_1 \cdot \frac{1}{\{c_2^2 \, U_{om}^2 - U_{cr,ave}^2\}^2} \tag{E.2}$$

in which

$$c_2 = \beta \cdot \omega \cdot y_0 / \{y_0 + y_{max}\} \tag{E.3}$$

and

$$c_1 = 10^{-7} \, D*^4 \cdot \nu \cdot a_1 \cdot (u_s/u_m)^4 / (1 - p) \tag{E.4}$$

| | | |
|---|---|---|
| T | = time from the start of the erosion process to the moment at which the equilibrium scour is reached | (s) |
| w | = fall velocity of bottom material | (m/s) |
| $\theta$ | = shape factor, depending of the geometry and the flow pattern (with and without an hydraulic jump) | (-) |
| $U_{om}$ | = averaged flow velocity upstream of the scour hole | (m/s) |
| $U_{cr.ave}$ | = depth averaged flow velocity at the initiation of motion | (m/s) |
| D* | = sedimentological diameter of bottom material | (-) |
| p | = porosity | (-) |
| $\omega$ | = factor depending on $y_{max}/y_0$ | (-) |
| $\beta$ | = factor depending on the geometry and the bed protection | (-) |
| $a_1$ | = factor depending on the relative turbulence intensity and the sediment transport intensity | (-) |
| $u_s$ | = flow velocity near the bottom | (m/s) |
| $u_m$ | = depth averaged flow velocity | (m/s) |

If T goes to infinity then (E.2) reduces to:

$$y_{max}/y_0 = \{\beta \cdot \omega \cdot \bar{U} - U_{cr,ave}\}/U_{cr,ave} \tag{E.5}$$

This formula is of the same type as the approximation of Dietz in (E.1) if $\beta \cdot \omega = c \cdot \alpha$, This seems to be not completely correct because $\beta \cdot \omega$ seems to be a function of time.

These two expressions (E.5) and (E.1) can be compared with the results of a scour-tests T5 and T6 in a scale model of the Brouwersluis, see lit. [2.12]. As a function of time $\beta \cdot \omega = 1$ to 2 and this can be compared with

c. $\alpha$   = { 0.5 to 1 } . { 1.9 to 2.1 } = 0.95 to 2.1.

For the final stage of the scouring process $\omega$ . $\beta$ = 2 and therefore c = 1.
It can be concluded that c is also a function of time:
during  the development phase of the scouring process c = 0.4 to 0.5 and in
the final phase of equilibrium scour depth c = 1.

After  a  first  application  of the formula of Zanke in lit. [2.12] it was
concluded that the determination of the value of the different constants in
the  formula  of  Zanke  requires  at  least  three tests in a scale model.
Therefore this formula was considered to be  too  complicated  and  further
applications were not recommended.

Now we recommend a further examination of the equilibrium formulas of Dietz
and  Zanke,  because  more information about $\alpha$ and new test results are now
available. Probably the results of long lasting tests in scale  models  can
be used for a more detailed verification of these formulas.

Appendix F

**Analysis of the scour formulas of Bormann (equation 2.30)**

The requirement that the calculated value of $D_{sd}$ is more or less the same as the value of $D_{sa}$ suggests to write both original formulas as one equation:

$$c_2 = c_d^2 \cdot U_0^{1.5 \text{ to } 1.6} \cdot Y_0^{0.45 \text{ to } 0.6} \cdot g^{-0.7 \text{ to } -0.8} \cdot \Delta^{-0.8}$$

$$\cdot D_{50}^{-0.3 \text{ to } -0.4} \cdot \sin \beta^{0.65 \text{ to } 1} - D_p \qquad (F.1)$$

$$Y_{s,max} = c_2 - y_0$$

and

$$c_d^2 = Y_t^{0.12} \qquad \text{or} \qquad (F.2a)$$

$$c_d^2 = 1.64 \cdot [\tan \phi / \{\cos \beta \cdot (\tan \phi + \tan \beta)\}]^{0.8} \qquad (F.2b)$$

In these formulas the exponents have been rounded off to one decimal.
In general, 1 ft $< Y_t <$ 100 ft that means after substitution in (F.2a)

$$1 < c_4 < 1.7$$

In general, 30 degrees $< \phi <$ 40 degrees and 0.3 $<$ tan $\beta$ $<$ 1 and after substitution in (F.2b):

$$0.95 < c_4 < 1.3$$

These ranges confirm that in general $D_{sd}$ is approximately equal to $D_{sa}$ and that these ranges are rather limited.
Next, we try to compare this formula for $c_2$ (F.1) with the formulas of the Breusers method. The combination of the formulas (2.5) and (2.6) results in:

$$y_{s,max} = 0.11 \cdot \Delta^{-0.7} \cdot y_0^{0.2} \cdot (\alpha U - U_c)^{1.7} \cdot t^{0.4} \qquad (F.3)$$

The comparison of (F.3) with the combined formula (F.1) shows a rather good agreement in the exponents:

|  | (F.1) | (F.3) |
|---|---|---|
| $\Delta$ | -0.8 | -0.7 |
| $y_0$ | 0.45 to 0.6 | 0.2 |
| $U_0$ or $\alpha\, U - U_c$ | 1.5 to 1.6 | 1.7 |

However, the definition of $y_0$ in both formulas is not the same! If we suppose that $U_{max} \gg U_c$ then the difference between $U_0$ and $\alpha \cdot U - U_c$ can be neglected in a rough comparison ($U_0$ is the average velocity above the crest of the sill and U is the average velocity upstream of the sill).
From formulas (F.1) and (F.3) a rough estimation of t for the equilibrium scour depth can be obtained:

$$\frac{y_{s,max}}{0.3 \cdot (D_s + D_p)} = \frac{0.11 \cdot t^{0.4}}{c_4 \cdot g^{-0.7 \text{ to } -0.8} \cdot D_{50}^{-0.3 \text{ to } -0.4} \cdot \sin \beta^{0.65 \text{ to } 1}}$$

$$(F.4)$$

Suppose: $0.001$ ft $< D_{50} < 0.01$ ft, g = 32.2 ft/s2, $18 < \beta < 45$ degrees
then

$$\frac{y_{s,max}}{D_s + D_p} = (0.003 \text{ to } 0.037) \cdot t^{0.4} \quad (4.40) \qquad (F.5)$$

Suppose $y_{s,max}/(D_s + D_p)$ = 0.6 to 0.9 then t,equilibrium = 45 days to 200 years! These values, which are not unrealistic, are only tentative to illustrate the considerable variation in the time, after which equilibrium scour depth can be expected. Some results of the time dependent development of the maximum scour depth are published by Colaric and others, see [2.7]. These results suggest that y = 0.4 should be reduced to y = 0.22. With this value of y after very long times the equilibrium scour depth will be reached.

The good similarity between the values of the exponents of the parameters in the Breusers formula and the Bormann formula is of more importance.

Suggestion: investigate the possibility to extend the Bormann formulas by replacing the parameter $U_0$ by $\alpha \cdot U - U_c$ in which $\alpha$ influence of different geometries represent, and reducing y = 0.4 to y = 0.2 according to formula (3.2) in the chapter about spurdikes.

After a strong simplification of formula (F.1) a formula with dimensionless parameters can be obtained:

$$\frac{D_s + D_p}{Y_0^{0.5} \cdot D_{50}^{0.5}} = c_4 \cdot Fr^{1.5} \cdot \{\frac{Y_0}{\Delta \cdot D_{50}}\}^{0.8} \cdot \sin \beta^{0.65 \text{ to } 1} \qquad (F.6)$$

in which

Fr = Froude number based on $U_0$, $Y_0$ and g                                    (-)

The structure of this formula is of the same type as the structure of some formulas for bridge pier scour, see section 4.6.

The equilibrium depth can be estimated with the formulas of Bormann, if $U_{max} \gg U_c$, else the formula of Dietz should be considered as a first approximation.